

A 5902 II

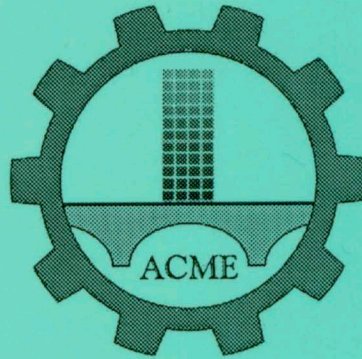
Dz. 6

POLISH ACADEMY OF SCIENCES – WROCLAW BRANCH

WROCLAW UNIVERSITY OF TECHNOLOGY

ISSN 1644-9665

INDEX 375667



**ARCHIVES
OF CIVIL AND MECHANICAL
ENGINEERING**

Quarterly

Vol. VII, No. 4

WROCLAW 2007

ADVISORY COMMITTEE

Chairman – JAN KMITA¹
JAN BILISZCZUK (Poland)
CZESŁAW CEMPEL (Poland)
JERZY GRONOSTAJSKI (Poland)
ANTONI GRONOWICZ (Poland)
M.S.J. HASHMI (Ireland)
HENRYK HAWRYLAK (Poland)
RYSZARD IZBICKI (Poland)
WAĆLAW KASPRZAK (Poland)
MICHAEL KETTING (Germany)
MICHAŁ KLEIBER (Poland)
VADIM L. KOLMOGOROV (Russia)

ADOLF MACIEJNY (Poland)
ZDZISŁAW MARCINIAK (Poland)
KAZIMIERZ RYKALUK (Poland)
ANDRZEJ RYŻYŃSKI (Poland)
ZDZISŁAW SAMSONOWICZ (Poland)
WOJCIECH SZCZEPIŃSKI (Poland)
PAWEŁ ŚNIADY (Poland)
RYSZARD TADEUSIEWICZ (Poland)
TARRAS WANHEIM (Denmark)
WŁADYSŁAW WŁOSIŃSKI (Poland)
JERZY ZIÓLKO (Poland)
JÓZEF ZASADZIŃSKI (Poland)

EDITORIAL BOARD

Editor-in-chief – JERZY GRONOSTAJSKI²
ROBERT ARRIEUX (France)
AUGUSTO BARATA DA ROCHA (Portugal)
GHEORGHE BRABIE (Romania)
LEŚLAW BRUNARSKI (Poland)
EDWARD CHLEBUS (Poland)
LESZEK F. DEMKOWICZ (USA)
KAZIMIERZ FLAGA (Poland)
YOSHINOBI FUJITANI (Japan)
FRANCISZEK GROSMAN (Poland)
MIECZYŚLAW KAMIŃSKI (Poland)
Scientific secretary – SYLWESTER KOBIELAK

ANDRZEJ KOCANĀDA (Poland)
WAĆLAW KOLLEK (Poland)
PIOTR KONDERLA (Poland)
ZBIGNIEW KOWAL (Poland)
TED KRAUTHAMMER (USA)
ERNEST KUBICA (Poland)
CEZARY MADRYAS (Poland)
TADEUSZ MIKULCZYŃSKI (Poland)
HARTMUT PASTERNAK (Germany)
MACIEJ PIETRZYK (Poland)
EUGENIUSZ RUSIŃSKI (Poland)
HANNA SUCHNICKA (Poland)

¹ The Faculty of Civil Engineering, Wrocław University of Technology
Wybrzeże Wyspiańskiego 27, 50-370 Wrocław, Poland
Tel. +48 71 320 41 35, Fax. +48 71 320 41 05, E-mail: jan.kmita@pwr.wroc.pl

² The Faculty of Mechanical Engineering, Wrocław University of Technology
ul. Łukasiewicza 5, 50-371 Wrocław, Poland
Tel. +48 71 320 21 73, Fax. +48 71 320 34 22, E-mail: jerzy.gronostajski@itma.pwr.wroc.pl

POLISH ACADEMY OF SCIENCES – WROCLAW BRANCH
WROCLAW UNIVERSITY OF TECHNOLOGY



ARCHIVES OF CIVIL AND MECHANICAL ENGINEERING

Quarterly
Vol. VII, No. 4

WROCLAW 2007

EDITOR IN CHIEF

JERZY GRONOSTAJSKI

EDITORIAL LAYOUT AND PROOF-READING

WIOLETTA GÓRALCZYK

TYPESETTING

SEBASTIAN ŁAWRUSEWICZ

SECRETARY

TERESA RYGLOWSKA

Publisher: Committee of Civil and Mechanical Engineering
of Polish Academy of Sciences – Wrocław Branch,
Faculty of Civil Engineering and Faculty of Mechanical Engineering
of Wrocław University of Technology

© Copyright by Oficyna Wydawnicza Politechniki Wrocławskiej, Wrocław 2007

OFICyna WYDAWNICZA POLITECHNIKI WROCLAWSKIEJ
Wybrzeże Wyspiańskiego 27, 50-370 Wrocław
<http://www.oficyna.pwr.wroc.pl>
e-mail: oficwyd@pwr.wroc.pl

ISSN 1644-9665

Drukarnia Oficyny Wydawniczej Politechniki Wrocławskiej. Zam. nr 675/2007.

Contents

M. WARMOWSKA, Problem of water flow on deck	5
D. BIELIŃSKI, Tribological consequences of rubber composition and structure – case studies	15
D. BRUZZONE, A. GRASSO, Nonlinear time domain analysis of vertical ship motions	27
D. CAPANIDIS, Selected aspects of the methodology of tribological investigations of polymer materials	39
M. GAWLIŃSKI, Friction and wear of elastomer seals	57
S. GHAZI-ASGAR, H. ZERAATGAR, M. GHIASI, Introducing an effective new ship rudder type, telescopic rudder	69
J. KLECZEWSKA, D. BIELIŃSKI, Friction and wear of resin-based dental materials	87
L. KOBYLIŃSKI, System and risk approach to ship safety, with special emphasis of stability	97
P. KOWALEWSKI, W. WIELEBA, Sliding polymers in the joint alloplastic	107
S. KRAWIEC, The influence of polymer fillers in a grease lubricant on tribological performance of friction nodes operating under mixed friction conditions	121
J. KULCZYK, Ł. SKRABURSKI, M. ZAWIŚLAK, Analysis of screw propeller 4119 using the fluent system	129
Z. LAWROWSKI, Polymers in the construction of serviceless sliding bearings	139
J. MATUSIAK, On certain types of ship responses disclosed by the two-stage approach to ship dynamics	151
W. OKULARCZYK, Experimental investigations of guide rings made of UHMWPE and PTFE composite in water hydraulic systems	167
Z. RYMUZA, Tribology of polymers	177
W. WIELEBA, The mechanism of tribological wear of thermoplastic materials	185

Spis treści

M. WARMOWSKA, Zagadnienie ruchu wody na pokładzie	5
D. BIELIŃSKI, Tribologiczne następstwa budowy i struktury gumy – przykłady	15
D. BRUZZONE, A. GRASSO, Nieliniowa analiza pionowych ruchów statku w dziedzinie czasu	27
D. CAPANIDIS, Wybrane aspekty metodyki badań tribologicznych materiałów polimerowych	39
M. GAWLIŃSKI, Tarcie i zużywanie uszczelnień elastomerowych	57
S. GHAZI-ASGAR, H. ZERAATGAR, M. GHIASI, Nowy efektywny ster okrętowy – ster teleskopowy	69
J. KLECZEWSKA, D. BIELIŃSKI, Tarcie i zużycie ściernie materiałów dentystycznych na baize żywić	87
L. KOBYLIŃSKI, Systemowe i oparte na analizie ryzyka podejście do bezpieczeństwa statku ze szczególnym podkreśleniem problematyki statecznościowej	97

P. KOWALEWSKI, W. WIELEBA, Polimery ślizgowe w alloplastyce stawów	107
S. KRAWIEC, Wpływ polimerowych napelniczy w smarze plastycznym na charakterystyki tribologiczne węzłów ślizgowych pracujących przy tarciu mieszanym	121
J. KULCZYK, Ł. SKRABURSKI, M. ZAWIŚLAK, Analiza opływu pędnika śrubowego 4119 przy zastosowaniu systemu Fluent	129
Z. LAWROWSKI, Polimery w budowie bezobsługowych łożysk ślizgowych	139
J. MATUSIAK, O pewnych rodzajach ujawnianych przy dwuetapowym podejściu do dynamiki statku	151
W. OKULARCZYK, Badania eksperymentalne pierścieni prowadzących wykonanych z UHMWPE i kompozytu PTFE pracujących w hydraulice wodnej	167
Z. RYMUZA, Tribologia polimerów	177
W. WIELEBA, Mechanizm zużycia tribologicznego tworzyw termoplastycznych	185



Problem of water flow on deck

M. WARMOWSKA

Polski Rejestr Statków, al. Gen. J. Hallera 126, 80-416 Gdańsk

A ship moving in waves is exposed to various undesired phenomena. Among them is water trapped on deck that affects ship safety. This paper presents a numerical model, based on shallow water flow, describing water flow on deck. Simplified methods have been applied to determine forces due to the water on deck influencing ship motion in waves. The presented method is developed to be included in the ship motion equation.

Keywords: *shallow water flow, free surface problem*

1. Introduction

The effect of water flow on deck, especially for small vessels, is substantial. Water trapped on deck may prove detrimental to ship motion. The changing water mass and flow of water across the deck and bulwark contribute to the forces and moments acting on the ship. Detailed description of this problem is presented by Belenky [1].

The problem of water on deck model describes:

- changing mass of water caused by water in- and outflow,
- shifting mass of green-water-on-deck.

Dillingham [2] presents a formula describing water flow through scrubbers and over bulwarks. The mass of flowing water depends on the size and shape of openings, the height of sea wave and on the water height above the opening. The changing mass does not depend on the water velocity field.

The problem of shifting mass of water on deck is usually described by a model of shallow water. Numerical solutions of 2D problems are obtained by Dillingham [2]. The equation used is valid for a level ship at rest. The author applies random choice method for solving hyperbolic equations. The three-dimensional flow is described by Dillingham and Falzarano [3] who transform equation to a coordinate system coupled to the ship's centre of gravity. Panatazapoulas [4] presents 3D equation of shallow water motion on deck of a ship moving in waves with yaw equal to zero. His method is further developed by Huang and Hsiung [5] who apply the flux differential splitting method to solve the non-linear three-dimensional problem describing water flow on deck. The forces and moments of water moving on deck are added to equations of ship motion.

Jankowski & Laskowski [6] present a method which takes into account the additional pressure acting on the change of water on the deck as well. This method is

based on the evaluation of Newton's momentum relations for a control mass volume over the deck (Buchner [7]).

The study presented in this paper shows modelling water motion on deck. 3D shallow water flow is used to model the flow.

2. The problem of shallow water flow

The flow of water on ship's deck is the dynamic displacement of shallow water which can be characterised by:

- small vertical velocity and negligible acceleration,
- negligible viscosity forces.

The problem is described in the OXYZ reference system fixed to the moving vessel deck. The OZ axis is perpendicular to the deck and is directed upwards. The system O'X'Y'Z' is an inertial system moving with constant forward speed. The gravity direction is downward vertical with g equal to 9.81 m/s^2 .

Velocity (u_x, u_y, u_z) describes the motion of water particles in relation to the system OXYZ (in relation to the deck):

$$\begin{aligned}\frac{dx}{dt}(x,y,z) &= u_x(x,y,z), \\ \frac{dy}{dt}(x,y,z) &= u_y(x,y,z), \quad (x,y,z) \in \Omega, \\ \frac{dz}{dt}(x,y,z) &= u_z(x,y,z),\end{aligned}\tag{1}$$

The phenomenon is described by the following 3D non-linear equation of water motion (Euler equation):

$$\begin{aligned}\frac{du_x}{dt}(x,y,z) &= f_x - \frac{1}{\rho} \frac{\partial p}{\partial x}(x,y,z), \\ \frac{du_y}{dt}(x,y,z) &= f_y - \frac{1}{\rho} \frac{\partial p}{\partial y}(x,y,z), \quad (x,y,z) \in \Omega, \\ \frac{du_z}{dt}(x,y,z) &= f_z - \frac{1}{\rho} \frac{\partial p}{\partial z}(x,y,z),\end{aligned}\tag{2}$$

where:

Ω is the changing in time domain occupied by water,

ρ is the water density,

$(du_x/dt, du_y/dt, du_z/dt)$ is the acceleration of water particles in OXYZ system,

p is the pressure in point (x, y, z) ,

(f_x, f_y, f_z) are the components of the resultant external force (gravity and generated by accelerated vessels) per unit mass.

For shallow water the change in time of vertical velocity u_z is small and it is assumed that:

$$\frac{du_z}{dt}(x, y, z) = 0. \quad (3)$$

The assumed dynamic condition is $p = p_a$ on free surface. Taking into account (2) and (3) the following formulas describe the scalar field of pressure in water on deck is obtained:

$$p(x, y, z) = p_a + \rho \int_{z_{\text{deck}} + h(x, y, z_{\text{deck}})}^z f_z(x, y, s) ds, \quad (4)$$

where:

$h(t, x, y, z_{\text{deck}})$ is the distance between deck in the point (x, y, z_{deck})
the point $(x, y, z_{\text{deck}} + h(t, x, y, z_{\text{deck}}))$ belongs to the free surface.

Additionally, it is assumed that horizontal velocities u_x and u_y do not depend on the vertical coordinate z : $u_x(x, y, z) = u_x(x, y)$, $u_y(x, y, z) = u_y(x, y)$. The equation determining the vertical velocity u_z is obtained from the principle of mass conservation:

$$u_z(x, y, z) = \left(-\frac{\partial u_x}{\partial x}(x, y) - \frac{\partial u_y}{\partial y}(x, y) + q \right) (z - z_{\text{deck}}), \quad (5)$$

where:

q represents the changes of water mass on deck.

The pressure field enables to determine the force \mathbf{F} and movement \mathbf{M} generated by moving water on deck:

$$\begin{aligned} \mathbf{F} &= -\int_S \mathbf{n} p ds, \\ \mathbf{M} &= -\int_S (\mathbf{n} \times \mathbf{R}) p ds, \end{aligned} \quad (6)$$

where:

S is the wetted part of surface of the deck and bulwark,

\mathbf{R} is the position vector of points belonging to S and \mathbf{n} is normal vector.

The problem is solved in the following steps which determine:

- the domain Ω occupied by water – Equations (1) determine the displacement of the free surface in each time step,
- the pressure field according to (4),
- the horizontal velocities u_x, u_y according to (2),
- the vertical velocity u_z according to (5),
- the force \mathbf{F} and moment \mathbf{M} generated by moving water and deck and acting on the vessel according to (6).

The solution of the shallow water problem is reduced to finding the position of the free surface and two components u_x and u_y of the velocity field, which determines the remaining parameters u_z and p (by Formulae (5) and (4)).

The solution of the shallow water problem is determined by the boundary conditions. The motion of water particles is bounded by the deck and bulwark. The water amount is changing in time (the value q changes in time) due to water inflow and outflow through openings and over the bulwark. In case of waves jumping on the deck and in case of submerging the bulwark, the appropriate velocity field of the wave on the boundary has to be given.

The Equations (1) are integrated using the Runge–Kutta method. The numerical grid approximating the free surface is determined for corresponding constant points $(x_i, y_i, z_{\text{deck}i})$ of the Euler net. The points of free surface $(x_i, y_i, z_{\text{deck}i} + h(t^n, x_i, y_i, z_{\text{deck}i}))$ are moved according to equation of water particles motion (1) or they are slipped on the deck or bulwark. The new point $(x_i, y_i, z_{\text{deck}i} + h(t^{n+1}, x_i, y_i))$ of free surface is determined by interpolation of function h for points of constant Euler net.

3. Results of calculations

The program simulating shallow water flow on the deck has been developed in PRS. The algorithm is based on equations presented above. The program simulates:

- the inflow and outflow of water on deck in rest,
- the flow of shallow water with constant mass in moving tank.

The simulation depends on such parameters as:

- the parameters of sea wave (height, period of oscillation, wave direction),
- the shape of the deck and bulwark, level of water on deck,
- the parameters of ship motion on sea waves.

In effect we obtain:

- the shape of free surface elevation,
- the velocity field of water particles,
- the pressure, forces and moments acting on the deck.

3.1. Deck moving with constant acceleration

To verify the method applied, the simulation of water motion on the rectangular deck, moving with constant acceleration $\mathbf{a} = (0 \text{ m/s}^2, 1 \text{ m/s}^2, 0 \text{ m/s}^2)$ has been carried

out. The result shows the flat free surface inclined at the angle 5.82° to the deck (Figure 1). The velocity field, responsible for the inclination of the free surface, appears during the simulation. After reaching the angle 5.82° the velocity field starts to disappear.

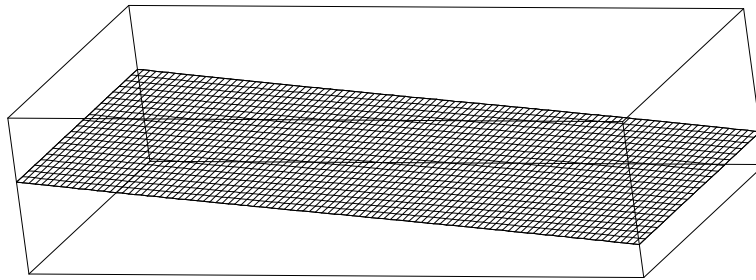


Fig. 1. The form of free surface of water on deck moving with constant acceleration $a_y = 1 \text{ m/s}^2$

3.2. Inflow of wave on deck in rest

The inflow of wave on deck at rest determines the boundary conditions. Numerical procedures were prepared describing this phenomena. Figure 2 and Figure 3 shows the regular wave affecting the water on deck.

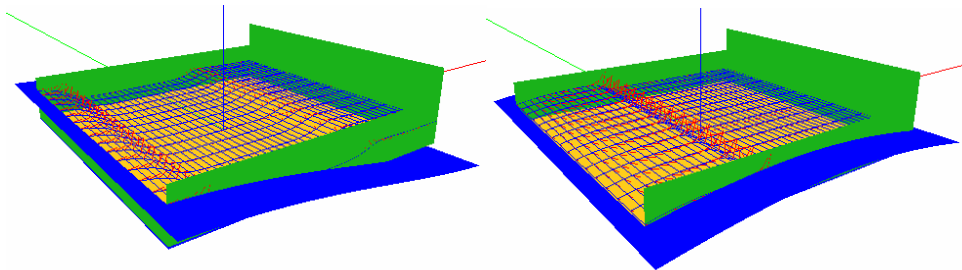


Fig. 2. The running wave inflowing on the deck at rest

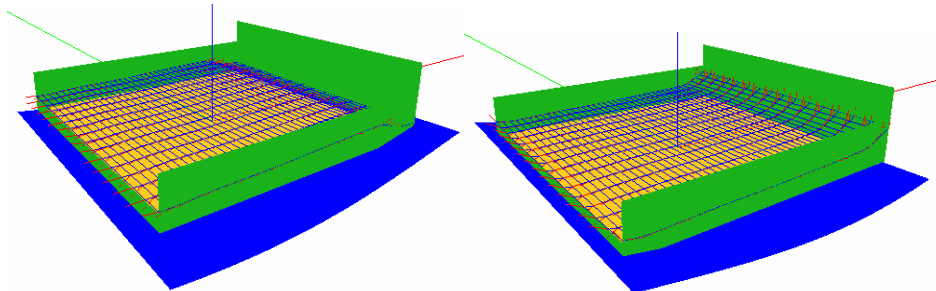


Fig. 3. The wave outflowing on the deck in rest

The height of sea wave is equal to 1 m and period of wave oscillation equals 6 s. The length of deck is equal to 20 m. The deck is on the level of the sea surface. The changing in time mass of water of deck, motion of water on deck and superposition of incoming and reflected wave can be observed.

3.3. Water motion on oscillating deck

The simulation of water motion on deck, moving with a harmonic acceleration has also been carried out and verified with numerical results obtained Huang Z.-J. and Hsiung C. [5]. Their results were experimentally verified by Adee and Caglayan.

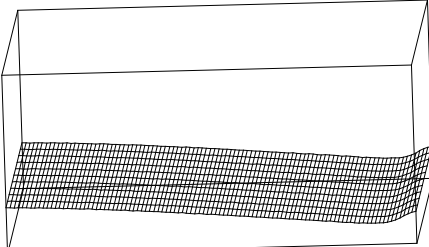
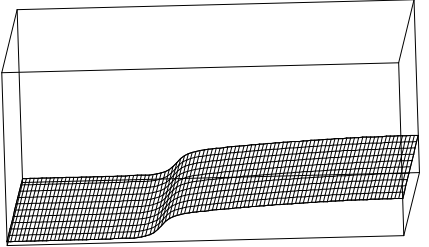
The original O of the reference system OXYZ is fixed in the geometric centre of the deck. The mass of water on the deck is constant. The parameters applied to make the simulation are given in Table 1.

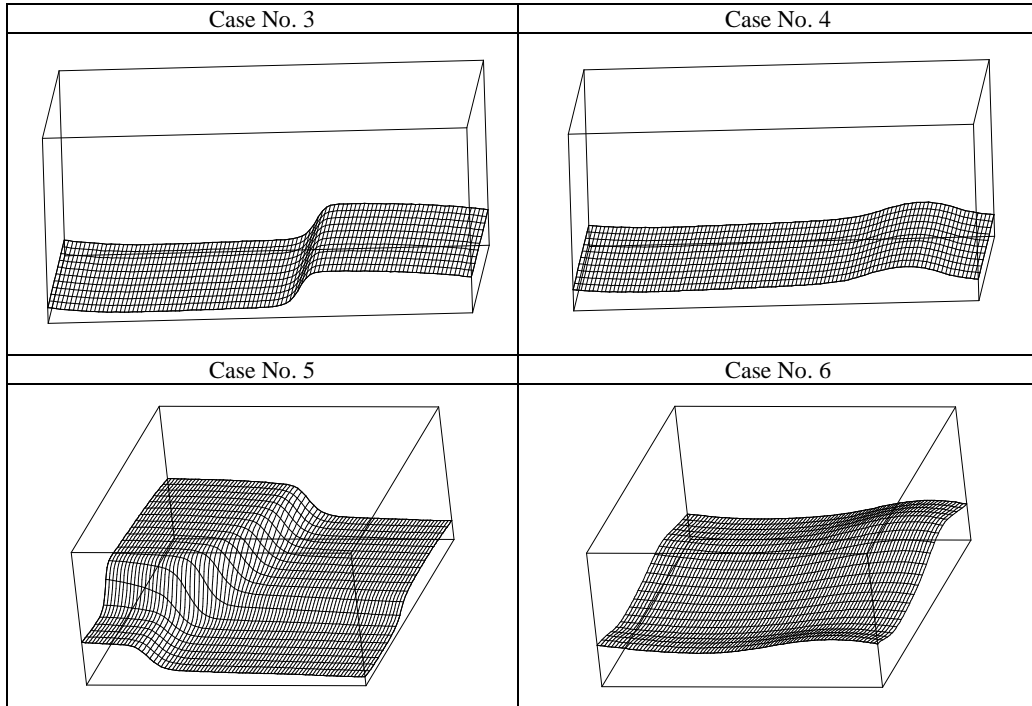
Table 1. Parameters of the simulation

	Length [m]	Wide [m]	Water depth [cm]	Frequency [rad/s]	Pitch amplitude [°]	Roll amplitude [°]
Case No. 1	1.0	0.91	7.62	1.57	–	9.5
Case No. 2	1.0	0.91	5.08	2.07	–	5
Case No. 3	1.0	0.91	5.08	3.644	–	7.5
Case No. 4	1.0	0.91	5.08	4.71	–	7.5
Case No. 5	1.0	0.8	10	4	5	5
Case No. 6	1.0	0.8	10	7.8	5	5

In Case 1, the frequency of the deck oscillation is close to one half of the first natural frequency. Case 2 corresponds to the first natural frequency, in Case 3 frequency of deck motion is equal to one and half of primary resonant frequency. In case 2 and 3 the bore can be clearly observed (see Table 2). In Case 4, the frequency is equal to second resonant frequency. This case presents the wave which is composed of two waves: coming and reflected. Case 5 and Case 6 represent the superposition of two waves generated by coupled sway and pitch excitation.

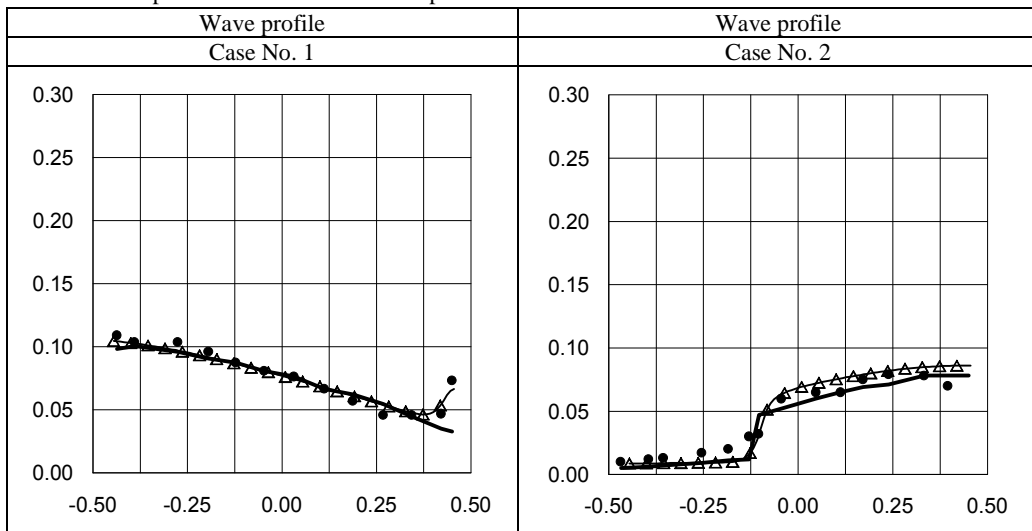
Table 2. Free surface deformation (corresponding to cases given in Table 1)

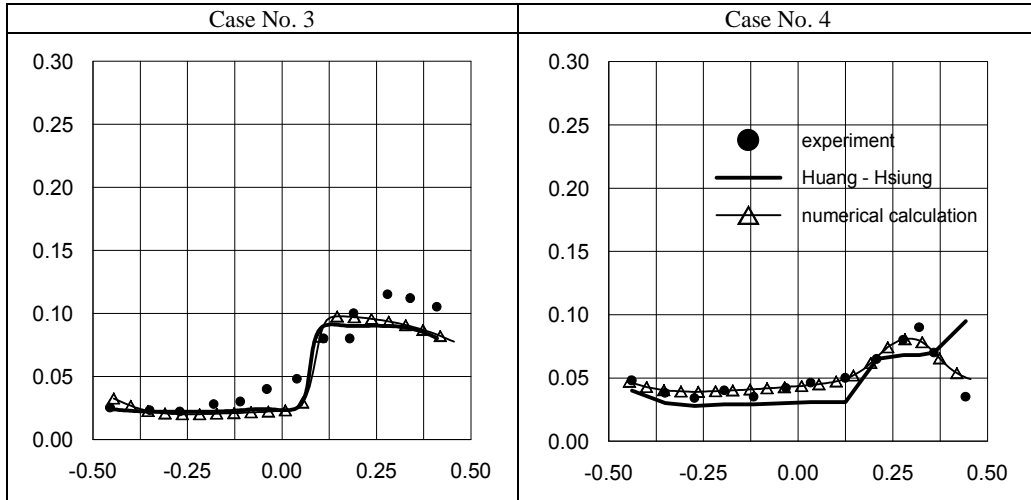
Free surface Case No. 1	Free surface Case No. 2
	



Verification of the presented results with those obtained in the experiment and from calculations by Huang and Hsiung [5] are presented in Table 3. The verification shows correctness of the model applied.

Table 3. Wave profile – verification with experiment and numerical calculations





The simulation enables visualisation of the velocity field changing in time. In case of progressive wave formation, the largest velocity values are created in the head of the wave (Figure 4 and Figure 5).

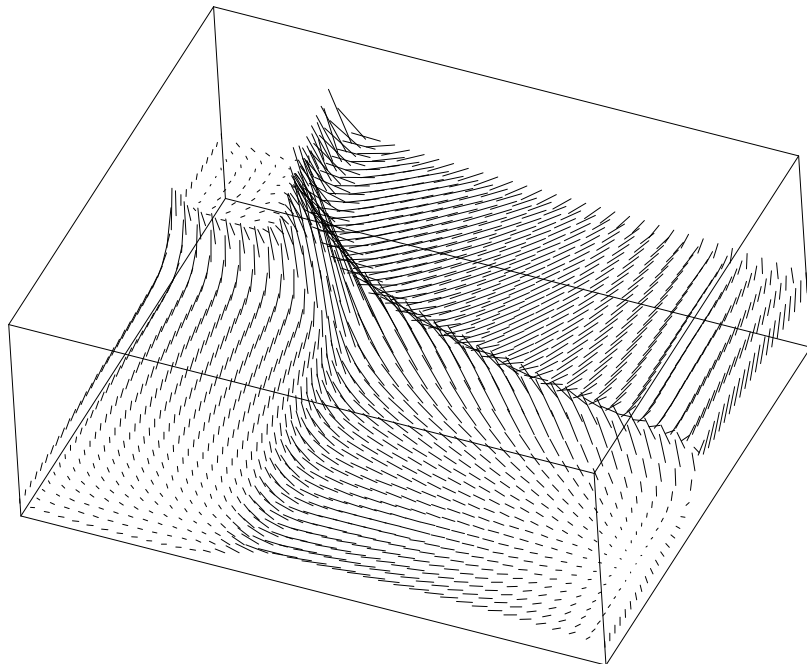


Fig. 4. The velocity field distribution, Case 5

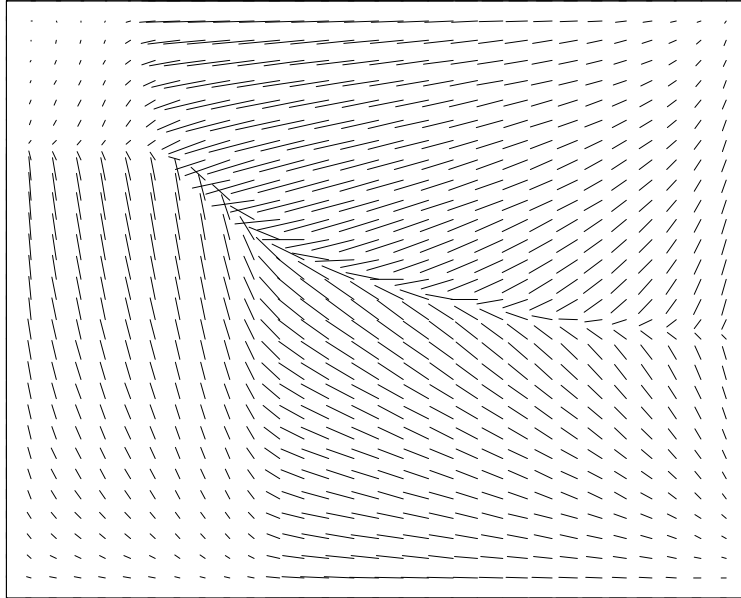


Fig. 5. The velocity field distribution, projection on the plane OXY, Case 5

4. Conclusions

Studies have been conducted on the possibility of approximating water motion on vessel deck by shallow water flow. The results obtained were successfully verified using results of experiment and numerical methods obtained by Huang and Hsiung [5]. The velocity field is determined correctly. The method applied model of the dynamics water motion on deck. The model also describes the bore phenomena. In the next step this model will be included in the algorithm and computer program simulating ship motion in waves with water trapped on deck (Jankowski & Laskowski [6]). This will be feasible after proper determination of velocity field of the water trapped on deck.

References

- [1] Belenky V., Luit D., Weems K., Shin Y.-S.: *Nonlinear ship roll simulation with water-on deck*, Proceedings of the 2002 Stability Workshop, Webb Institute, 2002.
- [2] Dillingham J.: *Motion studies of a vessel with water on deck*, Marine Technology, Vol. 18, No. 1, 1981.
- [3] Dillingham J.T., Falzarano J.M.: *Three-dimensional numerical simulation of green water on deck*, 3rd International Conference on the Stability of Ship and Ocean Vehicles, 1986.
- [4] Pantazopoulos M.S.: *Three-dimensional sloshing of water on deck*, Marine Technology, Vol. 25, No. 4, October, 1988.

- [5] Huang Z. J., Hsiung C. C.: *Nonlinear shallow-water flow on deck coupled with ship motion*, Proceedings of the Twenty – First Symposium of Naval Hydrodynamics, 1997.
- [6] Jankowski J., Laskowski A.: *Capsizing of small vessel due to waves and water trapped on deck*, Proceedings of the 9th International Conference STAB2006 – Stability of Ships and Ocean Vehicles, 2006.
- [7] Buchner B.: *Green water on ship type offshore structures*, PhD Thesis, Delft University of Technology, 2002.

Zagadnienie ruchu wody na pokładzie

Statek poruszający się na fali narażony jest na obciążenia wynikające ze zjawiska wdarcia sfałowanej wody na pokład. W Polskim Rejestrze Statków, w zakresie prac nad poprawą bezpieczeństwa małych jednostek, prowadzone są prace badawcze, mające na celu opisanie tego zjawiska. Praca ma stanowić uzupełnienie opracowanych wcześniej symulacji ruchu statków rybackich na fali nieregularnej o elementy ruchu cieczy na pokładzie statku z uwzględnieniem odkształcalnej swobodnej powierzchni. Artykuł przedstawia metodę ruchu wody płytkiej zastosowanej do opisu zagadnienia ruchu wody na pokładzie statku. Zaprezentowana została weryfikacja wyników z eksperymentem i wynikami obliczeń numerycznych.



Tribological consequences of rubber composition and structure – case studies

D. M. BIELIŃSKI

Institute of Polymer & Dye Technology, Technical University of Łódź, ul. Stefanowskiego 12/15,
90-924 Łódź

Rubber Research Institute “STOMIL”, ul. Harcerska 30, 05-820 Piastów

The paper discusses characteristic features of the structure of elastomers and the composition of rubber. Special attention has been paid to differences in structural organization between polymers and metals. Actually existing, mechanistic theory on the friction of elastomers, together with all its drawbacks has been demonstrated. Based on it, another approach to the interpretation of friction phenomenon – from the point of view of material engineering, has been presented on some examples of our own work. The influence of: 1. composition and structure of macromolecules 2. crosslink density and the composition of crosslink constituting a 3-D network, 3. filler loading, the degree of agglomeration and distribution of its particles, as well as 4. the surface migration of low molecular components of rubber mix and segregation in polymer blends, on the friction and wear of vulcanizates have been discussed.

Keywords: *elastomer, rubber, composition, structure, crosslink, filler, surface migration and segregation, friction*

1. Introduction

1.1. Characteristics of rubber

Polymers, contrary to metals, exhibit molecular organization, what means that instead of an atom, the basic structural unit is a macromolecule. It manifests itself by the specific behaviour of polymers under stress, which is additionally temperature dependent – Figure 1 [1].

Below glass transition temperature (T_g) the free rotation of macromolecules, even their fragments (backbone fragments or side chains) is blocked (“frozen”), so polymers behave like metals, obeying the Hooke’s law. However, above T_g , the “mobility” of macromolecular chains is released and becomes to be limited only by intermolecular interactions, what results in unique, elasto-plastic characteristics of the material [2], which can be described by the equation of high elasticity. In the case of elastomers, which macromolecules are very flexible, it allows for relative elastic deformations exceeding even 1000 %. Further increase of temperature makes eventually these interactions diminished, allowing – above melting temperature (T_m), for totally unlimited free movements of macromolecules, what manifests itself by the flow of material, which can be described by the Newton’s law. From the engineering point of view a “window” between T_g and T_m determines conditions for polymer processing and defines frames for their exploitation.

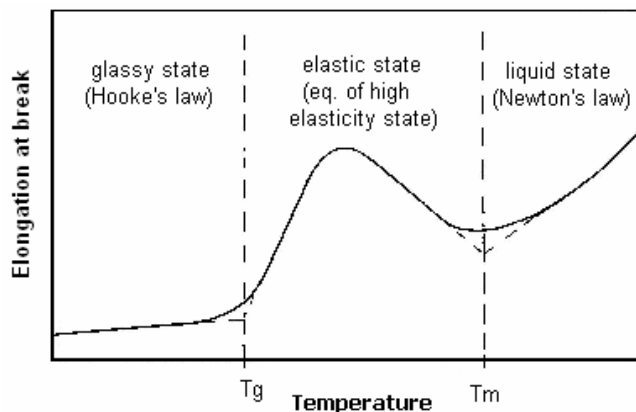


Fig. 1. Mechanical characteristics of rubber in the field of temperature [1]

In order to increase mechanical properties of elastomers, as well as to improve their thermal and chemical stability, they have to be crosslinked [3]. Crosslinking is realized by production of intermolecular chemical links. Properties of materials depend on the density of crosslinking, their length and chemical composition. Generally, short C–C bonds make the material stiffer and more thermally resistant, whereas longer S_x links improve its dumping properties and mechanical strength. Apart these two basic groups, there are also a lot of other kinds of specific and unconventional crosslinks.

Very often, again especially in the case of elastomers, even the crosslinking of their macromolecules is not able to meet requirements for mechanical strength. They have to be accomplished filling an elastomer matrix with a solid phase [4]. The preparation of new composite material depends on the kind of filler, being usually characterized by following factors:

- its chemical compatibility with an elastomer matrix,
- the value of specific surface area,
- the degree of agglomeration, and
- the homogeneity of distribution in an elastomer.

The first two factors determine the so-called filler activity, whereas the last two ones are dependent on the quality of mix preparation. The most common fillers used by the rubber industry are carbon black (CB) and silica.

To improve mixing conditions and further processing of rubber mix, apart an elastomer and fillers, it also contains: softeners, processing agents, compatibilizers (adhesion promoters, e.g. silanes) and other ingredients, such as: pigments, ageing protectors (antioxidants and antiozonants) or flame retardants. They are usually low molecular weight substances, influencing the system morphology.

Finally, it can be summarized that rubber is a multicomponent and a multiphase composite material, which morphology is of a key importance to tribological characteristics of the material.

1.2. Friction of rubber

Very first works on mechanisms of rubber friction were published by Shallamach in the late fifties [5]. He proposed deformational model, describing the phenomenon as the propagation of deformations in a material – called “Schallamach’s waves” – Figure 2.

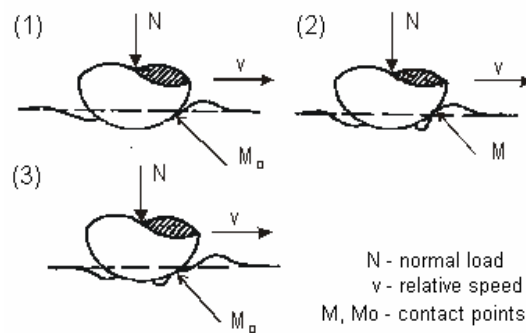


Fig. 2. The mechanisms of Schallamach’s waves propagation in rubber [5]

Despite a lot of experimental work being performed, a satisfactory explanation on the origin of Schallamach’s waves has not been presented so far [6]. However, attempts have been mainly undertaken from the mechanistic point of view, putting less attention to polymer engineering [7]. Nevertheless, some factors influencing the propagation of deformational waves, have been defined and namely: adhesion and the contact geometry of a friction pair, rubber elasticity, sliding speed, normal load and temperature. The critical value of sliding speed required for waves formation decreases with the decrease of normal load, roughness and temperature. Friction force discontinues – after an initial increase up to a maximum value, when being in an adhesive contact (“stick”) with a counterface, the sample slips, what results in the dramatic decrease of a friction force. The situation called “stick-slip” repeats, producing a typical only for this mechanism “saw-like” friction force characteristics. However, the mechanism is valid only for soft (usually unfilled), low loaded elastomers.

From the practical point of view, the friction of rubber has been well described by Moore [8], who proposed to divide a friction force into two components: deformational (hysteretical) and adhesional. It is commonly accepted, that adhesion plays a major role in the friction of materials exhibiting high elasticity, sliding with a low speed over a smooth surface under limited load [9]. Such conditions facilitate the “stick-slip” mechanism of friction. The hysteresis component of friction appears when an elastomer sliding over a rough surface is subjected to deformations, trying to keep contact with it [10]. Despite a fact, that some quantitative relationships between the strength and hysteresis of rubber have already been elaborated by Payne [11], the explanation on its “response” to dynamic loading still remains unsatisfactory [12].

This work is aimed at the description of a role played by rubber morphology in friction. The influence of macromolecular composition and structure, crosslink density and composition, filler loading, its agglomeration and distribution, as well as the surface segregation in polymer blends and blooming of low molecular weight components in rubber, are discussed in terms of their influence on adhesional and deformational components of friction. This knowledge creates a base for tailoring the properties of rubber to dedicated tribological applications.

2. Results and discussion

2.1. Macromolecular composition and structure

The replacement of side methyl groups with chlorine atoms results in significant changes to the friction of elastomers. Chlorine atoms present in a backbone make it stronger and stiffer, what is reflected by the lower coefficient of friction of chloroprene (CR) in comparison to isoprene rubber (IR) of similar crosslink density. However, for poly(vinyl chloride) elastomer, less substituted by chlorine, the influence of adhesion together with the additional plastification of polymer, make its coefficient of friction the highest among the polymers studied – Figure 3. Apart stiffness, also the ability of macromolecules to dumping external stresses imposed on elastomers is important, what is clearly visible when natural rubber (NR) is compared to vulcanizates of its synthetic analogue, polyisoprene – Figure 3. The former dissipates the energy of deformations easily, whereas the latter is slightly more prone to its accumulation. The difference however becomes significant for higher loading, when the elasticity of macromolecules is able to manifest itself. NR is much more abrasion resistant than IR, what comes from the higher tear strength (TES) of natural rubber vulcanizates. High loaded isoprene rubber vulcanizates wear extensively, but the roller shape debris make the coefficient of friction decreased due to a change in the mechanism of friction from sliding to rolling.

Copolymerization of polybutadiene (BR) with other monomers like styrene (SBR) or acrylonitrile (NBR) also results in lowering of the coefficient of friction. Again limitation to the free rotation of macromolecules, either by a bulky side group – for the former, or introduction of a stiff segment to the backbone – for the latter, prevails over the increase of polymer polarity (NBR).

The same explanation is valid for the lower coefficient of friction for block copolymers, being able to crystallization, in comparison to these of a random structure (conventional elastomers) – Figure 4. This fact indicates on a tribological potential for thermoplastic elastomers (TPE), e.g. styrene-butadiene-styrene (SBS) or block EPDM.

The configuration of macromolecules also plays a role in the friction of elastomers. Isomers “trans” make a chain stiffer than “cis” ones, what results in the lower coefficient of friction for the former. The difference is clearly visible for the stereoisomers: cis- and trans-polyisoprene (gutta-percha) – Figure 5. Similarly to trans-1,4-polyisoprene, trans-1,4- and 1,2-polybutadiene are plastics under normal conditions, of sig-

nificantly lower the coefficient of friction in comparison to BR – Figure 5. Regioselectivity, similarly to a chain conformation does not seem to be important from this point of view, due to the limited range of changes affecting coiled macromolecules. Another structural factor affecting mechanical and tribological properties of polymers is their tacticity. However, it is less important for elastomers, usually being atactic. Isotactic or syndiotactic distribution of side groups makes macromolecules stiffer. The stereoregularity of macromolecules is a prerequisite condition for a polymer to crystallization, however very seldom taking place in the case of elastomers.

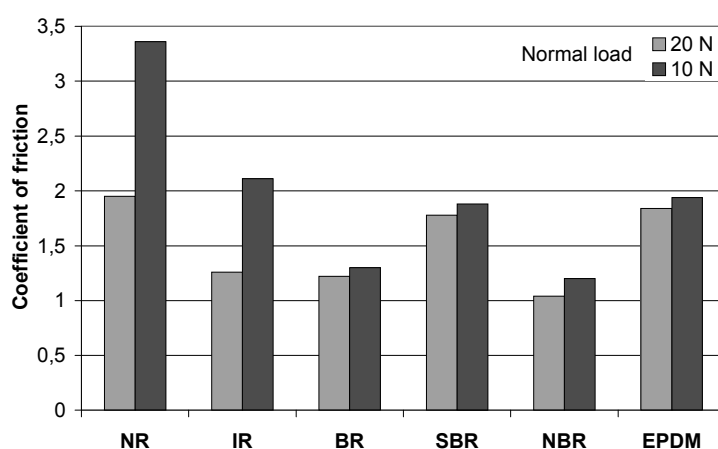


Fig. 3. Comparison between the coefficient of friction for some elastomers studied – the influence of macromolecular composition

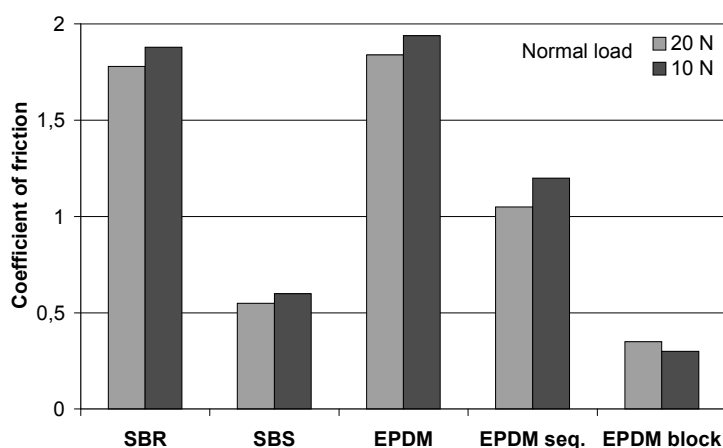


Fig. 4. Comparison between the coefficient of friction for some elastomers studied – the influence of copolymer composition and structure

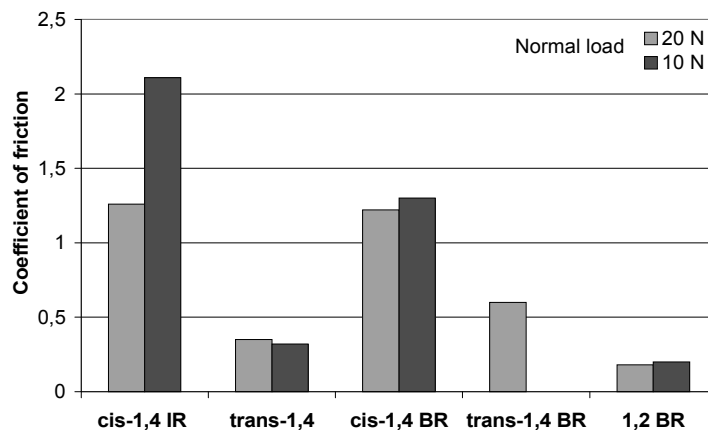


Fig. 5. Comparison between the coefficient of friction for some elastomers studied – the influence of macromolecular configuration

2.2. Density and composition of crosslinks

Crosslinks limit the possibility of macromolecules to free rotation. The value of molecular weight (M_w) between network nodes decides physical properties of elastomers [13]. The higher the degree of crosslinking the harder the material, eventually – for links being present every monomer unit, converting from an elastomer to a resin form, eg. ebonite. An influence of the degree of crosslinking on the friction of peroxide vulcanizates and γ -irradiated IR is presented in Figure 6. The coefficient of friction increases within the range of peroxide vulcanizates studied, whereas in the case of γ -cured samples one can see the optimum dose of radiation. The exceeding of 100–120 kGy results in the extensive degradation of rubber.

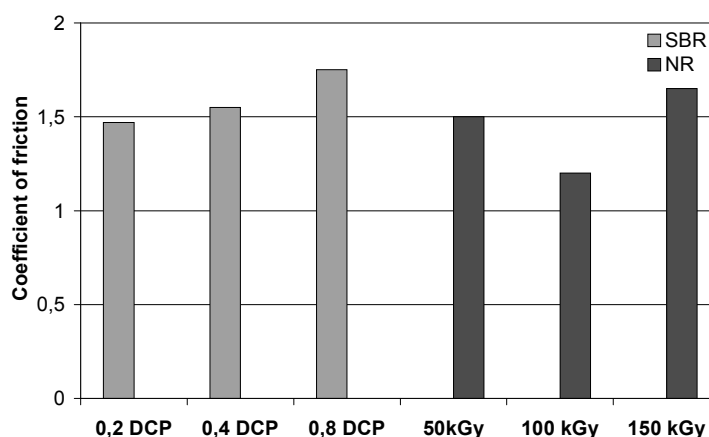


Fig. 6. Comparison between the coefficient of friction for peroxide SBR vulcanizates and radiation crosslinked NR rubber – the influence of crosslinks density

Apart density, also the composition of crosslinks influences properties of rubber vulcanizates. From Figure 7 one can see the influence of crosslinks sulphidity on friction.

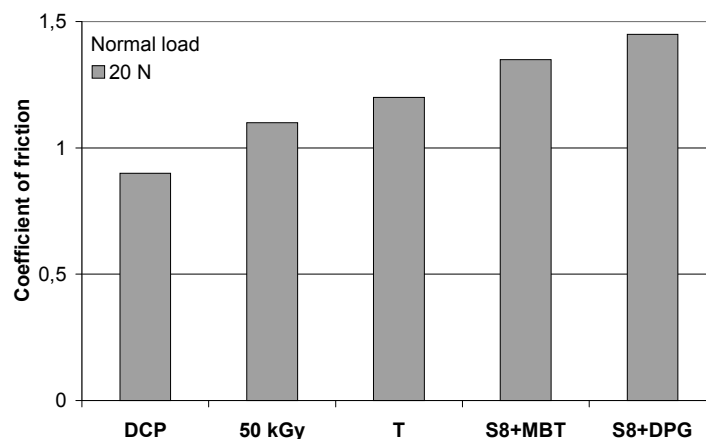


Fig. 7. Comparison between the coefficient of friction for IR vulcanizates – the influence of crosslinks sulphidity

According to expectations, IR vulcanizates of the highest content of polysulphide crosslinks ($S_8 + \text{DPG}$), characterizing themselves by the highest polarity and the highest hysteresis of material, exhibit the highest coefficient of friction. Despite high friction the abrasion resistance of sulphur vulcanizates is higher in comparison to peroxide or γ -crosslinked ones, what decides their common engineering application. Material engineering of rubber makes possible designing of crosslinks, what in turn enables tailoring tribological properties of the material.

Due to the low heat conductivity of elastomers, the conditions of vulcanization in the surface layer and in the bulk of material are different, what results in the surface gradient of hardness. The creation of a hard “skin” on an elastic substrate has been explained by a phenomenon called “maturing of network”, consist in the breaking of long polysulphide crosslinks with the creation of higher amount of mono- and disulphide ones [14]. In the matter of fact it leads to higher crosslinks density, what is reflected by higher hardness. The gradient character of rubber, being negligible for its macro-scale properties, manifests itself when tribological experiments are carried out in the micro-scale [15].

2.3. Filler loading, agglomeration and distribution

Generally, despite the activity of fillers, their addition makes rubber stiffer what results in the reduction of friction. However, contrary to plastics, admixing of solid lubricants like MoS_2 or graphite is much less effective due to the simultaneous plastifi-

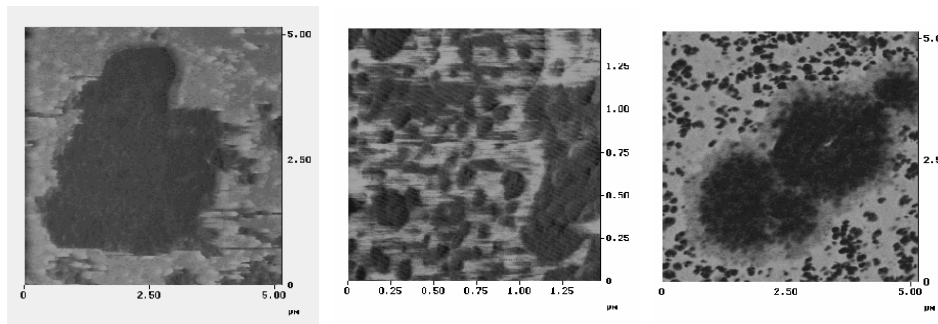
cation of rubber taking place, reflected by the significant increase of the deformational component of friction [16].

Active fillers, like silica or carbon black (CB) are the most effective ingredients in terms of mechanical and tribological properties of rubber. Their effectiveness depends on the following factors [17]:

- an amount being incorporated into rubber matrix (a curve with an optimum),
- interactions with rubber (measured by the amount of macromolecules immobilized onto the particles of solid phase – the so-called “bound rubber”, BdR),
- the degree of agglomeration (the number of filler clusters of dimensions exceeding 20 μm , given by the value of the so-called “dispersion index”, DI), and
- the quality of distribution in rubber matrix (characterized by the homogeneity of a rubber mix composition).

Apart the first relation, which seems obvious, the rest ones are more complicated. The tribological properties of rubber do depend on its morphology, but deciding factors are difficult to quantify. For example the amount of bound rubber (BdR), despite the same amount, can be of various origin, as visualized by AFM pictures presented below – Figure 8.

A) carbon black mixes



B) silica mixes

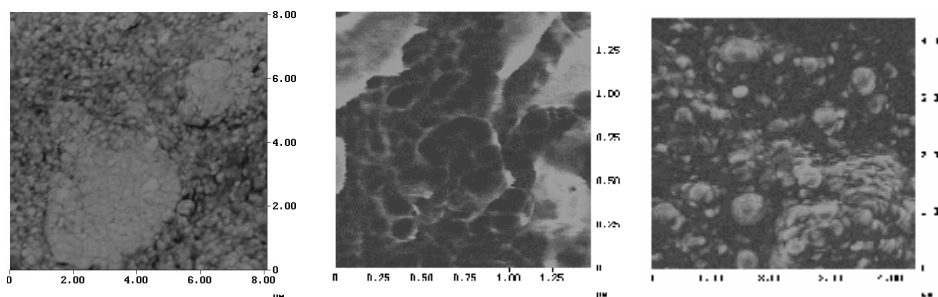


Fig. 8. Examples of the internal structures of filler agglomerates in rubber

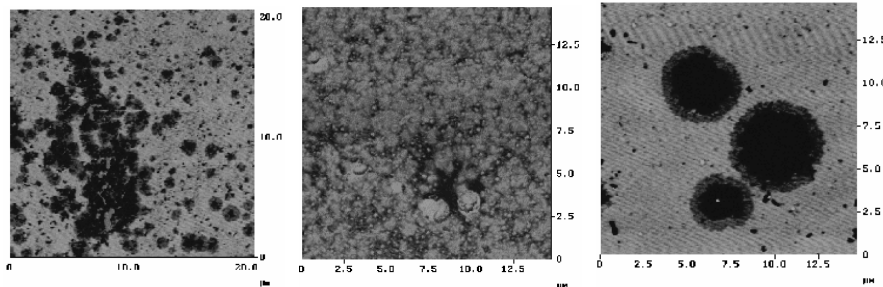
BdR is present inside or outside filler agglomerates. The interphase layer (darker in colour in comparison to the light matrix) is thicker or thinner, as well as stiffer (similar in colour to filler particles) or softer (closer to the colour of rubber matrix), what all influence the hysteresis of rubber – important in terms of friction, and its tear strength – deciding friction and abrasion resistance of material.

From our recent works it follows, that traditional approach to the quantification of filler agglomeration is inaccurate. The internal morphology of filler agglomerates is more important in terms of the mechanical and tribological properties of rubber than the contribution of “big” agglomerates, given by DI values [18, 19]. The presence of so-called “fatal” agglomerate of weak internal interactions, makes the process of rubber deterioration started.

Apart an agglomeration, also the ability of filler particles to create their own network, being responsible for the hysteresis of material, is also important. It creates a big difference between silica and carbon black filled vulcanizates, as determined by AFM – Figure 9.

There are different kinds of carbon black, varying according to networking ability, which is called “structural ability”. The more active the lower the structure of carbon black. However, all this is incomparable to silica, for which the strength of interparticle interactions has to be reduced in order to prevent rubber from overheating, being produced by internal deformations of the filler network during friction. This is the main reason why not silica but carbon black is commonly used by tyre manufacturers.

A) carbon black mixes



B) silica mixes

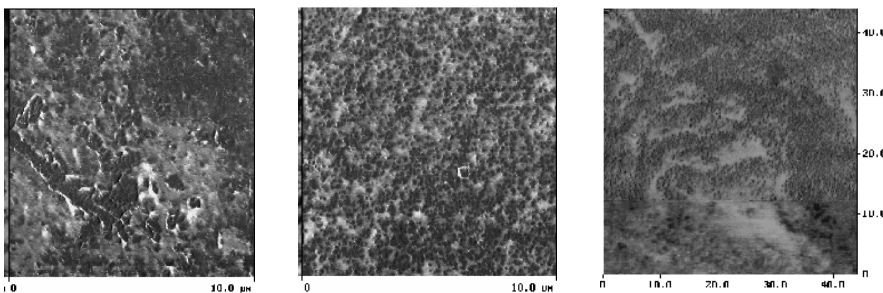


Fig. 9. Examples of filler networking in rubber

2.4. Surface segregation and blooming

The blooming of low molecular weight components of rubber is well known in rubber industry. Some of them can create a lubricating layer on the surface, eg. micro-crystalline paraffin waxes, whereas the others plastify the surface layer, what results in an increase of the coefficient of friction, e.g. silicone oils. During the vulcanization of rubber, chemical reactions taking place between the components of a curing system produce substances which can play the role of lubricant, eg. zinc stearate. Some examples of blooms, being created on the surface of rubber, are presented by AFM pictures – Figure 10.

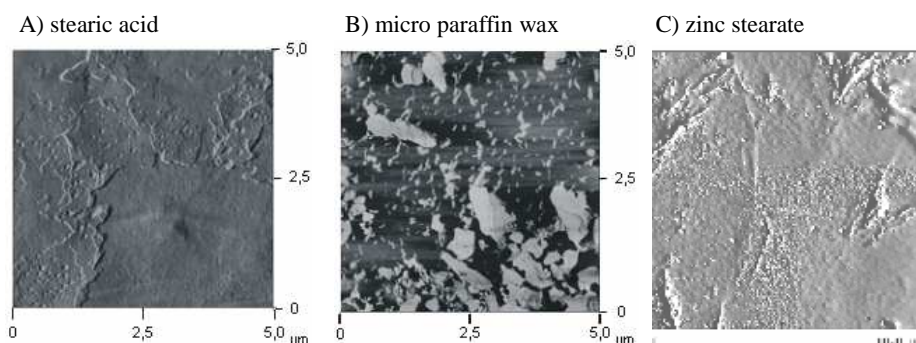


Fig. 10. Examples of the blooms of low molecular weight substances on the surface of rubber

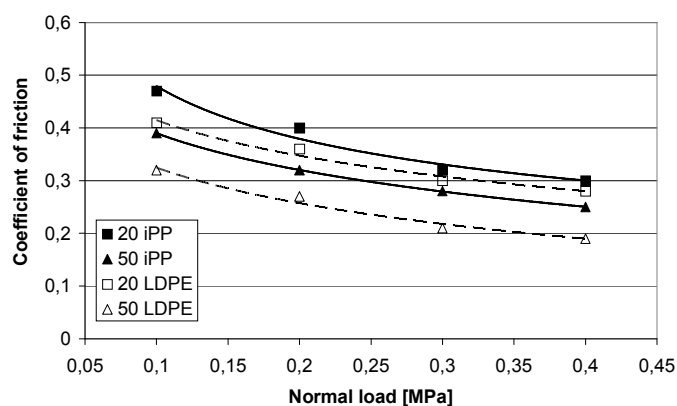


Fig. 11. The influence of polyolefine addition on the coefficient of friction of their blends with EPDM. A) PE-LD/EPDM, B) iPP/EPDM (figures in the legend inform on the amount of plastomer added in phr)

However, the surface migration is not only limited to low molecular weight substances, but has also been confirmed for polymer blends. The surface layer of ethylene-propylene-diene rubber filled with low density polyethylene (PE-LD/EPDM) was

found to be enriched with the low molecular weight fraction of polyethylene, as suggested by the surface-sensitive infrared spectroscopy analysis (FTIR) [20]. Segregated oligomer fraction plays the role of some kind of lubricant, lowering the coefficient of friction of EPDM more effectively than the addition of higher modulus iPP – Figure 11.

The data presented points on the possibility of tailoring tribological properties and processing of elastomers by their blending with plastomers, taking an advantage of the surface segregation phenomenon. The driving force for migration originates either from the difference in the solubility parameters between components or their crystallization ability [21]. The appropriate choice of these factors makes possible to play with the extent of the surface segregation in polymer blends.

3. Summary and conclusions

Rubber, contrary to other polymer materials, is usually a multicomponent and a multiphase system. This is why its tribological properties are difficult to be modelled only from the mechanical point of view. An approach from the side of material engineering seems to be more accurate. Presented differences in molecular organization and structure, composition of crosslinks and morphology of rubber, makes possible to explain its friction and wear more deeply. Undoubtedly, any dedicated progress in the modification of tribological properties of rubber cannot be achieved without the careful analysis of the material.

References

- [1] Cowie J.M.G.: *Polymers: Chemistry and physics of modern materials*, 2nd Ed., J. Wiley & Sons, Chichester (UK), 1994.
- [2] Fischer-Cripps A.C.: *Mater. Sci. Eng. A*, Vol. 385, 2004, pp. 74.
- [3] Dogadkin B.A.: *Chemistry of elastomers*, WNT, Warsaw, 1974.
- [4] Praca zb. pod red. Gaczyński R.: *Rubber. Handbook for engineers and technicians*, WNT, Warsaw, 1985.
- [5] Schallamach A.: *Wear*, Vol. 17, 1971, pp. 301.
- [6] Bieliński D.M.: *Structure of the surface layer and friction of elastomers*, Scientific Bulletin of the Technical University of Łódź, Vol. 882, Łódź, 2001.
- [7] Moore D.F.: *The friction and lubrication of elastomers*, Pergamon Press, Oxford-NY-Toronto-Sydney-Braunschweig, 1972.
- [8] Barnard D., Baker C.S.L., Wallace I.R.: *Rubber Chem. Technol.*, Vol. 58, 1985, pp. 740.
- [9] Barquins M.: *Wear*, Vol. 158, 1992, pp. 87.
- [10] Moore D.F., Geyer W.: *Wear*, Vol. 30, 1974, pp. 1.
- [11] Frakley P.K., Payne A.R.: *Theory and practice of engineering with rubber*, Applied Science, London, 1978.
- [12] Zhang S.W.: *Tribol. Int.*, Vol. 31, 1998, pp. 49.
- [13] Ślusarski L.: *Kautsch. Gummi Kunstst.*, Vol. 45, 1992, pp. 705.

- [14] Boochathum P., Prajudtake W.: *Eur. Polym. J.*, Vol. 37, 2001, pp. 417.
- [15] Bieliński D.M.: *Polimery*, Vol. 46, 2001, pp. 684.
- [16] Bieliński D.M., Janczak K.J., Ślusarski L., Loden A.: *Wear*, Vol. 169, 1993, pp. 257.
- [17] Bieliński D.M., Głąb P., Dobrowolski O., Ślusarski L.: *Elastomery*, Vol. 9, 2005, pp. 42.
- [18] Bieliński D.M., Ślusarski L., Dobrowolski O., Głąb P., Dryzek E.: *Kautsch. Gummi Kunstst.*, Vol. 57, 2004, pp. 579.
- [19] Bieliński D.M., Dobrowolski O., Głąb P., Ślusarski L.: *Kautsch. Gummi Kunstst.*, Vol. 58, 2005, pp. 239.
- [20] Bieliński D.M., Ślusarski L., Włochowicz A., Douillard A.: *Composite Interf.*, Vol. 5, 1997, pp. 155.
- [21] Bieliński D.M., Ślusarski L., Boiteux G., Parasiewicz W.: *Proc. of the 38th World Polymer Congress IUPAC Macro*, Warsaw, 07.2000, pp. 1175.

Tribologiczne następstwa budowy i struktury gumy – wybrane przykłady

W pracy omówiono charakterystyczne cechy budowy elastomerów i gumy. Zwrócono uwagę na różnice w organizacji strukturalnej pomiędzy polimerami a metalami. Przedstawiono, obowiązującą obecnie, mechanistyczną teorię tarcia elastomerów z wszelkimi jej niedostatkami, prezentując – na wybranych przykładach prac własnych, podejście do interpretacji zjawisk tribologicznych od strony inżynierii materiałowej.

Omówiono wpływ:

1. budowy i struktury makrocząsteczek,
2. gęstości usieciowania i budowy węzłów sieci przestrzennej,
3. stopnia napełnienia, aglomeracji i dystrybucji napełniacza, oraz
4. zjawisk migracji powierzchniowej małych cząsteczkowych składników mieszanki gumowej i segregacji w mieszaninach polimerowych, na tarcie i zużycie cierne wulkanizatów.



Nonlinear time domain analysis of vertical ship motions

D. BRUZZONE, A. GRASSO

Department of Naval Architecture and Marine Technology, University of Genoa, Italy

A nonlinear time domain seakeeping analysis has been performed for ships advancing in head seas with regular waves. A hybrid approach has been employed, solving the unsteady hydrodynamic problem in the frequency domain and the equations of motion in the time domain. This procedure transfers radiation and diffraction forces, supposed linear, from frequency to time domain, where nonlinear Froude-Krylov and hydrostatic forces are computed considering the actual hull wetted surface at each time step. In a first test case, a monohull, both a strip theory and a three-dimensional Rankine panel method have been used for the frequency domain analysis, while for another test case, a trimaran, only the three-dimensional methodology has been applied. A comparison of the results shows a good agreement with experimental data and the hybrid approach appears to be actually independent of the technique used in the frequency domain, even if the reliability of the results is strongly related with the accuracy of the evaluation of the hydrodynamic terms.

Keywords: *nonlinear motions, time domain, seakeeping*

1. Introduction

Linear strip theory, due to its simplicity and to the minimal computational effort required, is still the most employed model used for the prediction of ship responses in an incident wave field. Also several linear three-dimensional models have been developed in order, particularly, to better take into account problems related to high speed and to the complex free surface flow pattern between the hulls of multi-hull vessels. Several researchers have focused their studies on methodologies capable of including nonlinear effects in the solution of the seakeeping problems, as the interest for motions and loads in heavy weather, when nonlinear effects become no more negligible, is remarkably increased in the years.

Even if small perturbation methods may be applied in the frequency domain, allowing to represent weak nonlinearity under the hypothesis of small amplitude motions and waves, frequency domain formulations are unsuitable to predict the behavior of the ship response when linear hypotheses turn out to be no more correct.

Different time domain formulations have been proposed in literature in order to include nonlinear effects in the solution of the problem, both in two and in three dimensional approaches. Some of them combine linear with non linear terms, others apply fully nonlinear potential flow methods. Studies have also been carried out in order to treat the viscous flow seakeeping problem, solving the Reynold averaged Navier-Stokes equations in the time domain (called unsteady RANS). An extensive bibliography can be found in literature, but a comprehensive classification and review is given in [1].

Hybrid approaches (also called “blending methods”) have been examined because of the problems associated with fully non linear computations. These methods allow to introduce nonlinearities in the linear model, evaluating hydrostatic and Froude-Krylov forces, which are in fact easy to compute in time domain in their intrinsic nonlinear form, by pressure integration over the instantaneous wetted surface. Hybrid approaches are used because they are fast and provide results with engineering accuracy, allowing long time simulations and couplings with other design issues.

In this paper, a nonlinear time domain analysis based on the foregoing approach has been performed for two test cases, a destroyer vessel and a trimaran. In the first case, radiation and diffraction forces have been computed applying both a strip theory and a three-dimensional Rankine panel method, in order to assess the influence of the linear frequency domain analysis on the nonlinear time domain simulations.

2. Mathematical model

The hybrid approach to the prediction of ship responses in time domain is divided into two steps: the frequency domain and the time domain analysis. The first step allows to evaluate the radiation and the diffraction forces, solving the unsteady hydrodynamic problem for a given number of meaningful arbitrary frequencies. The latter solves the equations of motion in time domain, gauging at each time step Froude-Krylov and hydrostatic forces by integration of the hydrostatic pressure over the actual hull wetted surface under the incident wave profile. Implicitly, this methodology assumes that nonlinear contributions related to radiation and diffraction forces are small compared with those related to Froude-Krylov and hydrostatic forces. Hence the firsts are supposed linear, while the latter are evaluated fully nonlinear.

Since added mass and damping are frequency dependent whereas ship motions are directly evaluated into the time domain and nonlinear effects are included, impulse theory is applied in order to transfer the radiation forces from frequency domain to time domain [2].

2.1. Frequency domain analysis

The strip theory code employed for the simulations proposed in this paper is a public domain open source program which applies, for the prediction of motions, a method developed by Söding [3]. The mathematical model underlying the code will not be covered, referring to [4] for a comprehensive treatment of the subject.

A short description of the three dimensional Rankine panel method follows; more details, however, can be found in [5].

Let define a right handed orthogonal coordinate system (x, y, z) advancing at the vessel speed U maintaining the xy plane coincident with the undisturbed free surface. X is the symmetry axis of the still waterplane and is assumed positive astern. The z -axis is positive upwards. Ship motions are defined by the instantaneous position of

a body fixed reference system with respect to the previous system, that may be described by a vector $\eta_k(t)$, with $k = 1, \dots, 6$. Under the hypothesis of small amplitude motions, $\eta_k(t)$ can be assess solving the following differential equations system:

$$\sum_{k=1}^6 (M_{jk} + A_{jk}) \ddot{\eta}_k + B_{jk} \dot{\eta}_k + C_{jk} \eta_k = F_j(t). \quad (1)$$

Assuming incompressible and inviscid fluid and irrotational flow, the hydrodynamic problems related to the determination of the added mass and damping coefficients (A_{jk} and B_{jk}) and of the exciting forces $F_j(t)$ may be solved applying the potential theory.

Assuming a total velocity potential Φ , which satisfies the Laplace equation in the fluid domain Ω :

$$\Delta \Phi = 0 \text{ in } \Omega. \quad (2)$$

The boundary conditions are imposed over the linearised boundaries $\partial\Omega$. Denoting with \vec{V}_B the velocity of a point on the hull wetted surface and with \vec{n} its outward normal vector, the boundary condition on the hull surface S_H is:

$$\frac{\partial \Phi}{\partial \vec{n}} = \vec{V}_B \cdot \vec{n} \text{ on } S_H \quad (3)$$

Over the free surface the kinematic and dynamic conditions are imposed, obtaining:

$$\frac{\partial^2 \Phi}{\partial t^2} + 2\nabla \Phi \cdot \nabla \left(\frac{\partial \Phi}{\partial t} \right) + \frac{1}{2} \nabla \Phi \cdot \nabla (\nabla \Phi \cdot \nabla \Phi) + g \frac{\partial \Phi}{\partial z} = 0 \text{ on } z = 0 \quad (4)$$

Finally, a radiation condition at infinity must be enforced to ensure the uniqueness of the solution.

The total potential Φ may be expressed as the sum of the potential of a steady base flow Φ_S and of a small unsteady perturbation potential Φ_{US} .

$$\Phi = \Phi_S + \Phi_{US}. \quad (5)$$

The unsteady perturbation potential may be written as superposition of an incident wave potential ϕ_I , a diffraction potential ϕ_D and six radiation potentials:

$$\Phi_{US} = \phi_I + \phi_D + \sum_{k=1}^6 \phi_k. \quad (6)$$

Considering that the incident wave potential can be expressed in analytical form, the decomposition of the unsteady potential enables to study the total boundary value problem solving a set of six radiation problems and a diffraction problem.

By using a Rankine source distribution $\sigma(Q)$ each potential in (6) may be expressed as:

$$\phi(P) = \int_{\partial\Omega} \frac{1}{r(P,Q)} \sigma(Q) dS, \quad (7)$$

where $r(P, Q) = |P - Q|$.

The hull and a part of the free surface are approximated with quadrilateral panels, considering constant source strength on each. In this way, all the involved boundary value problems are solved in terms of these unknown source strengths.

A suitable radiation condition is finally posed at the forward border of the computational domain. In the present method radiated and diffracted waves are considered not to propagate ahead the ship. So the method can be applied for $\omega_e U/g > 0.25$.

Since the free surface computational domain is limited, it must be carefully considered in order to avoid wave reflection.

2.2. Time domain analysis

Considering a ship as an unconstrained rigid body subjected to gravity, radiation, diffraction, Froude-Krylov and hydrostatic forces and applying the impulse theory and Fourier analysis to the Equation (1), it is possible to rewrite the equations of motion as:

$$\sum_{k=1}^6 \left(M_{jk} + A_{jk}^{\infty} \right) \ddot{\eta}_k + B_{jk}^{\infty} \dot{\eta}_k + \int_0^t h_{jk}(\tau) \dot{\eta}_k(t - \tau) d\tau = F_j^D(t) + F_j^{FKH}(t) \quad (8)$$

with $k = 1, \dots, 6$ where A_{jk}^{∞} and B_{jk}^{∞} mean infinite-frequency added mass and damping coefficients, $F_j^D(t)$ are the linear diffraction and $F_j^{FKH}(t)$ the nonlinear Froude-Krylov and hydrostatic forces and moments.

h_{jk} is the impulse response functions (or retardation functions) and can be evaluated by the following relation:

$$h_{jk} = -\frac{2}{\pi} \int_0^{\infty} \omega_e \left(A_{jk} - A_{jk}^{\infty} \right) \sin(\omega_e t) d\omega_e = \frac{2}{\pi} \int_0^{\infty} \left(B_{jk} - B_{jk}^{\infty} \right) \cos(\omega_e t) d\omega_e \quad (9)$$

in which ω_e is the encounter frequency

The system of Equations (8) is solved in the time domain by a numerical procedure. Hydrodynamic radiation forces are obtained by convolution with the impulse re-

sponse functions in (9). Diffraction forces are obtained simply transforming in the time domain the corresponding frequency domain terms. Froude-Krylov and hydrostatic forces, which in the frequency domain are considered relative to the mean hull shape and linearized, can here be estimated considering the actual wetted hull body surface, known at each time step.

3. Numerical results

The method described above is here applied for the prediction of heave and pitch motions in regular head waves for two test cases.

The first case presented is a destroyer vessel, on which numerical simulations of vertical motions in regular head seas have been performed employing both the strip theory and the three-dimensional Rankine panel method. Results have been compared with experimental data provided by Gerritsma et al. [6]. Calculations have been carried out considering two Froude numbers (0.18 and 0.36) and three different wave steepness ka (0.01, 0.05 and 0.1), in order to evaluate how nonlinear effects are related to these parameters.

The linear response amplitude operators for heave and pitch are represented in Figure 1 for $F_N = 0.18$ and in Figure 2 for $F_N = 0.36$. The strip theory results show a better agreement with experimental data in the prediction of heave motions, while the three-dimensional method appears to better represent pitch motions.

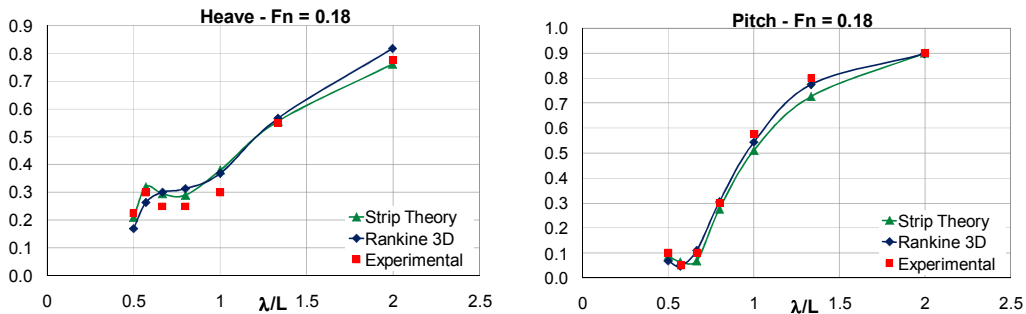


Fig. 1. Linear heave and pitch transfer functions for the destroyer at $F_N = 0.18$

In Figures 3 and 4 a comparison between added mass and damping coefficients, evaluated with the strip theory and the three-dimensional Rankine panel method, is reported. Differences in the prediction of added mass coefficients are generally limited, while calculation of damping turns out to be a critical issue.

In Figures 5 and 6 a comparison between nonlinear transfer functions obtained with different wave steepness is proposed. At $F_N = 0.18$ the response amplitude operators for heave and pitch appear to be poorly influenced by this parameter and, in general, by nonlinear effects like motions asymmetry and higher harmonic components, at least in the range of frequencies considered. At $F_N = 0.36$ the transfer functions result more

affected by the wave height and by the related nonlinear effects, which appear to be magnified by the ship motions.

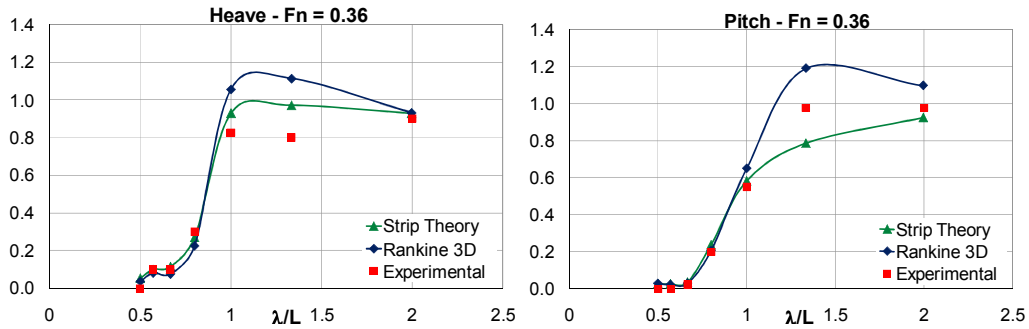


Fig. 2. Linear heave and pitch transfer functions for the destroyer at $F_N = 0.36$

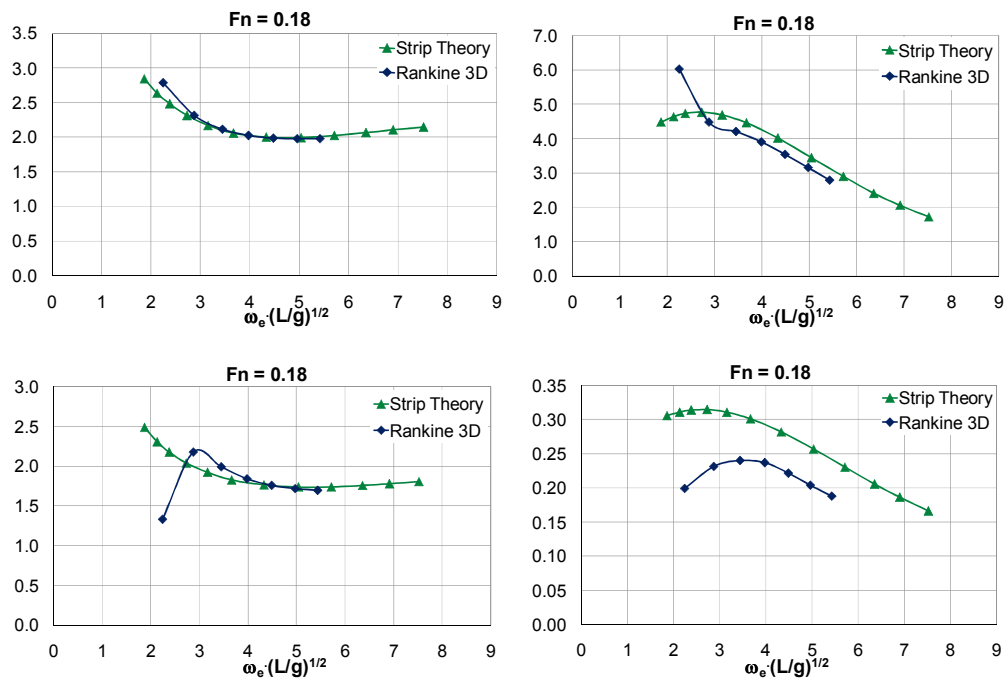


Fig. 3. Comparisons of added mass and damping coefficients for the destroyer at $F_N = 0.18$

The trends of variation appear to be similar with both the methodologies employed in the frequency domain analysis, even if the modules are different and their values seem connected with the motion amplitudes. However, it must be remarked that, when the relative motions between the vessel and the free surface are too large to consider negligible other highly nonlinear effects, e.g. force due to green water, the results

obtained could be questionable; moreover, the validity of the assumption of linear radiation and diffraction forces become arguable in this condition.

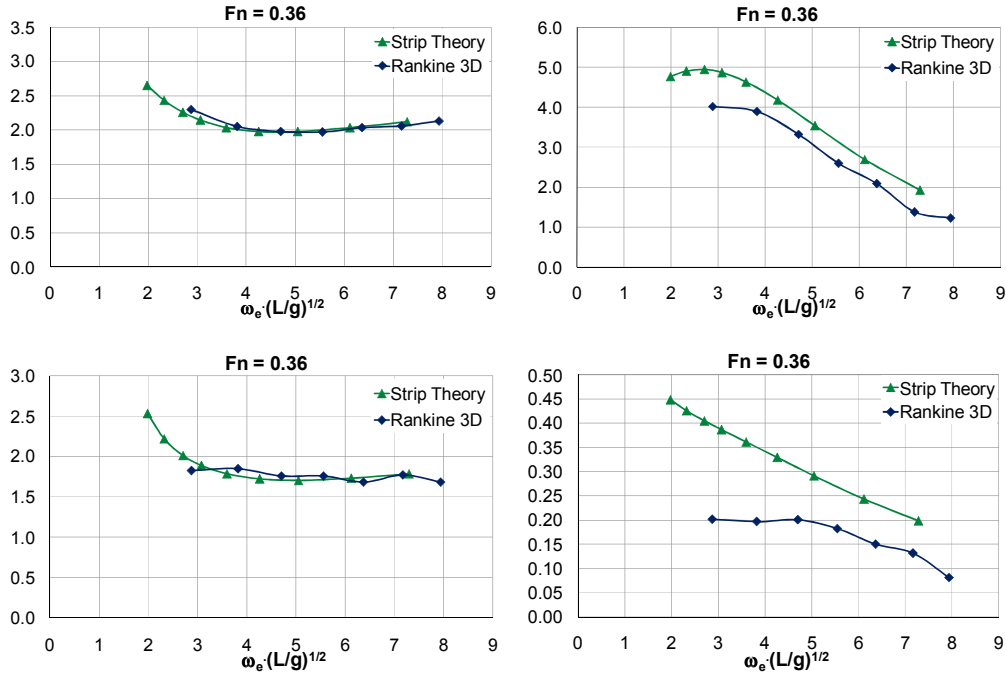


Fig. 4. Comparisons of added mass and damping coefficients for the destroyer at $F_N = 0.36$

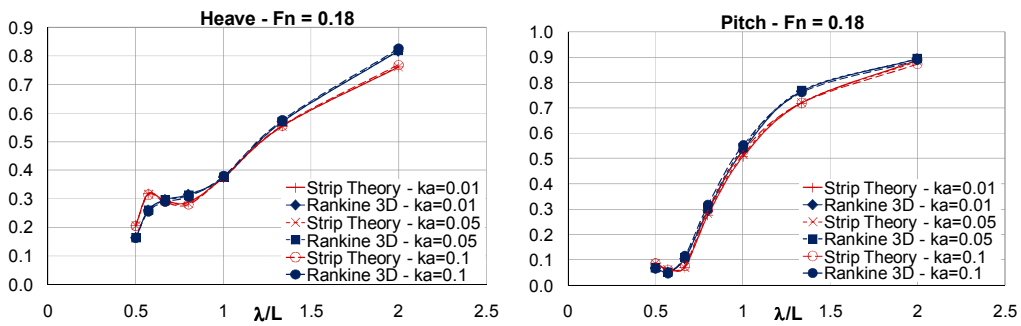


Fig. 5. Nonlinear heave and pitch transfer functions for the destroyer at $F_N = 0.18$, evaluated considering different wave steepness

As shown, the hybrid approach is capable to be applied employing different techniques for the frequency domain analysis. However, nonlinear simulations are strongly conditioned by the evaluation in the frequency domain of linear radiation and diffrac-

tion forces and errors in this calculations could affect the correct assessment of nonlinear effects.

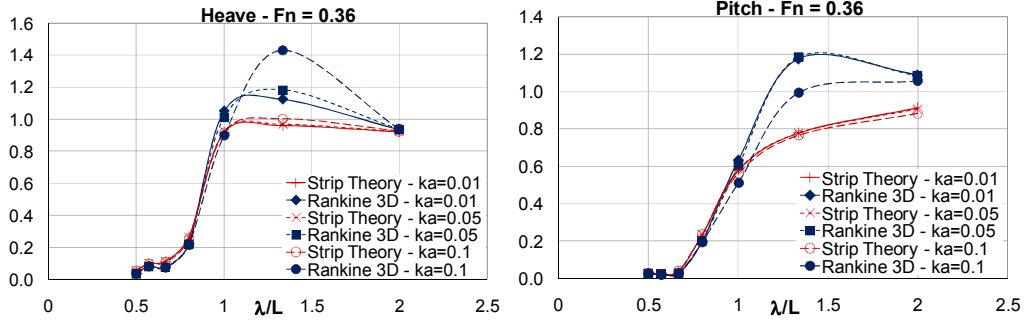


Fig. 6. Nonlinear heave and pitch transfer functions for the destroyer at $F_N = 0.36$, evaluated considering different wave steepness

A second application here presented regards a trimaran vessel, in which the component hulls are three modified Wigley parabolic hulls [7]. The frequency domain analysis has been performed employing only the three-dimensional Rankine panel method, as standard strip theory codes do not allow to deal with multi-hull vessels or neglect the interaction between the hulls. In Figure 7 the mean position underwater hull with free surface mesh used for linear unsteady hydrodynamic calculations is shown, while in Figure 8 a frontal view of the full surface employed for nonlinear simulations is reported. Numerical results for a Froude number $F_N = 0.2$ are compared with experimental data derived from towing tank tests performed by INSEAN [8].

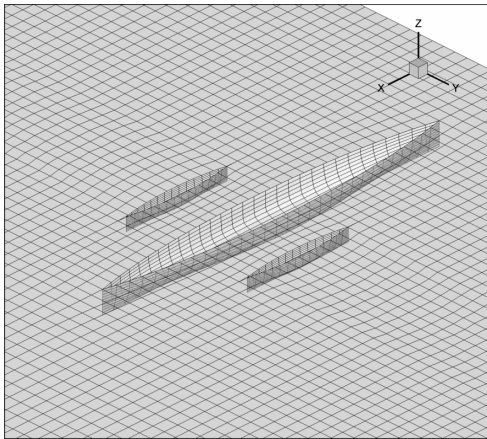


Fig. 7. Mesh of the mean position underwater hull with free surface

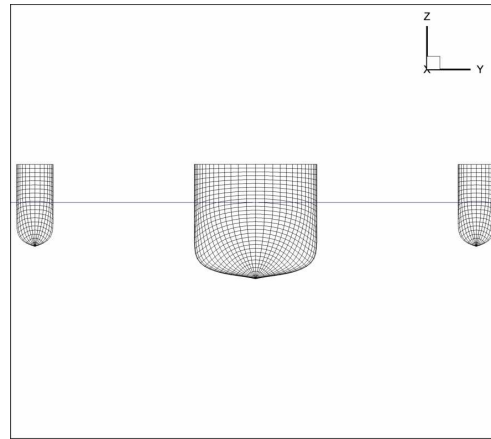


Fig. 8. Frontal view of the full hull surface

Figure 9 shows heave and pitch response amplitude operators, evaluated with a linear analysis and three nonlinear simulations considering wave steepness of 0.01, 0.05 and 0.1, also experimental results are reported for comparisons. Correspondence between numerical results and experimental data appear to be fairly good for $\lambda/L > 1.3$ while the responses turn out to be overestimated in a λ/L range between 1 and 1.3 for heave and corresponding to the resonance peak for pitch motion. Nonlinear effects on the heave transfer function, increasing the wave height, generate firstly a raise and then a reduction of the second resonance peak, which also tend to be shifted to lower frequencies. Also the value of pitch resonance peak decreases with the raising of the wave steepness and is progressively shifted to lower frequencies.

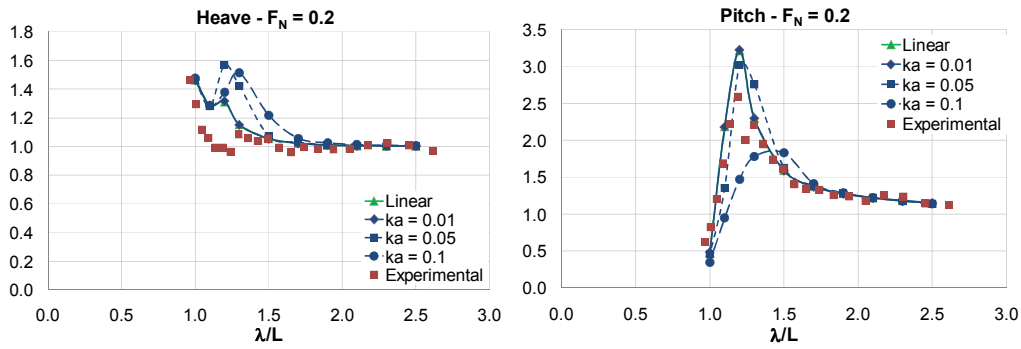


Fig. 9. Part of heave and pitch transfer functions for the Wigley trimaran at $F_N = 0.2$, evaluated considering different wave steepness

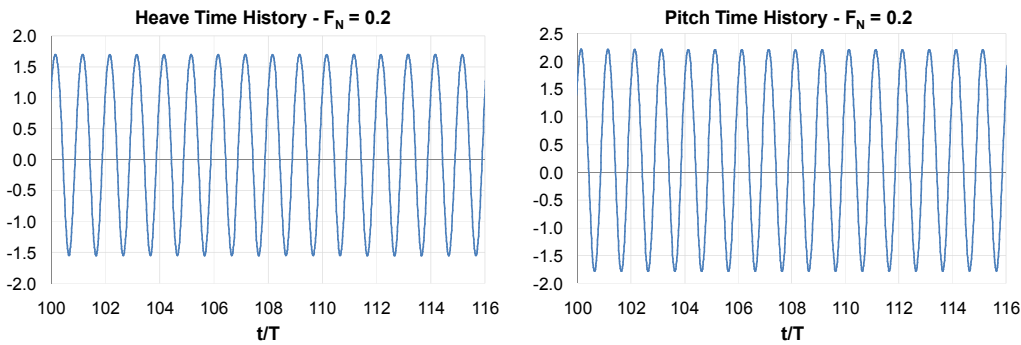


Fig. 10. Heave and pitch time histories for the Wigley trimaran at $F_N = 0.2$, $ka = 0.1$ and $\omega_e(L/g)^{1/2} = 3.16$

In Figures 10 time histories of heave and pitch, evaluated in the time domain considering a wave steepness of 0.1 and $\omega_e(L/g)^{1/2} = 3.16$, are reported, showing the dissymmetry of motion for both heave and pitch.

4. Conclusions

The paper presents a time domain analysis for heave and pitch motions performed on two test cases, a destroyer vessel and a Wigley trimaran. A hybrid approach has been employed, combining linear radiation and diffraction forces, evaluated in the frequency domain, with nonlinear Froude-Krylov and hydrostatic forces, computed in the time domain. Simulations have been performed considering three different wave steepness, assessing its influence on the response amplitude operators. In the first test case, the frequency analysis has been performed employing both a strip theory and a three-dimensional Rankine panel method, in order to check the independence of the time domain simulations from the frequency domain calculations, at least in terms of the radiation and diffraction forces transfer.

A comparison between numerical results and experimental data shows a generally good agreement, even if the strip theory gives better results for heave motions and the three-dimensional Rankine panel method is more accurate predicting the pitch. The methodology adopted in order to transfer the linear radiation forces from frequency to time domain appears not to be affected by the technique used in the frequency domain, but the results depend largely on the accuracy of the prediction of the hydrodynamic terms.

The validity of the assumption of linear radiation and diffraction forces has to be further investigated, particularly when there are noticeable variations of the hull wetted surface in time.

References

- [1] Beck R., Reed A.: *Modern seakeeping computations for ships*, Twenty-Third Symposium on Naval Hydrodynamics, Val de Reuil, 2000.
- [2] Cummins W.E.: *The impulse response function and ship motions*, Schiffstechnik, N. 47, 1962, pp. 101–109.
- [3] Söding H.: *Eine modifikation der streifenmethode*, Schiffstechnik, No. 16, 1969, pp. 15–18.
- [4] *PDSTRIP User Manual*, <http://sourceforge.net/projects/pdstrip>.
- [5] Bruzzone D.: *Application of a Rankine source method to the evaluation of motions of high speed marine vehicles*, Proceeding of the 8th International Marine Design Conference, Athens, May 2003, Vol. II, pp. 69–79.
- [6] Gerritsma J., Smith W.E.: *Full scale destroyer motion measurements*, Journal of Ship Research, Vol. 11, No. 1, 1967, pp. 1–8, 27.
- [7] Journèe J.M.J.: *Experiments and calculations on 4 Wigley hull forms in head waves*, Report 0909, Delft University of Technology, 1992.
- [8] Colagrossi A., Lugni C., Landrini M., Graziani G.: *Numerical and experimental transient tests for ship seakeeping*, Tenth International Offshore and Polar Engineering Conference, Seattle, 2000, pp. 406–413.

Nieliniowa analiza pionowych ruchów statku w dziedzinie czasu

Przedstawiona została nieliniowa analiza właściwości morskich statku w dziedzinie czasu dla statków poruszających się przy regularnej fali przeciwnej. Zastosowana została metoda hybrydowa polegająca na rozwiązywaniu nieustalonego zagadnienia hydrodynamicznego w dziedzinie częstotliwości i równań ruchu w dziedzinie czasu. Siły radiacyjne i dyfrakcyjne, z założenia liniowe, są przekazywane z dziedziny częstotliwości do dziedziny czasu, gdzie w każdym kroku czasowym obliczane są nieliniowe siły Froude'a-Kryłowa i siły hydrostatyczne z uwzględnieniem rzeczywistej powierzchni zwilżonej kadłuba. W pierwszym prezentowanym przypadku – statku jednokadłubowego, do analizy w dziedzinie częstotliwości została zastosowana zarówno metoda paskowa (strip theory), jak i trójwymiarowa metoda panelowa Rankine'a, natomiast w drugim przypadku – trimarana, zastosowano tylko metodę trójwymiarową. Porównanie wyników pokazuje dobrą zgodność z danymi doświadczalnymi. Metoda hybrydowa okazała się rzeczywiście niezależna od metody zastosowanej w dziedzinie częstotliwości nawet, jeżeli wiarygodność wyników jest silnie zależna od dokładności wyznaczania członów hydrodynamicznych.



Selected aspects of the methodology of tribological investigations of polymer materials

D. CAPANIDIS

Wrocław University of Technology, Wybrzeże Wyspiańskiego 27, 50-370 Wrocław

The paper presents selected problems relating to carrying out experimental investigations aimed at determining the tribological properties of polymer materials mating with metal or polymer elements in different friction conditions in sliding joints. The types of tribological investigations and the most commonly adopted types of sliding pair contact are presented. The possible space of tribological investigations is described and the criteria for the choice of key input and output quantities for tribological investigations of sliding pairs incorporating a polymer material are given. The benefits stemming from experiment design are demonstrated and the rotatable design's and the simplex design's advantages and range of application in tribological investigations are presented.

Keywords: *tribological properties of polymers, methodology of investigations, experiment design*

1. Introduction

The failure-free operation of sliding joints in given friction conditions depends mainly on the proper match between the mating materials, good sliding joint design and the adherence to the operating specifications. For this reason the properties of sliding pair materials, mainly their tribological properties, need to be known [1–2].

The growing demand for ever higher durability and operational reliability of sliding joints, chiefly unattended joints, working in technically dry friction or sparing (e.g. assembly) lubrication conditions at the ever higher motion parameters has spurred search for new, better sliding materials [3–4]. Full information about the course of friction and wear of the materials mating in sliding pairs can be obtained only through experiment. The complexity of the physicochemical phenomena occurring in the surface layer and the resultant variety of wear of the mating materials are due to the large number of factors having a bearing on the phenomena [5]. One can gain a deeper insight into a given sliding pair only if the latter is investigated by different methods and techniques. Hence state-of-the-art equipment, offering high measurement precision and a possibility of comparing the results with the ones reported by other research centres, is used for comprehensive tribological investigations and complementary physicochemical tests. One should note that in some cases it is difficult or impossible to compare research results since either no essential information about the experimental conditions, the way in which the specimens were prepared, etc., is provided or different investigative techniques (making direct comparison of results impossible) were used [6].

In view of the large increase in the number of researches into the tribology of polymers conducted by numerous research centres (as evidenced by the constantly growing number of publications, conferences, etc.) and considering the possibility of comparing the results obtained by the different research centres as highly important for the exchange of information, a laboratory tribological methodology for investigating polymer materials in technically dry friction or mixed friction conditions has been proposed.

2. Types of tribological investigations

Tribological investigations can be divided into two main types [7]:

- operational investigations conducted in real conditions on real objects. Their main advantage is that their results are directly applicable, whereas their disadvantages include the high cost associated with the technique itself, the long investigation time and usually considerable measurement difficulties.
- laboratory investigations on models of real objects or on isolated equipment units have similar disadvantages as above. Another kind of laboratory investigations are tests on material samples (sliding pairs) which have no such disadvantages, especially with regard to high investigation costs. They are characterized by ease of measurement and the highest replicability of results – which is crucial in material testing. Such investigations also offer the possibility of comparing results obtained in different research centres.

3. Investigative equipment

Laboratory equipment for tribological investigations of polymer materials has not been fully standardized yet. However, criteria relating to the macrogeometry of the sample/counterface contact have been defined. The most common types of contact between mating elements occur in the following configurations [8]:

- a) cylinder/plane,
- b) plane/plane,
- c) cylinder/cylinder (both cylinders may have positive curvature or one cylinder – positive curvature and the other – negative curvature, or they may have parallel or twisted axes),
- d) ball/ball,
- e) cone/cylinder,
- f) ball/plane.

All equipment for tribological investigations can be divided depending on the character of the sample/counterface contact, according to which sliding pairs belong to one of the three groups:

- group I – area contact,
- group II – linear contact,

– group III – point contact.

The above types of contact occur by and large in initial conditions since in the course of testing a point or linear contact may become an area contact as a result of elastic or plastic deformations and also due to the progressing wear of the sliding pair components.

Mainly group I devices (with area contact between the sample and the counterface) are used for the tribological testing of polymer materials because of the latter's physicochemical properties. Pin on disk devices are the most common. Figure 1 shows the basic load and relative motion schemes for this type of sliding pair [9].

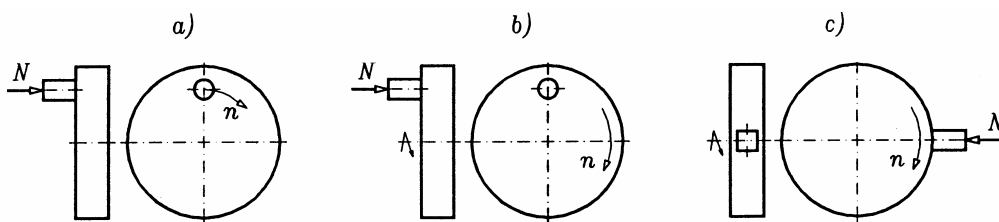


Fig. 1. Schemes of most common sample/counterface configurations in pin on disk devices

Because of their great popularity such devices can be regarded as the standard equipment for the laboratory testing of polymer materials and the obtained tribological test results can be compared (also internationally). The popularity of such sliding pair schemes (particularly the ones shown in Figure 1a and 1b) is due to the simple way of making samples and counterfaces, but mainly to the high accuracy of the sliding pair's geometric features thanks to the lack of mutually fitted dimensions. As a result, one can have high certainty about the value of the applied unit pressure and its uniform distribution on the sample's surface (thanks to the participation of the whole nominal sliding surface in the friction process). Moreover, the flat sliding surfaces of the sample and the counterface and the good access to them make it easy to perform measurements (of such quantities as roughness, hardness and linear wear), microscopic examinations and other examinations of the surface layer [10].

A test device should make it possible to smoothly adjust (in a proper range) the individual input quantities (unit pressure, sliding velocity, ambient temperature, etc.) so that a given sliding pair could be tested under different friction conditions, including extreme ones. Such a device should also be equipped with proper control-measurement equipment ensuring precise and repeatable (preferably continuous) measurements of input and output quantities during friction. An example of such a device is the tribometer described in [11–12].

4. Space of tribological investigations

Having only friction coefficient values and data on the wear of sliding pair materials one cannot sufficiently reliably assess the tribological properties of polymer mate-

rials since the properties depend on many factors relating to the friction process and stemming from the properties of the paired materials themselves.

In order to fully assess the tribological properties of polymer materials one must know what kind of material was used for the counterface in the sliding pair. It is also important to know the condition of the surface layer of both the polymer material and the counterface (especially a metal one) [5–8]. A description of the condition of the mating materials' surface layers usually includes: chemical composition, sliding surface hardness, phase microhardness and its distribution along surface layer thickness, surface roughness (expressed by various parameters, e.g. R_a , R_z , R_{3z}) and lay of tool marks and how they were made (by turning, grinding, polishing, chromium plating) [13–14].

In the case of polymer materials, it is essential to know the history of the material, i.e. how the sample was made (by injection, press moulding, machining, etc.), what were the processing parameters and how long and in what environment the material was aged. All of this affects the supermolecular structure of polymer materials, particularly in their surface layer, and consequently determines the sliding pair's tribological properties.

The tribological properties of polymer sliding pairs also very much depending on the environment (oxygen atmosphere, vacuum, humidity, ambient temperature, environment dustiness, chemical environment aggressiveness, type of lubrication or its absence) in which the tests were conducted, the kind of motion (rotational, swinging, translational, to-and-fro) and the friction process motion excitations (unit pressure, sliding velocity). It follows from the above that the space of tribological investigations is vast and can be generally divided into two categories: input quantities and output quantities.

4.1. Input quantities

In tribological investigations of polymer materials the input quantities can be assigned to different groups of controlled parameters, such as:

1. *Motion parameters*, e.g. p – unit pressure, v – sliding velocity, T_p – initial friction temperature (of the counterface), S – path (distance) of friction.

2. *Sample (polymer material) parameters*, e.g. M_p – type of material, SP – way of processing, Sch – chemical composition (type and fraction of the particular components in polymer composites), PS – ageing parameters (heat treatment, environmental conditions, temperature, time and other), X – different kinds of surface irradiation, ion or atom implantation or bombardment, etc.

3. *Counterface parameters*: M_{pp} – counterface material (usually metal), R_x – selected sliding surface roughness parameter, C – surface geometric structure, KR_x – tool mark lay relative to the direction of friction, H_x – sliding surface hardness, mH_x – microhardness in the surface layer.

4. *Test environment*, e.g. At – type of atmosphere (oxygen, inert gas, vacuum, etc.), W – relative humidity, T_o – ambient temperature, Sm – lubrication (type of lubricant, lubrication rate), ZS – impurities and other factors.

4.2. Output quantities

As output quantities in tribological investigations of polymer sliding pairs usually the following groups of measured quantities are adopted:

1. *Directly measured quantities*, e.g.: Z_h – linear wear, Z_m – massive (weight) wear, Z_v – volumetric wear, M_t – moment of friction, T_t – friction temperature, $p \cdot v$ – acceptable product of unit pressure and sliding velocity, N_{ob} – number of performed revolutions (cycles), etc.

2. *Directly determined quantities*, e.g. I_{zx} – wear intensity, μ – coefficient of (kinetic, static, start-up) friction, S – friction distance covered, R_{xp} , R_{xpp} – roughness of sample and counterface sliding surface after friction, etc.

3. *Complementary quantities*, e.g.: K_r – degree of crystallinity of polymer in the surface layer, H_{ww} – surface layer depth after friction, mH_t – distribution of microhardness in the surface layer after friction, h_{mp} – thickness of the polymer film transferred onto the counterface, etc.

4.3. Output quantities from auxiliary investigations

In order to explain the phenomena occurring during friction and to identify the types of friction and the mechanisms of wear of the mating materials complementary physicochemical investigations are carried out. These include:

1. Microscopic examinations of samples and counterfaces, in particular their sliding surfaces and surface layer cross sections.

2. Roentgenography.

3. Spectrophotometry.

4. Thermography and other.

5. Aims of tribological investigations

The character and range of tribological investigations depend on the aims to be achieved. As shown above, the space of tribological investigations is vast and so the spectrum of possible research subjects is wide. It covers (among others): comparative research on various polymer materials mating with identical counterfaces, conducted in the same friction conditions, aimed at selecting the best sliding pair, i.e. materials testing; research on the effect of friction process motion parameters on a given material pair's sliding and antiwear properties, i.e. the determination of the pair's tribological characteristics; research on the effect of the chemical or physical modification of a given polymer material on its tribological properties, i.e. the search for new sliding materials for specific friction conditions; optimization research aimed at determining

the most favourable friction conditions for a given sliding pair, such as the optimum roughness of the steel counterface and the recommended unit pressures, sliding velocities, friction temperatures, etc.; and comprehensive investigations covering several groups of factors simultaneously, usually conducted in stages with the investigation range narrowed down at each stage until the objective is reached.

Regardless of the aim and kind of investigations, not only the obtained results but also the specific investigation conditions (including all the groups of factors) should be reported in detail. Then the results of such investigations can be compared with the results obtained in other research centres.

6. Carrying out tribological investigations

Besides the choice of aim, experimental research (including tribological research) usually involves:

- selecting key input quantities,
- fixing the range of values for the input quantities,
- selecting the output quantities to be measured and the measuring methods,
- adopting an experiment design,
- handling the research results.

6.1. Selection of key input quantities

A large number of factors have a bearing on the tribological properties of a sliding pair. Depending on the research goal, the kind and number of input quantities can vary widely. Prior to experiment design one should make a preliminary analysis of the investigated object and consider the relations between the particular input quantities, known from previous experience or the literature on the subject. In order for the research results to be fully useful, i.e. for the model to describe well the investigated object, one should include possibly the largest number of input quantities which determine the object's output. On the other hand, a large number of input quantities complicates the model and increases the costs and labour intensity of the research. Therefore only the most important variables should be taken into account so that the model is sufficiently accurate and possibly not too complicated [15–16].

6.2. Range of change of input quantities

The range of change of input quantities (variables in experimental investigations) is usually determined on the basis of the following criteria:

- the experimenter's knowledge and experience from his/her previous investigations (into similar research subjects);
- a literature survey of the values adopted by other researchers in different research centres;

- a preliminary study of admissible values at which an experiment can be conducted without any signs of failure friction;
- the minimum values dictated by good grinding-in ability of a sliding pair, ensuring efficient performance of the experiment when the minimum values do not follow from the sliding pair's intended use (e.g. too low values of p and v may disproportionately lengthen the grinding-in period relative to the duration of the investigations themselves);
- the minimum and maximum values dictated by the intended use of the tested sliding pair (polymer material);
- in the case of comparative testing of different sliding pairs, such tests are usually conducted at fixed friction process parameters and the values of the parameters follow from the intended use of the tested sliding pairs, or the values most commonly used in such investigations by other researchers (e.g. $v = 0.5, 1.0, 1.5$ m/s, $p = 0.5, 1.0, 1.5$ MPa) are adopted whereby it becomes possible to directly compare the test results.

6.3. Selection of measured output quantities

The kind and number of measured output quantities depend on the aim and range of the investigations. One should try to gain possibly the fullest information about the investigated object. Therefore besides the outputs traditionally adopted in tribological investigations, such as the coefficient of friction, friction temperature and sample and counterface wear, one should include other quantities, e.g. sample and counterface sliding surface roughness after friction, the thickness and composition of the material film transferred onto the counterface surface, as well as other quantities from complementary (sect. 4.2) and auxiliary (sect. 4.3) investigations. The adoption of a larger number of output quantities does not contribute to a significant increase in the investigations' costs and time (assuming that the laboratory has proper equipment) while ensuring more reliable inference and correct interpretation of the phenomena occurring during friction.

Reliability and replicability of test results are determined by the choice of proper methods of measuring the output quantities and by the control of the values of the input quantities and in the case of tribological investigations, also by the proper grinding in of the investigated sliding pairs. The development of measuring techniques opens up ever greater possibilities in this regard. Generally, methods based on direct measurement yield the most accurate results. But it is not always possible to use them to measure, for example, friction moment or temperature. Then in order to eliminate the adding up of partial inaccuracies from the individual instruments in the measuring circuit is recommended to calibrate the latter. The measured output values are more reliable when several independent methods are employed to measure the same quantity. For example, in some cases it is necessary to employ different measuring methods to determine the wear of a sample made of a polymer material since it may happen that the wear determined by the gravimetric method has a negative value (due to moisture

absorption or inclusion of counterface wear metal products by the lubricant) whereas linear (or volumetric) wear measurement indicates positive wear of the sample.

As mentioned above, in order to obtain correct results from tribological tests it is necessary to properly grind in the sliding pairs. The grinding in is usually assessed by applying the following criteria:

- the coefficient of friction and wear intensity have stabilized at constant levels;
- friction temperature has stabilized;
- the whole nominal (flat) contact area of the sliding pair takes part in the friction process, as determined by microscopic examinations;
- the roughness of the two mating sliding surfaces (of the sample and the counterface) has stabilized at a constant level.

The values of grinding-in parameters are determined by preliminary tests and they should be lower than the ones in the tests proper. For the adopted values of p , v , T grinding-in time (friction distance) is determined. Sliding pairs which grind in slowly are pre-ground with abrasive paper (in the testing device).

6.4. Adoption of experiment design

In multi-factor investigations (which tribological tests usually are) the use of the experiment design technique will bring about notable effects – it will reduce the number of experiments to the absolute minimum and so reduce the amount work, the costs and the duration of the investigations. The planning of experiment, understood to be a series of experiments, includes the selection of a matrix of experiment inputs. The quality of identification or optimization of the investigated object may to a substantial degree depend on the choice of experiments (measuring points). Hence experiment design, i.e. the choice of the number of experiments and the values of the particular variables in the successive experiments, is highly important.

With regard to tribological investigations, from among the many kinds of experiment design one should distinguish the simplex design and the rotatable design. But there are no limitations as the use of other types of experiment design [15–16].

6.4.1. Simplex experiment design

The simplex design is used to investigate, among others, the properties of mixtures dependent on the latter's composition. The simplex design exploits the fact that the composition of composites can be described by the vector of x_1, x_2, \dots, x_S (composite components) satisfying balance constraints given by the formula:

$$\sum_{s=1}^S x_s = 100, \quad (1)$$

where:

x_s – the percentage of the s -th component
or for standardized values:

$$\sum_{s=1}^S t_s = 1, \quad (2)$$

where: $t_s = \frac{x_s}{100}$,

in which: $x_s \geq 0$ at $s = 1, 2, \dots, S$, where S is the number of composite components.

This means that the sum of all the variables (composite components) is equal to 100%, or that the sum of their standardized values amounts to 1 (constitutes a whole). Moreover, each of the components must be positive or may not occur at all. A factor design for investigating the properties of S -component mixtures may include only such experiments whose points belong to an S -dimensional simplex constituting the area of an $(S-1)$ -dimensional space. This means that the points lie on an $(S-1)$ -dimensional hyperplane bounded by an S -dimensional regular simplex being a convex polyhedron spread over S vertices in the $(S-1)$ -dimensional space. The simplexes for the number of input variables $S = 2-4$ are graphically represented in Figure 2.

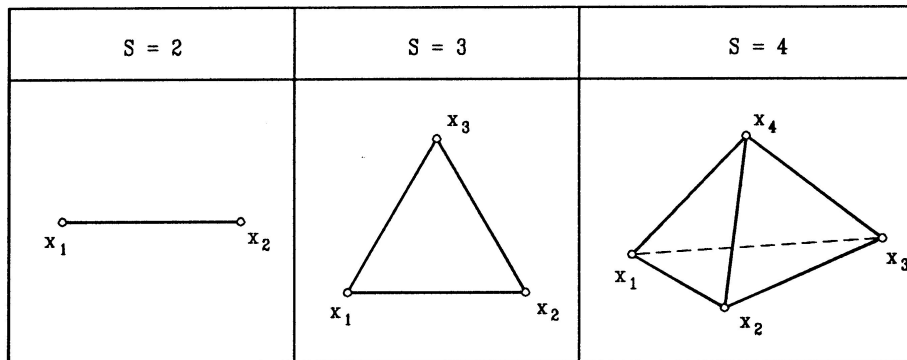


Fig. 2. Graphic representation of simplexes for number of input variables $S = 2-4$.

It follows from the above that from among the S input variables only $(S-1)$ are linearly independent. Thanks to this one can use reduced polynomials (with a smaller number of coefficients) for description. Consequently, the number of experiments (composites) required to determine the coefficients of such a polynomial is smaller. At high dimensionality S and higher degrees I reduced polynomials still have a too high number of coefficients. That is why simplified reduced polynomials are often employed. To approximate results one can also use other polynomials (e.g. with singular forms) provided that the condition that the number of experiments be lower than the number of the polynomial's coefficients ($N \geq N_b$) is satisfied.

Two main types of simplex designs are distinguished [15]:

- integral simplex designs of type $\{S, I\}$, referred to as whole simplex designs, enabling the identification of I -th degree reduced polynomials with S variables (at $I \leq S$);
- integral simplex designs of type $\{S\}$, referred to as fractional simplex designs, enabling the identification of S -degree simplified reduced polynomials with S variables.

Fractional designs are more important for the investigation of multicomponent composites since they allow one to better determine the investigated properties inside a simplex. Fractional simplex designs of type $\{S\}$ are formed by a set of all the points of standardized values t_1, t_2, \dots, t_S calculated from the formulas:

$$(1, 0, \dots, 0); \left(\frac{1}{2}, \frac{1}{2}, 0, \dots, 0\right); \dots, \left(\frac{1}{S}, \frac{1}{S}, \dots, \frac{1}{S}\right), \quad (3)$$

and points obtained through the transposition of the coordinates at fulfilled condition (1) or (2). The number of values of the particular input variables in fractional designs is greater or at the most equal to their number in whole designs (for which $n_{\max} = I + 1$), given by the relation:

$$n_{\max} = S + 1. \quad (4)$$

The number of experiments (systems) in fractional designs is:

$$N = 2^S - 1 \quad (5)$$

and it is lower than in whole designs. This makes it possible to identify simplified reduced polynomials with a lower number of coefficients. Also the required number of experiments, and so the number of formed composites, is lower. The arrangement of measuring points in a fractional simplex design for $S = 4$ composite components is shown in Figure 3.

The effect of the individual components on the properties of a composite is examined only in a certain range of their quantitative share. Then local design, i.e. investigation of a simplex subarea, is employed [15]. A local design is obtained through the transformation of a whole or fractional simplex design. This boils down to assigning to a whole simplex's vortices:

$$x_1 = [1, 0, \dots, 0]^T, \quad x_2 = [0, 1, \dots, 0]^T, \quad x_S = [0, 0, \dots, 1]^T, \quad (6)$$

respectively S vortices: w_1, w_2, \dots, w_S confining the simplex area (as shown in Figure 4), defined by the vectors:

$$w_S = [w_{S1}, w_{S2}, \dots, w_{SS}]^T, \quad (7)$$

where:

$$s = 1, 2, \dots, S.$$

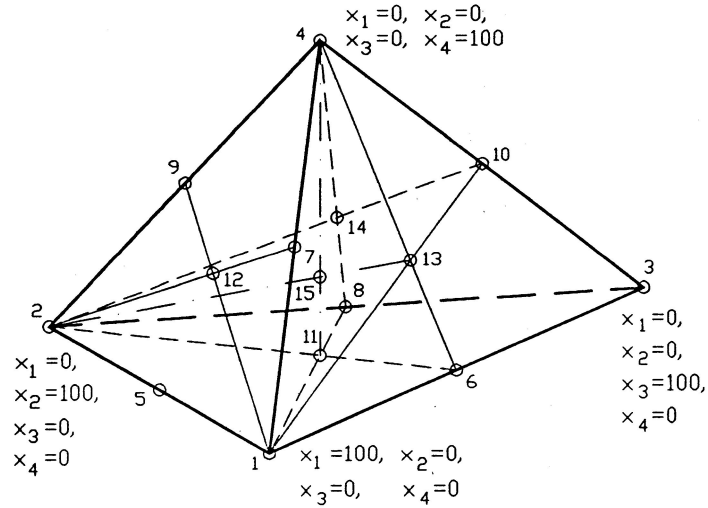


Fig. 3. Arrangement of measuring points in fractional simplex design for $S = 4$

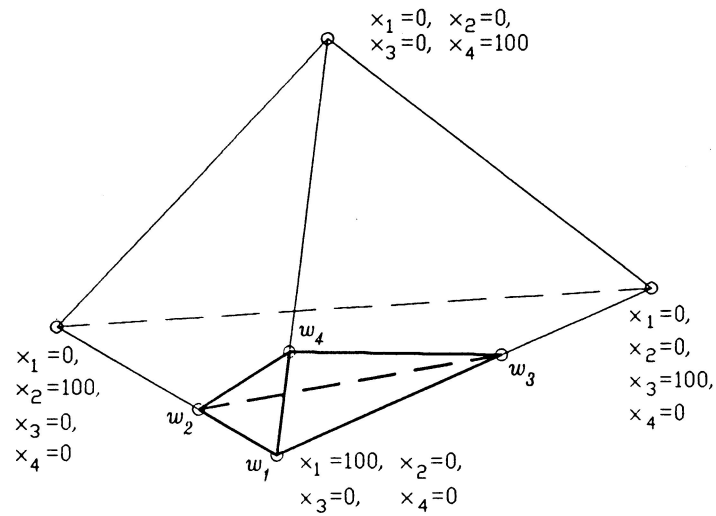


Fig. 4. Simplex subarea confined by vortexes w_1, w_2, \dots, w_4

By introducing matrix denotations one can represent a theoretical design spread over a whole simplex as input matrix \mathbf{X} and the vortexes of the simplex subarea as transformation matrix \mathbf{L} :

$$\mathbf{X} = \begin{bmatrix} \mathbf{x}_1^T \\ \mathbf{x}_2^T \\ \cdot \\ \mathbf{x}_S^T \\ \cdot \\ \mathbf{x}_N^T \end{bmatrix}, \quad (8)$$

$$\mathbf{L} = \begin{bmatrix} \mathbf{w}_1^T \\ \mathbf{w}_2^T \\ \cdot \\ \mathbf{w}_S^T \end{bmatrix}. \quad (9)$$

The local design's input matrix \mathbf{W} is determined by transforming design \mathbf{X} by means of matrix \mathbf{L} , according to the relation:

$$\mathbf{W} = \mathbf{XL}. \quad (10)$$

6.4.2. Rotatable experiment design

Rotatable experiment design with a spherical distribution of information, also referred to as design with rotational symmetry, is highly useful for determining linear-square-model tribological motion characteristics. Unlike other types of multilevel design, it is characterized by reproducibility of regression function estimates in the neighbourhood of the experiment's central point, guaranteeing a constant accuracy of the obtained model. Practically, it is assumed that it is a uniformly accurate design with an identical variance – the same as in the design's central point [15–16].

When an experiment is conducted on 5 levels, number of experiments N is calculated from the formula:

$$N = 2^S + 2S + N_0 \quad (11)$$

where:

S – the number of experiment input variables,

N_0 – the number of experiments in the experiment design's central point.

Input quantities x_s (where $s = 1, 2, \dots, S$) assume the following values:

$$x_{s(\min)}, \quad x_s^O - \Delta x_s, \quad x_s^O, \quad x_s^O + \Delta x_s, \quad x_{s(\max)}, \quad (12)$$

where:

x_{\min} , x_{\max} – respectively the minimum and maximum value of variable “s”, and

$$x_s^o = \frac{x_{s(\min)} + x_{s(\max)}}{2}, \quad (13)$$

the value of input variable “s” in the experiment’s central point

$$\Delta x_s = \frac{x_{s(\max)} - x_{s(\min)}}{2 \cdot \alpha}, \quad (14)$$

the value of the elementary jump of input variable “s” in the experiment design

α – the star radius value following from the rotatability condition [15], which for designs connected with the identification of second-degree polynomials, is determined from the formula:

$$\alpha = \sqrt[4]{2^S}. \quad (15)$$

In order to simplify the procedure in the factor analysis involved in the calculation of regression function coefficients, the input quantities are standardized according to the formula:

$$t_s = \frac{x_s - x_s^o}{\Delta x_s}, \quad (16)$$

then the values given by formula (12) for the standard input quantities will be:

$$-\alpha, -1, 0, +1, +\alpha. \quad (17)$$

One should note that in the days of computers, standardization of input quantities diminishes in importance and does not have to be used; practically, it is used only for demonstrative purposes.

A rotatable experiment design is created similarly as a composition or orthogonal design [15–16], except that it differs in the value of star arm α and in number N_0 of experiments in the experiment design’s central point. Experiment input matrix \mathbf{T} forms N systems – vectors $[x_1, x_2, \dots, x_S]$, whose coordinates x_1, x_2, \dots, x_S can assume values given by formula (12) or (17).

The arrangement of the individual systems of values of input variables in the designs for respectively $S = 2$ and $S = 3$ is shown graphically in Figure 5.

6.5. Handling research results

The handling of research results boils down to the determination of the relation between the measured outputs and the experiment input quantities, in the form of a regression function. Fractional simplex designs allow one to identify S -degree simplified reduced polynomials with S variables. For example, formula (18) represents a 4th-degree simplified reduced polynomial with 4 variables (four-component composites), which includes only 14 coefficients b_i , (and so only 14 composites with different compositions). The polynomial has this form:

$$\begin{aligned}
 y = & b_1x_1 + b_2x_2 + b_3x_3 + b_4x_4 + b_5x_1x_2 + b_6x_1x_3 + b_7x_1x_4 + \\
 & + b_8x_2x_3 + b_9x_2x_4 + b_{10}x_3x_4 + b_{11}x_1x_2x_3 + b_{12}x_1x_2x_4 + , \\
 & + b_{13}x_2x_3x_4 + b_{14}x_1x_2x_3x_4
 \end{aligned} \tag{18}$$

where:

y – an output research quantity (I_h, μ, T_t),

b_1, b_2, \dots, b_{14} – regression function coefficients (without a free term – without a constant),

x_1, x_2, x_3, x_4 – variables representing the volumetric percentages of the composite components.

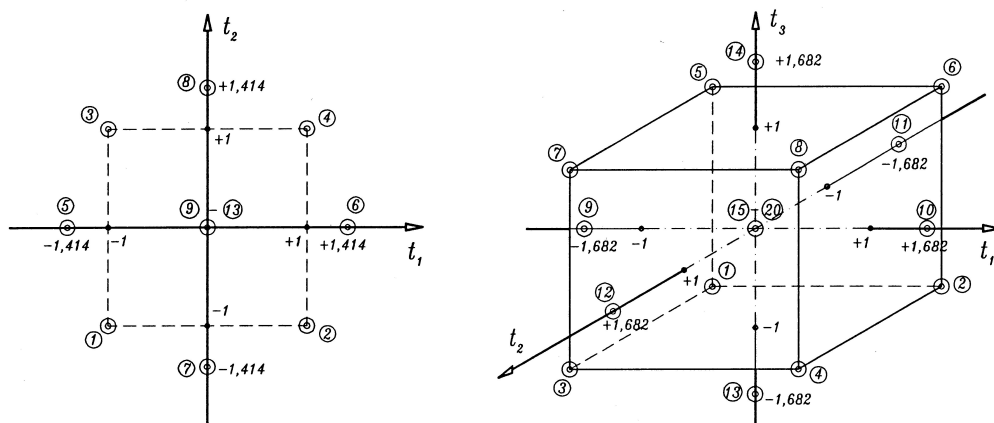


Fig. 5. Arrangement of particular systems of values of input variables in designs for $S = 2$ and $S = 3$

Simplex designs are open designs. This means that when the number of components in the investigated composites is increased, one can use the results of the previous investigations. Then one must appropriately modify the experiment design, supplementing it with new compositions containing the additional components and carry out experiments only for them. The results of the previous investigations supple-

mented in this way will be used to determine appropriately modified, new regression functions.

In rotatable designs the multidimensional regression function is usually a 2nd-degree polynomial having this form:

$$y = b_0 + \sum_{s=1}^S b_s \cdot x_s + \sum_{s=1}^S b_{ss} \cdot x_s^2 + \sum_{\substack{i=1 \\ j=1 \\ i < j}}^S b_{ij} \cdot x_i \cdot x_j, \quad (19)$$

where:

- b_1, \dots, b_s – regression function coefficients,
- S – the number of experiment input variables,
- y – an experiment (measured) output quantity.

Examples of applications of the simplex design and the rotatable design in tribological investigations can be found in respectively [17–18] and [19–20].

The coefficients of the regression functions expressed by formulas (18) and (19) are calculated by the least squares method, using the relation:

$$b = (X^T X)^{-1} X^T y, \quad (20)$$

where:

- X – an experiment matrix,
- y – a vector of experiment outputs (the measured quantity),
- b – a vector of regression function coefficients.

The determined regression functions are verified through their statistical estimation combined with the testing of the regression functions' adequacy from the F-test point of view and the testing of the significance of the regression function terms from the t-Student point of view [15]. The regression functions are used in the design-construction process for optimization calculations connected with the choice of sliding joint geometric features or for determining the optimum chemical composition of composites, ensuring the most advantageous tribological properties in specific friction conditions [17–21].

References

- [1] Capanidis D., Wieleba W., Ziemiański K.: *Wpływ warunków eksploatacji na dobór polimerów i kompozytów polimerowych jako materiałów ślizgowych*, Trybologia, Nr 28, Nr 5–6, 1997, pp. 529–539.
- [2] Rymuza Z.: *Trybologia polimerów ślizgowych*, Warsaw, WNT, 1986.

- [3] Szczerek M.: *Badania tribologicznych własności materiałów*, Tribologia, Teoria i Praktyka. Nr 4/5'93. VII Krajowe Sympozjum Eksploatacji Urządzeń Technicznych, Radom – Kozubnik, 1993, pp. 43–70.
- [4] Wieleba W., Capanidis D., Ziemiański K.: *Polimerowe łożyska ślizgowe z tworzyw termoplastycznych*, Cz. I – Materiały ślizgowe. Poradnik tribologii i tribotechniki (23) – wkładka do TRYBOLOGII, Nr 6/95, pp.125–131.
- [5] Leszek W.: *Fizyko-chemiczne zjawiska występujące na powierzchni ciał stałych przy tarcii*, Materiały na III Sympozjum Tribologiczne pt. „Szkola jesienna”, Tribologiczne problemy warstwy wierzchniej, 1973, pp. 221–239.
- [6] Leszek W.: *Wybrane zagadnienia metodologii badań trybologicznych*, Wybrane problemy tribologii, PWN, Warsaw 1990, pp. 209–219.
- [7] Lawrowski Z.: *Tribologia – Teoria, tarcie, zużywanie i smarowanie*, Wydawnictwo Naukowe PWN, Warsaw, 1993.
- [8] Hebda M., Wachal A.: *Trybologia*, Warsaw, WNT, 1980.
- [9] Capanidis D., Ziemiański K.: *Metodologia badań właściwości tribologicznych polimerów*, Krajowa Konferencja Naukowo Techniczna „Problemy tarcia i zużycia elementów maszyn z tworzyw sztucznych”, Częstochowa, 11–12 listopada 1987, pp. 6–30.
- [10] Ziemiański K., Capanidis D.: *Laboratoryjne badania własności tribologicznych tworzyw sztucznych*. XII Sympozjon Podstaw Konstrukcji Maszyn. Lublin–Kazimierz Dolny, 9–12.10.1985, Politechnika Lubelska, pp. 421–422.
- [11] Capanidis D., Ziemiański K.: *Urządzenie badawcze do określania kompleksowych charakterystyk tribologicznych skojarzenia ślizgowego polimer-metal*, III Seminarium „Tworzywa sztuczne w budowie maszyn”, Kraków–Janowice, 1982, Zeszyty Naukowe Politechniki Krakowskiej, pp. 89–99.
- [12] Capanidis D., Wieleba W., Ziemiański K.: *Zmodyfikowane stanowisko badawcze typu „pin on disc” do badań właściwości tribologicznych materiałów ślizgowych i ciernych*, VI Seminarium „Tworzywa sztuczne w budowie maszyn”, Cracow, 10–12.10.1991, pp. 13–18.
- [13] Capanidis D., Cichosz P.: *Wpływ chropowatości powierzchni na właściwości tribologiczne skojarzenia poliformaldehyd-stal*, 4-ta Międzynarodowa Konferencja Naukowo-Techniczna pt. *Wpływ technologii na stan warstwy wierzchniej* – WW 99, Gorzów Wlkp.-Lubniewice, 21–22.10.1999, pp. 321–326.
- [14] Wieleba W.: *The statistical correlation of coefficient of friction and wear rate of PTFE composites with steel counterface roughness and hardness*, Wear, 2002, Vol. 252, pp. 719–729.
- [15] Mańczak K.: *Technika planowania eksperymentu*, Warsaw, WNT, 1976.
- [16] Polański Z.: *Planowanie doświadczeń w technice*, Warsaw, PWN, 1984.
- [17] Capanidis D., Ziemiański K.: *Planowanie sympleksowe eksperymentu w badaniach właściwości wieloskładnikowych kompozytów polimerowych*, Ogólnopolskie sympozjum kompozyty i kompozycje polimerowe, Szczecin, 22–24.06.1994, pp. 257–260.
- [18] Capanidis D.: *Metody polioptymalizacji w projektowaniu właściwości wieloskładnikowych kompozytów*, Ogólnopolskie sympozjum kompozyty i kompozycje polimerowe, Szczecin, 22–24.06.1994, pp. 261–265.

- [19] Capanidis D., Wieleba W., Ziemiański K.: *Computer Techniques for Optimization of the Polymer Composites Content by Tribologic Measurements*, EUROTRIB'93, Budapest, pp. 106–111.
- [20] Capanidis D., Wieleba W., Ziemiański K.: *Tribological investigations of new multi-component slide composites on the basis of PTFE*, Vth International Symposium INTERTRIBO'93 „Tribological Problems in Exposed Friction System”, 26-28 August, 1993, Bratislava, pp. 82–87.
- [21] Capanidis D.: *Problemy związane z optymalizacją składu wieloskładnikowych kompozytów polimerowych*, VII SEMINARIUM „Tworzywa sztuczne w budowie maszyn”, Cracow, 6–8.10.1994, pp. 47–53.

Wybrane aspekty metodyki badań tribologicznych materiałów polimerowych

W artykule przedstawiono wybrane zagadnienia związane z realizacją badań doświadczalnych dotyczących określania właściwości tribologicznych materiałów polimerowych, współpracujących w skojarzeniu z elementami metalowymi lub polimerowymi, w różnych warunkach tarcia. Omówiono rodzaje badań tribologicznych i najczęściej przyjmowane rodzaje makrogeometrii styku badanych par ślizgowych. Opisano możliwą przestrzeń badań tribologicznych oraz podano kryteria związane z wyborem najistotniejszych wielkości wejściowych i wielkości wyjściowych zazwyczaj uwzględnianych w badaniach tribologicznych. Przedstawiono korzyści wynikające ze stosowania eksperymentu planowanego, a także podano zalety oraz zakresy stosowania planu rotalnego i planu sympleksowego w realizacji badań tribologicznych.



Friction and wear of elastomer seals

M. GAWLIŃSKI

Wrocław University of Technology, Wybrzeże Wyspiańskiego 27, 50-370 Wrocław

The paper contains discussion of the influence of both friction and wear on the operation of the elastomer seals. Friction is critical factor not only in rotating or reciprocating seals but also in static seals. Its minimization cannot be achieved by means of improving lubrication since it can result in unacceptable leakage. There are shown means to lower deformation component of friction coefficient as well as change of adhesion component of friction for dry and lubricated surfaces.

Keywords: *seal, elastomer, friction, wear*

1. Introduction

A basic function of any seal is either to protect an environment against the leakage from engines, machines and different devices or protection of machines inside against contamination (e.g. humidity, abrasives) from surroundings. There are different types of the seals; in general, one can distinguish static and dynamic seals. Static seals are installed between two surfaces which do not move relatively each other. Dynamic seals are those which contact one of either rotating or reciprocating surfaces.

It follows, that the friction and wear will be of minor importance for the static seals operation while for dynamic seals they will play important role. Most of static and dynamic seals are produced from elastomers; their properties predispose them for seals.

One should specify following positive features:

- high elasticity (e.g. rubbers),
- moderate creep and stress relaxation,
- relatively good resistance to abrasion,
- impermeability (important at sealing of gases),
- chemical resistance to different media.

Less or more negative features of elastomers as materials for the seals are following:

- high friction coefficient and friction dependence on time in the seal staying at rest,
- low coefficient of heat conductivity,
- change of properties resulting from elastomer ageing,
- brittleness at low temperatures.

Some of the specified negative properties are interrelated: high friction and low heat conductivity coefficients can lead to the dramatic increase of temperature in the

dynamic seals. High temperature, on its side, accelerates ageing of elastomer. The ageing is the process of the progressive and permanent deterioration of the elastomer properties, especially: decrease of tensile stress, increase of hardness and material cracking. Therefore, it seems to be important to discuss the influence of both friction and wear on the operation of the static and dynamic elastomer seals.

2. Friction and wear of static seals.

O-rings are the most often used static seals; they are used as primary or secondary seals. O-ring (Figure 1a) has to be compressed in order to get the load necessary for sealing. Installation of the seal in the groove of the height h being smaller than O-ring diameter d causes its deformation (Figure 1b). The measure of this deformation is the reaction (load) which the O-ring exerts on the upper and lower surface of the groove, (Figure 1c). It is so-called assembly load. Let assume that the O-ring occupies the central position in the groove just after installation.

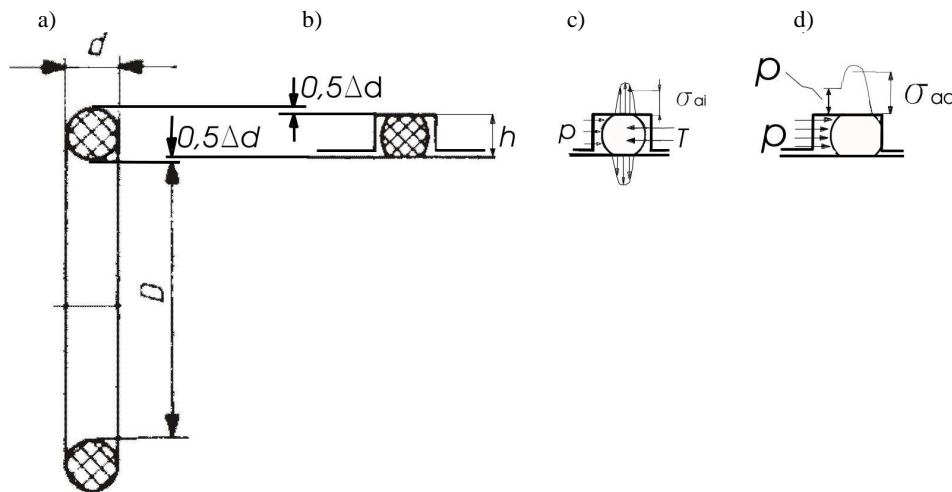


Fig. 1. Generation of contact pressure at O-ring – shaft interface, a) free O-ring, b) O-ring compression in the groove, c) contact pressure distribution at O-ring-walls interface, d) transfer of the gas/liquid pressure through the O-ring on the groove wall

The friction forces T hold the seal in this intermediate position. Now, this is the moment when one can allow the pressurized gas/liquid to flow towards the O-ring. If the break-out friction is too big then, it can appear that the O-ring will not change its position in the groove. This moment can be recognized as a critical one since the gas/liquid pressure p is bigger than the average contact pressure σ_{ai} and the leakage can occur. Average contact pressure σ_{ai} after seal assembly can be determined from the formula [1]:

$$\sigma_{ai} = \frac{\pi}{6} \cdot E_{\infty} (2 \cdot \varepsilon + 0,13), \quad (1)$$

where:

E_{∞} – elastic modulus at the end of relaxation,

ε – relative compression; $\varepsilon = \frac{\Delta d}{d}$.

It results from Equation (1) that the bigger elasticity modulus E_{∞} of rubber the bigger average contact pressure. For rubbers there is known relation between elastic modulus and hardness; bigger E_{∞} corresponds with bigger hardness. In general, bigger rubber hardness gives smaller friction in dynamic conditions. However, it is necessary to keep in mind that the bigger hardness the smaller compression of the O-ring. Keeping the same compression rate and enlarging rubber hardness brings on the increase of both break-out friction and running friction.

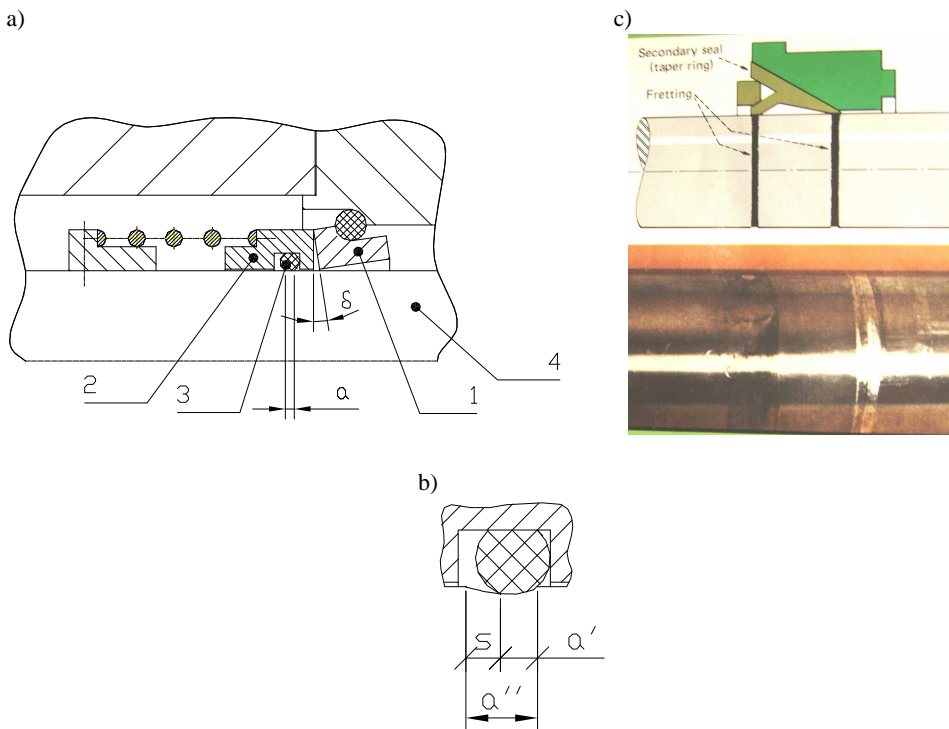


Fig. 2. Mechanical face seal, a) seal before operation, 1 – stationary ring, 2 – rotating ring, 3 – O-ring, 4 – shaft, b) wear track on the shaft surface, c) example of the real wear on the shaft surface

The tightness requirement necessitates the O-ring shifting in the groove and its contact with the vertical wall (Figure 1d). This contact enables the transfer of the me-

dium pressure through the O-ring made of elastic rubber on the confining walls of the groove. It means, that the operating contact pressure σ_{ao} will be equal [1]:

$$\sigma_{ao} = \sigma_{ai} + 0.9p, \quad (2)$$

where:

p – gas/liquid pressure.

The rubber fills up all potential surface irregularities while the operating contact pressure is sufficient to oppose the gas/liquid flow along the O-ring –walls interface.

O-rings and other elastomer seals can also be used as secondary seal in mechanical face seals, (Figure 2). It is a good example to show that in static seals it is exceptionally possible to meet an abrasive wear. Inclination δ of the stationary ring face 1 causes the vibrations of the rotating ring 2 together with the O-ring 3 (Figure 2a). High frequency of axial vibrations, poor lubrication at O-ring-shaft interface results in wear of both rubbing surfaces, (Figure 2b).

The wear of the O-ring increases its contact width with the shaft ($a' > a$, Figure 2b) what results in decrease of contact pressure value. Moreover, there is some wear of shaft surface; vibration of O-ring gives the wear track of slight depth and width of $a'' = s + a'$, where s is the amplitude of O-ring vibrations. Moreover, wear track is usually covered with scratches. All these circumstances, i.e. smaller contact pressure and the presence of the scratches can give rise to the leakage.

3. Friction and wear of dynamic seals

Friction force/torque can be recognized as the limiting factors in the case of the seals operating on the high-speed shafts. Elastomer oil lip seals sealing the engine crankshafts generate relatively small torque of the order of 0.4 Nm but their power consumption is very big because of big angular speed being equal to even 500 rad/s. This excessive power consumption leads, when combined with small heat conduction, to high temperature at lip-shaft interface and, in consequence, to fast rubber ageing. It results, that reduction of the power consumption is of vital importance for the seals co-operating with the high-speed shafts.

Friction decreasing is also important in the reciprocating seals for pneumatic cylinders. The lower friction the bigger efficiency of pneumatic cylinder and the easier positioning of its piston. There is practically no problem with the seals of the hydraulic cylinders due to better lubrication and high tightness level.

3.1. Friction and wear of elastomer seals rubbing against rotary shafts

It is not possible to reduce power consumption by means of the lubrication improvement since this latter can lead to the leakage. Although, recently, there are the attempts to improve lubrication at lip-shaft interface but only in the micro-scale.

There are two possibilities to reduce power consumption: through decreasing normal load which the lip exerts on the shaft [2] or by means of lowering the friction coefficient. It is well known [3] that friction coefficient f can be expressed as a sum of two components:

$$f = f_{\text{def}} + f_{\text{adh}}, \quad (3)$$

where:

f_{def} – deformation component,

f_{adh} – adhesion component.

According to Grosch [4] deformation component of the friction coefficient results from the internal friction in the rubber. Hence, one can write on:

$$f_{\text{def}} = C \cdot \text{tg} \varphi, \quad (4)$$

where:

C – constant,

φ – angle of internal losses.

The angle φ of internal losses depends on the rubber type, temperature as well as on the frequency of deformation. The external layer of the sealing lip is deformed by the surface roughness of the rotating shaft. Thus, there is an idea to lower f_{def} by means of the choice of the relevant shaft surface roughness. Let assume, that the area of local contact between the lip and the shaft surface is a function of the distributions of both profile ordinates and radii values of the shaft irregularities along the profile height. It has been found [5] that the most important profile of the shaft surface is that determined in circumferential direction; distribution of the ordinates density is left-hand for plunge ground surfaces with the roughness $0.12 \leq R_a \leq 0.64 \mu\text{m}$. Stabilization of the radii values on the level of mean \bar{r} value takes place at the relative approach ε to the shaft surface being $0.2 \leq \varepsilon \leq 0.3$. This approach can be easily realized in the oil lip seals where the average contact pressure is close to 1.0 MPa. The mean radius r^* of the local contact spot can be calculated from the equation

$$r^* \cong \sqrt{2\bar{r}h} \quad (5)$$

where:

\bar{r} – mean irregularities radius,

h – relative approach to the shaft surface profile; $h = d/\sigma$,

d – distance from mean line of profile,

σ – standard deviation of the ordinates distribution.

The knowledge of the mean radius r^* makes easy calculation of the deformation frequency ω of the local contact: $\omega \cong v/2r^*$, where v – linear speed of the shaft sur-

face. The results of deformation frequency of the local contact spots for the shaft linear speed $v = 13.2$ m/s (which corresponds to the rotary speed $n = 3000$ rpm of the shaft diameter $d = 88$ mm) are presented in Table.

Table. Deformation frequency of the local contact spots depending on the relative approach of the lip to the shaft surface profile.

spot radius	Shaft					
	$R_a = 0.12 \mu\text{m}$		$R_a = 0.32 \mu\text{m}$		$R_a = 0.64 \mu\text{m}$	
	$\bar{r} = 163 \mu\text{m}$		$\bar{r} = 67 \mu\text{m}$		$\bar{r} = 37 \mu\text{m}$	
frequency	$h = 3\sigma$	$h = 1\sigma$	$h = 3\sigma$	$h = 1\sigma$	$h = 3\sigma$	$h = 1\sigma$
$2r^*$, m	$\sim 20 \cdot 10^{-6}$	$\sim 11 \cdot 10^{-6}$	$\sim 20 \cdot 10^{-6}$	$\sim 11 \cdot 10^{-6}$	$\sim 18 \cdot 10^{-6}$	$\sim 10 \cdot 10^{-6}$
ω , s^{-1}	$\sim 7 \cdot 10^5$	$\sim 1.2 \cdot 10^6$	$\sim 7 \cdot 10^5$	$\sim 1.2 \cdot 10^6$	$\sim 7.3 \cdot 10^5$	$\sim 1.3 \cdot 10^6$

There are two important conclusions for plunge ground shaft surfaces resulting from the analysis of the data presented in Table:

- 1) in one and the same seal the deformation frequency can vary within one order of magnitude depending on the variation of the load over the lip perimeter,
- 2) it is sufficient to standardize the relative approach $h = d/\sigma$ of the lip to the shaft surface profile to get the same, independently on the mean radius \bar{r} value of asperities roundness, deformation frequency.

For the given range of the frequency variation $7 \cdot 10^5 \leq \omega \leq 1.3 \cdot 10^6 \text{ s}^{-1}$ the angle of internal losses varies within $2.5 \leq \varphi \leq 6.2^\circ$ for different grades of fluorinated rubbers (FKM) at ambient temperature. Its maximal value, and hence, maximal value of deformation component of friction coefficient, exists at lower frequency $10^3 \leq \omega \leq 10^4 \text{ s}^{-1}$.

Adhesion component f_{adh} of friction coefficient can be determined from the tests of the rubber samples on the one-ball tribometer [5] or from the knowledge of both the deformation component, and resultant friction coefficient f (Equation 3). For clean and dry fluor rubbers the adhesion component found during experiments on one-ball tribometer appeared to vary in the range of $0.46 \leq f_{\text{adh}} \leq 0.64$ at the average contact pressure: $0.57 \leq p_a \leq 0.86$.

Lubrication of the rubber samples lowered adhesion component to the following values: $0.07 \leq f_{\text{adh}} \leq 0.10$. These values are typical for either boundary or mixed friction.

The wear of the sealing lip can be, depending on the load distribution and the shaft surface roughness, not uniform or uniform. The first case (Figure 3) takes place when the shaft surface roughness is small ($R_a < 0.32 \mu\text{m}$) with right-hand ordinates distribution.

Seals operating on the rougher shafts ($R_a = 0.64 \mu\text{m}$) distinguish themselves with well developed uniform wear over whole lip perimeter (Figure 4).

Another seals produced from ACM rubber with the lip diameter of $\Phi 26.5$ mm cooperated with the drawn sleeves made of hardened steel. Sleeve surface roughness was isotropic with $R_a = 0.25 \mu\text{m}$ and mean radius of asperities $\bar{r} = 95 \mu\text{m}$. The average torque value was (0.2–0.37) Nm at the shaft speed $n = 1500$ rpm.

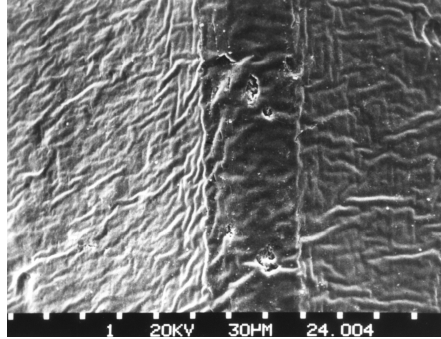


Fig. 3. Sealing edge of the lip made from FKM rubber rubbing against the shaft surface with $R_a = 0.12 \mu\text{m}$, there are only random wear traces

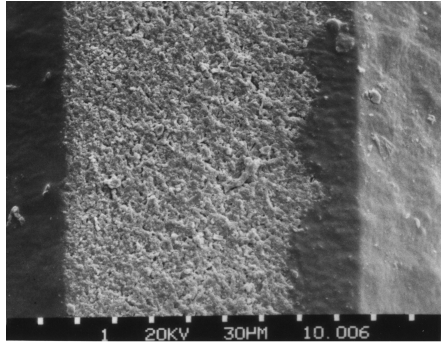


Fig. 4. Sealing edge with uniform wear track over the whole lip perimeter

Power consumption of these seals changed in the range of $(2.6\text{--}4.9) \text{ W/mm}^2$. It gives very high thermal load of the sealing edge. The outlook of the worn lip gives the evidence of adhesive wear with typical cracks distributed over the smooth rubber surface (Figure 5).

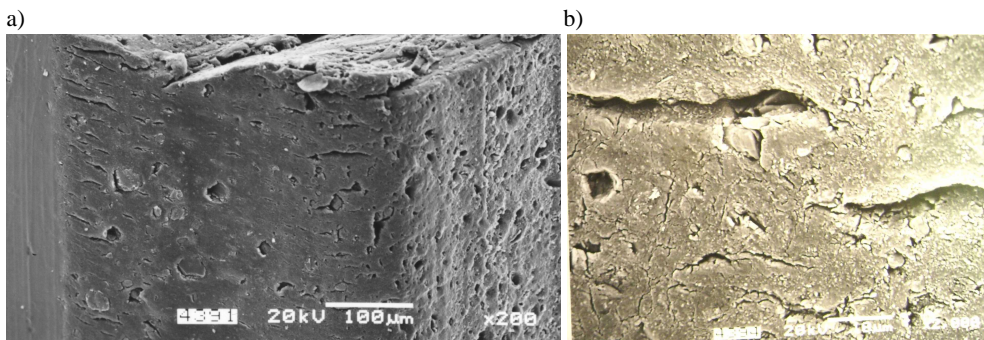


Fig. 5. The worn lip surface, a) general view, b) magnification

It was possible to anticipate this type of wear during analysis of the shaft roughness. Shaft surface had right-hand distribution of ordinates frequency density, with high concentration of ordinates, small value of reduced height R_{pk} of upper part of surface roughness and small ratio $R_t/\bar{r} = 0.03$ where R_t – profile height. All these roughness features made difficult an oil access to the sealing edge.

3.2. Friction and wear of elastomer seals operating in pneumatic cylinders

Seals for pneumatic cylinders operate under pressures not bigger than 1MPa. Shape of the seal should ensure low friction. Pneumatic seals more often work in dry conditions than in wet ones. Seals can be lubricated through oil-mist, oil-fog or by special greases. Frictional losses in pneumatic cylinders should not exceed 5% of total force required at the end of the rod. O-rings are used for smaller sizes and lighter duties as reciprocating seals. The most favorable conditions for O-ring operation are: short piston/rod stroke, adequate lubrication and moderate velocities, (Figure 6). Slow speed and low air pressure tend to develop high friction which can lead to the O-ring failure.

U-rings made from relatively soft elastomer give good sealing at low pressure and with small friction. There are also used composite seals like ring made of low friction material (e.g. PTFE) energized by O-ring.

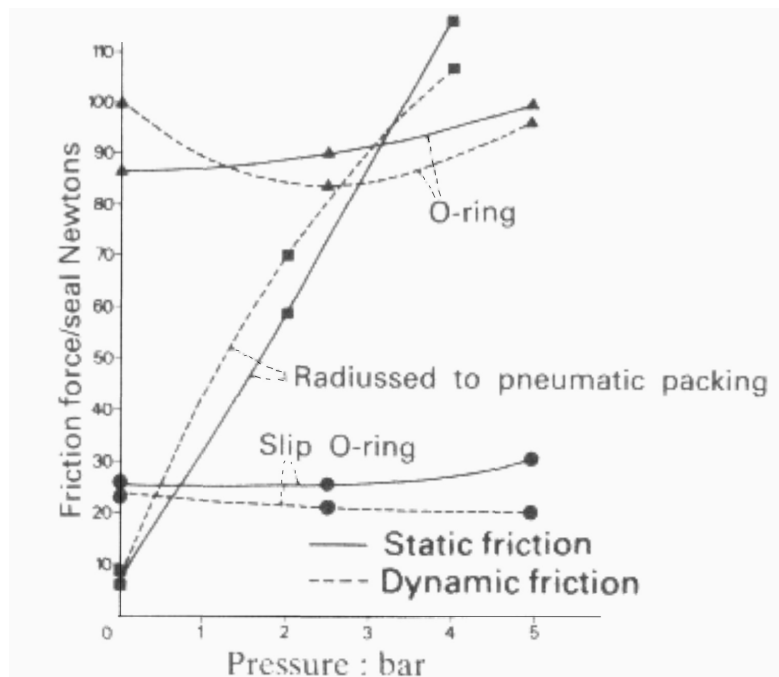


Fig. 6. Friction force versus pressure under dry conditions [6]

The variation of friction with rubbing speed comprises three stages (Figure 7). Static friction is usually big but once break-out has been initiated the friction coefficient drops down to a low value at low velocities and becomes bigger as the velocity increases.

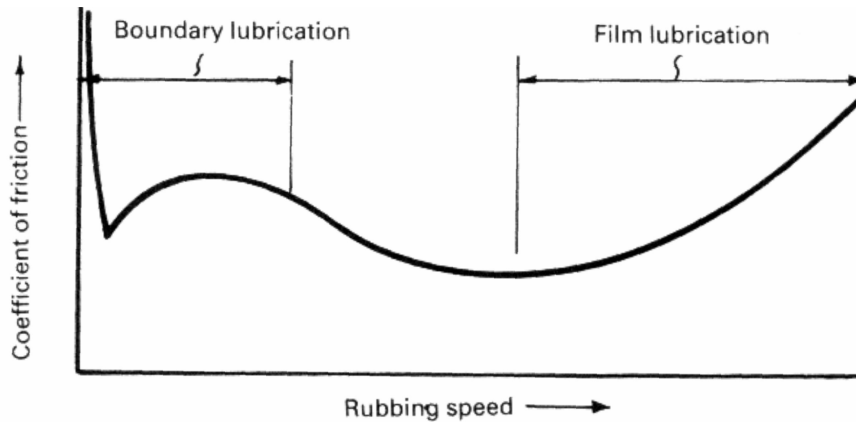


Fig. 7. Variation of friction coefficient versus speed [6]

The most dangerous to the seal operation in pneumatic cylinders is the effect of idle time since the increase of friction coefficient is quite fast with the stay at the rest. Friction coefficient of the dry seal can be ten times bigger than that of the same seal operating under lubricated conditions (except for PTFE seals). One can minimize this adverse effects protecting the seal against drying and producing the cylinder surface with such roughness that the seal material will not adhere.



Fig. 8. Abrasive wear of the guiding ring

Stick-slip motion takes place then, when the seal is allowed to dry out, when the surface finish is poor and when there is inadequate lubrication. Figure 8 presents the worn surface of the guiding ring used on the piston.

4. Conclusions

The paper can be summarized by means of the following conclusions:

- 1) the break-out friction should be minimized by means of the choice of adequate squeeze of the seal made of given grade of rubber,
- 2) minimization of power consumption of the seals co-operating with high-speed shafts can be achieved through lowering normal force exerted by the seal on the surface and by lowering friction coefficient,
- 3) deformation component of friction coefficient is determined by internal friction in the elastomer. It can be minimized by the choice of relevant shaft surface roughness ensuring adequate deformation frequency of the contact spots,
- 4) the wear of sealing edge depends on both the contact pressure and shaft surface roughness; it is recommended to have surface roughness with left-hand distribution of ordinates density frequency and with mean radius of all asperities in the range of $30 \leq \bar{r} \leq 90 \mu\text{m}$ in order to get uniform wear track over whole seal perimeter,
- 5) adhesion component of friction coefficient is important then, when the seal operates at dry condition; it can amount up to 0.64 at the contact pressure values met in oil lip seals. There is dramatic drop of this coefficient in lubricating conditions.

References

- [1] Karaszkievicz A.: *Hydrodynamics of the seals used in hydraulic drives* (in Polish), Prace Naukowe P.W., z.159, Oficyna Wydawnicza P.W., Warszawa, 1994.
- [2] Gawliński M., Konderla P., Upper G.: *Optimization of crankshaft seals*, Vol. 41, SAE Transact., 1989.
- [3] Kragelski J.V.: *Friction and wear* (in Russian), Mashinostroenie, Moskva, 1978.
- [4] Grosch K.A.: *The relation between the friction and visco-elastic properties of rubber*, Proc.R.Soc., A274, 1996, pp. 21–39.
- [5] Gawliński M.: *Local contact conditions and frictional losses in oil lip seals* (in Polish), Oficyna Wydawnicza PWr., Wrocław, 2004.
- [6] *Seals and sealing handbook*, 2nd Edition, The Trade&Technical Press Ltd., Anglia, 1986.

Tarcie i zużycie uszczelnień elastomerowych

W artykule omówiono wpływ zarówno tarcia jak i zużycia na działanie uszczelnień elastomerowych. Tarcie należy traktować jako niezwykle ważny czynnik determinujący działanie nie tylko uszczelnień zespołów obrotowych i posuwisto-zwrotnych maszyn, ale również działanie uszczelnień spoczynkowych. Zmniejszenie współczynnika tarcia w uszczelnieniach ruchomych

nie można przeprowadzić poprzez poprawę smarowania powierzchni trących, bowiem może to prowadzić do zwiększenia wycieku. W referacie przedstawiono sposoby obniżenia oporów ruchu uszczelnień elastomerowych poprzez zmniejszenie składowej deformacyjnej jak i adhezyjnej współczynnika tarcia zarówno w warunkach smarowania granicznego/mieszanego jak i braku smarowania.



Introducing an effective new ship rudder type, Telescopic Rudder

S. E. GHAZI-ASGAR

Msc graduate of Amirkabir University of Technology, Iran Shipbuilding and Offshore Industrial Complex Co.

H. ZERAATGAR

Assistant Professor Amirkabir University of Technology Faculty of Marine Technology

M. GHIASI

Assistant Professor Amirkabir University of Technology Faculty of Marine Technology

Rudder is the most important controlling device in ship maneuvering. Usually, it is a passive equipment of a ship, which generates the control forces and moments by inflow velocity and loses its performance when the ship speed reduces. Many parameters are involved in rudder design such as rudder's shape, area and span. By increasing rudder span, the aspect ratio, rudder area and rudder forces are increased. In addition, research shows that the increasing of rudder aspect ratio is the best option to receive highest performance of rudder than any other change of rudder parameters. Having known that the rudder dimensions limited by ship stern form, rudder span is limited to the ship overall geometry and the stern geometry.

In this research, a new and innovative ship rudder type (Telescopic Rudder) is suggested that allows enlarging the rudder height hence increasing the rudder aspect ratio. This improves the controllability (maneuverability) of vessel by increasing the hydrodynamic coefficients of rudder.

The telescopic rudder made by two pieces, which secondary part slides into the main part. A hydraulic system is used to facilitate sliding thus increasing the rudder height, increasing the aspect ratio and area of rudder producing larger forces. A computer code is also developed to investigate the hydrodynamic characteristics of telescopic rudder by boundary element method (3D-panel). The effectiveness of the new rudder type is studied by the said code in comparison with the conventional type.

Keyword: *telescopic rudder, hydrodynamic force, maneuverability, aspect ratio*

Nomenclature

Y_δ – derivative of Y with δ , rudder deflection angle

N_δ – derivative of with δ

\bar{b} – mean span

\bar{c} – mean chord

A_r, A_R – rudder area

λ, Λ – aspect ratio

α – angle of attack

L – lift force

D – drag force

Y_{rudder} – rudder control force

N_{rudder} – rudder control moment

- β_R – drift angle
 x_R – distance from the origin of the ship to the C.P. of the rudder
 x, y, z – system of reference axis
 ϕ – potential function
 u, v – velocity components
 $r = \dot{\psi}$ – angular velocity
 $\dot{u}, \dot{v}, \ddot{\psi}$ – acceleration components
 Δ – displacement
 I_Z – mass moment of inertia
 X, Y – resultant total force
 N – resultant total moment
 $X_u, X_{\dot{u}}$ – derivative of X with u, \dot{u}
 u_1 – initial value of u
 $Y_v, Y_{\dot{v}}, Y_r, Y_{\dot{r}}$ – derivative of Y with v, \dot{v}, r, \dot{r}
 $\Delta u_1 = u - u_1$
 $N_v, N_{\dot{v}}, N_r, N_{\dot{r}}$ – derivative of N with v, \dot{v}, r, \dot{r} .

1. Introduction

Nowadays, considering the increasing number of ships and shipping lines in merchant ship market and also the navy ships, necessity of good maneuvering characteristics is obvious. Consequently, a large variety of control devices of ship motion and maneuvering have been presented.

Rudder is the most important part of ship maneuvering system; so about 15 different types of rudder are suggested till now for various vessel types with different operation and efficiency. In this paper, we will introduce a new type of ship rudder with improved hydrodynamic force and ship maneuverability.

A control surface has one sole function to perform in meeting its purpose and that is to develop a control forced in consequence of its orientation and movement relative to the water [1]. The control force produced by a rudder at the stern of a vessel creates a moment, $N_{\delta}\delta_R$ which causes the ship to rotate and orient herself at an angle of attack to the flow. These forces and moments which are created due to this rotation and angle of attack, will determine the maneuvering characteristics of the ship.

2. Rudder

Some parameters such as principal dimensions of the ship, geometry and body lines of the vessel, rudder and other control surfaces, propulsion system containing engine, gearbox, shafting and propeller are the most important parameters in ship maneuvering and steering. Ship steering means determine the ship location and the direction of her positioning.

Based on this description, the surge, sway and yaw motions are the main movements in the ship maneuvering. The rolling motion has a minor effect on the maneuvering calculations; but because of generating the roll in turning, this motion has been investigated in maneuvering too.

The equations of motion can be simplified as below in the local coordinate system fixed on the ship:

$$\begin{aligned}
& -X_u(u - u_1) + (\Delta - X_{\dot{u}})\dot{u} = 0, & \text{Surge} \\
& -Y_v v + (\Delta - Y_{\dot{v}})\dot{v} - (Y_r - \Delta u_1)r - Y_{\dot{r}}\dot{r} = 0, & \text{Sway} \\
& -N_v v - N_{\dot{v}}\dot{v} - N_r r + (I_z - N_{\dot{r}})\dot{r} = 0, & \text{Yaw}
\end{aligned} \tag{1}$$

where $\frac{\partial x}{\partial u} = x_u$, $\frac{\partial y}{\partial u} = y_u$, ..., $\frac{\partial N}{\partial \dot{\psi}} = N_{\dot{\psi}} = N_{\dot{r}}$.

By adopting the non-dimensional form of equations of motion and neglecting the surge, Equation (1) becomes as follows:

$$\begin{aligned}
& -Y'_v v' + (\Delta' - Y'_{\dot{v}})\dot{v}' - (Y'_r - \Delta')r' - Y'_{\dot{r}}\dot{r}' = 0 \\
& -N'_v v' - N'_{\dot{v}}\dot{v}' - N'_r r' + (I'_z - N'_{\dot{r}})\dot{r}' = 0
\end{aligned} \tag{2}$$

where:

$$\begin{aligned}
\Delta' &= \frac{\Delta}{0.5\rho L^3}, & v' &= \frac{v}{V}, & \dot{v}' &= \frac{\dot{v}L}{V^2}, \\
I'_z &= \frac{I_z}{0.5\rho L^5}, & r' &= \frac{rL}{V}, & \dot{r}' &= \frac{\dot{r}L^2}{V^2}.
\end{aligned} \tag{3}$$

In Equation (1) and (2) must include the effect of the ship's rudder held at zero degree. On the other hand, if we want to consider the path of the ship with controls working, the equation of motion must include terms on the right-hand side expressing the control forces and moments created by rudder deflection as a function of time [1].

The linearized component of the force created by rudder deflection acting at the center of gravity of the ship is $Y_{\delta}\delta_R$ and the linearized component of the moment created by rudder deflection about the z-axis of the ship is $N_{\delta}\delta_R$ where δ_R is the rudder deflection angle and Y_{δ} , N_{δ} are the linearized derivatives of Y and N with respect to rudder deflection angle δ_R [1].

With these assumptions and some simplifications, the equations of motion including the rudder force and moment are as follows:

$$\begin{aligned}
\Delta'_y \dot{v} - Y'_v v' - (Y'_r - \Delta) r' &= Y'_\delta \delta_R, \\
n'_z \dot{r}' - N'_v v' - N'_r r &= N'_\delta \delta_R, \\
n'_z &= I'_z - N_r \cong 2I_z, \\
\Delta'_y &= \Delta' - Y'_v \cong 2\Delta'.
\end{aligned} \tag{4}$$

The simplest and most common type of control surface is the all-movable rudder. Chord dimension parallel to the direction of motion, span dimensions normal to the direction of motion and thickness dimension normal to both the span and the chord. The mean value of chord is \bar{c} and the mean span \bar{b} is the average of the span of leading and trailing edges of the rudder. The ratio $\lambda = \bar{b} / \bar{c}$ is the geometric aspect ratio and the profile area A , may be taken as $\bar{b} \times \bar{c}$ [1].

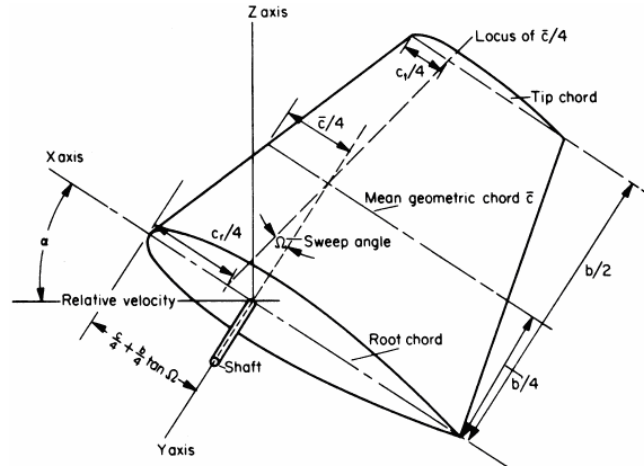


Fig. 1. Typical Rudder Shape

Consider a rudder as a separated body which fully immersed in an inviscid fluid and a uniform flow which unaffected by ship hull and propeller hits the rudder by angle of attack α . The combination of forward velocity and angle of attack will induced a circulation around the rudder which produces a lift force on the rudder. Since the flow is considered in the steady state, two dimensional, ideal, non-viscous and deeply submerged, there is no drag force and the total force due to the angle of attack will act normal to the direction of free-stream velocity. However, because rudder has a finite aspect ratio, two dimensional theory dose not accurately predict the acting forces. When the rudder is at an angle of attack, vortices are shed over the root and tip of the rudder, which induce velocities in the plane determined by the span and thickness. These velocities when added to the stream velocity cause an induced drag force in the direction of motion [1].

The total resultant hydrodynamic force in a real fluid arising from the effects described in above is shown in Figure 2 as acting at a single point called the center of pressure. This force may be variously resolved into any number of components. The three components which involve in ship control are a lift (L), normal to the direction of motion; drag (D), parallel to the direction of motion, and a y -component normal to the axis of the ship. This latest component is the reason for having rudder. If there were no interaction between the pressure field around the rudder and the adjacent ship and its appendages, this y -component would be the control force $Y_{\delta}\delta_R$ and the moment of this component about the z -axis of the ship would be the control moment $N_{\delta}\delta_R$.

$$\begin{aligned} Y_{\delta}\delta_R &= Y_{rudder} = \pm(L \cos \beta_R + D \sin \beta_R) \\ N_{\delta}\delta_R &= N_{rudder} = Y_{rudder} \cdot x_R \\ X_{rudder} &= L \sin \beta_R - D \cos \beta_R \end{aligned} \quad (5)$$

Where the drift angle at the rudder is β_R , x_R is the distance from the origin of the ship to the C.P. of the rudder [1].

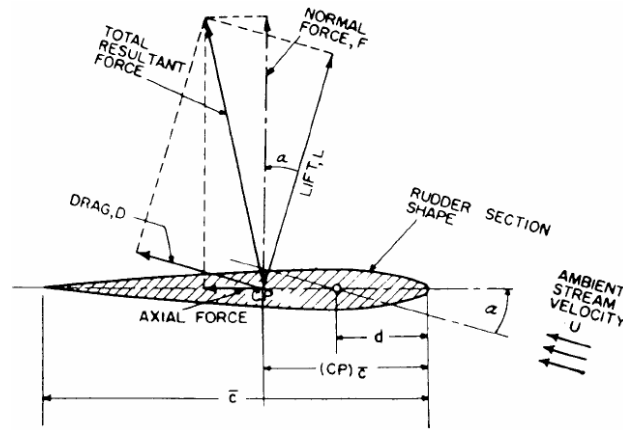


Fig. 2. Rudder Force

Whose component of the total rudder force which introduced, F is of importance in rudder design and the production of this component times the distance of the center of pressure from the centerline of the rudder stock yields the hydrodynamic torque experienced by the stock. The rudder effectiveness in maneuvering is mainly determined by the maximum transverse force acting on the rudder. Rudder effectiveness can be improved by:

- rudder arrangement in the propeller slipstream,
- increasing the rudder area,
- better rudder type,

• shorter rudder steering time [2]. There are various kind of rudder developed over the years.

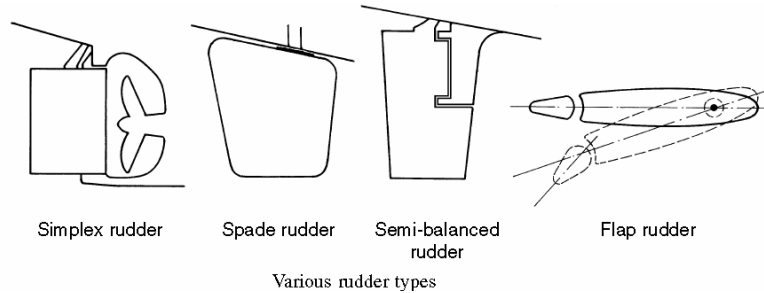


Fig. 3. Rudder Type [2]

- Rudder with hell bearing (simplex),
- spade rudder,
- semi-balanced rudder,
- flap rudder,
- rudder with rotating cylinders,
- active rudder/rudder propeller,
- voith schnider,
- speed z-drive,
- kitchen rudder,
- jet flap rudder [2].

And now we present the new one type called telescopic rudder.

3. Primary plan of a new rudder (Telescopic Rudder)

In present study a new rudder type is developed which provides the arbitrarily increasing of rudder height, so a more effective rudder will be achieved. Because of restricted aspect ratio, there is no similar flow pattern in parallel level with rudder section area, normal to its vertical axis. In addition in both ends of rudder, three dimensional cross flows will be created which by decreasing of the aspect ratio; these cross flows will increase and lead to reduce of the generated lift force by rudder in various angles of attack.

Whatever the rudder's root will close to the hull, the creation of cross flows in this part will be avoided; thus the lift coefficient of rudder will increase. Also because of small distance between rudder tip and the outward flow from the propeller, the cross flows are strongly created in this region (rudder tip) which causes to generate flow in-plane of rudder and reduce the lift coefficient. In addition there are many factors involved in rudder design. The most important parameters are rudder shape, area and height.

Rudder must be located in the limited region by the stern geometry. This restricts the rudder dimensions. The telescopic rudder idea makes it possible to loose these limitations during free navigation and achieve more effective rudder.

Increasing the rudder height has a direct influence on some parameters such as aspect ratio, rudder area and decreasing the 3-d cross flow over the rudder root and tip. In addition increasing the stability of ships with high block coefficient, more control on rolling angle and having a more efficient rudder even at low speed near the harbor are some benefits of increasing the rudder height.

The telescopic feature makes it possible to save the previous gains and in necessary conditions such as crossing the shallow channels or in docking condition, comply with shape of ship restrictions and brings out the rudder to initial shape.

4. Structure of telescopic rudder

The telescopic rudder design consists of two parts which the smaller rudder is located inside of the main one and has the ability to slide through it (open/close). The main part is similar to a conventional rudder and in close situation (when the smaller part locates inside the main part) it is exactly a conventional rudder.

The second part which is located inside the main part structure (mother), is smaller and in certain time it can slide out by a control system (hydraulic control) and increase the rudder span; therefore the aspect ratio of rudder will be increased due to increased rudder span and regarding enlargement of rudder area, the greater force and torque will be created.

The telescopic rudder design is more suitable for a large vessel with single passive rudder and propeller. At occurring an accident such as ship collision, by using the telescopic rudder escape from the dangerous area in shorter time and space can be done.

In addition this rudder can help faster maneuvering in harbor area if the water depth would be suitable for its usage. Also this feature is more useful for various sizes of naval vessels during missions. It can provide more powerful maneuvering according to ship speed and it is suitable for track of a target faster and escape from torpedo. Regarding the structural considerations, rudder should be stiffened with vertical and horizontal webs. For installation of the sliding part in main rudder, the arrangement of stringer plate should be in a manner state that in addition to the strength of the main rudder, the required space for moving of the sliding part can be provided. Worthy of mention, this feature is capable to done for various kind of rudder type such as all-movable or horn rudder, etc.

There are some structural configuration and manner of telescopic rudder operation shown in below Figures.

Just as seen in model A, by increases the number of horizontal web plate instead of vertical and hollowed one, the structural strength of rudder have been provided. Model B stiffened as usual however because of hollow stringer the number of stiffening web increased. Model C is a simple prototype of horn rudder which can be stiffened similarly as both previous models.

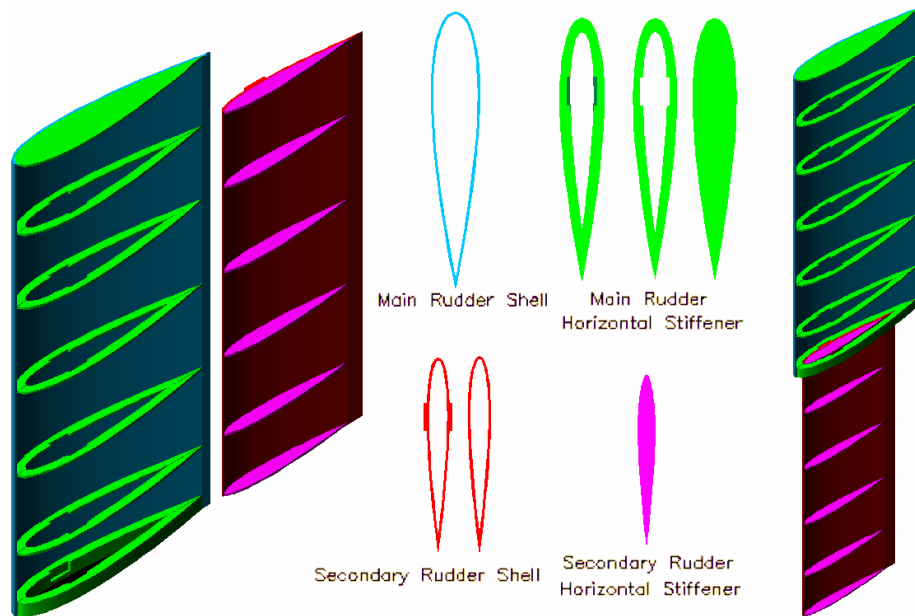


Fig. 4. Telescopic Rudder – Model A

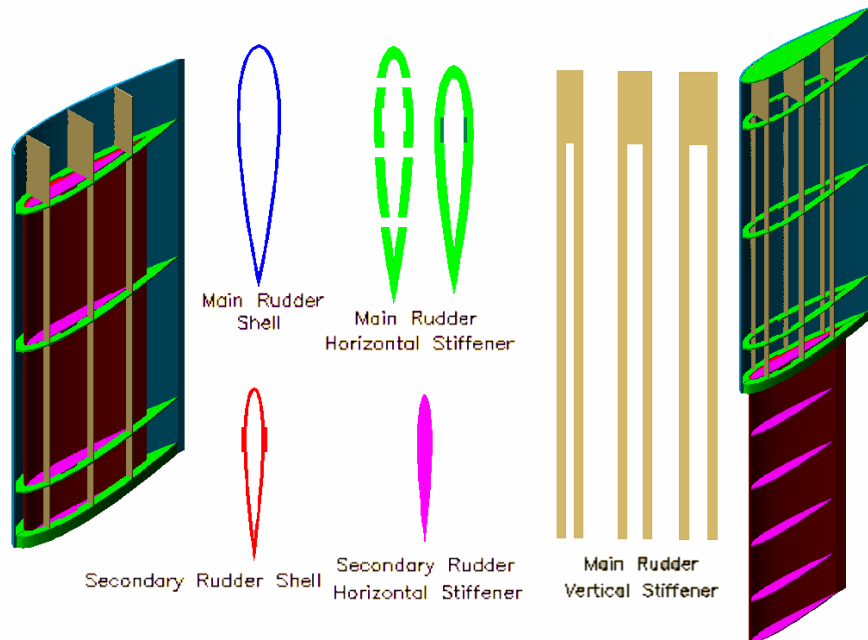


Fig. 5. Telescopic Rudder – Model B

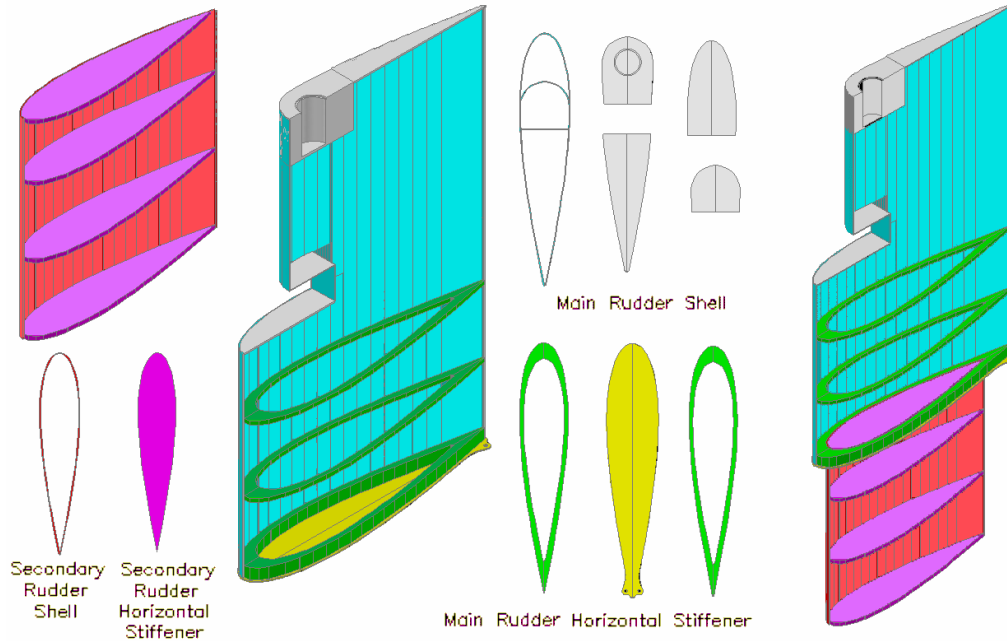


Fig. 6. Telescopic Rudder (horn) – Model C

There are several challenges in field of machinery and equipment in telescopic rudder which mentioned briefly as following:

- designing of the control system for rudder movement,
- designing of the steering gear and bearing for rudder,
- designing the proper structure to achieve an acceptable requirement,
- sealing the rudder containing design a seal or sealing system (e.g. using compress air system to prevent water influence during slide telescopic part),
- examine the fouling of sliding part and its effect on seal system.

5. Mathematical model for hydrodynamics aspects

Potential theory is an extremely well developed and elegant mathematical theory, devoted to the solution of Laplace's Equation:

$$\nabla^2 \varphi = 0. \quad (6)$$

There are several ways to view the solution of this equation. The one most familiar to aerodynamicists is the notion of "singularities". These are algebraic functions which satisfy Laplace's equation, and can be combined to construct flowfields.

The most familiar singularities are the point source, doublet and vortex. We can write the expression for the potential at any point P as

$$\phi(p) = \frac{1}{4\pi} \oint_{S_0} \left[\frac{1}{r} \nabla \phi - \phi \nabla \left(\frac{1}{r} \right) \right] n ds. \quad (7)$$

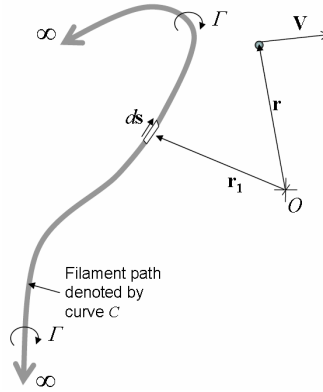


Fig. 7. Filament vortex and flow field

The value of ϕ at any point P is now known as a function of ϕ and $\partial\phi/\partial n$ on the boundary. By using filaments vortex for distribution of singularities along surface we can determine the velocity field from the Biot Savart law as below:

$$V(r) = -\frac{\Gamma}{4\pi} \int_c \frac{(\vec{r} - \vec{r}_1) \times d\vec{s}(\vec{r}_1)}{|\vec{r} - \vec{r}_1|^3}. \quad (8)$$

6. Relation between aspect ratio and hydrodynamic coefficient

In present numerical modeling, we use below model for study aspect ratio and hydrodynamic coefficient relationship.

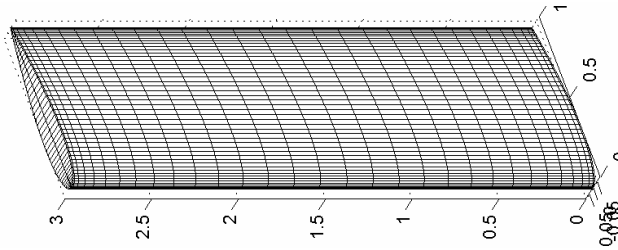


Fig. 8. NACA 0018, 100×20 mesh size

Gain result shown in Figure 9.

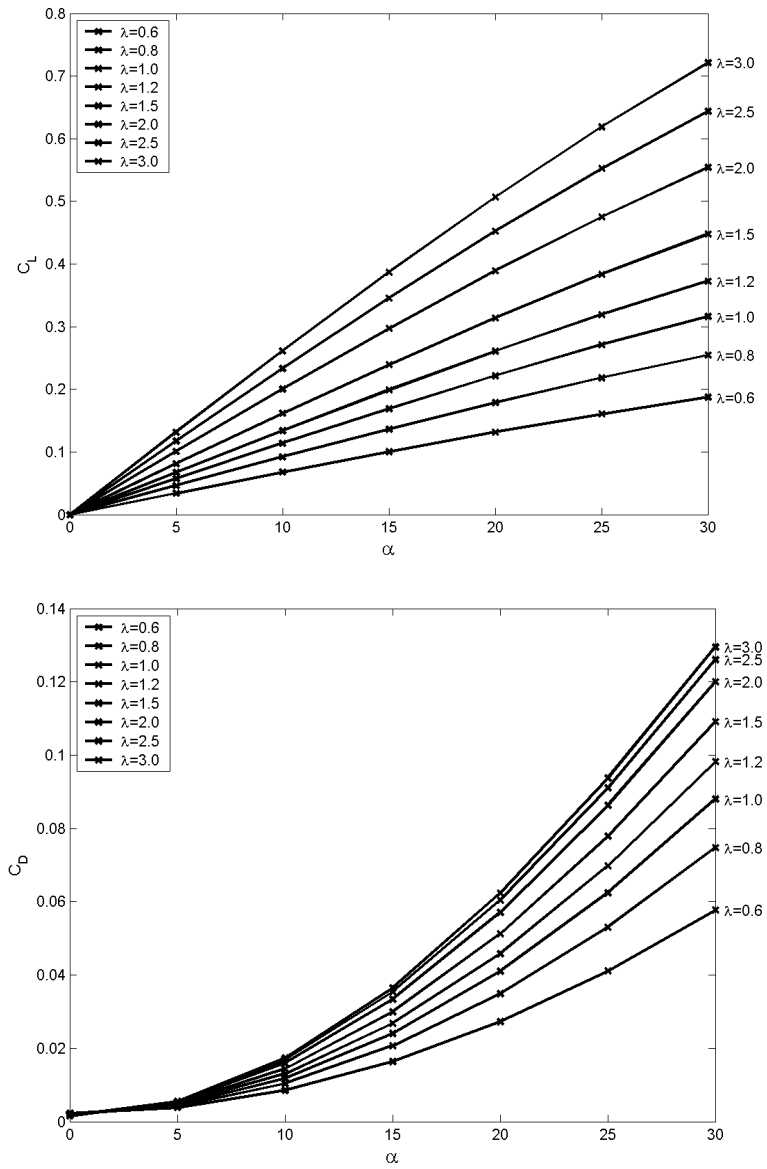


Fig. 9. Relation between Lift & Drag coefficient with α and λ

Conform to suppose, by increasing the aspect ratio the lift and drag coefficient will be increased. In Figure 10 the changing location of center of pressure with increasing aspect ration has been shown.

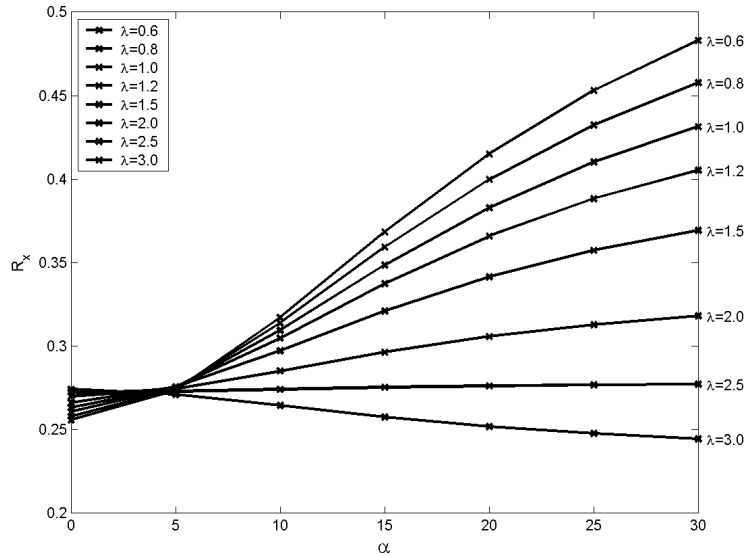


Fig. 10. Relation between R_x with α and λ

Regarding this Figure we can find that when λ increase the position changing in CP will decrease. Therefore the hydrodynamic torque acting on rudder stock will have a brief changes, which is appropriate for design of rudder shaft. This is a one of the other advantage of using telescopic rudder.

7. Effect of enlarging rudder span on hydrodynamic coefficient

According to above obtained results, we investigate the enlarging rudder span on lift and drag coefficient now. We consider below models:

Rudder with NACA 0018, span height $h = 3$, chord length $C = 1$, angle of attack $\alpha = 15^\circ$, taper ratio = 1.3, telescopic chord length $0.75 \times C$, leading edge offset 0.1.

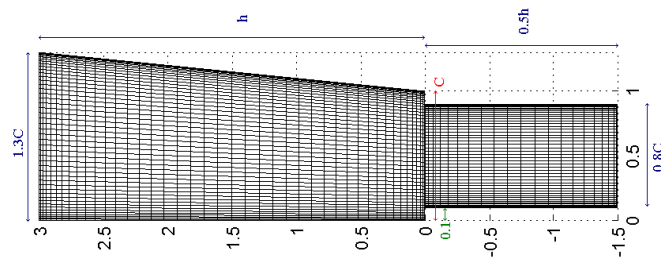


Fig. 11. Rudder Geometry Data

Mesh size table as follow, where n is the number of panel on rudder circumference, m is the total number of panel along span (include main and sliding part).

Table. Mesh size

h' / h	$n \times m [m_1]$	type
0	119×54	1
0.05	119×50 [42]	2
0.10	119×53 [43]	3
0.15	119×55 [43]	4
0.20	119×55 [41]	5
0.25	119×59 [43]	6
0.30	119×61 [43]	7
0.35	119×59 [40]	8
0.40	119×61 [40]	9
0.45	119×61 [38]	10
0.50	119×59 [36]	11
0.55	119×61 [36]	12
0.60	119×61 [34]	13

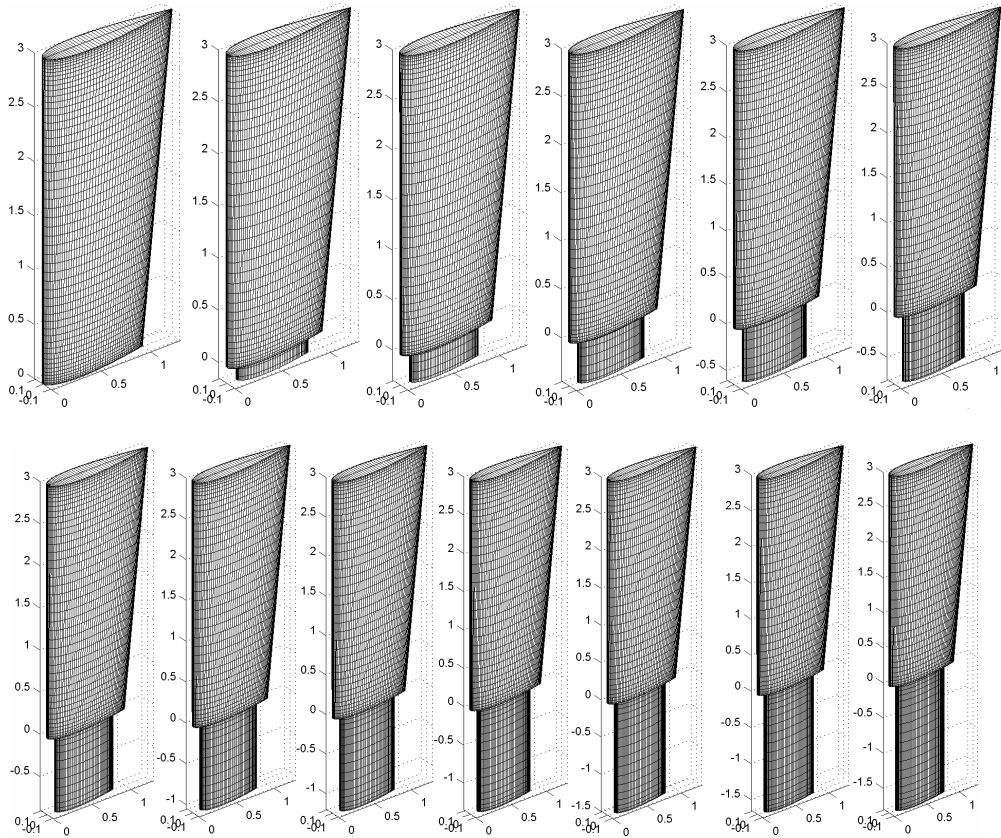


Fig. 12. Telescopic Rudder Geometry

As it expected by increasing rudder span the hydrodynamic rudder force increased.

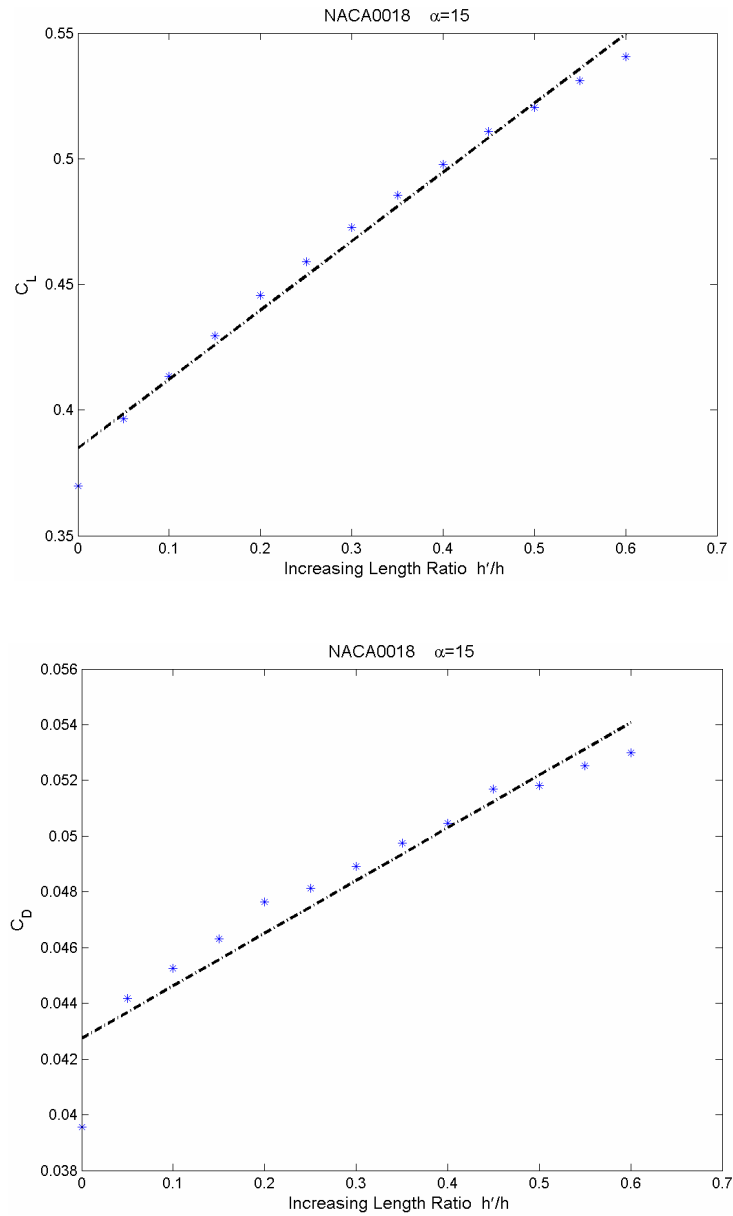


Fig. 13. Lift & Drag Coefficient Vs Increasing height

Regarding Figure 13 there is linear relation between increasing rudder span with hydrodynamic coefficients. If the rudder height increases 0.6 time to initial height the lift and drag coefficient will increase 1.46 and 1.34 times respectively and improve the maneuvering characteristics.

The Figure 14 and 15 show the contour of pressure coefficient on rudder and the stream lines in model 13.

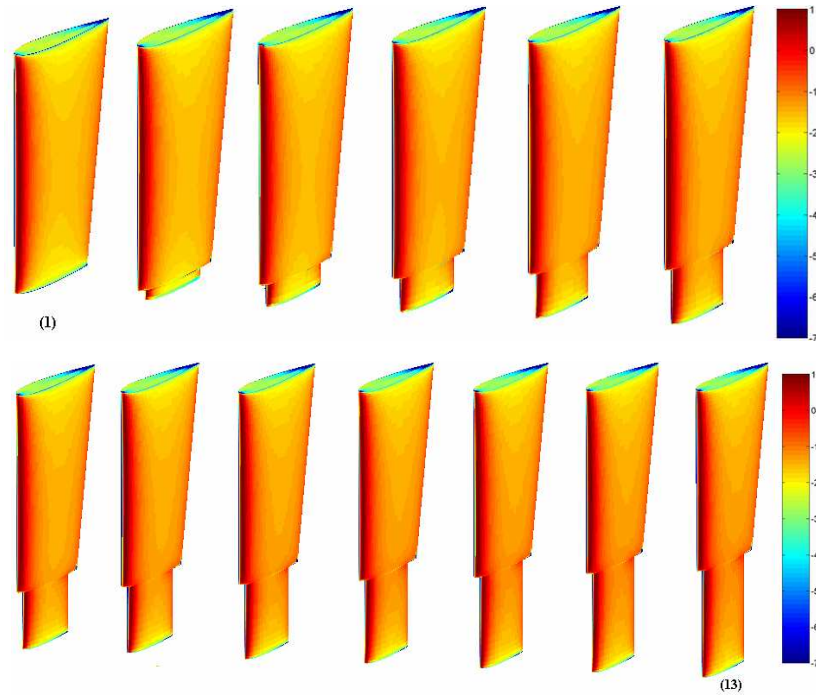


Fig. 14. Contour of Pressure Coefficient

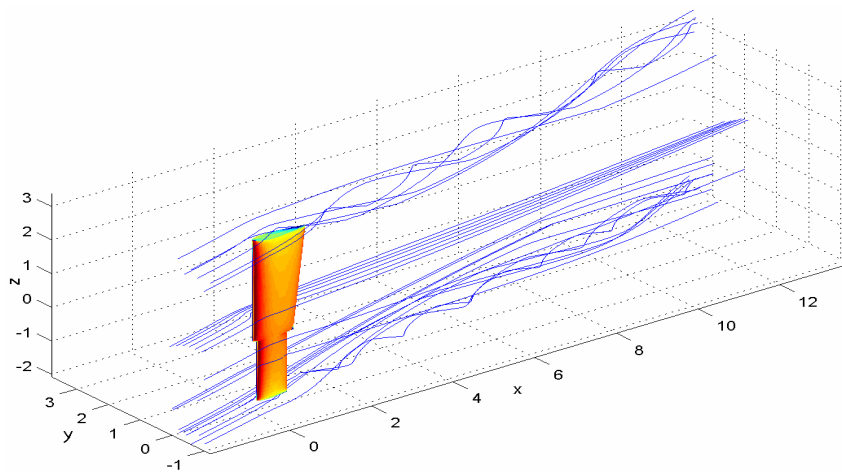


Fig. 15. Streamline on telescopic rudder

8. Conclusions and closing remarks

- There are linear relationship between enlarging rudder span with lift and drag coefficient.
- Position changing of CP in high span rudder is less than low span. Therefore the hydrodynamic torque acting on rudder stock will have a brief changes, which is appropriate for design of rudder shaft.
- Increasing the rudder height has a direct influence on aspect ratio, rudder area and decreasing the 3-d cross flow over the rudder root and tip. Therefore we observed increasing lift coefficient value.
- Because of discontinuity in connection of main to telescopic part of rudder, vortex flows have been created in downstream flow.
- Increasing the lift and drag coefficient will increase the lift and drag force consequently maneuvering characteristic of vessel will improved.

References

- [1] Lewis E. V.: Editor. *Principles of naval architecture*, Vol. III Second Edition, Pub. The Society of Naval Architects and Marine Engineers, Jersey City, New York, 1989.
- [2] Volker Bertram: *Practical Ship Hydrodynamics*, Pub. Butterworth-Heinemann. First published, 2000.
- [3] Mason W. H.: *Applied computational aerodynamics*, Professor of Aerospace & Ocean Engineering Virginia Polytechnic Institute & State University, 1998.
- [4] Devenport W.: *Wings in ideal flow & non-lifting 3D flow*, Virginia Tech Department of Aerospace and Ocean Engineering, 2005.

Nowy efektywny ster okrętowy – ster teleskopowy

Ster jest najważniejszym urządzeniem kontrolującym w trakcie manewrowania statkiem. Zazwyczaj jest pasywnym elementem wyposażenia statku, który wytwarza siłę i moment dzięki napływowi wody, i traci sprawność, gdy prędkość statku się zmniejsza. Z projektowaniem steru związanych jest wiele parametrów takich jak kształt, pole powierzchni i rozpiętość steru. Przy zwiększaniu rozpiętości steru rosną wydłużenie, pole powierzchni i siły. Badania pokazują, że zwiększenie wydłużenia steru jest, w porównaniu ze zmianą każdego innego parametru, najlepszym rozwiązaniem, żeby uzyskać najwyższą sprawność steru. Ponieważ wymiary steru są ograniczone przez kształt rufy statku, rozpiętość steru zależy od rozmiarów statku i rufy.

W trakcie badań opracowano nowy typ steru - ster teleskopowy, który pozwala na zwiększenie wysokości steru, a dzięki temu na zwiększenie wydłużenia. To rozwiązanie pozwala na poprawienie sterowności statku poprzez zwiększenie wartości współczynników hydrodynamicznych steru.

Ster teleskopowy składa się z dwóch części. Część ruchoma przesuwa się wewnątrz części podstawowej. Do przesuwania części ruchomej został zastosowany układ hydrauliczny. Po wysunięciu części ruchomej zostaje zwiększona wysokość steru, co powoduje wzrost wydłużenia, powierzchni steru i siły hydrodynamicznej. W celu zbadania charakterystyki hydrodynamicznej steru teleskopowego opracowany został program komputerowy oparty na metodzie elementów brzegowych (trójwymiarowa metoda panelowa). Przy pomocy wspomnianego programu zbadana została efektywność nowego steru w porównaniu ze sterem konwencjonalnym.



Friction and wear of resin-based dental materials

J. KLECZEWSKA

Institute of Polymer & Dye Technology, Technical University of Łódź, Stefanowskiego 12/16, 90-924 Łódź, Poland

D. M. BIELIŃSKI

Institute of Polymer & Dye Technology, Technical University of Łódź, Stefanowskiego 12/16, 90-924 Łódź, Poland

Rubber Research Institute "STOMIL", Harcerska 30, 05-820 Piastów, Poland

Commercially available resin-based dental composites were studied. Their friction and wear kinetics were determined, together with the microhardness of materials. Tribological examinations evidenced that friction force characteristics are different for various composites - equilibrating slower or faster. However, in some cases, friction may also present a constant value during the whole experiment. The friction force characteristics have been found being related to abrasion kinetics of dental composites.

Microindentation experiments provided interesting information on the hardness of dental composites. It has been found, that in the most cases, composites studied exhibit the surface gradient of hardness. Generally, the harder and the stiffer the material the higher its abrasion, what follows a micromechanical model of friction.

Keywords: *dental materials, hardness, friction, wear*

1. Introduction

Amalgam has been used for more than century to fill posterior tooth. Its low price and rapid application have made it the most economic dental filling material. The material is also stronger and more durable than most of available alternatives. However, the increasing demand for more esthetic restorations has made posterior composites a strong alternative to amalgams.

The esthetic revolution began in 1970s, "accidentally" with an observation that mercury vapor was released itself from amalgam and could be inhaled. Controversy about mercury toxicity was a principal reason for replacing amalgam restorations with other, safer materials. Nowadays, the usage of amalgam is in demise and composite resins replace it gradually. Popularity and proliferation of this kind of material are connected with its advantages: good mechanical properties, high resistance to dissolution and esthetic qualities. But its poor abrasion and fracture resistance when placed in stress-bearing areas may limit its application. It is obvious, that if material scientists want to develop more resistant composite, they should try to deeper understand wear process, from the structural and clinical point of view. It must be pointed up, that not only the amount and the rate of wear are important but, first and foremost, wear

mechanisms. It is really tough problem, because the wear of tooth and dental fillings is a very complicated and multi-factorial process. From that reason, it is still an important issue for researchers, ...in the spite of numerous studies and papers have already been done and published on [1, 2].

1.1. Mechanisms of wear

Wear can be defined as “the ultimate consequence of interaction between surfaces, which is manifested in gradual removal of material”. Generally, we may distinguish four main types of wear process [1, 3]:

- *adhesive wear* – occurs when surfaces slide one against another. Volume of material transferred from one surface to another is proportional to real contact area and sliding distance;

- *abrasive wear* – probably the most widespread type of wear; occurs when hard asperities (integral part of the surface – „two-body abrasion” or separate particles which are entrapped between the surfaces – „three-body abrasion”) plough into softer surface. Generally, this type of wear is proportional to the hardness of materials in contact, the geometry of abrasive particles, sliding distance and load;

- *fatigue wear* – as the result of repeated stress caused by clearance size particles trapped by two moving surfaces. The plastic deformation of material causes the zone of tension behind the motion. The surfaces are dented and cracking is initiated. These cracks propagate as the result of repeated stress produced by bearing load. Eventually materials that was surrounded by cracks is lost. This displaced material may itself form wear debris, causing three-body abrasion.

- *corrosive wear* – occurs as the result of chemical reactions on worn surfaces. If a chemical reaction layer forms on the surface then it can be removed by contact with the counterface. Removed material results in debris which are likely to agglomerate, producing larger particles.

1.2. Wear of dental resin-based composites

In general, resin-composite restorations are diphase with: 1. hard phase – silane-coated inorganic filler particles embedded in 2. softer matrix – dimethacrylate resin (either Bis-GMA or urethane dimethacrylate UDMA). In some cases, the proportion of lower molecular weight monomer such as TEGDMA is introduced to decrease overall viscosity of the system.

Friction of the surface with hard asperities makes the response of composites, which depends on the size of a hard phase region and the scale of deformation. If the size of hard filler particles and space between them are smaller than deformation caused by asperities, materials behave like homogeneous solids and their wear resistance is similar to that of a resin base. If filler particles and the scale of deformation are of approximate size or filler particles are larger, then the material behaves like a heterogeneous solid and its wear rate decreases [1].

To sum up, wear of dental resin-based composites is the result of a number of fundamental processes, especially: erosion, attrition and abrasion, which may occur simultaneously or sequentially, acting in various combinations. Their mutual interaction is very complex, what results in the general tendency of wear process hardly to be predicted.

Traditionally, in the subject literature, the term *erosion* is used to describe the loss of the surface layer attributed to chemical effects (usually acidic). *Attrition* characterizes surface loss at sites of direct occlusal contact. This type of wear occurs as the result of direct contact with sharp asperities of counterfaces and may induce substantial changes in surface texture (smear layer, roughness, etc.). *Abrasion* is used to describe wear at non-contact sites and also to some other situations which cannot be ascribed to erosion or attrition. This mechanism – “occlusal” material loss, is considered to be the significant type of wear for composites. Fundamentally, abrasion is caused by frictional surface interactions of dental materials with toothbrush and paste or food and fluid ingredients during chewing.

These three terms describe rather clinical manifestation than mechanisms of wear, thus it is reasonable that an each case should be considered rather in terms of a site and mechanism, than its nomenclature. It cannot be denied, that the mechanism of wear process, which has the great influence on wear rate, strongly depends on both factors, originating from: 1. material and 2. conditions under which the material is used [1, 4].

1.2.1. The influence of filler loading and morphology

The long-term wear of posterior composite restorative materials is influenced by wide range of factors, falling into two main groups:

1. inter alia – the chemistry of resin matrix and filler, and
2. composition and morphology of the system – for which the content and the size of filler particles and their distribution in a soft matrix, seem to be the most important ones [3]. Inorganic particles are well known from their ability to improve mechanical properties of polymers.

In the subject literature some theoretical and experimental evidences on the role of morphology for wear resistance of polymer composites can be found. Jørgensen et al. [5] suggests that decreasing the size of particles, space between them and increasing the volume fraction of filler, are the key factors to improve the wear resistance of materials. The authors have considered that filler particles situated very closely to each other can protect a softer resin matrix from abrasives, what results in the reduced wear of material. Turssi et al. [6] have studied wear of materials filled to the same extent, but with particles of various shapes. They have noticed that composites made of spherical filler particles had significantly lower wear resistance than those containing irregularly shaped ones. It has also been confirmed that abrasion reduces with the decrease of filler particle size.

1.2.2. The influence of filler size distribution and homogeneity

It cannot be denied that particle size is an important factor for tribological properties of polymer composites. In vitro wear tests indicate on resin-based dental composites containing the smallest sized spherical particles exhibiting a considerably higher wear resistance in the comparison to materials containing fillers of larger size. However, it must be pointed up, that mean particle size does not adequately describe the solid phase. Especially particle size distribution, composition homogeneity and the participation of the largest filler particles, dominate the tribological behaviour of composite materials [4].

It has been found, that in the most cases composites exhibit the surface gradient of composition (filler loading), as well as dimensions and size distribution of the solid phase particles. Non-uniform size distribution of filler particles in the surface layer of composites facilitates their tribological properties [7].

Turssi et al. have studied the wear behaviour of dental composites containing fillers of different size, geometry and particle distribution, but of the same chemistry and content [6]. They confirmed that the application of irregular shape fillers, having additionally a broad particle size distribution leads to the creation of significantly more wear-resistant composites in comparison to those made of similar sized spherical filler particles. Mono-modal materials containing the largest filler particles exhibit the highest abrasion.

The analysis of literature survey leaves no doubt that the mechanism of wear for resin-based dental composites still remains difficult to explain and describe. Taking into account, that this problem is connected with our, human health, it seems obvious, that tribological studies on these materials should be continued.

2. Experimental

2.1. Materials and sample preparation

Commercially available resin composites formulations (Filtek Supreme A2B, Filtek P60, Valux Plus, Filtek Z250, Tetric Ceram, QuixFil Universal) have been studied. The materials have been extruded directly into a home made silicon mould and their surface secured with a microscope cover glass to minimize contact with air oxygen. Then, the top surface has been photo-polymerized using a light-curing unit (Heliolux DLX, Ivoclar Vivadent, Switzerland) operating in a standard mode and emitting the radiation of 550 mW/cm².

2.2. Methods. Wear tests and microindentation

Wear test. Friction has been determined with a block-on-ring T-05 tribometer (ITeE, Radom, Poland). The tribometer was equipped with a multi-channel electronic PC measurement unit – Spider 8 (HBM, Germany) for data acquisition.

A 35 mm of diameter stainless steel ring, was rotating against the flat block sample of dental composite material. Measurements have been carried out with the sliding speed of $v = 12$ cm/s and the normal load of 100 N, at ambient temperature (20^{+5} °C). Friction experiments were running for six hours. After every hour samples were removed from the instrument and weighed to determine the wear of material.

Microindentation. Mechanical properties of the surface layer of dental composites have been carried out with a NanoTest 600 instrument (Micro Materials, UK) [8]. A Berkovitch diamond penetrated the surface layer of material with the loading/unloading rate of $dP/dt = 0.1$ mN/s and a force increasing from 0.5 mN to 5 mN. All the experiments were run in controlled conditions of temperature ($T = 20^{+2}$ °C) and relative humidity (60^{+5} %). Data registered were analyzed using the method proposed by Oliver and Pharr [9].

3. Results and discussion

Friction characteristics of the dental composites studied are presented in Figure 1 and 2. To make the figures more clear, only the traces of friction force in first, third and sixth hours have been presented and compared.

Tribological examinations have evidenced that in general, the friction force characteristics fall into three groups:

1. when friction force equilibrates slowly. The value of friction force increases from 20 N to approx. 40–45 N during the first hour (Filtek Supreme A2B, Valux Plus) – Figure 1,

2. when friction equilibrates more rapidly. The value of friction force stabilizes already after 20–30 minutes (QuixFil Universal, Filtek Z250) – Figure 2.

3. friction presents generally a constant value during the whole experiment (Filtek P60, Tetric Ceram) – Figure 3.

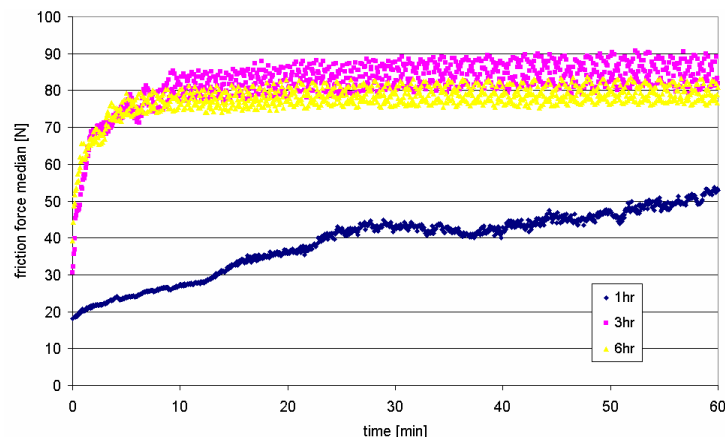


Fig. 1a. Changes to the median of friction force in time for dental composites Filtek Supreme A2B

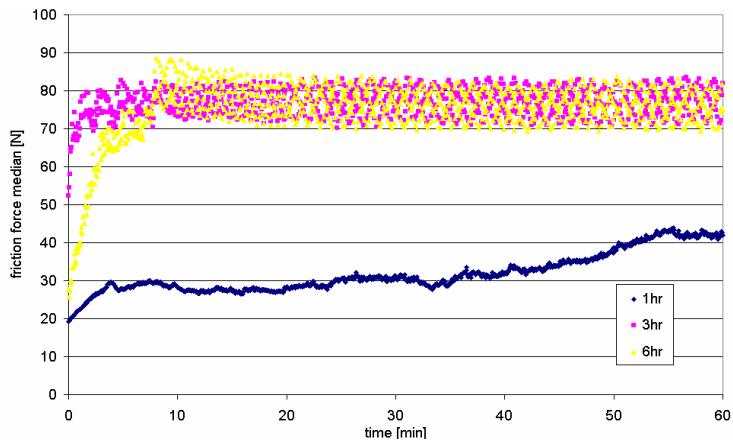


Fig. 1b. Changes to the median of friction force in time for dental composites Valux Plus, (during the 1st, the 3rd and the 6th hour of experiment)

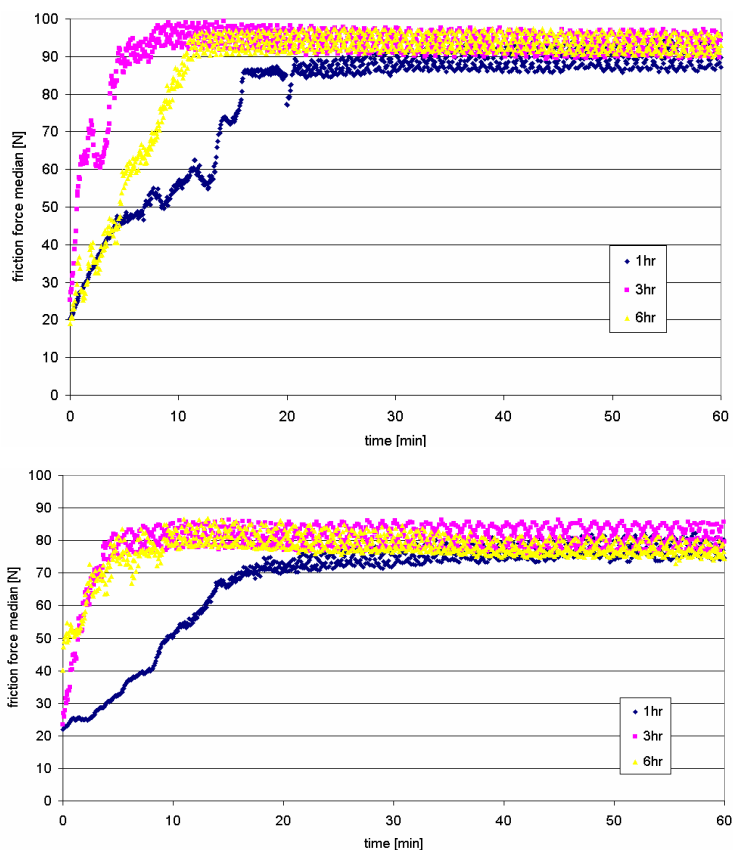


Fig. 2. Changes to the median of friction force in time for dental composites: a) QuixFil Universal, b) Filtek Z250 (during the 1st, the 3rd and the 6th hour of experiment)

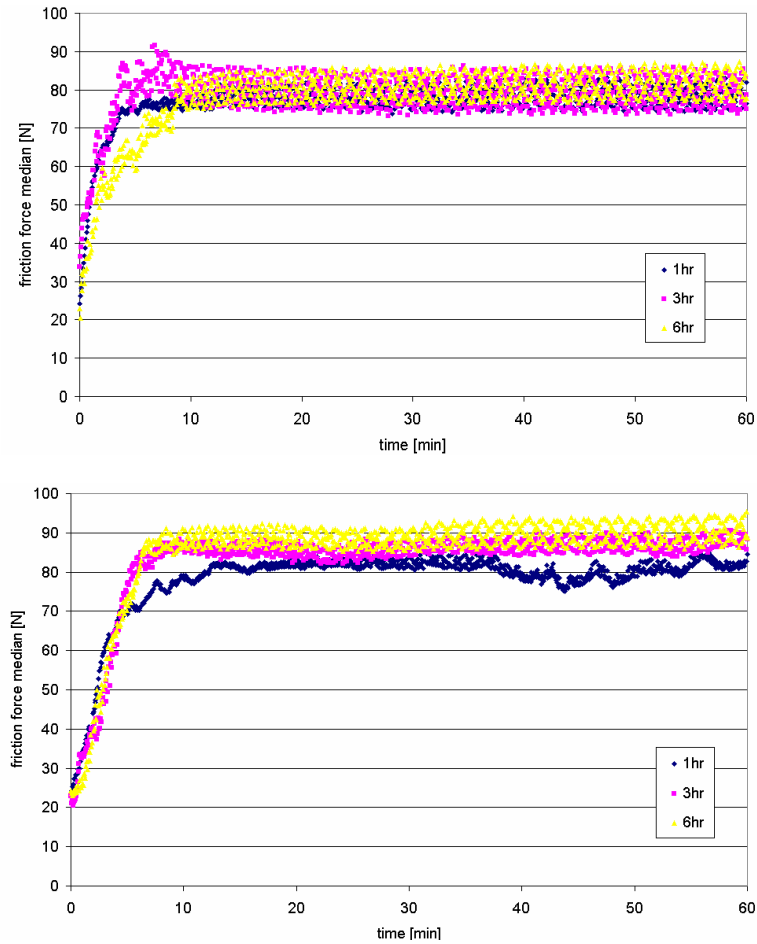


Fig. 3. Changes to the median of friction force in time for dental composites:
 a) Filtek P60, b) Tetric Ceram (during the 1st, the 3rd and the 6th hour of experiment)

It seems likely that the lack of changes to friction force for these composites is related to their abrasion kinetics. The abrasion kinetics for Tetric Ceram and Filtek P60 samples represent a straight line, with the correlation factor of $R^2 = 0.9995$ for former and $R^2 = 0.9928$ for the latter, whereas for other materials studied some changes to the slope are present – Figure 4.

These changes are the most visible for the first group of composites and could be related to the variation of friction force during the first hour of tribological experiment.

It has been found, that in the most cases, the composites studied exhibit the surface gradient of hardness. Microhardness decreases from the surface to the bulk of sample.

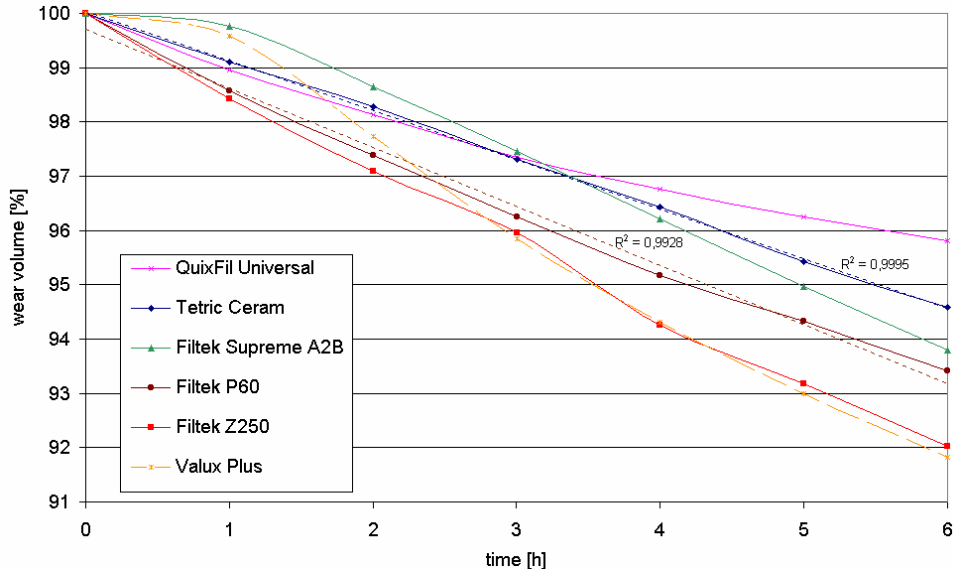
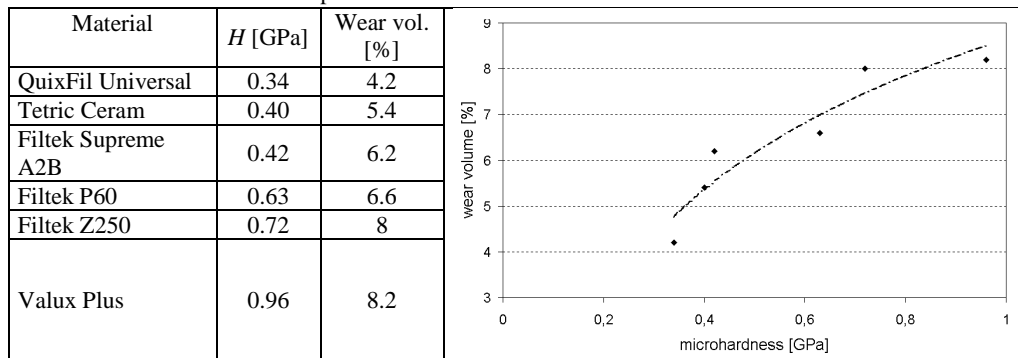


Fig. 4. Abrasion kinetics of some polymer-based dental composites

A relation between microhardness and wear loss of the dental composites studied has been observed – Table.

Table. Relation between microhardness (on depth approx. 500 nm) and wear loss for the dental composites studied



Generally, the harder and stiffer material the higher its abrasion. The mechanism of friction can be described by micromechanical Bowden and Tabor model [10].

4. Summary

Tribological experiments carried out in this study have shown that polymer-based composite materials can exhibit various wear behaviour. The friction force character-

istics of each material might be distinctly different, despite very similar chemical composition. This friction variation is related to the abrasion kinetics of dental composites. The lack of changes to friction force makes abrasion kinetics a straight line with approx. correlation factor of 1.

Microindentation measurements have provided interesting information about the hardness of dental composites. It was worthy of note, that in the most cases, the composites studied exhibit the surface gradient of hardness. The hardness has a great influence on tribological behaviour. In general, the softer materials the higher their wear resistance.

Our results confirmed that optimization of the wear behavior of dental composites is a very difficult process and may require a change in approach. The researchers should put more attention to the surface layer, not only being focused on the bulk properties of material.

References

- [1] Mair L. H., Stolarski T. A., Vowles R. W., Lloyd C. H.: *Wear: mechanisms, manifestations and measurement. Report of a workshop*, J. of Dent., Vol. 24, No. 1–2, 1996, pp. 141.
- [2] Ferracane J. L.: *Is the wear of dental composites still a clinical concern? Is there still a need for in vitro wear simulating devices?*, Dent. Mater., Vol. 22, 2006, pp. 689.
- [3] Bum-Soon L., Ferracane J. L., Condon J. R., Adey J. D.: *Effect of filler fraction and filler surface treatment on wear of microfilled composites*, Dent. Mater., Vol. 18, 2002, pp. 1.
- [4] Lambrechts P., Goovaerts K., Bharadwaj D., De Munck J., Bergmans L., Peumans M., Van Meerbeek B.: *Degradation of tooth structure and restorative materials: A review*, Wear, Vol. 261, 2006, pp. 980.
- [5] Jørgensen K. D., Hørsted P., Janum O., Krogh J., Schultz J.: *Abrasion of class I restorative resins*, Scand. J. Dent. Res., Vol. 87, 1979, pp. 140.
- [6] Turssi C. P., Ferracane J. L., Vogel K.: *Filler features and their effects on wear and degree of conversion of particulate dental resin composites*, Biomaterials, Vol. 26, 2005, pp. 4932.
- [7] Kleczewska J., Bieliński D. M., Sokołowski J., Klimek L.: *Analysis of the surface layer of polymer dental materials*, Inż. Mater., 2007 – in press.
- [8] www.micromaterials.co.uk.
- [9] Oliver W. C., Pharr G. M.: *A new improved technique for determining hardness and elastic modulus using load and sensing indentation experiments*, J. Mater. Res., Vol. 7, 1992, pp. 1564.
- [10] Bowden F. P., Tabor D.: *An Introduction to Tribology*, Heinemann, London, 1974.

Tarcie i zużycie ściernych materiałów dentystycznych na bazie żywic

Obiektem badań były dostępne komercyjnie polimerowe materiały dentystyczne na bazie żywic. Zbadano kinetykę zużycia wybranych kompozytów dentystycznych oraz ich mikro-twardość. Pomiary tribologiczne dowiodły, że krzywe obrazujące zmiany siły tarcia w czasie,

mogą mieć odmienny przebieg dla różnych kompozytów. Pomimo, że badane materiały odznaczały się podobnym składem chemicznym, w niektórych przypadkach siła tarcia miała stałą wartość w trakcie całego eksperymentu, w innych natomiast stabilizowała się z różną prędkością. Okazało się, że możliwe jest powiązanie przebiegów siły tarcia w poszczególnych godzinach, z kinetyką zużywania się kompozytów dentystycznych. W przypadku materiałów, dla których wartość siły tarcia nie zmieniała się w trakcie trwania procesu kinetyka zużycia przybierała kształt linii prostej. W pozostałych przypadkach obserwowano mniejsze lub większe odchylenia od liniowego trendu.

Pomiary techniką mikroindentacji dostarczyły wartościowych informacji na temat twardości warstwy wierzchniej badanych materiałów dentystycznych. Wyniki tych pomiarów można również powiązać ze zużyciem. Okazało się, że twardsze i sztywniejsze materiały dentystyczne odznaczały się wyższym zużyciem ściernym. Zatem tarcie kompozytów dentystycznych na bazie żywic można opisać za pomocą mikromechanicznego modelu Bowdena i Tabora. Pomiary mikrotwardości dowiodły również, że w przypadku większości materiałów mamy do czynienia z występowaniem powierzchniowego gradientu twardości.

Przeprowadzone badania potwierdzają, że optymalizacja właściwości materiałów dentystycznych pod kątem ich odporności na zużycie ściernie, jest sprawą skomplikowaną i wymaga przede wszystkim skoncentrowania się na właściwościach warstwy wierzchniej materiału, w której procesy tribologiczne są inicjowane.



System and risk approach to ship safety, with special emphasis of stability

LECH KOBYLIŃSKI

Foundation for Safety of Navigation and Environment Protection, 14-200 Iława-Kamionka

Present stability regulations developed over the years by IMO reached definite conclusion with the adoption of the Revised draft of the Intact Stability Code. The criteria included there are working comparatively well with regard to the majority of conventional ships. Advent of very large and sophisticated ships of non-conventional features caused that those criteria may be inadequate, and because of that currently IMO is considering development of criteria based on ship performance. However, with the application of the existing criteria risk level is not known, and there was still a number of ships satisfying criteria that did capsize due to different causes. The present criteria are design criteria of the prescriptive nature. As opposed to prescriptive criteria requirements based on risk analysis offer many advantages.

The author proposes that as alternative to existing criteria safety assessment based on risk analysis should be used. This would require holistic and system approach to stability. Safety against capsizing (or LOSA accident) is a complex system where design, operational, environmental and human factors have to be taken into account. The crucial point in safety assessment would be identification of all hazards the ship may be subjected. Although performing risk analysis to stability problems seems to be a very complex task, in the opinion of the author it may be manageable and could be applied for safety assessment of highly sophisticated and costly ships.

Keywords: *ship's safety, risk analysis, stability of ship, hazard identification, formal safety assessment*

1. Introduction

Seafaring at present days is not particularly dangerous. However, the international society shocked by serious marine casualties that happen from time to time where hundreds of lives are lost and oceans are polluted by several thousands tons of oil feels that it is necessary to take action to enhance safety. In particular, the International Maritime Organisation (IMO), the United Nations agency responsible for safety at sea is working since early sixties of the last century towards achieving this goal. This organisation develops international safety requirements for shipping. Creation of this organisation and its activity shows that the international society is crucially interested in promoting safety at sea. The attitude to safety of seafaring was, however, not always such as it is to-day.

From the earliest days shipping was associated with the risk of losing the ship and people onboard. Even in the nineteenth century it was never known whether the ship starting a journey will ever return and passengers, entrusting their lives to unreliable ships felt extremely lucky if the journey ended successfully. Ships were lost by hundreds. It is worth noticing that in the single year 1821–22 in North Sea 2000 ships

were lost with over 20 000 people onboard. Between the year 1876 and 1892 10 381 British ships were lost with 27 010 mariners and 3543 passengers. The cause of casualties was defined as “*force majeure*”.

The principle of economy was *laissez faire*, every intervention of governments was strongly rejected by ship owners and seafarers. As a result, crews were treated badly and ships were unsafe. The industrial revolution of the nineteenth century and rapid development of sea transportation, shipping and shipbuilding that follows caused that the problem of safety at sea gained importance. Because of the growing number and size of ships the high risk involved in shipping could not be accepted, on the other hand because of the technical and scientific progress there were realistic possibilities to build safer ships and carry on safer navigation. Ultimately marine administrations and ship owners gave up under pressure of public opinion moved by the high mortality on board ships and by the large number ships lost.

Stability was in the centre of attention of shipbuilders from the oldest times. They knew very well, that ships at sea must not capsize. There were no stability criteria available, and the knowledge of how to construct ships safe against capsizing was based solely on experience and skill of shipbuilders passed from generation to generation.

The foundations of the science of stability were laid down already in the middle of eighteenth century by Bouguer, Euler, Bernouille and others, but they did not influence the designing of ships. There were, however, developed certain simple rules how to design stable ships and attention was focused on ensuring adequate metacentric height.

After the capsizing of the naval ship *Captain* in 1870 with all hands onboard the importance of righting lever curve was recognized, and as a consequence in 1884 criterion proposed by Denny was adopted by the British Admiralty. In following years several proposed stability criteria were advanced, none of which found wider application. By late thirties Rahola proposed criteria based on the analysis of some capsized ships that later on were used in several countries. First official compulsory stability standards were adopted in SSSR in 1947 and they for the first time included “weather criterion”.

One of the first tasks taken by IMO in early sixties was development of stability standards. First part of this task was completed in 1968 by adoption of statistical criteria, supplemented in 1986 by weather criterion. In 1993 they were included into the Intact Stability Code for all ships covered by IMO instruments. The criteria were recommended and not compulsory. Recently the Code was revised, divided in two parts, the first one made compulsory by reference in the amended SOLAS convention. It will come into force in 2009. This, however, is not the final solution. The programme of work of IMO includes development of improved stability criteria that should take into account various hazards to which the ship may be subjected.

2. Concepts of safety

In the past the ability to build ships that were safe and had good seakeeping qualities was based entirely on experience gained over a long time and passed on from generation to generation.

This was the oldest concept of safety, where safety was achieved by the “trial and error” method. This traditional way of building ships has survived to this day in many developing countries, where small ships have been built without any drawings and calculations and the design was based solely on experience. There were, however, certain regulations specifying hull scantlings in relation to ship parameters. This concept not so long ago was used commonly by classification societies. Krappinger [14] defined this concept of safety as the assignment of hardware and this concept is often used as a basis of simple safety requirements up to this day.

A more advanced concept of safety does not include assignment of dimensions or proportions of an object, but assignment of its physical properties. In respect to stability, this means, for example, assignment of values of metacentric height or of the righting arms at various angles of heel. The method of estimation of these values could be, however, the same, i.e. the trial and error method. All older stability criteria or recommendations were actually based on this method.

Currently, especially with regard to stability, a more advanced concept of criteria is advocated, under the term “performance oriented criteria”. It is not entirely clear what this term may really mean, but it seems that with regard to stability most people understand under this concept the approach that may be defined as: *“the approach where the behaviour of vessel is analysed in a set of environmental and operational scenarios taken as realistically as possible on the basis of her performance in terms of safety against capsizing. The performance-oriented criteria should be based on calculations or measurements of performance of the vessel in deterministic or probabilistic terms in the analysed scenarios. Numerical simulation, analytical methods model experiments and full scale trials could be used”* [12].

Table 1. Five-tier system for goal-based requirements

Tier I:	Goals
Tier II:	Functional requirements
Tier III:	Verification criteria of compliance
Tier IV:	Technical procedures and guidelines, classification rules and industry standards
Tier V:	Codes of practice and safety and quality systems for shipbuilding, ship operation, maintenance, training etc

The most recent concept of safety regulations is goal-based standards. Goal based regulations does not specify the means of achieving compliance but sets goals that allow alternative ways of achieving compliance [4]. Goal-based standards are for some time considered at IMO and appraised by some authors [19], and they were introduced in some areas, albeit not in the systematic manner. Marine Safety Committee of IMO commenced in 2004 [IMO 2004] its work on goal-based standards in relation to ship construction adopting five-tier system (Table 1).

IMO MSC committee agreed in principle on the following tier I goals to be met in order to build and operate safe and environmentally friendly ships: *“Ships are to be de-*

signed and constructed for a specific design life to be safe and environmentally friendly, when properly operated and maintained under specified operating and environmental conditions, in intact and specified damage conditions, throughout their life” [IMO 2004].

3. Prescriptive versus risk based criteria

The basic dichotomy in the conception of safety requirements consists of prescriptive approach and risk-based approach.

Traditional regulations were of prescriptive nature and usually were based on deterministic calculations. They are formulated in the way where a ship dimensions or other characteristic (e.g. metacentric height) must be greater (or smaller) than certain prescribed quantity. Prescriptive regulations could be developed on the basis of experience (expert’s opinions) statistics, analytical methods, computer simulation, model tests and full-scale trials.

Prescriptive regulations have many advantages. They are formulated in a simple language, which is easily understood by everybody, they are easy in application, they also make checking adherence to the requirements easy. The main shortcoming of prescriptive regulations is that they are bounding designers and they do not allow introduction of novel design solutions. They are based on experience gained with existing objects and they are not suitable for novel types. Usually they were amended after serious casualties happened. The risk involved with the application of prescriptive regulations is not known.

At the opposite of the prescriptive regulations, there is risk-based approach. In the risk-based approach, the regulations specify objectives to be reached, which are safe performance of an object. The advantages of risk-based approach are obvious. They give free hand for the designer to develop new solutions, they actually allow taking optimal decisions from the point of view of economy and safety and the risk to the public and to the environment is assessed and accepted.

4. System approach to safety and stability

As mentioned above, existing criteria are design criteria intended to be applied during the design stage of a ship. However, even the preliminary analysis of stability casualties shows, that design features of the ship are not the most important nor most often cause of casualty. Casualty – it will be in the following called LOSA – (loss of stability accident) [13], is usually the result of a sequence of events that involve environmental conditions, ship loading condition, ship handling aspects and human factor in general.

Ship stability system is rather complicated. However, in most cases it could be considered as consisting of four basic elements: ship, environment, cargo and operation (Figure 1) [9]. The Venn diagram in this figure stresses strong interactions between the four elements. The use of the system approach to stability criteria was

proposed by the author quite long time ago and it was partly applied in development of the Intact Stability Code [10], but in general until this day stability requirements remain basically design oriented. Analysis of LOSA casualties reveals that the causes of casualty may be attributed to:

- functional aspects resulting from reliability characteristics of the technical system, therefore stability characteristics of the ship,
- operational aspects resulting from action of the personnel handling the system, therefore crew members but also ship management, cargo handling, marine administration and owners company organisation,
- external causes resulting from factors independent from designers builders and operators of the technical system therefore ship environment and climatology [2], [3],
- cargo related aspect resulting from characteristics of cargo and its way of transporting.

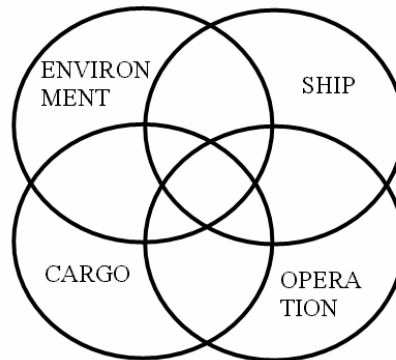


Fig.1. Four-fold Venn diagram for ship stability system

Human factor plays important part in all four elements of the system. Human and organisational errors, HOE, according to some authors, are responsible for approximately 80% of all marine casualties [15], other sources definitely stated that this percentage is 80% [18]. In order to achieve sufficient level of safety with respect of stability, all elements creating stability system have to be taken into account. Taking into account the fact, that less than 20% of all casualties are caused by faulty or bad design of the ship, the existing safety requirements that refer mainly to design features of the ship can not insure sufficient level of safety, in particular with regard to ships having novel design features.

5. Application of holistic and risk-based approach to safety and stability

It seems that there is some consensus on the need to apply holistic and risk-based approach to safety of ships at sea. The Marine Safety Committee of IMO recommended this approach as Formal Safety Assessment (FSA) [7]. The possibilities to use

this approach in the rule making process are still under investigation and rather few trial applications of FSA have been attempted, e.g. [5]). This in particular applies to stability problems, intact or damage, and existing IMO rules on stability, do not include possibility to apply such methods. Few partial applications of risk analysis to stability problems were published [1], [3], [16]. Risk approach is inherently involved in the total ship safety concept strategy proposed by Vassalos [19]. The author investigated possibilities of application of the FSA methodology to intact stability criteria in several papers e.g. [11], [13].

Recently, however, IMO SLF Subcommittee completed the task of revision of the Intact Stability Code (IS Code) dividing it in two parts, the first one of which will be made mandatory [8]. But still remains the long-term task of developing stability criteria that take into account various hazards, inter alia parametric resonance in following and head seas, broaching or loss of stability in wave crest. Some people think that it would be possible to develop prescriptive criteria based on systematic calculations of computer-simulated behaviour of the ship in a seaway. There are, however, strong arguments showing that it may not be possible.

First of all hazards posed by seaway, as mentioned above, are not the only ones. LOSA casualty is usually the end result of a sequence of events where various hazards play important part. Furthermore, behaviour of the ship in a seaway strongly depend on ship operation and in particular on decisions taken by the master in dangerous situations. There is no way to take account of those decisions in the design process of the ship. The author sees the only possibility to assure safety by applying risk analysis.

Risk-based approach according to IMO recommendation is formalized and includes the following steps:

- identification of hazards,
- risk assessment,
- risk control options,
- cost-benefit assessment, and
- recommendations for decision making.

It is rather obvious that application of FSA methodology is a tedious and time-consuming task, but in principle it is feasible. It would be not practical to apply this method to conventional ships that are reasonably safe, but it could be effectively applied to important and large ships of non-conventional design. FSA may, therefore, be recommended as an alternative to existing prescriptive criteria subject to the discretion of the Maritime Administrations involved. This idea is presented in the Table 2 and the general procedure for the application of system and the risk approach is shown in Figure 2.

Table 2. Methods of safety assurance

Ships	Method of stability safety assessment
Conventional, not sophisticated	Prescriptive criteria as in the IS Code
Novel types, large sophisticated ships	Risk analysis under the provision allowing application of alternative means of assuring safety

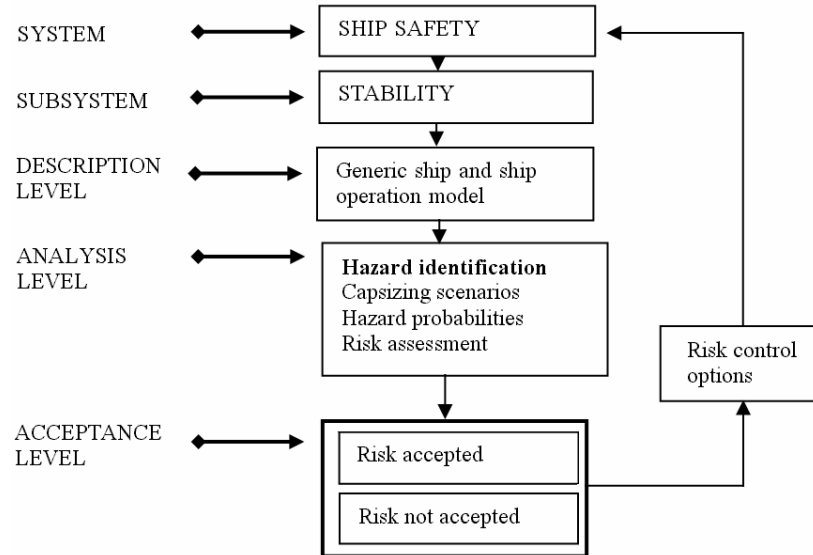


Fig.2. Block diagram of risk analysis

6. Hazard identification

The crucial problem in safety assessment analysis is proper identification of various hazards to which a ship may be subjected. According to the definition, hazard is “*a potential to threaten human life, health, property or the environment*” [6]. When performing risk analysis all relevant types of hazards must be taken into consideration – environmental, technical, operational and managerial. Human factor must be taken also into consideration.

Hazard identification is carried-out using hazard identification and ranking procedure (HAZID). Hazards could be identified using several different methods.

IMO resolution included general guidance on the methodology of hazard identification. With respect to stability, hazard identification could be achieved using standard methods involving evaluation of available data in the context of functions and systems relevant to the type of ship and mode of its operation. Stability is considered assuming that the ship is intact and accident evaluated is called LOSA (loss of stability accident). LOSA is a new definition covering capsizing, that means taking by the ship position upside down, but also covering a situation where amplitudes of rolling motion or heel exceed a limit that makes operation or handling the ship impossible for various reasons – e.g. loss of power, loss of manoeuvrability, necessity to abandon the ship etc. It does not necessary mean the total loss of the ship. [13].

According to general recommendation the method of hazard identification comprised mixture of creative and analytical techniques. Creative element was necessary

in order to ascertain that the process is proactive and is not limited to hazards that happened in past.

In general HAZID involves several possibilities used separately or in combination:

- statistical data concerning causes of accidents,
- historical data including detailed description of accidents,
- conclusions resulting from model tests of ships in waves,
- conclusions resulting from computer simulation of capsizing,
- event and fault trees method,
- analysis of accidents using TRIPOD method [17],
- opinions of experts organized according to DELPHIC method.

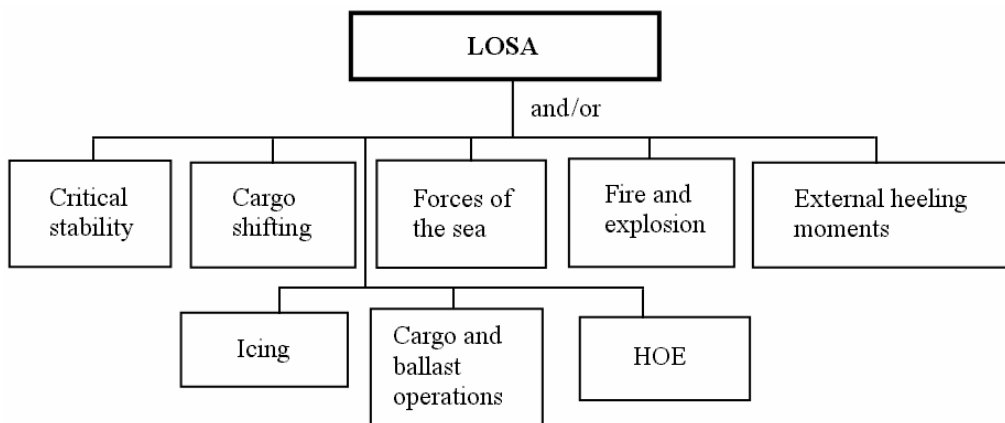


Fig. 3. Basic hazards to stability (HOE – human and organisation errors)

As an example of the application of this methodology the list of hazards in respect of stability is shown in Figure 3. In this example ranking of hazards is not shown, moreover the sketch could be considered as the first level of the fault tree leading to LOSA. When further decomposition of hazards is performed it could be easily seen that the hazards, taken as faults, are strongly interconnected and human factor is present in all of them.

Hazards identified as relevant to safety against LOSA are all strongly interconnected, moreover, human factor understood as a performance of an individual (in most cases the master) plays important part in each case. Hazards identified should be further decomposed preferably using fault trees and/or events trees reproducing various scenarios of LOSA casualty. The set and combination of fault trees and event trees as developed for all hazards identified and all scenarios (defined as risk contribution trees – RCT) is a basis for HAZOP (hazard and operability study) procedure that allows also assessment of frequencies (probabilities) of hazards required for risk assessment.

This is rather tedious task bearing in mind the multitude of possible scenarios. This problem, however, is not discussed here.

References

- [1] Alman P.R., Minnick P.V., Sheinberg R., Thomas III W.L.: *Dynamic capsize vulnerability: reducing the hidden operational risk*, SNAME Annual Meeting, 1999.
- [2] Cleary W.A.: *Marine stability criteria*, Proceedings of the 1st International Conference on Stability of Ships and Ocean Vehicles, Glasgow, 1975.
- [3] Erickson A., Person J., Rutgerson O.: *On the use of formal safety assessment when analysing the risk for cargo shift in rough seas*, International Conference on Design and Operation in Abnormal Conditions, Proceedings, Glasgow, 1997.
- [4] Hoppe H.: *Goal based standards – a new approach to the international regulation of ship construction*, IMO News, Issue 1, 2006.
- [5] IMO: *Formal Safety Assessment. Trial application to high speed passenger catamaran vessels*, Doc. DE 41/INF.7, 1997.
- [6] IMO: *Guidelines for Formal Safety Assessment (FSA) for use in the IMO rule-making process*, Doc. MSC/Circ.1023; MEPC/Circ.392, 2002.
- [7] IMO: *Revised Intact Stability Code Prepared by the Intersessional Correspondence Group*. Submitted by Germany. Doc. SLF 49/5, 2006.
- [8] IMO: *Subcommittee on Stability, subdivision and Safety of Fishing Vessels*, Report of 50th session. Doc.SLF 50/WP.6., 2007.
- [9] Kastner S.: *Safety and Stability of Ships*, Vol. 1, Elsevier, 2003.
- [10] Kobyliński L.: *Philosophische und Hydrodynamische Probleme der Internationalen Kenterkriterien von Schiffen*, Intern. Schiffstechnische Symposium, Rostock, 1984.
- [11] Kobyliński L.: *Application of the FSA methodology to intact stability criteria*, Marine Technology Transactions, Vol. 15 (2004), pp. 319–329
- [12] Kobyliński L.: *Appraisal of risk assessment approach to stability of ships*, International Workshop on Ship Stability, Istanbul, 2005.
- [13] Kobyliński L.: *Alternative stability requirements based on system and risk approach*, 9th STAB Conference, Rio de Janeiro, 2006.
- [14] Krappinger O.: *Die quantitative Berücksichtigung der Sicherheit und Zuverlässigkeit bei der Konstruktion von Schiffen*, Jahrbuch der STG, Bd. 61, 1997.
- [15] Manum I.A.: *What have guided international activities on intact stability so far?*, 4th STAB Conference, Naples, 1990.
- [16] McTaggart K., de Kat J.O.: *Capsize risk of intact frigates in irregular seas*, SNAME Annual Meeting, paper Nr.8, 2000.
- [17] ter Bekke E.C.A., van Daalen E.F.G., Willeboordse E.J., Boonstra H., Keizer E.W.H., Ale, B.: *Integrated safety assessment of small container ships*. 8th Intern. Conference on Probabilistic Safety Assessment and Management, New Orleans, 2006.
- [18] U.S.Coast Guard: *Prevention through people*, Quality Action Team Report, 1995.
- [19] Vassalos D.: *Total ship safety – a life-cycle risk-based DOR for safety*, The Stability Research Centre, NAME, Universities of Glasgow and Strathclyde, May 2002.

Systemowe i oparte na analizie ryzyka podejście do bezpieczeństwa statku ze szczególnym podkreśleniem problematyki statecznościowej

Przyjęcie przez IMO znowelizowanego Kodeksu stateczności zakończyło określony etap prac nad rozwojem przepisów statecznościowych. Przepisy te spełniają dość dobrze zadanie zapewnienia bezpieczeństwa w stosunku do statków konwencjonalnych. Mogą one być jednakże niewystarczające dla statków dużych, nowoczesnych i niekonwencjonalnych. Jednakże poziom ryzyka przy zastosowaniu obecnych kryteriów nie jest znany, ponadto od czasu do czasu zdarzają się wypadki przewrócenia się statku. Z tego powodu do programu prac IMO wprowadzono zadanie opracowania kryteriów opartych o osiągi statku. Alternatywą dla wymagań preskrypcyjnych są wymagania oparte na analizie ryzyka. Autor proponuje stosowanie alternatywnych wymagań opartych na analizie ryzyka. Wymaga to stosowania podejścia systemowego i holistycznego. Bezpieczeństwo przed przewróceniem się stanowi złożony system, w którym należy uwzględnić aspekty projektowe, operacyjne, otoczenie i ładunek. Istotnym elementem oceny bezpieczeństwa jest identyfikacja wszystkich zagrożeń, jakim podlega statek. Analiza ryzyka jest procedura złożoną, jednakże zdaniem autora w stosunku do stateczności jest możliwa do wykonania.



Sliding polymers in the joint alloplastic

P. KOWALEWSKI, W. WIELEBA

Wrocław University of Technology, Wybrzeże Wyspiańskiego 25, 50-370 Wrocław

Endoprostheses make it possible to replace a sick or damaged joint with man-made elements. Thanks to numerous clinical trials and to progress in the manufacturing technology, the devices of this type are now more and more modern and reliable. Materials used in endoprostheses have been subject to continuous modifications. The principal reasons of failures in the implantation of artificial joints are the loosening of the graft, often due to the infection caused by products of wear of polymer elements, improper grafting or improper co-operation between the implant and tissue. Additionally, after a dozen or so years of exploitation, needed is the reoperation of the endoprosthesis due to its wear. An improvement in the sliding properties and wear resistance of the polymer elements of endoprostheses will contribute to the reduction of pathologies and reimplantations as well as to the elongation of their service life. Numerous studies have been carried out at present to explain the process of wear of polymer inserts used in hip and knee endoprostheses. In the case of an implanted joint, the forces of friction are higher than those in a natural joint. Additionally, these forces are variable in time, which adds fatigue aspects and bone/implant integration impacts to the problem. Mechanical and tribological properties of ultra-high molecular weight polyethylene contributed to the fact that this material has been the principal sliding polymer employed in the joint alloplastic. Improvement in reliability and anticipation of wear patterns in endoprosthesis are priorities in the current research.

Keywords: *friction, sliding polymers, alloplastic, endoprosthesis*

1. Introduction

1.1. Role of plastics

Natural tissues of a human being perform different tasks. The optimal physical and chemical structure of these tissues perfectly fits the functions involved in these tasks. Millions of years of evolution formed organs that a human being has been trying to replace based upon its humble knowledge. The elaboration of a device that is able to fully replace a sick or devastated organ and to take over all its functions is practically impossible. Of the many organ groups, the functions of which are taken by implants, motor organs are those the most often replaced. In the last half-century, the number of grafted orthopaedic implants has significantly increased. Specific types of those implants, due to their function as an artificial joint, are endoprostheses.

1.2. Operational complexity

Natural human joints have a complicated anatomical structure that is fit to the mobile functions performed. The properties of the cartilage and synovial fluid as well as

the very form of the sliding surfaces of a joint makes it possible for such a biobearing to operate in a broad range of loading and sliding velocities under minimum friction losses. It may be assumed, to a high degree of probability, that a healthy joint operates under full film lubrication [9, 30] assisted by the so called “weeping lubrication” mechanism [9 after 27]. The mechanism consists in pressing and depressing the synovial fluid from porous layers of the joint cartilage [9]. Additionally, bioelastohydrodynamic, mixed or boundary friction is also possible. Biotribology has for a long time been a subject of extensive, worldwide research. It shall be stressed that the mechanism of joint friction has not been fully identified and explained as yet. Consequently, the reconstruction of the specific structure of a natural joint is not possible [9].

The progress experienced in the bioengineering has made it possible to replace practically all synovial joints with artificial ones [20]. The most frequently replaced joints are hip and knee ones. Any dysfunction of these joints influences significantly the overall state of health and impairs human mobility. These joints are subject mostly to deformations or to mechanical damage [9].

The full reconstruction of a joint brings about the removal of the joint capsule. As a result, the natural lubrication fluid (synovial fluid) is absent in the joint. The operational environment of the implanted joint is such that it cannot be additionally lubricated. In the engineering practice, these lubrication-free bearings are mostly lined with plastics. Additional features of plastics such as resistance to corrosion, dumping capability contributed to their status as the fundamental sliding material for the production of endoprostheses.

1.3. Reliability and bio-tolerance

Operational environment of endoprostheses, due to their very specific application, is also very specific. Reliability and quality are of tremendous importance as both factors influence directly the health or even life of a human being. A need for reoperation as a result of a faulty implant shall be nullified. The standardization of products made of polymer became one of the objectives of the ASTM Committee F-4 on Medical and Surgical Materials and Devices, which was established in 1962. Yet another aspect playing a considerable role in the implantation of plastics is bio-tolerance. Marciniak remarks that the problem of bio-tolerance of plastics is more complex than in the case of other biomaterials as catalysts, stabilizers or other substances may become toxic or allergic depending upon their concentration or uneven distribution in tissues [29].

The most important phenomena associated with the bio-tolerance of plastics in organisms are:

- toxic or allergic reactions,
- tissue reactions involved with the functional adaptation of tissues co-operating with a polymer implant,

- resistance of a polymer to biodegradation and depolymerization, which governs the constancy of physical and chemical properties,
- carcinogenic impacts.

2. Materials employed

2.1. Development of bio-materials in the joint alloplastic

The evolution of subsequent generations of endoprostheses gave reason to the application of ever new materials. First reports on the application of artificial joints surfaces date back to 1860: Carnochan attempted to restore the mobility of temporomandibular joint by replacing the elements of joint with wooden blocks [28]. In 1890 Gluck introduced the first total endoprosthesis of the hip joint by making its components of ivory [14 after 4]. In the first decades of the 20th century, a broad spectrum of materials was being used for endoprostheses: mentions concerning the use of implants made of rubber (Delbert 1919 [28]; glass, celluloid, pyrex glass or bakelite (Smith-Petersen 1923 [26]) can be found in the literature.

Attempts to use traditional materials like stainless steel (introduced for the first time by Wiles in 1938) and brass (MKee in 1940) were undertaken. In 1950 J. Judet and R. Judet presented the results of resection-reconstruction alloplastics with the use of semi-endoprosthesis made of polymethyl methacrylate (PMMA) [12].

The rapid growth of interest in plastics in the 50-ties of the previous century was also noticeable in bio-medial engineering. Marciniak [19] specifies target properties of plastics to be applied in medicine. These are:

- ease in obtaining steady material properties for different lots of products,
- ease of formation making it possible to obtain different functional forms without degradation of material,
- ease of sterilization without the loss of properties or shape,
- adequate physical and chemical properties of material,
- non-triggering of toxic or allergic reactions,
- bio-tolerance in the tissue environment,
- adequate functional service life and reliability.

Advantages of plastics and the development of the relevant manufacturing processes brought about more and more attempts to employ polymers in the production of sliding elements for endoprostheses. At the break of the 50-ties and 60-ties, common were sliding materials made of polytetraethylene (PTFE). Unfortunately, products of operational wear caused severe allergic reactions and finally – the loosening of implants. Sir John Charney applied as first in 1962 an insert made of ultra high molecular weight polyethylene – UHMWPE. Low values of the coefficient of friction for friction pairs including polyethylene elements together with the absence of a clear reaction of the organism against this material contributed to its widespread application in the alloplastics of joints.

The UHMWPE features the following advantageous properties:

- good sliding properties,
- self-lubrication properties,
- resistance to body fluids,
- good damping properties,
- relatively low price.

Apart of ultra high molecular weight polyethylene, also polyoxymethylene (POM) was used for sliding components of endoprostheses [3], [23]; mostly Delrin® (by the DuPont company). Laboratory and model testing of a Polish equivalent, known under the brand name of Tarnoform (Zakłady Azotowe w Tarnowie-Mościcach), and filled with powders of bronze and PTFE has proved its fitness for the purpose of endoprosthesis construction [31]. The task of fillers is to enhance the tribological properties of the material and to reduce wear. Later laboratory studies [7] revealed, however, that the process of polyacetale wear is associated with the destruction of polymer chains with the dissipation of formaldehyde, a highly carcinogenic agent. The use of POM as a sliding biomaterial is therefore excluded.

2.2. Friction pairs used in the joint alloplastics

The selection of sliding pairs is a fundamental part of the design process for endoprostheses. In the last decade only modifications of the existing materials (modification of materials, modification of the surface layer) have been introduced. The following materials are used most frequently in the alloplastics of joints:

- 316 stainless steel,
- CoCrMo alloy: Vitalium (for metal working), Endocast (for casting),
- Zirconia (ZrO_2) ceramics,
- Alumina (Al_2O_3) ceramics.

In some of the endoprostheses (mostly the hip joint), applied are friction pairs that do not contain polymer. These are metal/metal or metal/ceramics pairs. The most frequently used are:

- 316L – UHMWPE,
- CoCrMo – UHMWPE,
- CoCrMo – CoCrMo,
- Ti6Al4V – UHMWPE,
- Al_2O_3 – UHMWPE,
- Al_2O_3 – Al_2O_3 ,
- ZrO_2 – UHMWPE.

Table 1 shows the fundamental mechanical properties of materials used in alloplastics. Tribological performance is evidently dependent upon properties of the two sliding materials. The chemical composition of typical metal materials used in endoprostheses is shown in Table 2.

Table 1. Mechanical properties of materials used for endoprostheses of joints [9]

No	Material property	CoCrMo En-docast Alloy	Ti6Al4V Alloy	UHMWPE Chirulen Polyethylene	Al ₂ O ₃ Ceramics
1	Density, g/cm ³	8.3	4.5	0.96	
2	Yield strength, MPa	700	895 to 1080	21.5	3.9
3	Tensile strength, MPa	1000	850 to 1120	46.2	
4	Elongation, %	15	10 to 15	434	
5	Modulus of elasticity, MPa	2.2 10 ⁵	1.08 10 ⁵	1000	3.8 10 ⁵
6	Endurance limit, MPa	400	500	–	
7	Poisson's ratio	0.3		0.4	

Table 2. Chemical composition of metal alloys used for implants [23]

	C	Mn	Si	Cr	Ni	Mo	W	Co	Fe	P	S
Co-Cr-Mo	0.22	0.48	0.97	27.9	0.05	6.27		base	0.38	0.006	0.006
316 L stainless	0.017	1.73	0.65	17.33	13.69	2.34			base	0.023	0.007
	Al	V	Fe	C	O	N	H	Ti			
Ti6Al4V	6.20	4.05	0.15	0.013	0.013	0.011	0.0058	base			

2.3. Ultra High Molecule Weight Polyethylene (UHMWPE)

Polyethylene is considered as an ultra high molecule weight material if its molecule mass is greater than 1 million g/mol. At the beginning of the 90-ties, there were 10 varieties of UHMWPE. They differed, among others, with the molecular mass and content of calcium stearate (added to reduce oxidation during gamma sterilisation) and by the method of manufacture. At the beginning of this century, the list of available polymer varieties was down to three [17]. There are three fundamental methods for the production of endoprosthesis elements made of UHMWPE [17]:

- direct compression moulding,
- extrusion into bars followed by machining,
- compression moulding into sheets followed by machining.

In the 60-ties of the previous century, gamma radiation was the fundamental method used for the sterilization of elements made of UHMWPE. The main chemical transformations driven by ion radiation in polyethylene are cross-linking, degradation, and oxidation [22]. The cross-linking consists in the creation of C-C links between molecules [8]. The degradation of elements made of polyethylene consists in the disruption of chemical bonds between a macromolecule of the polymer [8]. Oxidation developing at the surface or just below the surface [17] consists in the creation of oxides and hydroxides [8]. Sterilisation influenced changes in the mechanical properties the material and its tribological performance.

Attempts to improve the properties of UHMWPE have been undertaken for many years now. The objective was to reduce the rate of wear, to improve resistance to fatigue wear and impact loading.

At the end of 70-ties a new material known under its brand name of PolyII appeared. It was a composite material on the base of UHMWPE with a dispersive addition of carbon fibres [17]. The production of elements made of this material consisted in the direct compression moulding of a mixture of UHMWPE powder and carbon fibres to final shape moulds [17]. Poly II material featured considerable better resistance to creep and better resistance to wear than ordinary UHMWPE, as confirmed by testing on a pin-on-disc apparatus [17]. A reduced fatigue resistance was also a problem. This material was withdrawn from the market 7 years after its introduction due to manufacturing problems involved with the compression moulding [7].

The next variation of the UHMWPE, which appeared at the beginning of the 90-ties, was Hylamer; a material with enhanced mechanical properties without any fillers or fibres [17]. These enhanced properties of Hylamer were due to a strict control of its crystalline structure. The production process consisted in the application of a very high pressure (above 280 MPa), high temperature (above 250°C) and a slow cooling of the ready-made product. The material had a markedly higher rate of crystallinity (80%) and elevated value of the modulus of longitudinal elasticity (when compared to the previous one). During the following years, diverging results concerning the resistance of the materials against wear were published [17]. An increase in its longitudinal modulus of elasticity also did not contribute to its application for endoprostheses.

In 1995 Furman, Rasquinha, et al. presented the results of the influence of manufacturing methods used in the production of polyethylene bushings on their resistance to wear. The research done showed that the shells manufactured by the direct moulding method were two times more resistant to wear than those manufactured by machining methods [17].

Apart of the research involving polyethylene with ultra high molecular weight, research involving polyethylene with high density (HDPE) was also conducted. A considerable decrease in the wear of elements made of HDPE and subjected to 100 Mrad radiation was observed when compared to radiation free UHMWPE [17]. This increase in the resistance to wear was due to a better cross-linking of polyethylene molecules. By analogy, the resistance to wear of radiated UHMWPE also increases with the increasing amount of its radiation. With 20 Mrads of UHMWPE radiation, its linear wear was not available to measure (less than 0.01 mm/year [17]). The application of so high radiation doses reduces the wear rate but impairs at the same time other mechanical properties, especially fatigue strength [17]. Research on the influence of gamma radiation on the mechanical properties and frictional performance are described, among others, by Oonishi [21] and Podrez Radziszewska [22]. In the mid-90-ties, the highly cross-linked polyethylene was being introduced into practice.

Restriction in the access of oxygen during radiation by the use of neutral gas or vacuum atmosphere significantly reduces negative chemical transformations in the surface layer of the material (oxidation). A considerable improvement of tribological performance as a result of ion radiation and limitation of negative impacts of this process resulted in its widespread and successful application till the present day.

3. Friction

3.1. Coefficient of friction

The literature dealing with the subject of friction offers a lot of research reports presenting values of the coefficient of friction for specified sliding pairs operating under stable conditions. Research dealing with tribological performance in terms of friction characteristics for typical sliding pairs is also available. Divergences between values reported in the literature are big, and the reasons are, in the authors' opinion, due to different friction conditions that are not accounted for in the design of experiment.

The results of research concern frequently friction in a given endoprosthesis make. These results concern mostly the linear wear, mass wear, and—to a lesser degree—values of the friction resistance. It shall be noted that the results obtained are heavily governed by the very design solution of the endoprosthesis. The type of contact and distribution of pressure in the friction zone are of paramount importance to friction and wear. The coefficients of friction of real implants determined with the aid of a walk simulator shall be used as a comparative parameter between different design solutions. They should not be used for the definition of properties of the friction pair employed due to different friction conditions (e.g. different contact pressure distribution patterns).

3.2. Distribution of contact pressure

Similarly as for other sliding pairs, the type and character of contact is of crucial importance to the process of friction. The distribution of contact pressure between the rubbing elements influences the force of friction and the wear rate. In the literature, the results of estimated contact pressure values for real endoprostheses operating at given kinematical inputs could be found [6, 23]. Missing is, on the other hand, research explaining the influence of the friction force on the distribution of contact pressure in the contact zone. It shall be noted that an attempt to evaluate the service life of the friction node of an endoprosthesis is a very frequent topic undertaken by researchers. The main purpose of these experimental works is the elaboration of a wear model of the polymer insert. The principal method used in these research projects is a multi-cycle measurement of ready-made elements carried out using a walk simulator. A resulting wear model has a limited application range and cannot be used for other types of endoprostheses and, worse, does not contribute to the explanation of the phenomenon essence.

To find relationships between the wear of the elements of an endoprosthesis and other parameters, needed is the determination of pressure distribution in the contact area. Pressure in the contact area is variable and wear is directly linked (among others) to this pressure. It shall be also noted that the state of stress in the endoprosthesis is very complex; not only due to its structure but also due to a variation of displacements.

3.3. Surface roughness of the counter-element and lubrication fluids

The friction present in sliding nodes is dependent, among others, on the surface finish of the contacting surfaces [16, 24]. In the case of co-operation of a polymer element with a metallic or ceramic element, crucial for friction and wear is the surface finish of the counter-element (a harder one). The rough surface of the metal element increases the abrasive wear and resistance to sliding due to deformations of the surface irregularities. With smooth surfaces, more important is adhesion present between the two mating surfaces. To describe adhesion wear, Archard had introduced the coefficient K being a ratio of the number of adhesion wear contacts to the overall number of wear contacts between the mating surfaces [5]. As a result of testing of many material pairs, Archard concluded that under dry friction conditions the least value of the coefficient K features polyethylene sliding against steel. For such a pair $K = 10^{-7}$ [5]. That means that only one adhesion contact out of 1 million responsible for friction resistance contributes to wear [5].

The co-operation of a polymer with a smooth surface element makes it possible to reduce abrasive wear [24]. The presence of body fluids in the friction zone of two smooth surfaces may contribute, at certain conditions, to the creation of the elastohydrodynamic lubrication. This observation was confirmed by Hall and Unsworth's research [11]. A condition necessary for the creation of the full film lubrication in an endoprosthesis is, among others, a sufficiently high viscosity of the lubricating medium. Values of the friction coefficient of some selected sliding friction pairs operating in the presence of different lubrication fluids are shown in Table 3 [14].

Laboratory testing [13] proved that the least values of the friction coefficient in the presence of a lubrication fluid (Ringer's solution) were for the smoothest surface of the metallic element in friction pairs UHMWPE vs. 316L and UHMWPE vs. Co-CrMo. For the friction pair UHMWPE vs. 316L, at a value of the roughness parameter $Ra = 0.04 \mu\text{m}$, the unit pressure $p = 1.25 \text{ MPa}$ and sliding velocity $v = 0.085 \text{ m/s}$, the friction coefficient was equal to $\mu = 0.0284$.

Table 3. Values of the friction coefficients for some selected friction pairs operating in the presence of different lubrication fluids. Pin on plate tester $p = 3.45 \text{ MPa}$ [14]

Lubricant Counter-specimen	Bovine serum		Saline		Distilled water	
	U	R	U	R	U	R
Zirkona	0.049	0.040	0.082	0.060	0.055	0.028
Alumina	0.056	0.054	0.115	0.089	0.075	0.044
316L	0.078	0.065	0.156	0.123	0.097	0.061

U = unidirectional motion,

R = reciprocating motion.

4. Operational considerations

Motions performed by a human being may be defined as intermittent ones. The operation of joints on a daily basis cannot be compared to the operational mode of ma-

chinery. Motions are in short cycles (compared to those present in machinery) with frequent interruptions. During these breaks, a friction node is subject to changes. Polyethylene (similarly to other thermoplasts) exhibits a tendency to relaxation and creep, especially at elevated temperature.

Metallic element of endoprostheses co-operating with polyethylene do not display any noticeable wear [9]. Hard particles (wear scale) like, among others, particles of spalled bone cement may get into the contact zone and scratch the metallic surface of the endoprosthesis head. The research reported in [9] did not show any changes on the endoprosthesis head after 15 years of exploitation, even in the surface finish.

Based upon clinical trials and laboratory testing, the following typical modes of failure of polymer components may be listed [9, 15]:

- abrasive wear identified by changes in the micro and macro geometry of the surface,
- plastic deformations (as a result of violation of the allowable endoprosthesis loading) and creep,
- fatigue wear (pitting),
- changes in the chemical composition and colour,
- changes in the material structure,
- loosening and rupture.

4.1. Abrasive wear and wear products

The basic mode of failure of polymer bushing under friction conditions is abrasion. Numerous tests that have been carried out to determine the abrasive wear of polyethylene focus mainly on linear wear. This type of wear influences changes in the geometry of contact in a sliding node. To isolate plastic deformation and linear wear, it is necessary to measure mass loss of the tested components. The spread of the wear values is considerable depending upon the type of a friction pair and the type of endoprostheses (especially in the case of knee endoprostheses). The mean value of wear of the bushing of knee-joint endoprostheses for a friction pair Co/CrMo vs. UHMWPE was equal: 0.15 to 0.20 mm/year (linear wear) [25], and 50 to 100 mm³/year (volume), a significant growth after 10 years in service [35]. Markedly reduced wear was reported during friction of polyethylene with ceramic elements. For a friction pair Al₂O₃ vs. UHMWPE the linear wear was equal to a mere 0.03 mm/year [25]. It shall be stressed that the wear rate is influenced to a considerable degree by pressure in the contact zone [1, 9], kinematics of the friction node [2], and mobility of a patient. [9].

Products of wear differ depending upon the type of materials used for friction pairs. Impacts of the wear products on the organism reaction are also different. For polyethylene components, its scale dominate in the products of wear (size: from 1 to 20 μm [9], 3 to 25 μm on average [10]). Larger (20 to 50 μm) particles are also present [9]. Products of wear have a tendency to conglomerate. Worn particles are removed by lymphatic vessels but part of them accumulates on the implant ridges, around the fric-

tion node [9 after 27]. Table 4 contains a summary of approximate wear data for different materials (elaborated based upon [9, 17, 18, and 25]).

Table 4. Wear of polymer materials used for hip endoprotheses [9, 17, 18, and 25]

Material	Wear of bushings of hip joint endoprosthesis
Non-modified UHMWPE	0.12 – 0.25 mm/year – metal head
	0.098 – 0.03 mm/year – ceramic head
Crossed UHMWPE	0.022 – 0.15 mm/year – metallic head (2.5 – 4.0 Mrads)
	0 – (above 20 Mrads) – metallic head
Poly II (UHMWPE + 20% of carbon fibres)	$4.89 \cdot 10^{-9}$ g/cycle – metallic head
Hylamer (UHMWPE: specific manufacturing conditions)	0.13 – 0.4 mm/year – metallic head
	0.15 – 0.33 mg/mln. cycles – ceramic head
UHMWPE: direct compression moulding	0.05 mm/year – metallic head
HDPE: highly crossed (100 Mrads)	0.076 mm/year – metallic head
	0.072 mm/year – ceramic head

4.2. Plastic deformation and creep

The low yield stress of the UHMW polyethylene contributes to plastic deformations of endoprosthesis elements made of these materials during their usage. In knee joint endoprotheses, this phenomenon is present at the beginning of the endoprosthesis usage and during its overloading. It is especially pronounced in endoprotheses with flat surface of the polymer insert. In hip joint endoprotheses, due to the dominant pattern of pressure distribution (bearing pressure), the phenomenon of creep dominates. An additional factor contributing adversely to the yield limit and accelerating the process of creep is local temperature rise in the friction node [9].

4.3. Fatigue wear

Contact fatigue phenomenon (pitting) adversely affects the exploitation of knee joint endoprotheses. The shape of the mating surfaces and loading are such that the contact zone is subject to a high concentration of stresses. The maximum concentration occurs below the surface (Bielajev's point). Additionally, fluctuations in the direction of loading destroy the structure of the material and cause separation of big chunks of polyethylene. Fatigue wear is non-measurable until a chunk of material has been separated, and therefore dangerous.

Changes in the mechanical properties of the material caused by friction and radiation sterilisation have an additional influence triggering this phenomenon [22]. The augmentation of the gamma radiation doses during sterilisation reduces the material wear reducing at the same time its fatigue resistance. The best solution is setting the maximum wear limit free of the implant osteolysis during its usage and next, selecting a proper dose of radiation to obtain a material with the target wear limit. A maximum

value of the linear wear free of osteolysis for bushing in the hip joint endoprosthesis (28 mm in dia.) has been established for 0.1 mm per year [18].

Polyethylene properties are also changing during its exploitation as a result of friction and environmental conditions. Based upon the testing done, polyethylene subjected to cyclical loading with the presence of friction caused an increase in crystalline by 12% on average [9]. As a result, the material became brittle and vulnerable to wear [9].

5. Summary

Tribological problems present in the alloplastics of joints belong to the most complex ones. The number of factors influencing the operation of a joint is huge. As a result, there is a plurality of possible design solutions. A short history of alloplastics has many threads. A deterrent factor is the long time necessary for reliable results of clinical trials. The continuous improvement in the design of simulators notwithstanding, there are still divergences between the results of laboratory testing and clinical trials.

The progress in analytical methods (FEM) gives an opportunity to design implants compatible with the organism of a human being. Tribological aspects that directly affect the operation of a joint are still a problem. The two most important ones are: the mechanism of friction and wear processes.

The main direction of research at present is targeted to the anticipation and learning of the wear process in endoprostheses. The knowledge that has been accumulated for the last 60 years makes it possible to properly select materials for a friction pair. Strict manufacturing regimes and sterilisation give a possibility to modify and optimize the mechanical properties and tribological performance of sliding materials.

The knowledge concerning all factors influencing the process of friction and wear and their skilful application will make it possible to thoroughly control the operation of sliding frictional nodes. The acquisition of such knowledge stimulates further research on the phenomena and processes governing the operation of endoprostheses.

References

- [1] Barbour P., Barton D., Fisher J.: *The influence of stress conditions on the wear of UHMWPE for total joint replacements*, Journal of materials science: Materials in medicine, 8, 1997, pp. 603–611.
- [2] Barnett P., Fisher J., Auger D., Stone M., Ingham E.: *Comparison of wear in total knee replacement under different kinematic conditions*, Journal of materials science: Materials in medicine, 12, 2001, pp. 1039–1042.
- [3] Będziński R.: *Biomechanika inżynierska, zagadnienia wybrane*, Oficyna Wydawnicza Politechniki Wrocławskiej, Wrocław, 1997.
- [4] Boutin P.: *Arthoplaste totale de la hanche par prothese en alumine fritee*, Rev. Chir. Orthop. Reparatrice Appar. Mot., 1972, t. 58(3), pp. 229–246.

- [5] Bowden F.P, Tabor D.: *Wprowadzenie do trybologii*, Wydawnictwa Naukowo – Techniczne, Warszawa, 1980.
- [6] Burcan J., Witosławski P., Žytňanský M., Rehak L.: *Badanie oporów ruchu endoprotezy ceramicznej*, Materiały V Sympozjum Mechanika w medycynie, Rzeszów, 2000, p. 47–49.
- [7] Capanidis D.: *Ocena degradacji polioksymetyleny (POM) zachodzącej podczas jego tarcia po stali*, Tribologia, 2002, R. 33, nr 3, pp. 801–809.
- [8] Czupryńska J.: *Wpływ wysokoenergetycznego promieniowania elektronowego na zmianę właściwości niektórych polimerów*, Polimery, 1, 47, 2002, pp. 8–14.
- [9] Gierzyńska-Dolna M.: *Biotribologia*, Wydawnictwo Politechniki Częstochowskiej, Częstochowawa, 2002.
- [10] Gierzyńska-Dolna, M., Wieczorek A., Lacki P., Szfrański A.: *Ocena materiałów stosowanych na implanty w aspekcie badań tribologicznych*, Materiały IV Sympozjum Mechanika w medycynie, Rzeszów, 1998, pp. 105–110.
- [11] Hall R. M., Unsworth A.: *Friction in hip prostheses*, Biomaterials, 18, 1997, pp. 1017–1026.
- [12] Judet J., Judet R.: *The use of an artificial femoral head for arthroplasty of the hip joint*, J. Bone Surg. Br., 1950, t. 32–B(2), pp. 166–173.
- [13] Kowalewski P., Wieleba W., Woźniak J.: *Wpływ chropowatości powierzchni elementu metalowego na wartości współczynnika tarcia materiałów stosowanych w endoprotezie stawu kolanowego*, mat. X Jubileuszowy Kongres Eksploatacji Urządzeń Technicznych, Stare Jabłonki, 6–9 września 2005.
- [14] Kumar P., Oka M., Ikeuchi K., Shimizu K., Yamamuro T., Okumura H., Kotoura Y.: *Low wear rate of UHMWPE against zirconia ceramic (Y-PSZ) in comparison to alumina ceramic and SUS 316L alloy*, Journal of Biomedical Materials Research, Vol. 25, Issue 7, June 1991, pp. 813–828.
- [15] Kusz D.: *Rys historyczny i uwarunkowania rozwoju endoprotezoplastyk stawu biodrowego*, Inżynieria Materiałowa nr 2 (103), Rok XIX, Marzec–Kwiecień 1998, pp. 36–39.
- [16] Lawrowski Z.: *Tribologia*, wyd. Politechnika Wrocławska, 1985.
- [17] Li S.: *Ultra high molecular weight polyethylene: from Charney to cross-linked*, Operative Techniques in Orthopedics, Vol.11, Nr 4 (October), 2001, pp. 288–295.
- [18] Livingston B.J., Chmell M.J., Spector M.: *Complications of total hip arthroplasty associated with the use of an acetabular component with a Hylamer liner*, Journal of Bone Surgery, 79, 1997, pp. 1529–1538.
- [19] Marciniak J.: *Biomateriały*, Wydawnictwo Politechniki Śląskiej, Gliwice, 2002.
- [20] Morecki A., Ekiel J., Fidelus K.: *Bionika ruchu. Podstawy zewnętrznego sterowania biomechanizmów i kończyn ludzkich*, PWN, Warszawa, 1971.
- [21] Oonishi H., Kuno M., Tsuji E., Fujisawa A.: *The optimum dose of gamma radiation-heavy doses to low wear polyethylene in total hip prostheses*, Journal of Materials Science: Materials in Medicine, 8, 1997, pp. 11–18.
- [22] Podrez-Radziszewska M., Dudziński W.: *Wpływ promieniowania wysokoenergetycznej wiązki elektronów na własności UHMWPE*, Materiały X Seminarium „Tworzywa sztuczne w budowie maszyn”, Kraków, 2003, pp. 303–306.
- [23] Pytko A., Kowal A.: *Implanty stawu biodrowego człowieka*, Materiały IV Sympozjum Mechanika w medycynie, Rzeszów, 1998, pp. 197–209.

- [24] Rymuza Z.: *Trybologia polimerów ślizgowych*, Wydawnictwa Naukowo-Techniczne, Warszawa, 1986.
- [25] Santavirta S., Kontinen Y. T., Lappalainen R., Anttila A., Goodman S. B., Lind M., Smith L., Takagi M., Gómez-Barrena E., Nordsletten L., Xu J.-W.: *Materials in total joint replacement*, Current Orthopaedics, 1998, 12, pp. 51–57.
- [26] Smith-Petersen M.: *Arthroplasty of the hip*, J. Bone Joint Surg., 1339, t. 21 (2), p. 69–288.
- [27] Ungethum M., Winkler-Gniewek W.: *Tribologie in der Medizin*, Tribologia und Schmirungstechnik 1990, Nr 5, pp. 268–277.
- [28] Warren N.: *A short history of total hip replacement*, Joint replacement, Mosby year book, London, 1990.
- [29] Weisman S.: *Surgical Implant Materials*, ASTM Standardization News, November 1976.
- [30] Wierzcholski K., Czajkowski A.: *Rodzaje tarcia w biotribologii*, Mater. II Sympozjum Inżynieria Ortopedyczna i Protetyczna IOS'99, Białystok, 1999, pp. 357–369.
- [31] Ziemiański K.: *Zastosowanie tworzyw sztucznych w budowie maszyn: wybrane zagadnienia*, Oficyna Wydawnicza Politechniki Wrocławskiej, Wrocław, 1995.

Polimery ślizgowe w alloplastyce stawów

Endoprotezy pozwalają na zastąpienie chorego lub uszkodzonego stawu elementami wykonanymi przez człowieka. Istniejące obecnie urządzenia tego typu dzięki licznym doświadczeniom klinicznym oraz rozwojowi technologii ich produkcji stają się coraz bardziej nowoczesne. Ciągłej modyfikacji podlegają materiały wykorzystywane w węzłach tarcia endoprotez. Podstawowymi przyczynami niepowodzeń implantacji sztucznych stawów jest obłuzowanie się wszczepu, często spowodowane infekcją wywołaną produktami zużycia elementów polimerowych, nieprawidłowym wszczępieniem lub nieprawidłową współpracą implantu z tkanką żywą. Ponadto po okresie kilkunastu lat niezbędna jest wymiana wszczepionej endoprotezy na skutek jej zużycia. Poprawa właściwości ślizgowych i odporności na zużycie elementów polimerowych endoprotez, zmniejszyłoby ryzyko powikłań i reimplantacji, oraz wydłużyło okres stosowania implantu. Obecnie prowadzone są liczne badania mające na celu wyjaśnienie procesu zużywania polimerowych wkładek stosowanych w endoprotezach stawu kolanowego oraz biodrowego. W przypadku implantowanego stawu siły tarcia są większe niż w przypadku naturalnego biołożyska, dodatkowo obciążenia posiadają zmienny charakter, co powoduje pojawienie się aspektu wytrzymałości zmęczeniowej urządzenia oraz wpływu na zespolenie kość-implant. Właściwości mechaniczne i tribologiczne polietylenu o ultra wysokim ciężarze cząsteczkowym (UHMWPE), zdecydowały, iż stał się on podstawowym polimerem ślizgowym stosowanym w alloplastyce stawów. Poprawa niezawodności, trwałości oraz przewidywalność zużywania się węzłów tarcia endoprotezy są priorytetowymi kierunkami w badaniach prowadzonych w tej dziedzinie.



The influence of polymer fillers in a grease lubricant on the tribological performance of friction nodes operating under mixed friction conditions

ST. KRAWIEC

Wrocław University of Technology, Wybrzeże Wyspiańskiego 25, 50-370 Wrocław

The paper presents the results of a study upon the influence of the type of polymer filler in a lithium grease lubricant on the lubrication performance of steel friction pairs operating under mixed friction conditions. Grease compositions based upon the 1S lithium grease and powders of three polymers, i.e. polytetrafluoroethylene (PTFE), polyoxymethylene (POM) and PA6 polyamide were analysed. For the sake of comparison, compositions with an anisodesmic filler (graphite) and metallic filler (tin) were also tested. The tribological testing was carried in agreement with the guidelines of the PN-76/C-04147 standard using a four ball apparatus. The effectivity of the tested lubricants was evaluated using three criteria: the ball wear d , the limiting wear load G_{oz} and the limiting load F_g . It was found that a polymer featuring good tribological properties (when used as material for sliding bearings) might not always be equally efficient when used as filling powder. POM or PA powders used as fillers for the 1S lithium grease do not improve the effectivity of lubrication. A modification of the same grease with 6 wt % of PTFE powder results with an effective grease composition.

Keywords: *grease lubricants, polymer fillers, effectivity*

1. Introduction

Mixed friction, according to practice, is the dominant type of friction in friction nodes. Even in friction pairs operating under full film lubrication conditions, this phase is present during starting and stopping. It must be stressed that many friction assemblies, due to oscillating or reciprocating motion, operate continuously at mixed friction conditions. Examples are highly loaded, low speed joints, e.g. in loaders and excavators, in the suspension systems of automobile vehicles, in hoisting machinery (grippers), or in chains etc. The presence of boundary friction in the process of mixed friction results in elevated power losses (lower efficiency) and material losses (wear). Viewing the above, studies upon mixed friction lubrication with the finding of possible remedies for these deficiencies as the ultimate goal are generally justified.

According to the principle of Krachelski, a condition necessary for the friction and wear process under mixed friction conditions in friction nodes to be normal is to provide the upper surface of the mating elements with a positive gradient of the shear strength [1]. The optimum value of this gradient is sought by improving tribological properties of both mating materials and lubricant.

As experience points, actions aiming at the increase of the positive gradient by lubrication are very effective. Garkunov proved that a small amount of lubricant provided at the mating surfaces is sufficient for the creation of a thin lubrication layer of 100 nm thickness that is able to reduce 10 times forces of friction and 100 times wear.

The most efficient substances for the lubrication of friction nodes operating under mixed friction conditions are greases. This high effectivity of greases is due to their ability to create thick boundary layers. The research reported in [3, 4] proved that a lubrication layer created on the mating surfaces was 1.2 to 3.5 times thicker than that created by the base oil. Grease components do not guarantee, however, good lubrication properties in the range of high loading. This is due to a comparatively low temperature of desorption of the boundary layer created on the lubricated surfaces of the mating elements. The improvement of these properties is possible by many methods. The simplest one and sufficiently effective method is the introduction of so-called fillers to grease. These are substances of different structure and concentration that are not soluble in the plastic matrix and do not interfere with the colloidal structure of a grease lubricant [5], [6].

Among the many types of fillers, the earliest employed were anisodesmic structure substances. Graphite and molybdenum disulphide among them have found the widest application range. Newer generation of fillers consists of soft metals like copper, tin, zinc, and lead. A grease lubricant with the like filler forms a thin metallic layer (metal plating) on sliding surfaces, which protects these surfaces against sticking and lowers the thermal loading of the friction node [7, 8]. By virtue of these properties, the effectivity of lubrication of such modified grease becomes considerable enhanced.

One of the prospective directions of improving anti-friction and anti-wear properties of greases is their modification with polymer fillers. The application of polymer powder for this purpose is purposeful as it enables the elimination of the main faults of polymer sliding materials, i.e. their low thermal conductivity, often the high wear rate, and hygroscopy, and soaking contributing to dimensional instability of the manufactured sliding elements.

In this paper, the results of a study upon the effectivity of lubrication of steel sliding pairs with compositions containing different polymer fillers are presented. These compositions had been prepared based upon the 1S brand name lithium grease and contained 6 wt% of powder of each of the three polymers, i.e.: PTFE (polytetrafluoroethylene), POM (polyoxymethylene), and PA6 polyamide. These polymers have been widely used as materials for the construction of sliding friction nodes that do not require lubrication. A composition containing PTFE by-product powder was also tested. An incentive for the latter study was a need to make use of waste materials released during the production of PTFE by the Tarnowskie Zakłady Azotowe. For comparative reasons, a composition with anisodesmic structure (graphite) and a composition with soft metal powder (tin) were also tested and analysed.

2. The method and experimental

Experiments were conducted in agreement with the PN-76/C 04147 Polish standard “Testing of lubrication properties of greases and oils” using a four ball apparatus. According to this standard, three indexes were adopted for the evaluation of effectiveness of the tested compositions: the ball wear d , the limiting wear load G_{oz} and the limiting load F_g defined as the maximum load that is still safe against the ball welding. This load indicates the level of the maximum pressure that a lubricating layer is still able to sustain. The next, higher load causes the interruption of the lubricating layer and welding of the mating balls; this is the welding load F_z . Grease composition had been prepared using a mixer. A weighed portion of the grease and filler had been mixed for 30 minutes at a speed of the mixer $n = 800$ r.p.m. The mixing time $t = 30$ min was established experimentally according to a criterion of the uniform distribution of the filler particles in the grease carrier. This uniformity was assessed visually by observing the prepared composition under a biological microscope after 10, 20, and 30 minutes of mixing.

The measurement of wear of the balls was conducted parallel and perpendicular to the wear scar. Scars less than 1 mm in size were measured using a microscope with an accuracy of 0.01 mm, and the remaining scars – using a magnifying lens with an accuracy of 0.1 mm. The trials were repeated always 6 times. The results were statistically processed at a level of confidence equal to 95% using the t-Student test.

3. Specification of materials and their short characteristics

The following materials were used for testing:

1. The 1S all purpose vehicle grease as the carrier (the base grease) for the tested fillers. This grease, as proved by testing [9], features the worst lubrication properties among the three analysed grease lubricants designed for the lubrication of sliding bearings, i.e. the STP grease, 1S, and Machine 2 grease. The selection of the carrier according to the above criterion made it possible to limit the interfering influence of the lubrication properties of the carrier on the effectivity of lubrication of a composition made on its base. This decision agrees with the results of [10], where it was proved that anti-friction and anti-wear properties of copper powder filled compositions are best pronounced when the underlying carrier grease has the worst lubrication properties.

2. Powders of three polymers, i.e.:

- Polytetrafluoroethylene PTFE (suspension Tarflen®, symbol SM 1) manufactured by Zakłady Azotowe Tarnów with a granulation of 20 to 40 μm and waste PTFE (designated here as PTFE–o). PTFE is a derivative of polyethylene (PE) in which all atoms of hydrogen had been replaced by atoms of fluorine such that PTFE chains are built of carbon atoms surrounded by fluorine atoms. This is a material with some of its tribological properties unknown in any other polymer materials. When sliding on pol-

ished steel, PTFE displays the smallest value of the friction coefficient $\mu \approx 0.05$ [11, 12] and its value is stable with an increase in temperature [13]. Due to the small energy of cohesion, the transfer of PTFE onto the metallic surface of the mating element is especially easy creating thus a highly ordered layer of polymer [14, 15]. By virtue of this property, the mating of a steel/plastics friction pair is being converted into the mating of a PTFE/PTFE pair, what is more tribologically advantageous due to the presence of weak van der Waals forces between the mating surfaces. At the same time, such disadvantageous features as low wear resistance, low thermal conductivity, high thermal expansion and ease of deformation limit considerably the application range of PTFE (in its monolithic form) in the construction of sliding nodes. One of the methods that permits successfully to by-pass the deficiencies of this material is its use in a pulverised form as grease filler.

- Polyoxymethylene (POM, Tarnoform®) with a granulation of up to 50 μm . It belongs to a group of polyacetals, complexes containing a recurrent CHRO mer and polyacetal resins. This polymer is employed mostly as a construction material. Considering its beneficial properties under dry friction conditions [16] as well as its application in composite materials of the Glacier Company (DX type composites), this polymer was used as filler in this research.

- Polyamide (PA6) with a granulation of up to 60 μm . It belongs to polyamides featuring good strength and sliding properties. These favourable sliding properties in the monolithic material may suggest that the situation will be the same when this polymer is used in the form of powder as grease filler.

3. Graphite with a brand name of CR2. This is a material of natural origin with a granulation of up to 8 μm . An X-ray examination of the chemical composition of this graphite confirmed its high purity with respect to the content of mineral origin impurities. This graphite has been widely employed by domestic manufacturers to the production of graphite greases.

4. Tin powder with a granulation of up to 63 μm . This is a product of Zakłady Metalurgiczne in Trzebinia. Tin powder is obtained by blasting a stream of liquid metal with gas; powder particles are spherical in shape. The choice of tin powder as filler was decided by its two features: ability to plate the steel surface during sliding and secondly, tin as an element is able, similarly to copper, to create complex complexes.

5. Bearing balls made of LH15 steel, 12.7 mm in diameter and machined to 16 grade of accuracy in the dimensional group $S = 0 \mu\text{m}$. Other physical properties of the balls were in agreement with the PN-83/M-86452 Polish standard.

4. Results of experiments and conclusions

A summary of the results in a form of plots: ball wear vs. load for the tested compositions are shown in Figure 1. Calculated values of the limiting load G_{oz} are illustrated in Figure 2.

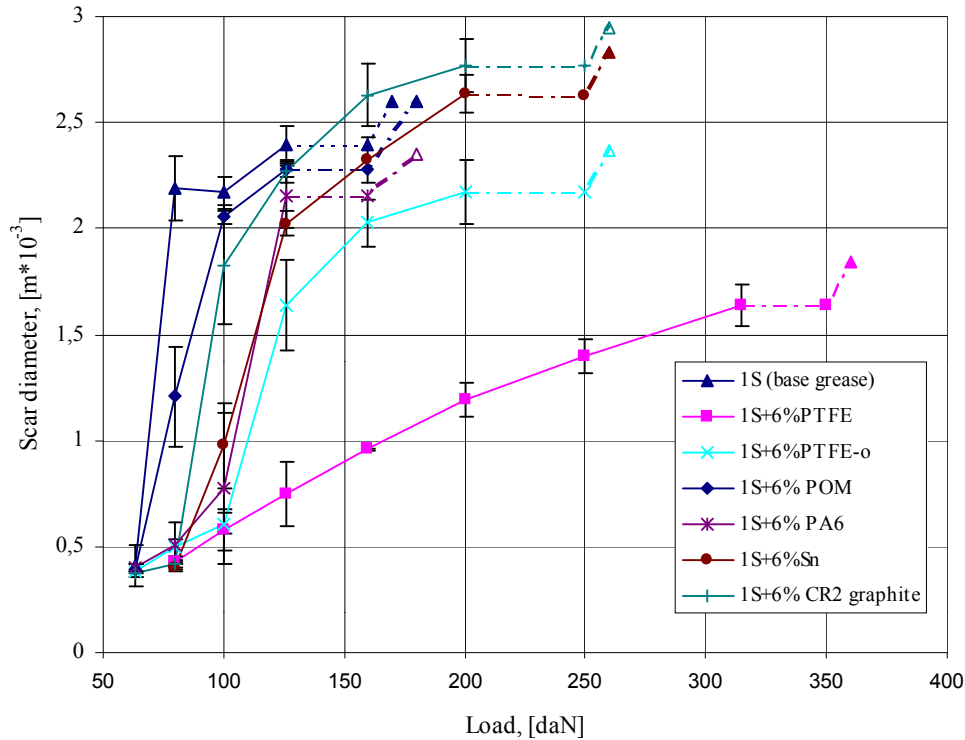


Fig. 1. Wear vs. load for the tested greases

Additionally, each figure includes, for the sake of comparison, characteristics for a composition with graphite, tin powder, and for the 1S grease (the base for the prepared grease compositions). A value of the G_{oz} indexes for the 1S base grease and for the POM composition is equal to zero, as three trials (out of six made) resulted in the ball welding.

By comparing values of the criteria magnitudes, i.e. wear, the limiting load, and the limiting wear load index that were obtained when lubricating with POM or polyamide compositions, it is seen that two of them (wear and the limiting load) are the same or their values are very close to each other. As an example, the limiting load for the 1S grease $F_g = 126$ daN. This load for a composition with POM or PA6 is also the same. Similar situation is with wear, which at a load of e.g. 126 daN is for all the three greases very close and equal to approximately 2.2 mm. A significant difference occurred in values of the limiting wear load G_{oz} . This index for the 1S grease and its composition with POM is equal to zero. As it was explained previously, testing with these greases resulted in welding of the balls. When lubricating with a PA6 composition the balls were free of seizure, a value of G_{oz} was equal to 14 daN/mm² and was equal to those obtained when lubricating with non-polymer compositions, i.e. with graphite and tin (Figure 2). The occurrence of this difference witnesses to the fact that

compositions with PA6 are slightly more effective than compositions with POM. In a general author's opinion the POM and PA6 polyamide powder do not increase the effectivity of lubrication of composition made with these powders. On the other hand, modification of the 1S with 6 wt% of PTFE powder significantly increases lubrication performance of this grease. Values of all the three accepted criteria magnitudes are decidedly better for this composition than those obtained for non-filled grease. As an example, the limiting load for this composition is 315 daN, what is a 150% increase when compared to the value obtained by lubricating with the non-modified grease or lubricating with the POM or PA6 filled grease. This high increase in the effectivity of lubrication of the 1S grease filled with PTFE is also confirmed by the wear criterion. By lubricating with this composition, the wear of the balls at a load of 315 daN is equal to 1.64 mm and is less by about 30% than the value obtained during the testing of the balls at a considerable lower load (126 daN) and with a non-modified grease lubricant. Concerning the influence of waste PTFEo on the criteria values, it is seen that a composition filled with this powder is clearly less effective than compositions filled with commercially available PTFE. Generally, the lubrication performance of a composition containing PTFEo is comparable to that obtained when lubricating with compositions containing non-polymer fillers, i.e. graphite or tin. As an example, the limiting load for these three compositions is equal to 200 daN, and the G_{oz} index – approximately 15.5 daN/mm².

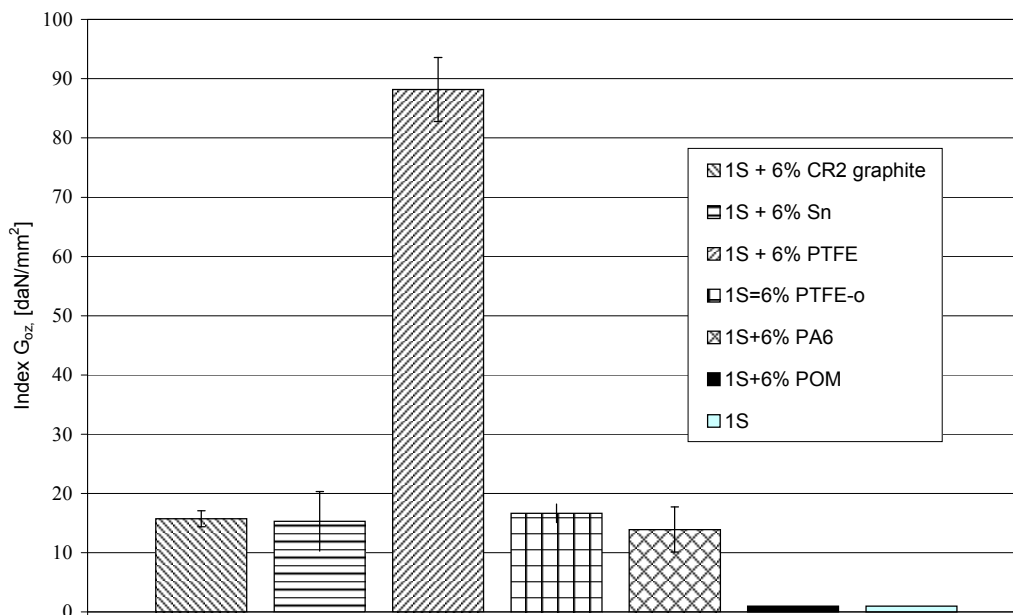


Fig. 2. Index of the limiting wear load G_{oz} for the tested greases

The results of investigations of the influence of polymer fillers in the lithium grease on tribological characteristic of friction pairs operating under mixed friction conditions can be summarised in the following way:

1. Polymer material that displays good tribological properties when used as materials for the construction of friction assemblies (e.g. bushing) might not be equally effective as fillers of greases. Polyoxymethylene and PA6 polyamide used in powdered form as filler to the 1S grease do not increase the effectivity of lubrication of the underlying base grease.

2. Polytetrafluoroethylene (PTFE), which has a limited application range as a construction material due to its poor wear resistance and dimensional instability, is an effective filling material when used as filler to the 1S grease. Modification of the 1S grease with this polymer (6 wt %) causes an increase of the seizure load from 126 daN to 315 daN, that is by approximately 150%. Also wear at this load (315 daN) is approximately 30% lower than the wear recorded when testing at a load of 126 daN with a non-modified grease lubricant.

3. Indexes of the lubrication performance for compositions containing waste PTFE are very close to those measured when using a grease lubricant filled with common, non-polymer fillers like graphite or tin.

References

- [1] Kragelskij I.V., Michin N.M.: *Uzly trenija mašin*, Mašinstroenie, Moskva 1984.
- [2] Staroselskij A.A., Garkunov D.I.: *Dolgovječnost truščichsja detalej mašin*. Mašinostronie, Moskva, 1967.
- [3] Bakašvili D.L., Imerlišvili T.V.: *Prognozirovanie tolščiny plenki plastičnych smazok v uprugogidrodinamičeskich kontaktach*, Trenie i iznos 1987, T. 8, No 2, pp. 236–243.
- [4] Švarcman V.Š., Šojchet V.H., Imerlišvili T.V., Čchaidze G.R.: *Tolščina plenki plastičnych smazok pri različnych režimach raboty tjaželonagružennych uprugogidrodinamičeskich kontaktov*, Trenie i iznos, 1988, T9, No 1, pp. 129–136.
- [5] Fuks I. G.: *Dobavki k plastičnym smazkam*, Chimija, Moskva, 1982.
- [6] Wachal A., Kulczycki A.: *Trybologiczne własności smarów plastycznych zawierających polimery niskotarciowe*, Trybologia, 1986, Nr 4–5, pp. 21–23.
- [7] Fuks G. I.: *Adsorbpcja i smazočnaja sposobnost maseł*, Trenie i iznos, 1983, T. IV, No 3, pp. 398–414.
- [8] Rajbov D.V., Matveeskij R.M., Fuks I.G., Bujanovski I.A.: *Vlijanie medsoderžaščich dobavok na antifrik cionnye svojstva plastičnych smazok*, Trenie i iznos, 1989, T.10, No 6, pp. 1100–1104.
- [9] Krawiec S.: *Wpływ synergizmu wybranych napełniaczy w smarze na zwiększenie trwałości ślizgowych węzłów maszyn*, Oficyna wydawnicza PWR, Wrocław, 1998.
- [10] Kračun A.T., Zobov E.V., Morar V.E., Bruchis M.M., Kračun S.V.: *Issledovanie vlijanija tverdogo sma zočnogo materiala na protivozadirnnye, protivozadirnye i antifrikcionnye svojstva plastičnych smazok*, Trenie i iznos, 1981, T. II, No 5, pp. 856–863.
- [11] Reick F. G.: *Energy – Saving Lubricants Containing Colloidal PTFE*, Lubricating Engineering, 1982, Vol. 38, Nr 10.

- [12] Spengler G., Wunsch F.: *Schmierung und Lagerung in der Feinwerktechnik*, Düsseldorf, VDI Verlag, 1970, pp. 182–185.
- [13] Senatrev A. N., Smurugov V. A., Savkin V. G.: *K mehanizmu frikcionnogo perenosa i samosmazыvaniya PTFE*, *Trenie i iznos*, 1991, T.12, No 6, pp. 1023–1027.
- [14] Baranov N. G.: *Klassifikacija svojstva, oblasti primenenija poroškowych antifrikcionnych materialov*, *Trenie i iznos*, 1991, T.12, No 5, pp. 905–913.
- [15] Semenov A. P., Noženkov M. V.: *K voprosu o mehanizme smazočnogo dejstvija tverdych antifrikcionnych materialov*, *Trenie i iznos*, 1984, T. V, No 3, pp. 408–416.
- [16] Capanidis D.: *Badania tribologiczne kompozytów ślizgowych na bazie polioksymetylenu (POM) – Tarnoformu*, *Trybologia*, 2004, R. 35, nr 3, pp. 25–33.

Wpływ polimerowych napełniaczy w smarze plastycznym na charakterystyki tribologiczne węzłów ślizgowych pracujących przy tarciu mieszanym

W artykule przedstawiono badania wpływu rodzaju napełniacza polimerowego w smarze plastycznym na efektywność smarowania stalowych węzłów ślizgowych pracujących w obszarze tarcia mieszanego. Analizie poddano kompozycje smarowe uzyskane z napełnienia smaru plastycznego litowego 1 S proszkami trzech polimerów, tj. policzterofluoroetyleny (PTFE), polioksymetyleny (POM) i poliamidu PA6. Dla celów porównawczych zbadano też kompozycje z napełniaczem o budowie anizodesmicznej (grafitem) oraz z napełniaczem metalicznym (cyną). Badania tribologiczne prowadzono na aparacie czterokulowym z zastosowaniem wytycznych normy PN-76/C-04147. Efektywność analizowanych smarów oceniano według trzech wielkości kryterialnych, tj. zużycia kulek d , granicznego obciążenia zużycia G_{oz} oraz obciążenia granicznego F_g . Stwierdzono, że nie zawsze polimer, który ma dobre charakterystyki tribologiczne, gdy jest stosowany jako materiał konstrukcyjny na węzły ślizgowe, jest jako proszek efektywnym napełniaczem smaru plastycznego. Proszki POM lub poliamidu PA zastosowane jako napełniacze smaru 1S nie polepszają efektywności smarowania utworzonej kompozycji smarowej. Modyfikacja tego samego smaru plastycznego 6% wagowo proszku PTFE tworzy bardzo efektywną kompozycję smarną.



Analysis of screw propeller 4119 using the Fluent system

JAN KULCZYK, ŁUKASZ SKRABURSKI, MACIEJ ZAWIŚLAK

Wrocław University of Technology, Wybrzeże Wyspiańskiego 27, 50-370 Wrocław

The aim of this paper was to carry out an analysis of screw propeller 4119 using the RANS method. A computer program for creating spatial propeller geometry was developed for this purpose. Two-equation turbulence models: $k-\varepsilon$ and $k-\omega$ were adopted for calculations. The calculations were performed for an isolated propeller. The results were used to determine the propeller's hydrodynamic characteristics. The calculation results were compared with experimental results.

1. Introduction

Despite the considerable advances in theory, model tests are still the main source of information about the hydrodynamic properties of isolated propellers. Model tests must satisfy geometric, kinematic and dynamic similarity requirements.

In order to express velocity/force ratios in the geometric scale one should preserve the equality between the relevant similarity numbers: the Froude number and the Reynolds number. Equality of the Froude numbers for the propeller and its model is technically easy to achieve. If the propeller operates in unbounded water, there is no need to preserve the equality between the Froude numbers. This need arises only when propeller operation produces waves on the free surface, which practically occurs only when the propeller axis depth is smaller than the propeller diameter. The equality between the Reynolds numbers of the actual propeller and its model leads to technically unfeasible relations for speed, revolutions and forces. Since it is impossible to preserve equality between Reynolds numbers in model tests of isolated propellers such modelling becomes partial. The resulting errors are referred to as the scale effect. Attempts are made at reducing them through the use of possibly large models (small geometric scales) and through corrections introduced when rescaling model test results to the actual ship.

In test models of noncavitating isolated propellers operating at a sufficient distance from the free surface, aimed at determining the hydrodynamic characteristics of such propellers one can use any revs and any forward speeds, provided that they allow:

- the measurement of the characteristics in the required advance coefficient range,
- measurement at Reynolds numbers higher than the critical one.

Testing by numerical methods eliminates the scale effect problems since tests can be performed at a scale factor of 1. Consequently, modelling accuracy, particularly for large propellers, can be considerably increased. One should note, however, that the results obtained in this way are loaded with other errors.

2. Principles of finite element mesh design

Finite element mesh design is a vital part of flow modelling. It is the most complex and time-consuming task in this process and to a large extent it determines the correctness of the results. The finite element mesh design problem can be approached in two ways:

- methodically – knowing the character of the flow one can try to generate a structural mesh whose shape matches that of the flow,
- by force – by applying, without any reservations, a nonstructural mesh with a large number of elements.

The first approach is justified in cases when the geometry of the investigated flow is simple and there is no problem with properly arranging the elements. In the case of more complex phenomena, such as the flow around a screw propeller, it may turn out to be impossible to generate a proper structural mesh.

Most researchers [3–5, 7, 10] are inclined to perform computations using a tetragonal nonstructural mesh. This solution has many advantages: firstly, it is a very simple way of generating such meshes and it can be automated by scripting and secondly, the results are characterized by a very small error whereby entire screw propeller-hull and propeller-nozzle assemblies, tandem arrangements and so on can be analyzed. Additionally, in order to improve analytical results the boundary layer can be modelled by prismatic elements [10].

A computer program specially written for this purpose was used to generate the geometry of a 4119-type screw propeller. The program transforms input data into the coordinates of points in space. The points describe the shape of a propeller blade surface and then they can be connected into curves, surfaces and a volume. Propeller data are fixed in the program's source code but the program can be modified to allow reading in data for individual types of screw propellers. The generated propeller blade should be completed with a corresponding propeller boss model (which is easy to generate). Standard cubic elements available in CAD software, such as the sphere, the cylinder and the truncated cone, are created.

When modelling an isolated propeller it is best to assume the largest possible calculation domain. But one should note that the larger the domain, the greater the number of mesh elements. As the number of mesh elements increases so does the computing time. On the other hand, thanks to a larger domain convergent and correct results are obtained faster. The best solution is a compromise between the domain size and the number of elements.

Taking into account the periodicity of the investigated phenomenon, a single propeller blade was designed.

In accordance with the recommendations given in [9] a domain with the following dimensions:

- the domain's beginning located at $1.5 D$ ahead of the propeller,
- the domain's end located at $3.5 D$ behind the propeller,

- the domain's diameter: $1.4 D$,

where:

D is the propeller's diameter, was adopted.

In order to construct a proper calculation mesh the shape functions available in the Gambit software were used. The shape functions were applied twice to determine:

- the element density distribution on propeller blade edges with the functions applied to the edges; the sources being the blade's vertex and points on the leading and trailing edges at the base of the blade; the adopted quantities: StartSize = 0, GrowthRate = 1.1, instance = 50, SizeLimit = 5;
- the element density distribution in the neighbourhood of the propeller blade with the shape functions applied in the volume; the source being the propeller blade surfaces; the adopted quantities: StartSize = 1, GrowthRate = 1.1, Distance = 20, SizeLimit = 50.

Thanks to the use of the shape functions the elements could be properly compacted in the propeller blade region without introducing an excessive number of elements in the more distant areas. As a result the calculation results for the adopted domain size were acceptable.

The value of coefficient y^+ was the main criterion for setting the mesh resolution. The coefficient should be in a range of $30 < y^+ < 500$ [11] in order to properly model the turbulent boundary layer and obtain correct pressure distributions on the propeller blade surfaces. Another criterion was to ensure smooth growth in size of the elements with the distance from the foil's surface and at the same time to prevent their excessive enlargement within the propeller slipstream.

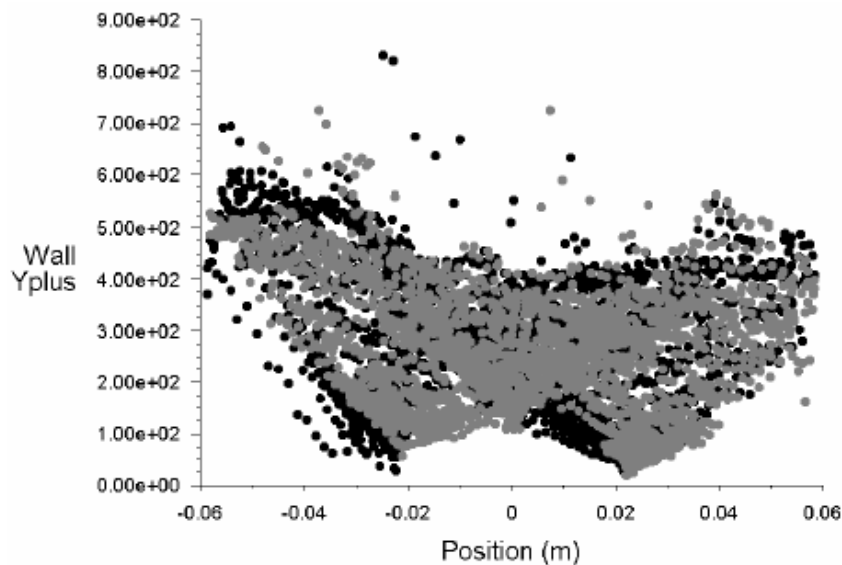


Fig. 1. Values of coefficient y^+ for $J = 0.833$

Figure 1 shows that the values of coefficient y_+ at advance coefficient $J = 0.833$ stay within the specified range. Similar values were obtained for the other advance coefficient values. Figure 2 shows surface meshes on the propeller blade and boss surfaces. The meshes were used to generate a 3-D mesh inside the volume. The mesh consists of 297230 elements.

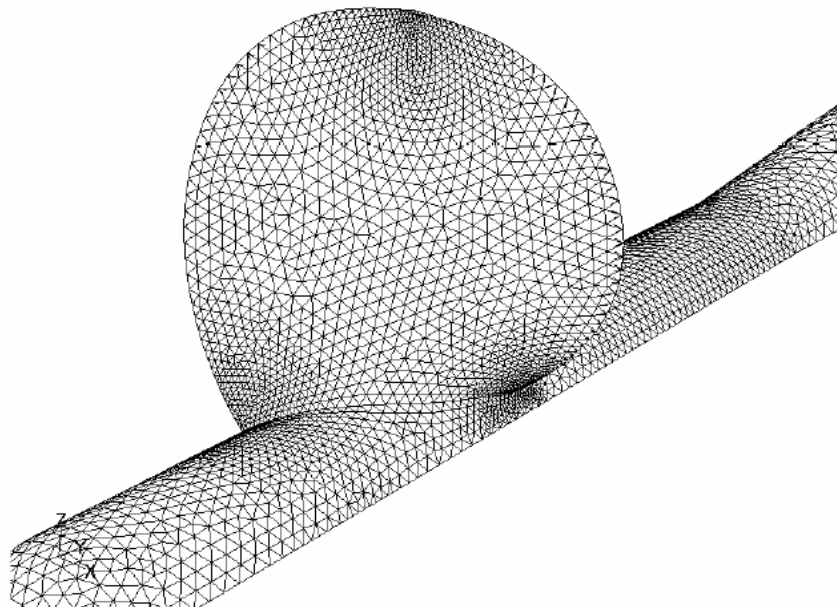


Fig. 2. Meshes on propeller blade and boss surfaces

Another important parameter is the quality of the mesh: the elements cannot be too much distorted, otherwise the obtained results will not be correct. It is best to assume the maximum cell equiangle skew below 0.9.

3. Calculations and their results

In the ship propeller analysis one can distinguish a few basic boundaries in the flow region:

- the inlet – inlet velocity was assumed; for this boundary condition one should specify, besides the velocity value, the values of $k-\varepsilon$ and $k-\omega$ or the turbulence intensity and the characteristic dimension;
- the outlet – outlet pressure was assumed;
- periodics – rotational;
- the propeller blades and the shaft – a viscous wall;
- the outer boundary – a nonviscous wall.

The calculation conditions were based on the paper by Jessup [2] since the experimental results had been taken from it. The rotational speed was set at 10 rps. The advance coefficient was changed by changing the velocity of inflow. This solution has two advantages: firstly, computations are performed at a constant Reynolds number and secondly, it is possible to determine the characteristics in all the propeller operation points [1].

The computations were performed using turbulence models $k-\varepsilon$ and $k-\omega$ with 2nd order discretization.

The rotational motion of the propeller was modelled by immobilizing the latter and rotating the calculation domain in the opposite direction (this gives exactly the same results as if the propeller were rotating). This solution was possible since the investigated case of the propeller was simple.

Computations for one operation point took about 48–72 h. During this time the program computed about 3000–4000 iterations. The convergence mostly amounted to 10^{-5} .

The angular distribution of axial velocity is shown in Figure 3. There is good agreement between the calculations and the numerical test results. The character of flow agrees with the experimental one and the velocity values do not diverge significantly from the reality. In the diagrams the values calculated using the $k-\varepsilon$ algorithm and the $k-\omega$ algorithm are denoted by respectively ke and kw and the experimental results by eks . The results for the other velocities similarly agree with the experimental ones [8].

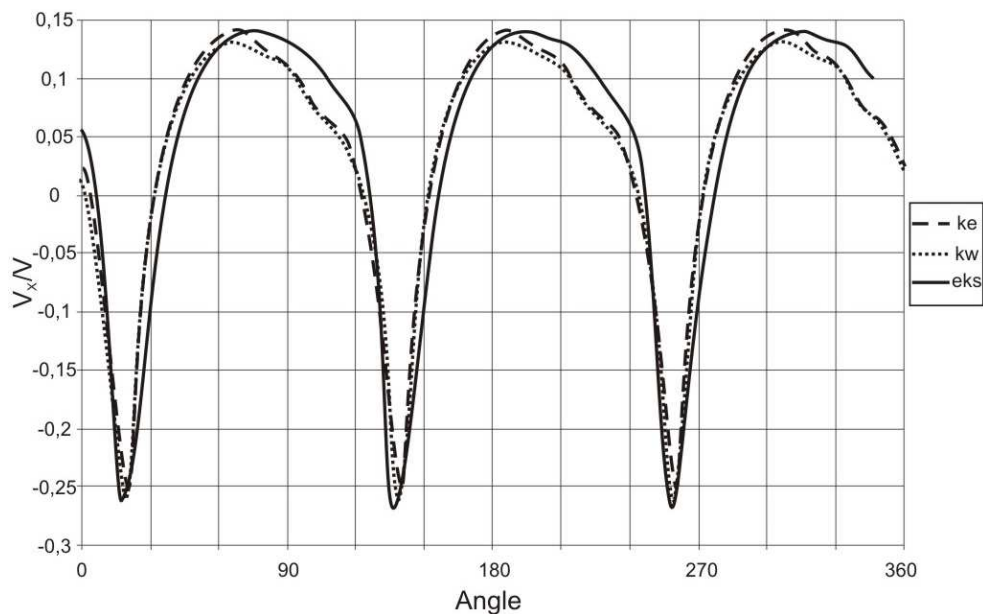


Fig. 3. Angular distribution $V_x/V - 1$ on circle $x/R = -0,3$, $r/R = 0,45$

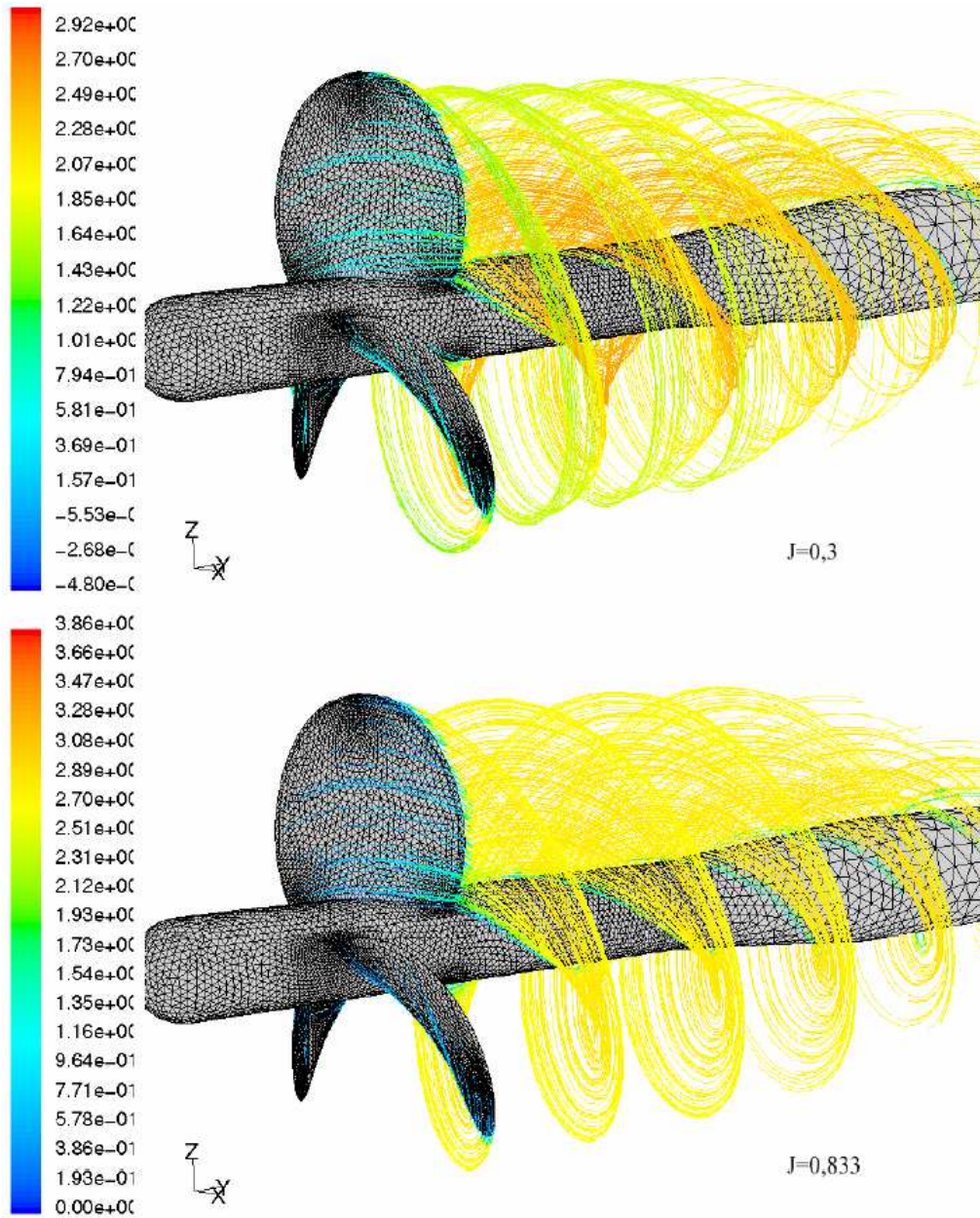


Fig. 4. Streamlines for advance coefficients $J = 0.3$ and $J = 0.833$

Figure 4 shows the streamlines for advance coefficients $J = 0.3$ and $J = 0.833$. One can see that the character of the investigated flow is in agreement with the reality and

a larger distortion of the propeller slipstream for the heavily loaded propeller is noticeable. Figure 5 shows hydrodynamic characteristic.

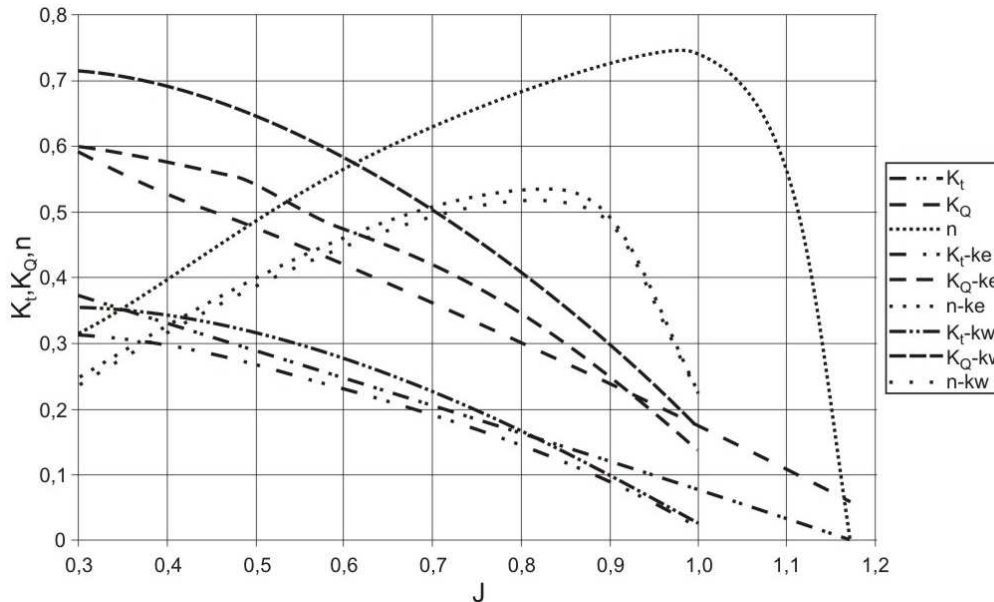


Fig. 5. Hydrodynamic characteristic of screw propeller 4119

4. Conclusions

The analysis of the screw propeller is highly complex (which has many consequences) and one must be aware that it is difficult and time-consuming, unless one has a ready methodology of carrying out such investigations. The aim of this research was to develop such a methodology. Some of its aspects have already been fully developed while a few others require further improvement.

The first task is to properly model the geometry which is not as easy as it seems. Practice has shown that not many CAD systems can handle such a complex geometry or generate all kinds of errors in the form of shape corruption. One should pay special attention to all kinds of strange bends in the surfaces. The Gambit software provides tools which allow one to model the propeller blade surfaces by spreading them out on a cloud of points or by drawing a surface through the curves that describe it. If any errors occur, they most probably occur at the leading edge or the trailing edge.

In the next step a calculation mesh is generated. It is much better to generate quickly and easily a nonstructural mesh and start calculations than to attempt to obtain a structural mesh. The literature on the subject [5–7, 9, 10] and practice indicate that the use of such a nonstructural mesh will give good results, provided that certain conditions are satisfied. If possible, one should try to model the boundary layer by means

of prismatic elements. Such an element resolution should be adopted that coefficient y^+ be in a range of 30–100.

In the considered case there were difficulties with reaching a compromise between the mesh scale and the properly low values of y^+ . This is certainly the main cause of the considerable divergence between calculated and experimentally determined thrust and torque values. The too low mesh density at the propeller's surface resulted in poorer accuracy of pressure distributions on the surface. The results for the part located at a distance from the surface were more accurate.

Numerical calculations have a major advantage over experimental investigations, namely one can neglect the scale effect since everything is modelled on the scale of 1:1. Also the computations are several times cheaper thanks to the available software.

It follows from the obtained results that in the considered case the choice of a turbulence model is of little consequence: practically identical results were obtained for the two models.

Taking all the above arguments into account one can say that analysis using finite volumes is suitable for investigating screw propeller operation. From all the calculation methods it is the most accurate and covers many phenomena, e.g. liquid viscosity, turbulence, cavitation, the occurrence of many phases, etc. By applying this method one can quickly obtain correct results. This method is also the only one which makes it possible to model propeller-hull assemblies, which until now could be investigated solely experimentally. Additionally, one can investigate the flow around the propeller as an unsteady phenomenon or add a free surface. Such problems can be solved using the Fluent system. The final argument is the fact that there is a worldwide trend to model flows around ship propellers using the method of finite volumes and such analyses yield correct results.

References

- [1] Dudziak J.: *Naval architecture* (in Polish), Shipbuilding Library.
- [2] Jessup S. D.: *An experimental investigation of viscous aspects of propeller blade flow*, The Catholic University of America, 1989.
- [3] Kelecy F.: *Study demonstrates that simulation can accurately predict fan performance*, Journal Article by Fluent User.
- [4] Rhee S. H.: *Marine applications*, Fluent UGM.
- [5] Rhee S. H., Joshi S.: *CFD validation for a highly skewed propeller*, Fluent Inc. materials.
- [6] Sanchez-Caja A., Sundell T., Martio J.: *Propeller and ship hull flows*, VTT Manufacturing Technology Finland.
- [7] Sanchez-Caja A.: *P4119 RANS calculations at VTT*, VTT Manufacturing Technology, Helsinki University of Technology.
- [8] Skraburski Ł.: *Analysis of screw propeller using FLUENT calculation system*, Wrocław, 2004.

-
- [9] Watanabe T., Kawamura T., Takekoshi Y., Maeda M., Rhee S. H.: *Simulation of steady and unsteady cavitation on a marine propeller using a RANS CFD code*, Fifth International Symposium on Cavitation.
- [10] *Performance of the 1903 Wright Flyer Propellers via Fluent's MRF Model*, Fluent Inc. materials.
- [11] FLUENT system documentation.

Analiza opływu śrubowego 4119 przy zastosowaniu systemu Fluent

W referacie przedstawiono sposób przeprowadzenia obliczeń numerycznych opływu śrubowego okrętowego przy zastosowaniu systemu obliczeniowego FLUENT. Przedstawiono sposób przygotowania kształtu oraz przygotowania siatki obliczeniowej. Omówiono sposób przeprowadzenia obliczeń. Obliczenia prowadzono przy wykorzystaniu dwóch modeli turbulencji $k-\varepsilon$ i $k-\omega$. Przedstawiono otrzymane wyniki, porównano z wynikami doświadczalnymi i omówiono.



Polymers in the construction of serviceless sliding bearings

Z. LAWROWSKI

Wrocław University of Technology, Wybrzeże Wyspiańskiego 25, 50-370 Wrocław

The application range of polymers and their composites in service-less sliding bearings, i.e. bearings that do not require lubrication supervision and maintenance, was defined. A survey of polymers having good sliding properties was done. A general characteristic and classification of polymer composites was presented. The structure and properties of the following composites were discussed: anti-friction coatings, filled composites, multi-layer composites and multi-layer filled composites. Exemplary design embodiments of slide bearing with the use of polymers were given. Remarks concerning specific features inherent to the design and operation of serviceless bearings summarise the paper.

Keywords: *serviceless sliding bearings, polymers, composites*

1. Serviceless sliding bearings

Under the name of serviceless sliding bearings are understood bearings that do not require operational supervision and maintenance. These are bearing without conventional lubrication systems, i.e. without the supply of lubricant from outside of the journal-bushing assembly. In these bearings, the lubricant is contained within the very assembly, e.g. in the bushing wall or on its surface layer.

Figure 1 shows a classification of sliding bearings with respect to lubrication supervision. The set I represents a conventionally lubricated bearing; it is considered as a bearing requiring lubrication supervision. Forced lubrication bearings might be an example. The set II illustrates a bearing in which the lubrication system and the lubricant are contained within the journal-bushing assembly. Glacier DX type bearings (see chapter 3.4) with grease pockets on the surface of the bushing are examples of this type. The set III presents a bearing in which the lubrication systems and the lubricant are contained within the bushing (or on the journal). Examples here may be bearings made of self-lubricating materials. The sets II and III illustrate schematically serviceless bearings.

Self-lubrication, i.e. an ability to reduce friction (mainly against steel) without conventional lubricants, consists in the use of the low shearing strength of some of the materials, including polymers. These materials have found an ever growing importance in serviceless bearings in the following application fields:

- in bearings where conventional lubrication cannot be employed due to its small effectiveness, e.g. at low (high) temperatures, in vacuum, in chemically active environment, etc.,

- in bearings where conventional lubrication may soil the product, e.g. food processing, paper, textile machinery and the like,
- in situations where lubrication servicing is impossible, difficult, dubious or not economically viable, e.g. in auxiliary vehicle devices, household appliances etc.

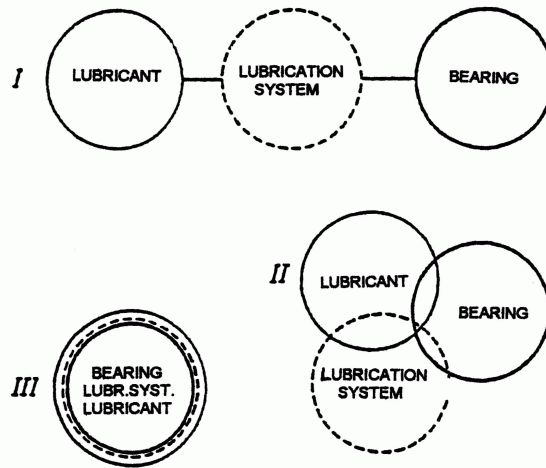


Fig. 1. Classification of sliding bearings with respect to lubrication supervision.
Discussion in the body of the text

Serviceless sliding bearings provided with self-lubricating materials can operate, due to thermal limitations and also due to wear, in the range of small and medium loads and sliding speeds. Figure 2 shows schematically the load carrying capacity of such bearings as opposed to that of conventionally lubricated bearings.

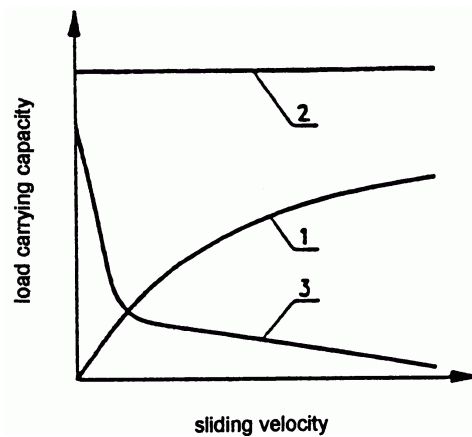


Fig. 2 Load carrying capacity of sliding bearings vs. sliding velocity: 1 – full film hydrodynamic bearing, 2 – hydrostatic bearing, 3 – serviceless self-lubricating bearing

It is seen that self-lubricating serviceless bearings complement the application range of full film bearings in its small sliding velocity part, as mentioned above.

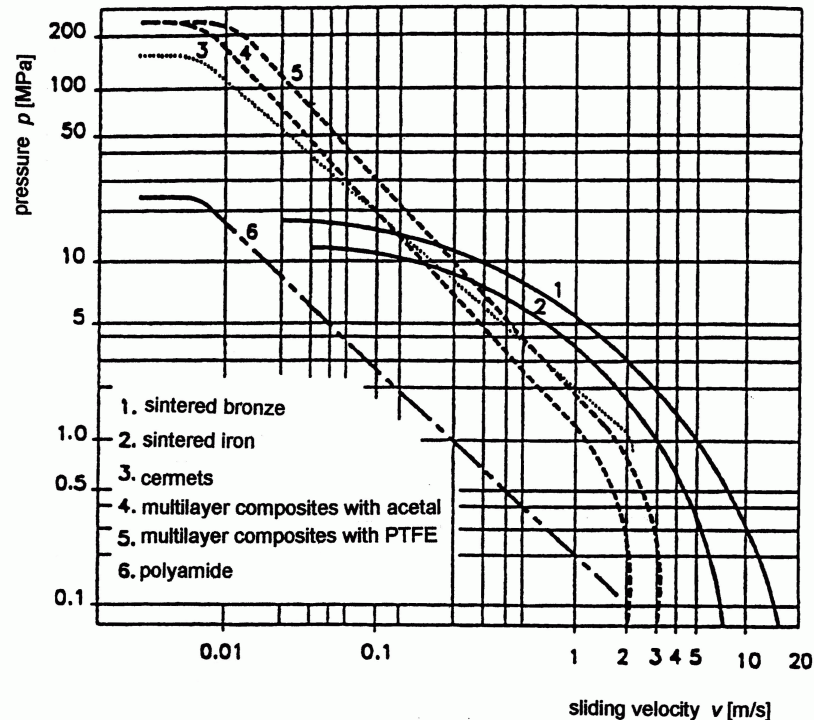


Fig. 3 Limiting curves (the load carrying capacity as a function of the sliding velocity) for different self-lubricating materials

Figure 3 shows plots of so called limiting curves, i.e. lines limiting loading for some of the self-lubricating materials depending upon the sliding speed. Data included in these graphs confirm the above given information on the application range of self-lubrication materials. Detailed data on the physical properties and lubrication performance of self-lubricating materials may be found in [1].

2. Sliding polymers

2.1. General characteristic of polymers as bearing materials

Tribological properties of polymers depend upon their structure. It was confirmed that a crystalline structure enhances the load carrying capacity and wear resistance of polymers whereas an amorphous structure makes sliding easier. Consequently, there is an optimum of these two phases that ensures a possibly high load carrying capacity together with low wear and small friction (usually against steel).

The following thermoplasts (partially crystalline polymers) are the most employed materials for serviceless bearings:

- Fluoroplasts: polytetrafluoroethylene (PTFE) and fluoroethylenepropylene (F.E.P),
- Polyacetals (polyoxymethylene, POM),
- Polyamides (PA),
- Polyethylene (PE).

The following amorphic polymers have found application in serviceless bearings:

- Polycarbonates (PC),
- Epoxy resins (EP); these are hardened resins (duroplasts),
- Polymanides (PI); these are mostly amorphic, available both as thermoplasts and duroplasts.

The wide application of polymers as bearing materials observed in recent years is due to many valuable advantages. These are, first of all, high resistance to seizure (absence of sticking against steel), good sliding properties of some of the polymers (low friction when operated against steel, also without lubricant), good chemical resistance, insensitivity to corrosion, ease of moulding of ready-made products (e.g. bushings) and a possibility to prepare thin anti-friction coatings. An additional advantage is a big potential for modifications and formation of composites.

Unfortunately, there are also disadvantage that must be borne in mind when both selecting polymers as sliding materials and operating frictional nodes containing polymers. The principal disadvantage of polymers is their low resistance to heat and a possibility of destruction after the allowable thermal state has been violated. Low thermal conductivity and a big value of thermal expansion constitute serious disadvantages of polymers as bearing materials. These disadvantages together with a tendency of some polymers to swelling in liquids can be eliminated by a skilful modification of the material or the design of a bearing assembly. Better thermal conductivity may be obtained by filling polymers with bronze or graphite powder as well as by the application of thin polymer coatings.

2.2. Survey of sliding polymers

Fluoroplasts

The most popular fluoroplast polymer of this group that is applied in the construction of serviceless sliding bearings is polytetrafluoroethylene. This material has been manufactured worldwide under different brand names, e.g. Teflon®, Fluon®, Hostalon®, Polyflon®, Halon®, Algaflon®, Rulon®, Tetraflon®, Soreflon®, Floroplast® and others. In Poland, PTFE is manufactured by Zakłady Azotowe in Tarnow under the brand name of Tarflen®.

Polytetrafluoroethylene has a highly crystalline structure with transition into an amorphic one at a temperature of 330 °C. By virtue of its molecular structure, it has so called “easy slippage planes”, what results with a very small coefficient of friction when sliding against steel (as low as 0.04).

Unfortunately, mechanical properties of polytetrafluoroethylene are poor: it flows as cold even at moderate values of pressure (2 to 4 MPa) and temperature (~ 110 °C). It is used therefore mostly as the base of polymer composites or as a filler (see: composites).

Polyacetals

Polyacetals are robust and rigid materials resistant to heat, humidity and solvents with good sliding properties and high resistance to wear. They react however with acids and oxidising substances. Polyacetals are employed mostly in pure form (i.e. without fillers), also as base materials in the construction of composites and their fillers.

Commercially available materials are known as Derin®, Ceclon®, Milicon®, Hostaform®, Tarnoform® (Zakłady Azotowe in Tarnów)

Polyamides

Polyamides are ones of the oldest and most widespread polymers. Their popularity is due to artificial nylon fibres. A variety of brand names carried by this material: Nylatron®, Kapron®, Stylon® (Polish), Tragamid®, Miramid®, Ultramid®, Grilon®, Renyl®, Technyl®, Amilan®, Akulon® and others witnesses to the great proliferation of polyamides.

Polyamides are part crystalline materials. Even if their coefficient of friction against steel is inferior to that of PTFE, a big advantage is their high resistance to wear (within the allowable values of $p\nu$).

Tribological properties of polyamides are frequently enhanced by their filling creating thus filled composites.

Polyethylenes

Low pressure PE-HOUHMW polyethylene with a high density and very large molecular mass has been employed mostly for sliding bearings. This material features a very high wear resistance and resistance to impacts together with small water absorption. Unfortunately, the coefficient of friction against steel is high (0.15 to 0.3). This property of polyethylenes shall be borne in mind if planned for application in serviceless bearings.

Polyethylene materials are also low thermally resistant. The temperature of operation shall not exceed 60 °C. These materials, similarly to polymers, are known by their brand names like Alathon®, Dylan®, Carlona®, Novatec®, Petrothene®, Lupolen®, Marlex®, Mirathen®, etc.

Polycarbonates

Polycarbonates feature some precious properties like a very high resistance to impacts, low thermal expansion, and a high temperature of thermal destruction.

Unfortunately, both friction and wear rate of polycarbonates are pretty high. Consequently, it is used only as the base for sliding composites filled with reinforcing fibres and sliding agents, e.g. PTFE.

Epoxy resins

In the construction of self-lubricating bearings, these duraplasts are used as the base of composites that are filled with solid greases like graphite and molybdenum disulphide and others. These composites serve as a raw material for the production of bushing or are coated in a form of thin layers onto steel substrates of these bearings.

Epoxy resins carry different brand names, e.g. Epibond®, Epidian®, Epicate®, Epocast®, Epodite®, Epon®, Eposet® and others.

Polyimides

Polyimides feature the best thermal stability among polymers. This is employed in the construction of self-lubricating bearing operating at elevated temperatures (up to 315 °C.) and at high momentary loading (up to 35 MPa at a temperature of 325 °C.).

Polyimides feature good sliding properties. Their resistance to wear is improved usually by filling with solid greases. Commercially known brand names of these materials carry names of the place of their development and manufacture, e.g. Vespel® (sintered elements), Kapton® (stretch foil), Apical® and others.

Polyimides are heat-hardened polymers. A thermoplastic modification of polyimides is also manufactured under the name of polyamidoimide. An extreme ease in processing, i.e. an ability to manufacture items using all methods available in the processing of plastics, is the main advantage of these materials. This ability, however, goes together with the decreased thermal resistance.

3. Composites

3.1. General characteristic and classification of composites

A composite material is understood to mean a material obtained by an aggregation of a few materials into one for the purpose of obtaining enhanced physical, chemical, and mechanical properties; and in the case of sliding composites, also enhanced tribological performance. These properties and tribological performance are different to those of individual components.

Composites have a heterogenic structure containing two or more phases formed out of its components. These phases may be continuous or one of them (or more) may be spread in the matrix.

As is clearly seen from the information provided above, the majority of polymers is used exactly as the carrier or filler of composites. This situation results from a need to compensate disadvantages of polymers: their low thermal conductivity, high thermal expansion, swelling in liquids, and low mechanical strength. An essential reason for the creation of sliding composites is a need to improve their sliding properties by decreasing dry friction and improving their wear resistance.

Figure 4 shows a general classification of sliding composites. It contains, as is seen, also metal composites (excluded from this elaboration). Composites containing polymers will be discussed in the further text.

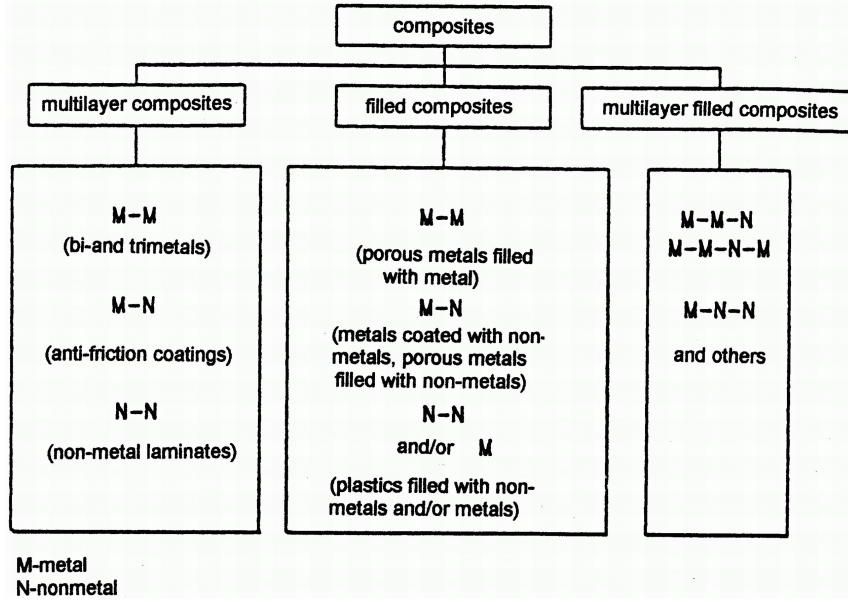


Fig. 4. Classification of sliding composites

3.2. Anti-friction coatings

The antifriction coatings are termed as thin (a fraction to one millimetre) surface layers coated onto and stuck into the substrate due to forces of adhesion. The substrate metals are usually steel, cast iron, and colour metal alloys.

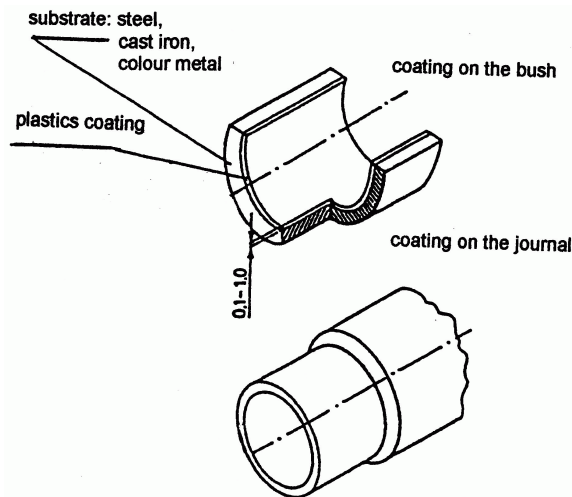


Fig. 5. Type M-N-coating layer composites

Anti-friction coatings are used mostly due to their ability to operate at a low value of the coefficient of friction (even at dry conditions) and ease in the dissipation of heat by the metallic substrate. The low thickness of the coating nullifies the effect of swelling and of thermal expansion in liquids.

Figure 5 shows two variants of coatings in a bearing: a coating on a bushing and a coating on a journal.

Coatings are formed on metallic surfaces using different techniques; by coating polymer powders on a preliminarily heated metallic element, by coating polymer powders on a cold element and the following heating and melting, and by spraying of the powder in the gaseous flame. Details of these techniques can be found in [1]

3.3. Filled composites of nonmetal-nonmetal and/or metal type

This type of composites is most widely employed due to possibilities involved with the application of different polymers as matrix, and above all, due to a possibility of using different fillers, both in types and concentration. Additionally, such a composite is part of filled layer composites (to be discussed later).

The above-mentioned sliding composites are used as matrix. The most widespread application have found polytetrafluoroethylene (PTFE), polyamides (PA), polacetales (POM) and epoxy resins (EP).

Fillers are added in order to improve the properties (physical, chemical, and mechanical) of composites and their performance (friction, wear). Based upon impacts involved with the application of fillers, a distinction shall be made between fillers and reinforcements. The latter ones concern fillers added to polymers to increase their strength.

Powders of copper, graphite, PTFE, PI, and molybdenum disulphide are used as fillers to improve thermal conductivity and sliding performance. Glass, carbon-graphite, and aramide fibres are used to improve thermal conductivity and strength.

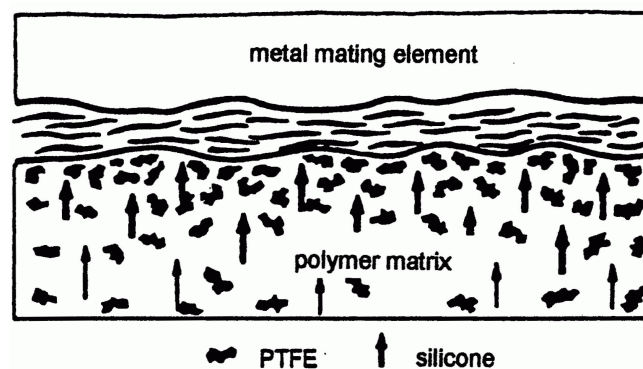


Fig. 6. Scheme of the self-lubrication process of a thermoplast + silicon composite [2]; silicone diffusing towards the surface amplifies the anti-friction action of PTFE

Apart of solid fillers, there are also liquid (synthetic lubricating oils) fillers. A combination of such fillers with solid fillers, e.g. PTFE, is also used. Figure 6 shows schematically the self-lubrication process of such a composite.

3.4. Filled multi-layer composites

The filled multi-layer composites combine the features of the earlier discussed types of materials. The idea of such composites is to form the upper layer made of a filled composite on the hard substrate, usually made of steel.

Figure 7 shows examples of one-layer filled composites, and Figure 8 – a summary of commercially available multi-layer filled composites.

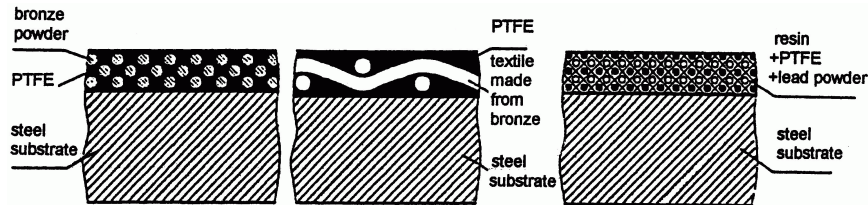


Fig. 7. Examples of composites with a sliding layer coated directly onto the substrate

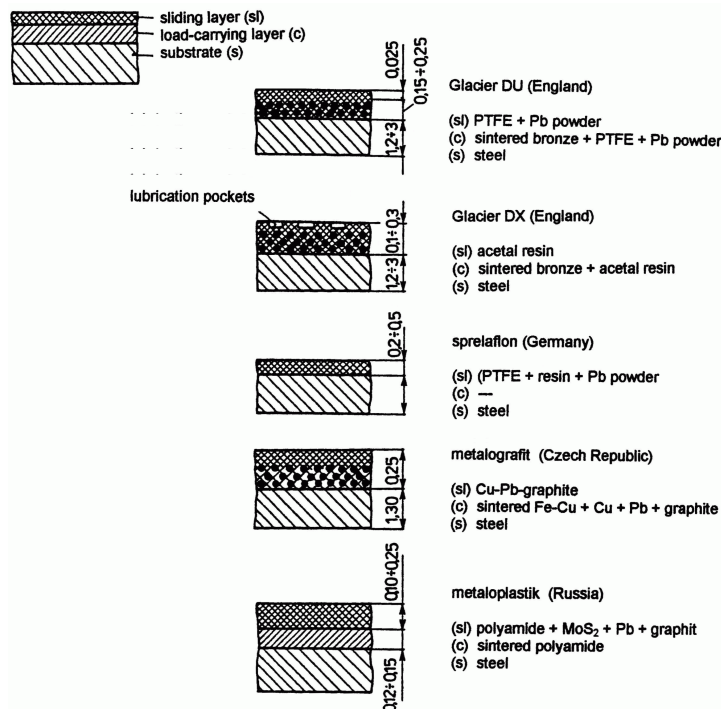


Fig. 8. Examples of brand multilayer filled composites

The most widespread are DU and DX composites of the *Glacier* Company: The first one is recommended as fully self-lubricating. This self-lubrication is ensured by a sliding layer made of PTFE, and in the case of its deterioration – by the very polymer contained in the pores of the bronze porous metal (sintered porous bronze), which constitutes the load carrying surface (evidently, at the expense of a certain amount of wear in the porous metal). The DX *Glacier* material is characteristic in that its surface has pockets for grease that are filled during assembly.

Bearings made of the above-described materials are manufactured usually as wound from a multilayer band.

4. Design of bearing assemblies made from polymer materials

The above mentioned disadvantages of polymers concerning their behaviour at elevated temperatures and in liquids call for a different approach in the design of bearings made of these materials, other than the approach valid for conventional bearings.

The design forms of polymer bearings belong to one of the two groups:

- bearings with the sliding layer made of polymers or their composites permanently bound with the substrate (anti-friction coatings and multi-layer filled composites), and
- bearings with polymer inserts mounted in the housing by friction or positive engagement.

Bearings of the first group are manufactured usually as sleeves or half-shells wound of a band (a semi-finished product). Their types, dimension and tolerances, and assembly methods are given in manufacturers' catalogues.

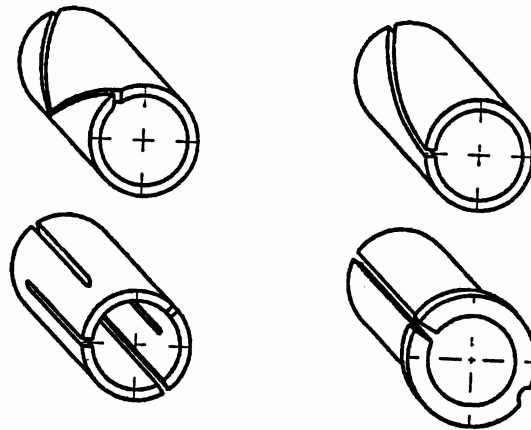


Fig. 9. Examples of polymer sleeves with dilatation gaps [4]

Bearings of the second group are manufactured as sleeves, which are press fitted to metallic housings. Due to the poor mechanical strength of polymers, sleeves (a few

mm in wall thickness) are press assembled and then the hole is machined to dimension decreasing thus the thickness to approximately 5% of the bearing hole diameter. However, the wall thicknesses should not be less than 2 mm.

To compensate for the swelling of thick-walled sleeves, dilatation gaps are used. Examples of such sleeves are shown in Figure 9.

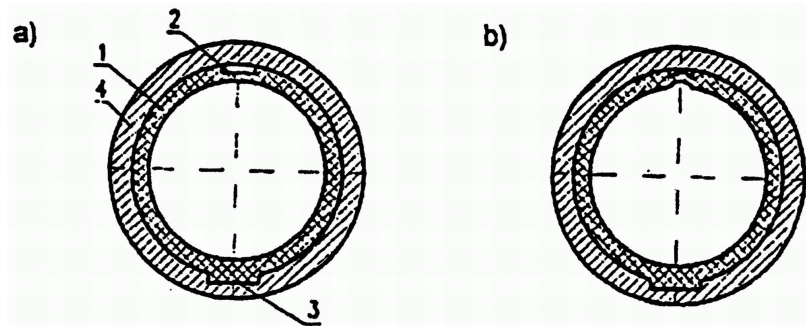


Fig. 10. Polymer sleeve with a positive securing tongue and a dilatation constriction

Due to a certain uncertainty of pressed fits, positive securing is also used. Figure 10 shows an example of such locking, also a replacement of the dilatation gap with a constriction.

5. Summary

Polymers and their composites are especially fit for sliding bearings that, due to different reasons, cannot be lubricated in a conventional way or such lubrication is economically non-viable. The self-lubricating property of such bearings is their undeniable advantage. They are also used sometimes in conventionally lubricated bearings as a precaution against seizure in the case of lubrication disruption. It shall, however, be borne in mind that lubrication hinders adhesive transportation of polymer onto the counter-surface and the creation of a continuous sliding layer.

Due to the low heat conductivity and swelling of polymers under the influence of heat and humidity, composites with a thin polymer layer or its composite shall be used at a high load rating of a bearing (high values of $p\nu$).

Operational recommendations may be formulated as follows:

The allowable value of $p\nu$ must be observed unconditionally; in the case of doubts, bearing temperature shall be monitored.

Good tribological properties notwithstanding (low friction against steel, low wear rate) polymers and their composites are subject to wear. The service life of bearings made of these materials may be evaluated based upon available data on their wear rate.

References

- [1] Lawrowski Z.: *Bezobsługowe łożyska ślizgowe*, Oficyna Wydawnicza Politechniki Wrocławskiej, Wrocław, 2001.
- [2] Bartz W. J.: *Selbstschmierende und wartungsfreie Gleitlager*, Ehningen, Expert Verlag, 1993.
- [3] Bhusan B., Gupta B.K.: *Handbook of tribology*, Malabar, Florida, Krieger Publishing Company, 1997.
- [4] Ziemiański K.: *Zastosowanie tworzyw sztucznych w budowie maszyn*, Wybrane zagadnienia, Wydawnictwa Politechniki Wrocławskiej, Wrocław, 1995.

Polimery w budowie bezobsługowych łożysk ślizgowych

Określono obszary zastosowania polimerów i ich kompozytów w ślizgowych łożyskach bezobsługowych, tj. łożyskach nie wymagających dozoru smarowniczego. Dokonano przeglądu polimerów o dobrych właściwościach ślizgowych. Przedstawiono ogólną charakterystykę i podział kompozytów polimerowych. Omówiono budowę i właściwości następujących kompozytów: powłok przeciwciernych, kompozytów wypełnianych, wielowarstwowych i wielowarstwowych wypełnianych. Podano przykłady konstrukcji łożysk ślizgowych z użyciem polimerów. Artykuł kończą uwagi dotyczące specyfiki konstrukcji i eksploatacji bezobsługowych łożysk ślizgowych zawierających polimery i ich kompozyty.



On certain types of ship responses disclosed by the two-stage approach to ship dynamics

J. MATUSIAK

Helsinki University of Technology, Ship Laboratory, Tietotie 1, 02150 Espoo, Finland

Some applications of the so-called two-stage approach to the determination of non-linear large amplitude motions of a ship in waves are presented. These include ship capsizing, parametric roll resonance and a time domain simulation of the so-called weather criterion. A brief description of the computational model is given, too.

Keywords: *non-linear ship dynamics, parametric roll resonance, capsizing*

1. Introduction

Linear models of ship dynamics in waves are well established. In most cases they result in a sufficiently accurate prediction of loads and ship motions. Perhaps the biggest benefit of using the linear models is that prediction of exceeding certain level of load or response can be easily derived. Analysis is conveniently conducted in the frequency domain. The biggest shortcoming of the linearity assumption is that it precludes prediction of certain classes of ship responses. The linear models can not predict the loss of ship stability in waves, parametric resonance of roll and asymmetry of sagging and hogging. Ship steering and maneuvering motion are disregarded.

Simulation of ship maneuvering is usually conducted for the still water condition. Time-domain simulation of ship motion is restricted to in-plane motion comprising of surge, yaw and sway motion components. If waves are encountered for, their effect is taken into account as a steady state one.

The method, called *LAIDYN*, which evaluates in time-domain ship rigid body motions in waves and manoeuvring is presented briefly. The *LAIDYN* method called also as the two-stage approach [1, 2] is used when evaluating non-linear large amplitude responses in waves. The method preserves best features of the linear seakeeping theory and takes into account most relevant non-linearities. As a result the loss of ship stability in waves and parametric resonance of roll are numerically predicted. Also transient type large amplitude response such as the one caused by a simultaneous action of waves and gusty wind can be evaluated. Ship maneuvering in regular waves can be simulated, too.

2. General model of ship rigid body motions

A ship is regarded as a rigid body possessing six degrees of freedom.

2.1. Motion kinematics

Three co-ordinate systems are used for describing ship motion. These are presented in Figure 1.

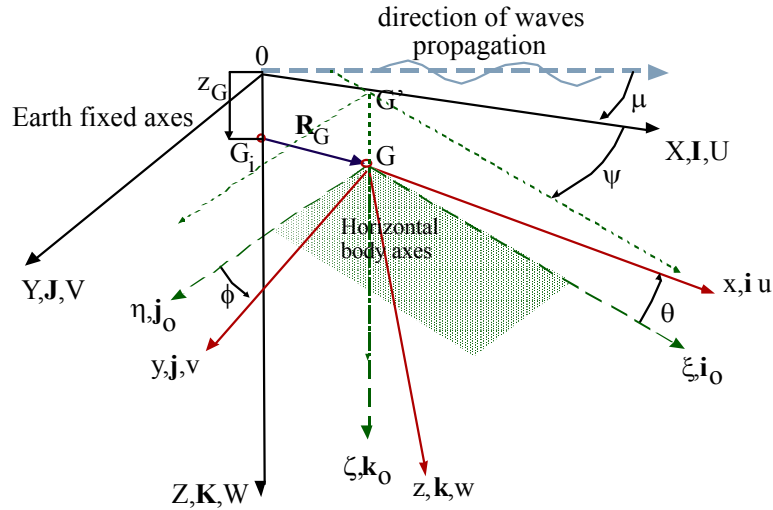


Fig. 1. Co-ordinate systems used to describe ship motion

An inertial Cartesian co-ordinate system fixed to Earth is denoted by XYZ . The X – Y plane coincides with the still water level. The origin O of this co-ordinate system is located at the vertical passing through the initial location G_i of the ship's centre of gravity. X -axis points to the initial direction of ship's bow. Ship is on course μ with respect to the direction of surface waves propagation. Ship's centre of gravity is denoted by G . It is the origin the moving Cartesian co-ordinate system xyz fixed with ship with x -axis pointing towards the bow. This system is called the body-fixed co-ordinate system. The so-called horizontal body axes co-ordinate system [3] denoted as ξ, η, ζ moves also with ship so that the axes ξ, η, ζ are parallel to the axes X, Y, Z of the Earth-fixed co-ordinate system.

The instantaneous position of ship's centre of gravity G is given by the following displacement components: surge (ξ or x_1), sway (η or x_2) and heave (ζ or x_3). These are the motion components of the centre of gravity in the moving co-ordinate system ξ, η, ζ . The velocity of the origin of ship is given as

$$U = \dot{R}_G = \dot{X}_G I + \dot{Y}_G J + \dot{Z}_G K = ui + vj + wk, \quad (1)$$

where:

u , v and w are the projections of the velocities of ship's centre of gravity in the Earth-fixed inertial co-ordinate system on the axes of the moving body-fixed system. The angular position of the ship is given by so-called modified Euler's angles denoted in Figure 1 as ψ , θ and ϕ . The relation between the velocities of the ship's centre of gravity in the inertial co-ordinate system and their projections u , v and w on the axes of the moving body-fixed system is [4, 5]

$$\begin{Bmatrix} \dot{X}_G \\ \dot{Y}_G \\ \dot{Z}_G \end{Bmatrix} = \begin{bmatrix} \cos\psi \cos\theta & \cos\psi \sin\theta \sin\phi & \cos\psi \sin\theta \cos\phi \\ \sin\psi \cos\theta & \sin\psi \sin\theta \sin\phi & \sin\psi \sin\theta \cos\phi \\ -\sin\theta & \cos\theta \sin\phi & \cos\theta \cos\phi \end{bmatrix} \begin{Bmatrix} u \\ v \\ w \end{Bmatrix}. \quad (2)$$

Angular velocity Ω of the ship in the body fixed co-ordinate system is

$$\Omega = P\mathbf{i} + Q\mathbf{j} + R\mathbf{k} \quad (3)$$

The dependence of the derivatives of the Euler angles and angular velocity components of Equation 3 is as follows [5]

$$\begin{Bmatrix} \dot{\phi} \\ \dot{\theta} \\ \dot{\psi} \end{Bmatrix} = \begin{bmatrix} 1 & \sin\phi \tan\theta & \cos\phi \tan\theta \\ 0 & \cos\phi & -\sin\phi \\ 0 & \sin\phi \cos\theta & \cos\phi \cos\theta \end{bmatrix} \begin{Bmatrix} P \\ Q \\ R \end{Bmatrix}. \quad (4)$$

2.2. Equations of motion

Equations of motion are given by the set of six non-linear ordinary differential Equations [5].

$$\begin{aligned} X_g - mg \sin\theta &= m(\dot{u} + Qw - Rv) \\ Y_g + mg \cos\theta \sin\phi &= m(\dot{v} + Ru - Pw) \\ Z_g + mg \cos\theta \cos\phi &= m(\dot{w} + Pv - Qu) \\ K_g &= I_x \dot{P} - I_{xy} \dot{Q} - I_{xz} \dot{R} + (I_z R - I_{zx} P - I_{zy} Q)Q - (I_y Q - I_{yz} R - I_{yx} P)R \\ M_g &= -I_{yx} \dot{P} + I_y \dot{Q} - I_{yz} \dot{R} + (I_x P - I_{xy} Q - I_{xz} R)R - (I_z R - I_{zx} P - I_{zy} Q)P \\ N_g &= -I_{zx} \dot{P} - I_{zy} \dot{Q} + I_z \dot{R} + (I_y Q - I_{yz} R - I_{yx} P)P - (I_x P - I_{xy} Q - I_{xz} R)Q. \end{aligned} \quad (5)$$

In Equations 5, X_g , Y_g , Z_g , K_g , M_g and N_g depict the components of global reaction force and moment vectors acting on the ship. These are given in the-body fixed co-ordinate system xyz . m and I_{ij} mean ship's mass and the components of the mass moment of inertia.

3. Reaction forces

Reaction forces and moments considered in the model comprise the ship resistance, propeller, rudder, restoring, radiation and wave forces and moments. Ship resistance and forces caused by propeller and steered rudder are represented using simple semi-empirical models.

3.1. Restoring forces and moments

Restoring forces are the hydrostatic forces caused by the hydrostatic pressure exerted by water on a hull, which is slowly moved from the static equilibrium position. Linear approximation of these forces mean, that the force is linearly related to the motion amplitude. In the discussed method, the non-linear three-dimensional model of evaluating restoring forces and moments is used instead. The ship hull is discretized by a number of triangular panels (see Figure 2). The wetted surface of a hull, which is dependent upon the instantaneous position of ship, is used when integrating hydrostatic pressures.

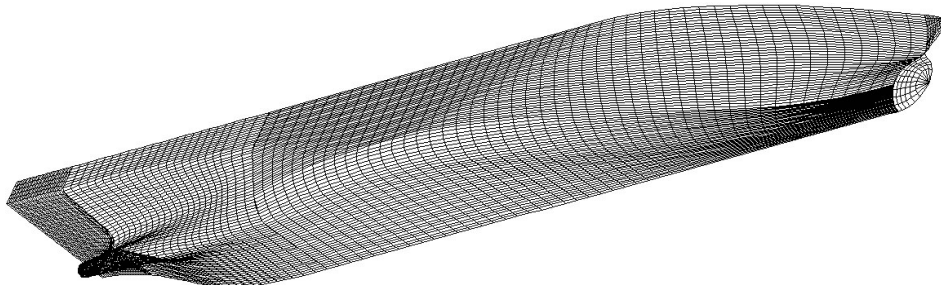


Fig. 2. Bottom view of a Ro-Ro ship

3.2. Radiation forces and moments

The non-zero acceleration motion of ship hull in still water causes certain reaction forces. We assume the hull flow to be inviscid. If restoring forces are subtracted from these reaction forces the components that are left are called *radiation forces*. For a harmonic motion with angular velocity ω and with the assumption of infinitely small amplitude these forces can be expressed using the so-called *added mass* and *damping* concept [6]. This linear model can be presented as

$$\begin{aligned}
X_{\text{rad}} &= -a_{11}\dot{u} - a_{15}\dot{Q} - b_{15}Q \\
Y_{\text{rad}} &= -a_{22}\dot{v} - b_{22}v - a_{24}\dot{P} - b_{24}P - a_{26}\dot{R} - b_{26}R \\
Z_{\text{rad}} &= -a_{33}\dot{w} - b_{33}w - a_{35}\dot{Q} - b_{35}Q \\
K_{\text{rad}} &= -a_{44}\dot{P} - b_{44}P - a_{46}\dot{R} - b_{46}R - a_{42}\dot{v} - b_{42}v \\
M_{\text{rad}} &= -a_{55}\dot{Q} - b_{55}Q - a_{53}\dot{w} - b_{53}w - a_{51}\dot{u} \\
N_{\text{rad}} &= -a_{66}\dot{R} - b_{66}R - a_{64}\dot{P} - b_{64}P - a_{62}\dot{v} - b_{62}v.
\end{aligned} \tag{6}$$

In Equations (6) a_{ij} and b_{ij} depict added masses and damping coefficients referred to the origin located in the centre of gravity (G in Figure 1). These have frequency dependent values. They are evaluated by a standard linear seakeeping theory based computer program [8]. Note that radiation forces are oriented in the body-fixed co-ordinate system.

Time domain approach requires the so-called convolution integral representation of the radiation forces [7]. In this approach radiation forces vector X_{rad} is represented by an expression

$$X_{\text{rad}}(t) = -a_{\infty}\ddot{x}(t) - \int_{-\infty}^t k(t-\tau)\dot{x}(\tau)d\tau, \tag{7}$$

where:

a_{∞} is the matrix comprising the added mass coefficients for an infinite frequency and x is the response vector. Matrix function k is the so-called retardation function, which takes into account the memory effect of the radiation forces. This function can be evaluated as

$$\mathbf{k}(t) = \frac{2}{\pi} \int_0^{\infty} \mathbf{b}(\omega) \cos(\omega t) d\omega, \tag{8}$$

where:

b is the frequency dependent added damping matrix.

The functions $\mathbf{k}(t)$ have to be evaluated only once before the simulation. The Fast Fourier Transform algorithm is used when evaluating discrete values of the retardation functions. Details of the algorithm are given in reference [2].

3.3. Wave excitation

Wave action on ship hull is usually represented by two components. At first, the so-called Froude-Krylov component is evaluated using the pressure in the oncoming wave. This pressure is integrated over the wetted portion of hull surface. In the linear

approximation the integration is conducted up to the still water level and a steady ship motion is assumed. The non-linear model allows six-degrees-of-freedom for ship motions.

Secondly, the so-called diffraction component of wave excitation takes into account the disturbance caused by a ship to oncoming wave. Theoretical model of the diffraction [6] assumes again that ship motion is restricted to a steady velocity in the horizontal X - Y plane.

4. Two-stage approach of evaluating non-linear dynamic response

4.1. Illustration of the two-stage approach using a single-degree-of-freedom non-linear system

When forming a mathematical model of ship, the vessel is regarded as a rigid body possessing in general six degrees of freedom. However, for the sake of simplicity the two-stage approach is explained in this section using a single-degree-of-freedom model. The model is extended to a multi-degree-of-freedom general model later on.

Let us consider a single-degree-of-freedom system given by a non-linear Equation

$$m\ddot{X} + g(\dot{X}) + h(X) = F(X; t) \quad (9)$$

where:

m is system mass, t is time. Dots denote time derivatives. The functions g and h are in general non-linear functions of response velocity \dot{X} and displacement X , respectively. Function F is also a non-linear function of X describing the external excitation of the system.

The linear version of the Equation (9) is given by

$$m\ddot{x}_L + c\dot{x}_L + kx_L = F_L(t), \quad (10)$$

where F_L is a linear, independent of the response forcing function. The total response is decomposed into a linear part x_L and a non-linear portion x as

$$X = x_L + x. \quad (11)$$

Subtracting linear approximation (10) from the general Equation (9) yields an equation for the non-linear part x of the response

$$m\ddot{x} + [g(\dot{x}_L + \dot{x}) - c\dot{x}_L] + [h(x_L + x) - kx_L] = f, \quad (12)$$

where:

$f = F(X; t) - F_L(t)$ is a non-linear part of the forcing function.

4.2. Linear approximation of the equations of ship motion in waves

A classical approach to predict ship motions in waves is based on a number of assumptions. Similarly as in the small oscillations models, it is assumed that motion amplitudes are small. This assumption means that the wetted surface of ship hull does not change and surface waves are of small amplitude. The cross-coupling terms of the body dynamics are disregarded as well. These linear models of ship dynamics in waves are well established. In most cases, they result in a sufficiently accurate prediction of loads and ship motions. The biggest shortcoming of the linearity assumption is that it precludes prediction of certain classes of ship responses for which non-linearities play important role.

The questions arise: Are the mathematical tools capable enough to solve the non-linear problem describing relevant physical phenomena? Which of the non-linearities should be taken into account in order to predict these particular types of ship behaviour in waves? Can we possibly restrict our model to the limited number of degrees of freedom?

The method starts with a linear approximation of the motion estimate in irregular or regular waves. The linear approximation takes care of the diffraction forces and it solves the added parameters (added mass and damping coefficients). Linear approximation of the responses in terms of the velocities

$$\begin{aligned} U_L &= u_L \mathbf{i} + v_L \mathbf{j} + w_L \mathbf{k} \\ \Omega_L &= P_L \mathbf{i} + Q_L \mathbf{j} + R_L \mathbf{k} = \dot{\phi}_L \mathbf{i} + \dot{\theta}_L \mathbf{j} + \dot{\psi}_L \mathbf{k} \end{aligned} \quad (13)$$

is obtained by the standard method [8]. Note that linear approximation does not distinguish between the inertial and body-fixed co-ordinate system. Motions are given in the co-ordinate system with the origin in the ship's centre of gravity. The linearised equations of ship motion can be presented as

$$\begin{aligned} m \dot{u}_L &= X_L = X_{\text{rad}} + X_{\text{diff}} + X_{\text{F.K,L}} \\ m \dot{v}_L &= Y_L = Y_{\text{rad}} + Y_{\text{diff}} + Y_{\text{F.K,L}} \\ m \dot{w}_L &= Z_L = Z_{\text{restoring,L}} + Z_{\text{rad}} + Z_{\text{diff}} + Z_{\text{F.K,L}} \\ I_x \dot{P}_L - I_{xz} \dot{R}_L &= K_L = K_{\text{restoring,L}} + K_{\text{rad}} + K_{\text{diff}} + K_{\text{F.K,L}} \\ I_y \dot{Q}_L &= M_L = M_{\text{restoring,L}} + M_{\text{rad}} + M_{\text{diff}} + M_{\text{F.K,L}} \\ I_z \dot{R}_L - I_{zx} \dot{P}_L &= N_L = N_{\text{rad}} + N_{\text{diff}} + N_{\text{F.K,L}}. \end{aligned} \quad (14)$$

The indices rad, diff, F.K and restoring stand for radiation, diffraction, the so-called Froude-Krylov and restoring forces and moments. Index L depicts linear approximation to the forces and moments. In the linear approximation of the wave exci-

tation, an important simplification is done. The integration of hydrodynamic pressure over the hull surface is conducted up to the still water level. This means that ship motion is restricted to a constant velocity V_S pointing in the x -direction. Other motion components are disregarded.

Mainly due to the linearity properties the solution of Equations (14) is sought in the frequency domain. As a result the responses are obtained in a form of transfer functions. Thus for instance linear x -response is given by

$$x_L = x_{L0}(\omega, \mu) \cos[\omega t - k(X_G \cos \mu - Y_G \sin \mu) + \alpha_x], \quad (15)$$

where x_{L0} is the motion amplitude, linear in respect to wave amplitude a_w , ω wave frequency, $k = \omega^2/g$ wave number and α_x phase angle.

4.3. Why to use two-stage approach?

The question arises why to use a two-stage approach? Why not to solve a non-linear equation of motion (5) directly in time domain by an appropriate numerical integration routine? Linear methods of the seakeeping theory are very well established. In particular, hydrodynamic forces (radiation and diffraction) are well represented by the linear approximation. As a result ship motions and loads are very well predicted. They are given in a form of reliable transfer functions provided that the ship is on a straight course and motion fulfils the linearity assumptions. Direct evaluation of ship motions with an aid of a non-linear model involves certain compromises. In particular, diffraction forces are often disregarded and a simplified constant added mass model usually represents the radiation forces. These drawbacks of the non-linear strip theory method are avoided when using a two-stage approach.

In the two-stage approach, the main part of the first order, fast response in waves is given by a linear approximation. These are evaluated for an actual heading and actual position in waves. Non-linear parts of hydrostatic and hydrodynamic load, rudder and propeller forces and non-linearities of ship rigid body dynamics yield non-linear part of the first order motions and slow manoeuvring motion.

4.4. Non-linear part of ship response

Having a linear approximation for the ship motions in waves obtained, the non-linear part of motions is evaluated in the time domain. This motion takes into account non-linearities of ship hydrostatics and non-linearities of wave loads at large amplitudes of motion. The only motion component that is not decomposed into the linear and non-linear part is the surge. The total surge motion is evaluated using the 1st of Equations (5). Propulsor action and rudder forces are included in this equation. The effect of added wave resistance is represented by x -directional component of the Froude-Krylov force. The total ship motion, or other type of response, being a sum of linear approximation and a non-linear part is thus obtained. In other words, total responses in terms of velocities are written in the form

$$\begin{aligned} \mathbf{U} &= u\mathbf{i} + (v_L + v)\mathbf{j} + (w_L + w)\mathbf{k} \\ \boldsymbol{\Omega} &= (P_L + P)\mathbf{i} + (Q_L + Q)\mathbf{j} + (R_L + R)\mathbf{k}, \end{aligned} \quad (16)$$

where variables without subscripts depict the non-linear part of the response. The linear approximation is evaluated with an aid of formula (15) for an actual ship position (X_G, Y_G) in waves and for an actual heading μ .

Subtracting Equations (14) of the linear approximation model from Equations (5) yields the lengthy equations for the non-linear part of response [1]. They govern the non-linear part of the rigid body motion in six degrees of freedom. In order to solve them we need to specify the non-linear part of the external (fluid) forces X, Y, Z and moments K, M, N acting on a body. These are qualitatively discussed above. More detailed discussion of them is presented in reference [1]. Moreover, we use Equations (2) and (4) to express body velocities in the inertial co-ordinate system. Numerical integration of these equations together with the division of responses given by Equations (16) yields the instantaneous position of ship in the inertial co-ordinate system XYZ . Additionally, thirteenth ordinary differential equation of a first order representing the action of autopilot is used to control the rudder angle. Integration is conducted using the 4th order Runge-Kutta scheme with an integration step being $\Delta t = 100$ ms. Computation is conducted for a full-scale ship. The zero initial conditions are used for all equations with an exception of surge velocity, which is set initially to a prescribed ship velocity in calm water. In order to dampen the spurious transients, the wave amplitude is gradually increased from zero to the prescribed final value $a_{w,\text{final}}$ using the expression

$$\begin{aligned} a_w(t) &= a_{w,\text{final}} \left[1 - \left(\cos \frac{\pi t}{2T_f} \right)^2 \right] \text{ for } t < T_f, \\ a_w(t) &= a_{w,\text{final}} \text{ for } t \geq T_f, \end{aligned} \quad (17)$$

where:

t is time and with $T_f = 50$ seconds in full scale being used.

5. Examples of ship motion simulation and method validation

5.1. Simulation and model test experiments dedicated to investigation of ship capsizing

Two ship cases were used in the benchmark study initiated by the International Towing Tank Conference and presented in [9]. First one, ship A1, is a containership of waterline length of $L_{PP} = 150$ m and low metacentric height ($GM_0 = 0.15$ m). This low GM_0 – value means that static stability of this ship is poor. Second vessel ship A2, is

a model of fishing vessel of the length $L_{PP} = 35.68$ m. Both models were run in regular waves, different headings and Froude numbers ($F_n = \frac{V_S}{\sqrt{gL_{PP}}}$). The summary of model test results and simulation results are given in two tables below. Wavelength is depicted by λ .

Table 1. Summary of the results for containership (Ship A1)

Case	λ/L_{pp}	$2a_w/\lambda$	F_n	Heading μ [deg]	Experiment	Computed
1	1.5	1/25	0.2	0	Parametric roll resonance, capsize	Parametric roll resonance, no capsizing
2	1.5	1/25	0.2	45	No- capsizing	No- capsizing
3	1.5	1/25	0.3	30	No- capsizing	No- capsizing
4	1.5	1/25	0.4	30	Capsize	Capsize

Table 2. Summary of the results for fishing ship (Ship A2)

Case	λ/L_{pp}	$2a_w/\lambda$	F_n	Heading μ [deg]	Experiment	Computed
A	1.637	0.1	0.3	-30	No-capsizing	No-capsizing
B	1.637	0.1	0.43	-10	Surfing, capsize	Surfing
C	1.127	0.115	0.3	-30	No-capsizing	No- capsizing
D	1.127	0.115	0.43	-30	Capsize	Capsize

A reasonable agreement of the computed results with the experimental ones is noted. An example of computed angular motion prior to capsizing is shown in Figure 3 and the corresponding experimental result is presented in Figure 4.

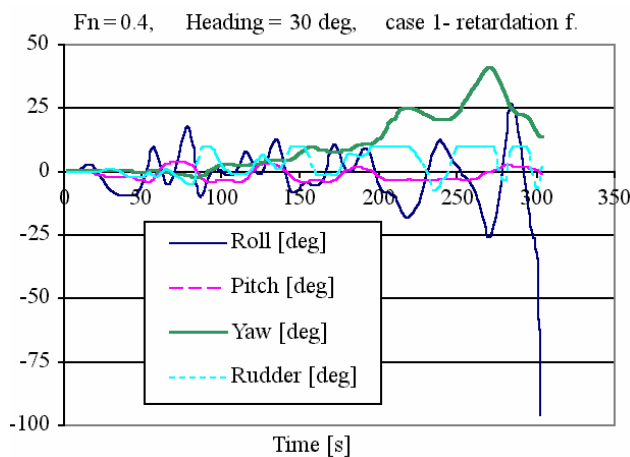


Fig. 3. Containership (ship A1) running at $F_n = 0.4$ capsizes in regular quartering regular waves (heading 30 deg). Simulated result

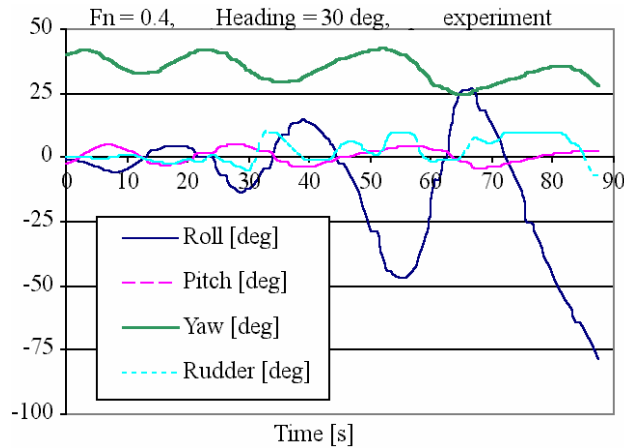


Fig. 4. Model of ship A1 running at $F_n = 0.4$ capsizes in regular quartering regular waves (heading 30 deg). Model test result scaled to full-scale [5]

Both time histories are similar. Capsizing is preceded by a couple of large heeling events. The surge motion and the position of ship in waves seems to have an important influence on the dangerous situation development.

5.2. Parametric roll resonance

Parametric roll resonance is an unexpected ship roll motion in head or following seas. The phenomenon is known to shipmasters. Linear seakeeping theory is not capable to predict this roll motion and for this reason we can call it an unexpected response. The phenomenon is generally attributed to the parametric variation of the restoring moment of heel caused by a large variation of water-plane area in waves. Thus, qualitatively, the phenomenon is often described by a single equation of the Mathieu type.

An extensive model test series of a modern, fast twin-screw Ro-Pax vessel was conducted at the Ship Laboratory of the Helsinki University of Technology. Tests were primarily concerned with the dynamic stability. In particular, a loss of stability on a crest of a following wave and parametric roll resonance were investigated both in regular and irregular waves for three KG-values with ship model without and with two different height bilge keels (450 mm and 900 mm in the full scale). Tests were run with the self-propelled model steered manually [10]. These model tests were used to validate the above described method. The results of the validation were presented in a bigger detail in reference [11]. In the following, in Figures 5 and 6, the example time histories of motions corresponding to a single test case is presented, only.

Both the simulations and the model test experiments gave similar conclusion. In this case of a pure parametric resonance, where the ratio of an encounter period to roll natural period is 0.5, roll amplitude seems to be related to wave amplitude squared.

Moreover, an increase of the wave amplitude results in a lower number of encounter periods required for a roll motion to start. Simulations indicated that there is a certain threshold value of wave amplitude below which parametric roll resonance does not develop.

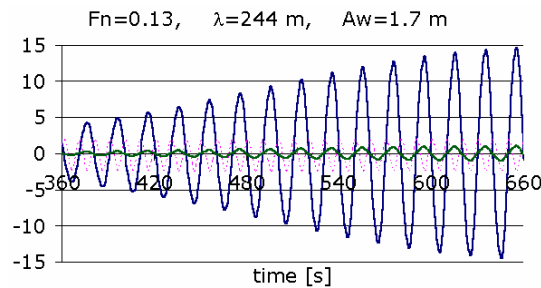


Fig. 5. Simulated angular motions for ship with low bilge keels and $KG = 12$ m; wave amplitude $A_W = 1.7$ m, $T\varphi = 20$ s, $\zeta = 0.046$. Ultimate roll amplitude 16 deg

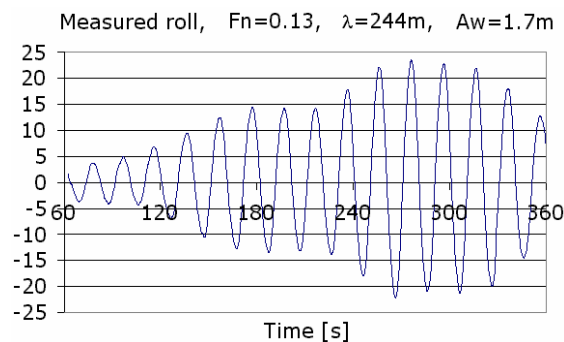


Fig. 6. Measured roll for ship equipped with low bilge keels and $KG = 12$ m, wave amplitude $A_W = 1.7$ m, $T\varphi = 20$ s, $\zeta = 0.046$

Both the simulations and the tests indicated that an increase of damping, achieved by bilge keels, results in a somewhat lower roll amplitude. Damping also delays and slows the development of the parametric roll resonance [11].

5.3. Weather criterion

In order to ensure safety of a vessel in a “dead ship condition”, the so-called weather criterion was made mandatory for ships in 2005. The criterion takes into account resonant beam waves and gusty wind [12]. As the origin of the criterion is quite old and there is a number of strong assumptions involved, its application to a modern large size passenger vessel can be questioned. In order to make it better suited for modern ships, an allowance for the alternative assessment using model tests was made. Tests

are believed to yield more realistic values of wind loading and better estimates of roll amplitude at the resonance. The first attempts to utilize model tests in validating fulfillment of the weather criterion were presented in [13, 14].

The LAIDYN method was used to evaluate the fulfillment of the weather criterion by an example passenger ship design [15]. The original idea was to substitute the model tests of the alternative assessment with the appropriate numerical simulations. The interesting findings of this study were:

- the so-called "effective" roll-back angle obtained by simulating ship's behaviour in beam seas was very close to the one given by the rule (-5 deg in the considered case).
- weather criterion considers the resonant beam seas as a critical situation yielding an initial heel at which wind gust impacts the vessel. Wave action as such is disregarded when considering transient response of ship caused by heeling moment due gusty wind loading. Thus the fulfillment of the weather criterion can be simulated (numerically or with an aid of model tests) by investigating ship's transient heel response in still water with an initial value set by a roll-back angle and step-wise heeling moment simulating gusty wind. The simulated result of this kind of response is shown in Figure 7 with ship heeling by 27 deg. The corresponding situation, as evaluated traditionally with an aid of dynamic lever concept, is shown in Figure 8 and yields maximum heeling of 30 deg.

If wind loading is represented by the horizontal force and the corresponding heeling moment then dynamic behavior, taking sway motion into account, yields still smaller maximum heel angle (see Figure 9).

The conclusion of the numerical simulation of the scenario set-up by the weather criterion is that it does not really pretend to evaluate capabilities of a ship in a realistic sea conditions and with a sound model of ship dynamics. It is merely a simple measure of intact ship stability. However, the criterion comprises important elements affecting ship safety and thus can be regarded as an important element of ship safety assessment.

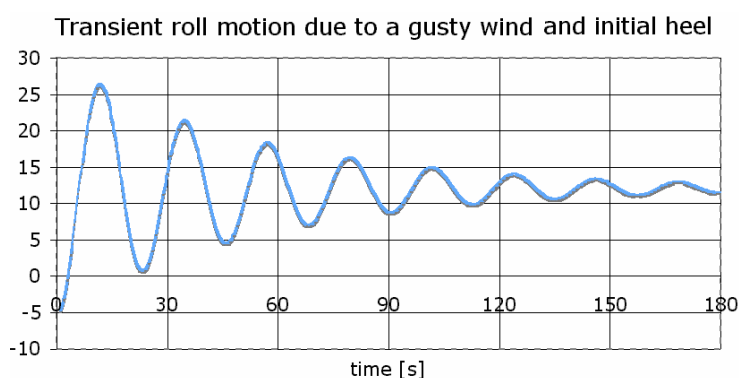


Fig. 7. Ship transient rolling caused by the gusty wind and initial heel. Gust loading is taken according to the weather criterion

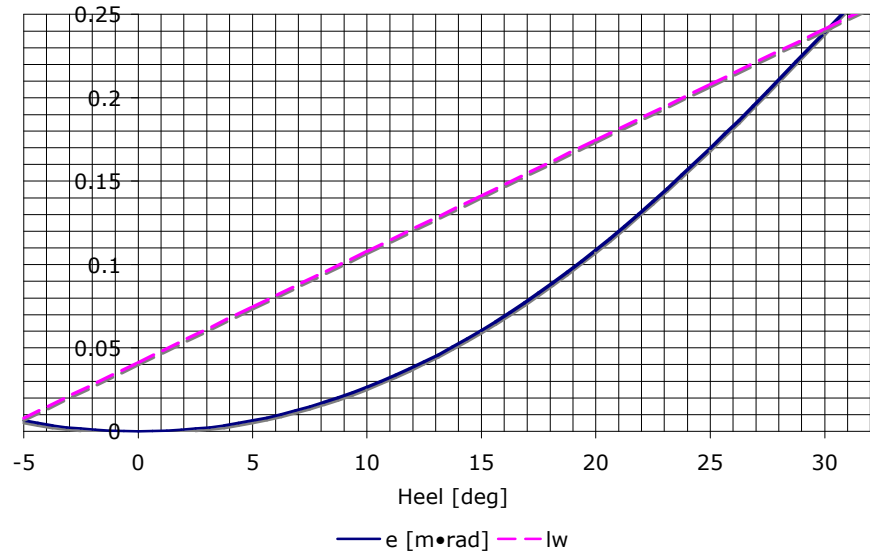


Fig. 8. Ship dynamic heeling according to the weather criterion. l_w is dynamic lever of gusty wind loading and e is dynamic lever of the restoring moment (integral over the GZ-curve)

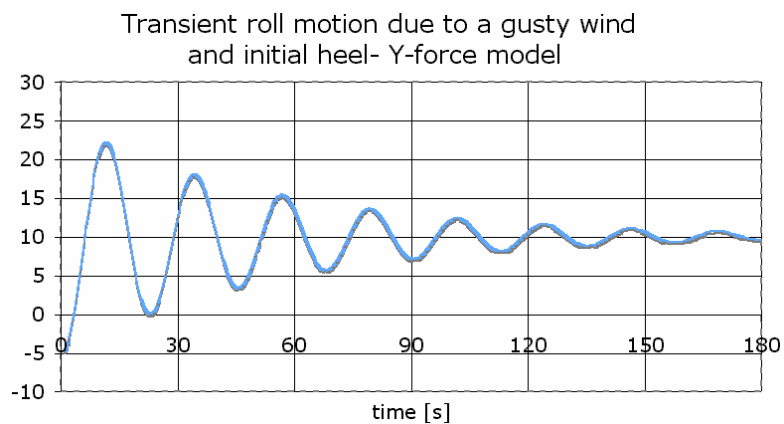


Fig. 9. Ship dynamic heeling according to the loading model represented by a horizontal Y-force and model of dynamics including the sway motion component

6. Concluding remarks

The two-stage approach yields ship motions, which at least qualitatively agree with the model test experiments. When dealing with the responses which are governed by strong non-linearities a small deviation in the initial conditions matters.

Although, in principle, a simulation of ship's maneuvering in waves is possible with a method in a present form a further development is needed. In particular an unified approach, taking into account different time scales of maneuvering and seakeeping, is needed to represent hull forces in unsteady motion. Also disclosing the factors responsible for stability loss and for parametric roll resonance would be valuable for both ship designer and for the operator.

References

- [1] Matusiak J.: *Two-Stage approach to determination of non-linear motions of ship in waves*, 4th Osaka Colloquium on Seakeeping Performance of Ships, Osaka, Japan, 17–21st October, 2000.
- [2] Matusiak J.: *Importance of memory effect for capsizing prediction*, 5th International Workshop On Ship Stability, University of Trieste 12–13 September, 2001.
- [3] Hamamoto M., Kim Y.S.: *A new coordinate system and the equations describing manoeuvring motion of a ship in waves*, J. Soc. Naval Arch., Vol. 173, 1993.
- [4] Clayton B.R., Bishop R.E.D.: *Mechanics of marine vehicles*, ISBN 0 419 12110-2, 1982.
- [5] Fossen T.I.: *Guidance and control of ocean vehicles*, ISBN 0 471 94113 1, 1994.
- [6] Newman J.N.: *Marine hydrodynamics*, Cambridge, Massachusetts, The MIT Press, 1980.
- [7] Cummins W.E.: *The impulse response function and ship motions*, Schiffstechnik 9, 1962, Nr. 47, 101–109.
- [8] Journee J. M.: *Strip theory algorithms*, report MEMT 24, Delft University of Technology, Ship Hydrodynamics Laboratory, 1992.
- [9] 23rd International Towing Tank Conference, Report of the Specialist Committee of Extreme Ship Motions and Capsizing, Venice Italy, September 8–14, 2002, in Proceedings of the Conference, Vol. 2.
- [10] Mattila M.: *An investigation of the dynamic stability of a fast RoPax vessel in waves* (in Finnish), Helsinki University of Technology, Mechanical Engineering Department, Master Thesis, 1999.
- [11] Matusiak J.: *On the effects of wave amplitude, damping and initial conditions on the parametric roll resonance*, Proceedings of the 8th International Conference on Stability of Ships and Ocean Vehicles, Madrid, Spain, September 2003, pp. 341–348.
- [12] International Maritime Organization, SLF 49/5 Revised Intact Stability Code prepared by the Intersessional Correspondence Group.
- [13] Hyeon Kyu Yoon et al.: *Application and review on interim guidelines for alternative assessment of the weather criterion*, In Proceedings of the 9th International Conference on Stability of Ships and Ocean Vehicles, STAB 2006, 25–29 September, 2006, Rio de Janeiro, Brasil.
- [14] Ischida S. et al.: *Evaluation of the weather criterion by experiments and its effect to the design of a RoPax ferry*, In Proceedings of the 9th International Conference on Stability of Ships and Ocean Vehicles, STAB 2006, 25–29 September, 2006, Rio de Janeiro, Brasil.
- [15] Matusiak J., Hamberg K.: *Considerations on the weather criterion applicability for the stability assessment of the large vessels*, In Proceedings of the 9th International Conference on Stability of Ships and Ocean Vehicles, Rio de Janeiro, Brasilia, 25–29.9.2006, Vol. 1, pp. 447–454.

O pewnych rodzajach reakcji ujawnianych przy dwuetapowym podejściu do dynamiki statku

Przedstawione zostały przypadki zastosowania tzw. dwuetapowego podejścia do wyznaczania nieliniowych ruchów o dużej amplitudzie statku na fali. Przypadki obejmują wywracanie statku do góry dnem, parametryczne kołysania rezonansowe, oraz symulację tzw. kryterium pogodowego w dziedzinie czasu. Podany został również krótki opis modelu obliczeniowego.

Experimental investigations of guide rings made of UHMWPE and PTFE composite in water hydraulic systems

W. OKULARCZYK

Częstochowa University of Technology, Institute of Polymer Processing and Production Management, Aleja Armii Krajowej 19c, 42-200 Częstochowa

In the present work two materials of guiding elements were tested in water hydraulic. During investigations of hardness conducted for stuffing box packings in water hydraulic systems an analysis of proper selection of piston rod guiding elements has also been carried out ($\phi 45f7$, $Ra = 0.07-0.20 \mu\text{m}$, $Rm \leq 2.5 \mu\text{m}$). Working piston rod has been used for investigations made of chromium-nickel steel AISI 431 ($Cr = 16.7\%$, $Ni = 2.08\%$). Some of the guiding elements, after proper selection of the material, could be still used, despite damaged seal. The tests have been performed maintaining water pressure on the sealing at a level of $p = 8 \pm 1 \text{ MPa}$ and the average velocity of the piston rod of $v \approx 0.35 \text{ m/sec}$. Water temperature during investigations was regulated within the range of $T_{\text{min}} = 291 \text{ K}$ and $T_{\text{max}} = 305 \text{ K}$. Variable value of friction coefficient has been obtained for the guide rings made of PTFE composite with the change in piston rod velocity. Application of guide rings made of UHMWPE has been estimated negatively.

Keywords: *engineering polymers, polymer seals, UHMWPE, PTFE composite, water hydraulic*

1. Introduction

The purpose of the investigations was to determine optimal combination of piston rod seal – guide ring. They concerned the type of the seal and materials of both seal and guide ring. The results of the investigations of seal selection on the basis of life-time and friction forces have been described before [1]. The purpose of this paper was to indicate the polymer suitable for water hydraulic systems.

2. Description of test stand

Figure 1 presents the test cylinder. The cylinder (2) is placed on the base (1) and fixed with two clamping rings (14). The piston rod (3), made of stainless steel, moves inside the cylinder forced by the movement of force sensor (4). Filling up of the cylinder (2) with water takes place after unscrewing upper head of hand pump (6) and loosening air vent (5). After water appears in the air vent and the water surface is found at the half of height of the hand pump cylinder (6) the air vent is tightened and the upper head of the pump is assembled. The pressure inside the cylinder is produced by the pressurised nitrogen from the gas cylinder (12). Pressure from the gas cylinder is reduced several times by means of pressure reducer (10) and then it is transferred through the hose (11) to the gas/water intensifier (13) with 10:1 ratio. Reading of the water

pressure transferred through the hose (9) from the cylinder (2) is made by means of the gauge (7). The possible leakage from the seal that can appear is drained through leakage pipes (15) into the measuring containers. Temperature measurements are read by sensors (8). Both cylinders are placed on one base and their piston rods are connected by means of force sensor working at the compression/tension conditions which enables the measurements of friction forces in sealing. The stroke was 0.5 m and the minimal cycle time amounts to ca. 3s.

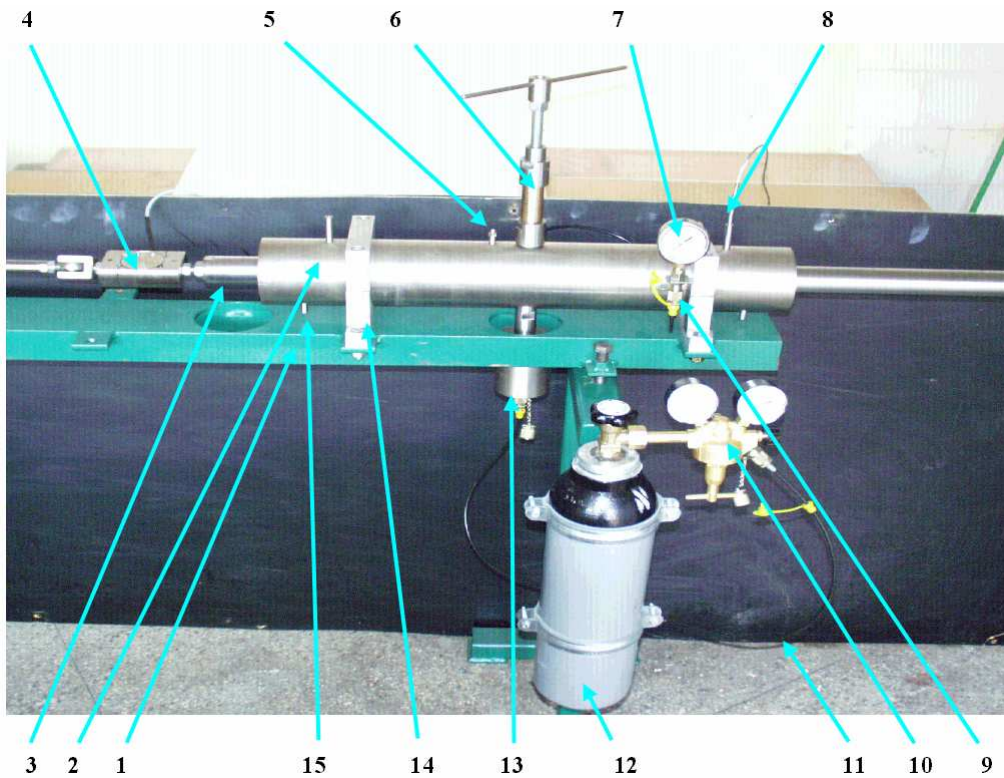


Fig. 1. Test stand: base (1), cylinder (2), piston rod (3), force sensor (4), air vent (5), hand pump (6), gauge (7), temperature sensors (8), hose (9), pressure reducer (10), hose (11), gas cylinder (12), gas/water intensifier (13), clamping ring (14), leakage pipes (15)

For typical hydraulic cylinder the guide elements are located before seal i.e. at the pressure side, which ensures their proper lubrication. The guide rings were placed under the seal rings (Figure 2) in order to achieve maximal concentricity. The external distance of test cylinder guide elements gives opportunity for the guide rings wear products to get into the interior of the cylinder only during the cycle of in-movement of the piston rod into the seal. Due to the leakages of lubricant, the self-lubricating

elements had to be used, proper for the material of piston rod. This arrangement also enabled better damping of vibration of piston rod free ends.

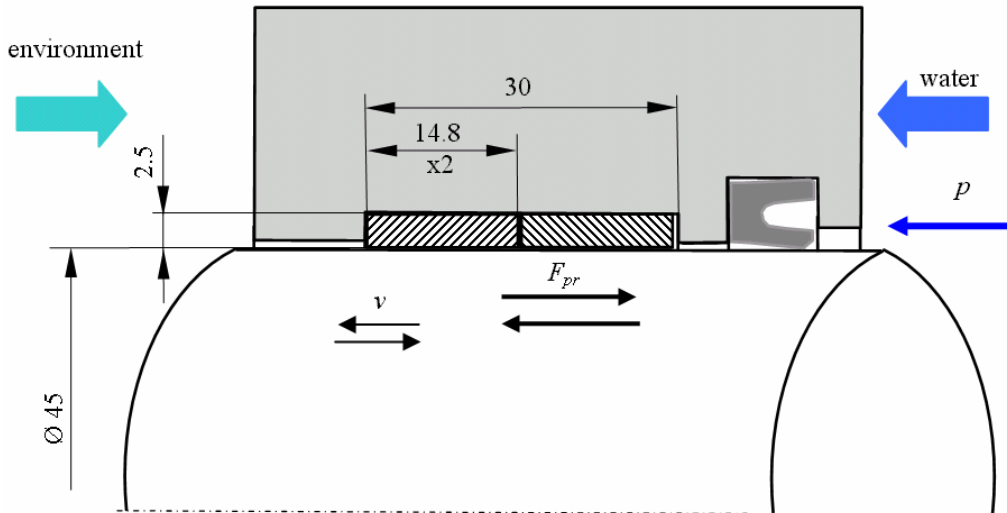


Fig. 2. Seal and guide rings in stuffing-box

The guide elements used for the test station were made of UHMWPE and PTFE filled with 23% of carbon and 2% of graphite (Kefloy 22) [2] (Table 1).

Table 1. Materials of guide elements

UHMWPE	UHMWPE virgin
PTFE composite	PTFE + 23% carbon + 2% graphite (Kefloy 22)

3. Research

Due to significantly high coefficient of linear thermal expansion of the polymers, the guide elements in pneumatic and hydraulic cylinders are produced from the cut tape, and a gap with a certain width is left between the ends [2]. Length of the tape is calculated as below:

$$L = 3.114(d + g) - 1 \text{ [mm]}, \quad (1)$$

where:

d – piston rod diameter, 45 mm;

g – thickness of the tape, assumed value: 2.5 mm.

Width of the rings was accepted as 14.8 mm; in both stuffing-boxes 2 rings were located (Figures 2–3).



Fig. 3. Packing nut (left), stuffing-box with guide rings made of PTFE composite in closed groove (central), stuffing-box with opened groove of seal and leakage holes (left) [2]

Parameters of working piston rod as well as the parameters of the investigations are shown in Table 2 and 3.

Table 2. Parameters of piston rod [3]

Diameter	45 f7
Ellipsoidality	$\leq 1/4$ f7 (for ϕ 45)
Material	chromium-nickel steel AISI 431 ($Cr = 16.7\%$, $Ni = 2.08\%$)
Covered chromium plating	≥ 20 μm
Roughness	$Ra = 0.07\text{--}0.20$ μm , $Rm \leq 2.5$ μm

Tab.3 Parameters of the investigations

Objects	Pressure p [MPa]	Velocity v [m/sec]	Temperature [K]	Investigation
Seals + guide elements	8 ± 1	0.35	291–305	Durability, total friction force
Only guide elements	0	0.05–0.40	291 ± 5	Friction force F_{cpr}

Initially, the guide rings made of UHMWPE (polyethylene ultra high molecular weight) were used for the investigations [4–9], however, it was found that during sealing tests conducted also on UHMWPE, there is still a water drops streaking effect at the piston rod ends protruding from the cylinder, which leads to clogging of the seal by wear products – lifetime only 20000 m (Figure 4). Wear products caused damage of the seals and investigations of guide rings made of UHMWPE. Only friction force after 108 000 m was determined.

In order to determine the friction force for the guide set (two guide rings in stuffing-box, see Figure 2) F_{pr} , a friction force was first determined for the two guide sets (in both stuffing-boxes) F_{cpr} .

$$F_{pr} = F_{cpr} / 2 \text{ [N]}. \quad (2)$$



Fig. 4. Mupuseal 30412 – 0450 – 90 – S seal after 20 000 m of friction distance. Visible wear products on the seal from the guide elements made of UHMWPE [1]

In order to obtain the measurements of friction force for F_{cpr} possibly close to the real state, the piston rod and the guide elements were several times washed by the technical acetone, which was then left to free evaporation. The layer of the material produced during operation and pushed into the piston rod structure was deliberately not removed. The seals were disassembled during tests from the stuffing boxes. During assessment of the elements made of polyethylene with very high molecular mass (UHMWPE) it was found that friction force (and the friction coefficient, respectively) after 108000 cycles (i.e. 108000 m), decreased only by 30%. It was also found that friction coefficient for UHMWPE μ_{UHMWPE} has a continuous value within the range of applied velocity of $v = 0.05$ to 0.40 m/s. In order to determine friction coefficient μ_{UHMWPE} the weight of the piston rod was calculated, whose mass $m = 15.5$ kg, thus pressing force $N = 152$ N. At the friction force for single guide element, after the distance of 3500 m, with $F_{pr} = 20$ N value of $\mu_{UHMWPE} = 0.26$. However after 108000 m of friction distance the friction coefficient $\mu_{UHMWPE} = 0.20$. It should be highlighted that these coefficients concern dry friction. Similar measurement have been performed for guide elements made of Kefloy 22, after 15000 m, 60000 m and 90000 m of friction distance s . The guide elements used in the test station were made of PTFE filled with 23% of carbon and 2% of graphite (Kefloy 22) [10–12]. Wear products from guide rings made of Kefloy 22 did not cause damage of the seals (Figure 5).

Figure 6 presents the example of the friction forces only for the guide elements made of Kefloy 22. The chart shows “soft” vibration damping and fluctuation of friction force. Vibration damping is a quality characteristic for polymers and PTFE has one of the best damping coefficient, if construction polymers are considered. Due to this properties the polymers have thoroughly superseded bronze from hydraulic systems. The vibrations with short wavelength are caused by the graphite on the piston rod [13]. This causes variable friction force (ca. 3.5–7.5 N). The charts for the

dependence of friction force on the velocity, for single guide element made of Kefloy 22 are presented in the Figures 7–9. Very broad range of friction coefficient $\mu_{Kefloy\ 22}$ was found, e.g. for the range of applied velocity, after the friction distance of 15000 m, together with the increase of the velocity its value changes from 0.20 to 0.065.



Fig. 5 Mupuseal 30413 – 0450 – 90 – S seal after 90 000 m of friction distance. Visible wear products on the seal from the guide elements made of Kefloy 22

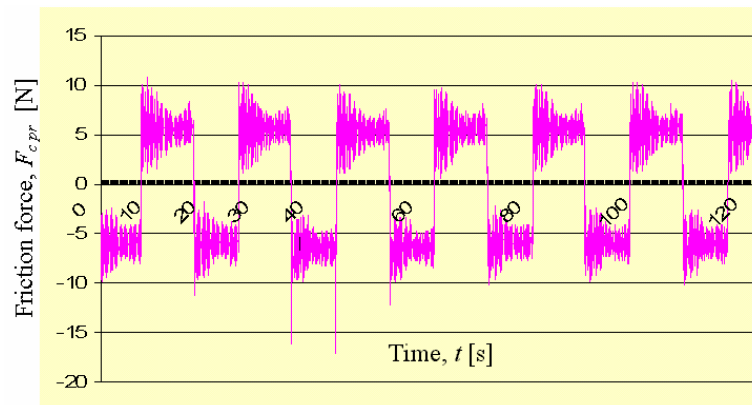


Fig. 6. Friction force diagram of guide elements made of Kefloy 22. Distance 99 000 m, sampling frequency 100 Hz, time of measurement 120 s, average velocity $v = 0,09$ m/s, average friction force value $F_{c,pr} = 6$ N

After friction distance of 90000 m the opposite situation takes place – while increasing the velocity the friction coefficient increases from 0.039 to even 0.37.

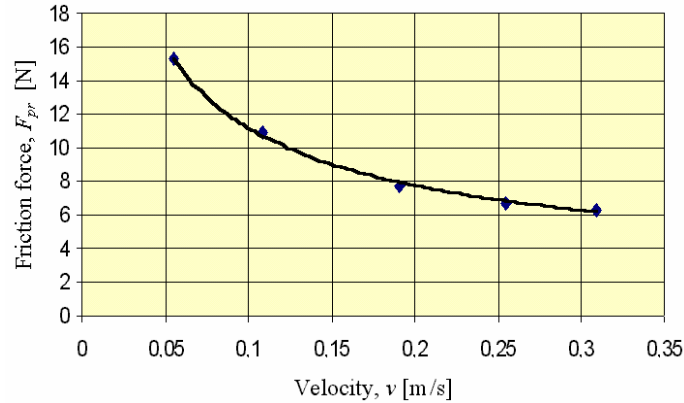


Fig. 7. Friction force as a function of the velocity of single guide element made of Kefloy- 22 after the distance of 15000 m

On the basis of Figure 7 it can be assumed that during initial period of mating of guide elements made of Kefloy 22 (PTFE + 23% of carbon + 2% of graphite) with the piston rod surface, an adhesion wear mainly occurred [14]. Friction node was also subject to running-in during this period. During first period the phenomena according to the theory of mechanical locking, typical for the polymer-metal contact, occurred. Next stage of running-in is an increase in friction force as a result of adhesion, visible especially at the lower velocity values. Separation of the surface by the products of abrasive wear, being also the lubricant, leads to the fluid friction – both surfaces, at this moment, do not contact with the point of highest irregularities of the surface. However, due to the increased thickness of the graphite on the piston rod a phenomenon of polymer material deformation of elastic nature occurs, especially visible on the charts of friction elements (Figure 6).

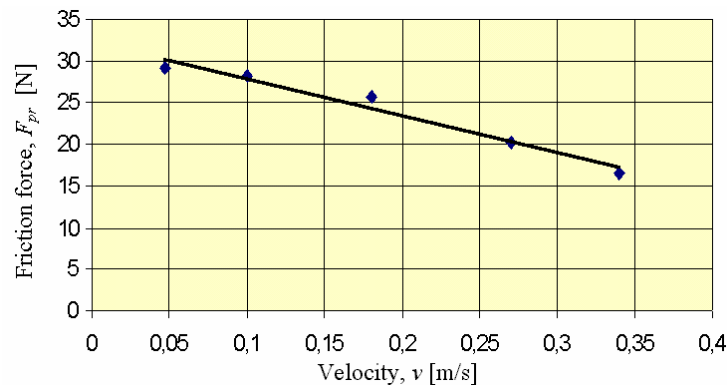


Fig. 8. Friction force as a function of the velocity of single guide element made of Kefloy- 22 after the distance of 60 000 m

The friction coefficient, from this moment increases with the increase of velocity (Figure 9). Friction begins to be of a mixed nature.

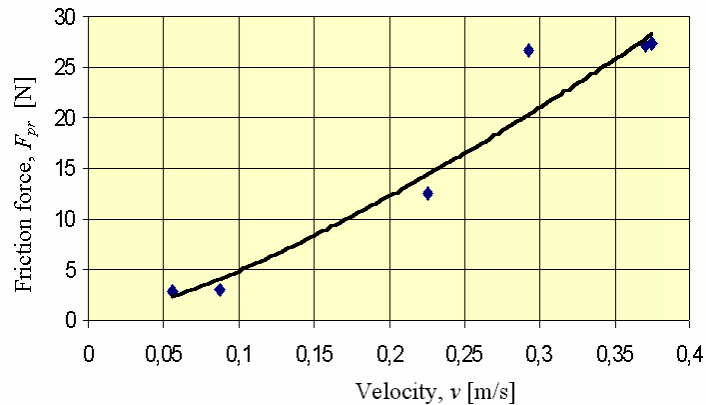


Fig. 9. Friction force as a function of the velocity of single guide element made of Kefloy- 22 after the distance of 90000 m

4. Conclusions

The assumed purpose of the investigations has been achieved. The combinations of the materials have been selected for piston rod sealing made of UHMWPE and guide rings made of PTFE composite (Kefloy 22). For the lifetime reaching friction distance of 200 km [1] the guide rings can be used several times. Kefloy 22 can be successfully used for guide rings in water hydraulic systems.

Application of the guide elements made from Kefloy 22 enable using wear products as a lubricant. In this paper the application of UHMWPE as a material for guide elements working in water hydraulic was investigated. Our studies revealed that it is not recommended to produce the guide elements from this material despite the fact that UHMWPE has the lowest abrasive wear rate from all polymers. Problem occurred due to wear particles disturbing the work of the cylinder.

Further investigations are recommended in order to reduce the amount of graphite and carbon from guide ring material. This should improve the lifetime of piston rod seal, which seem to depend on the thickness of the lubricant film on the push rod.

References

- [1] Okularczyk W., Kwiatkowski D.: *Prognosing the durability of polymer sealings*, Journal of Achievements in Materials and Manufacturing Engineering, Vol. 17, Gliwice 2006, pp. 125–128.
- [2] Catalog of O.L. Sealing Systems (DK).
- [3] Catalog of Urania Ltd. (IT).

- [4] Marcus K., Allen C.: *Effect of fillers on the friction and wear behaviour of ultra high molecular weight polyethylene during water-lubricated reciprocating sliding wear*, *Wear*, 162–164, 1993, pp. 1091–1102.
- [5] Bron K.J., Atkinson J.R., Dowson D.: *The wear of high molecular weight polyethylene – Part II: The effects of reciprocating motion, orientation in the polyethylene and a preliminary study of the wear of polyethylene against itself*, *Transactions of the ASME – Journal of Lubrication Technology*, 1982, Vol. 104, No. 1.
- [6] Cooper J.R., Dowson D., Fisher J.: *Macroscopic and Microscopic Wear Mechanism in Ultrahigh Molecular Weight Polyethylene*, *Wear*, 162–164, 1993, pp. 374–384.
- [7] Derbyshire B., Fisher J., Dowson D., Hardaker C.S., Brummitt K.: *Wear of UHMWPE sliding against untreated, titanium nitride-coated and “Hardcore” – treated stainless steel counterfaces*, *Wear*, 181–183, 1995, pp. 258–262.
- [8] Guo Q., Luo W.: *Mechanisms of fretting wear resistance interms of material structures for unfilled engineering polymers*, *Wear*, 249, 2002, pp. 924–931.
- [9] Marcus K., Allen C.: *The sliding wear of ultrahigh molecular weight polyethylene in an aqueous environment*, *Wear*, 178, 1994, pp. 17–28.
- [10] Landheer D., Meesters C.J.M.: *Reibung und Verschleiss von PTFE-Compounds*, *Kunststoffe*, 83, 1993, pp. 12–16.
- [11] Watanabe M.: *Wear mechanism of PTFE composites in aqueous environments*, *Wear*, 158, 1992, pp. 79–86.
- [12] Blanced T.A., Kennedy F.E.: *Sliding wear mechanism of polytetrafluoroethylene (PTFE) and PTFE composites*, *Wear*, 153, 1992, pp. 229–243.
- [13] Okularczyk W.: *Applications of multicriterial analysis for selection of polymeric seals in water hydraulics* (in Polish), *Polimery*, 2006, 51, no. 10, pp. 747–753.
- [14] Okularczyk W.: *Hydraulic rotating joint to special applications* (in Polish), *Materiały polimerowe i ich przetwórstwo*, Częstochowa, 2006, pp. 17–26.

Badania eksperymentalne pierścieni prowadzących wykonanych z UHMWPE i kompozytu PTFE pracujących w hydraulicie wodnej

Podczas wykonywania badań trwałościowych uszczelnień dławnicowych w układzie hydrauliki wodnej dobrano skojarzenie, w którym uszczelnienie tłoczyskowe wykonano z UHMWPE, natomiast pierścienie prowadzące z kompozytu PTFE (Kefloy 22). Do badań zastosowano tłoczysko robocze o średnicy $\varnothing 45f7$ wykonane ze stali chromowo-niklowej AISI 431 ($Cr = 16.7\%$, $Ni = 2.08\%$), pokrytej płytkami twardego chromu o $gr. \geq 20 \mu m$ (elipsoidalność $\leq \frac{1}{4} f7$, liczba mikropęknięć $\geq 5\ 000/mm^2$, $Ra = 0.07-0.20 \mu m$, $Rm \leq 2.5 \mu m$). Niektóre z elementów prowadzących, po prawidłowym doborze materiału mogły być używane nadal, mimo zniszczenia uszczelki.

Badania prowadzono, utrzymując ciśnienie wody obciążające uszczelki na poziomie $p = 8 \pm 1$ MPa oraz prędkość średnią tłoczyska $v \approx 0,35$ m/sek. Temperatura wody, a tym samym temperatura tłoczyska, podczas badań była regulowana w zakresie $T_{min} = 291$ K, $T_{max} = 305$ K. Otrzymano zmienną wartość współczynnika tarcia pierścieni prowadzących wykonanych z kompozytu PTFE wraz ze zmianą prędkości ruchu tłoczyska. Przy trwałości uszczelnień dochodzącej do 200 km drogi tarcia, pierścienie prowadzące mogły być stosowane kilkakrotnie. Kefloy 22 może być z powodzeniem stosowany na pierścienie prowadzące w hydraulicie wod-

nej. Oceniono negatywnie stosowanie pierścieni prowadzących wykonanych z PE-UHMW. Zaproponowano kompozyty o składzie pozwalającym na uzyskanie wyników zgodnych z założeniami dotyczącymi ich trwałości.



Tribology of Polymers

Z. RYMUZA

Warsaw University of Technology, Institute of Micromechanics and Photonics, 02-525 Warszawa, Poland

Tribology of polymers is very interesting area of research. The selection of polymers as materials for sliding (as well rolling) components of machines and devices is very important task for tribologists. Non-polymer-on-polymer as well as polymer-on-polymer contacts are important nowadays in design of machines and devices in modern technology. Understanding of tribological processes is very crucial. Tribological behaviour of polymeric tribosystems both for non-polymer-on-polymer and polymer-on-polymer combinations are discussed in this paper.

Keywords: *tribology, friction, wear, lubrication, polymers*

1. Introduction

Recently the application of polymers has rapidly increased generally in technology and also as materials for rubbing components in various machines and devices. This is particularly connected with low cost of materials and manufacturing in large amount of components. When the polymeric materials are rubbing in tribological contacts it is very useful and often the lubrication is not necessary. The friction coefficient can be similar to the lubricated metallic or ceramic contacts. This kind of contact is often called as oilless.

The tribology of polymers is different from tribology of metals and ceramic materials. The difference of application of polymers in frictional contacts in comparison to metals and ceramic materials relates mainly to the chemical and physical structures as well as to the surface and bulk properties. The polymers show very low surface free energy and also have the viscoelastic properties. It effects in drastic tribological differences when we consider adhesive and mechanical components of friction force. Also polymers can be easily modified both on surface and in bulk. Therefore there are often and easily used as a background material to produce many composites with easily varied physicochemical properties. This makes polymers very promising materials with ability to control their frictional and wear behaviours sliding contacts. Such "elasticity" of physical and chemical structures enables to produce interesting components for various tribosystems composed of polymers, metals, ceramic materials as well as polymer-on-polymer sliding (and even) rolling tribological contacts.

2. Non-polymer-on-polymer contacts

The non-polymer-on-polymer tribosystems are often applied in various machines and devices. This is probably due to good mechanical and thermal properties of the

counter-face rubbing element. The most popular and also practically confirmed as the best tribological combination is steel-on-polymer frictional tribosystem [1–3]. Relatively low friction coefficient and often sufficiently high wear-resistance can be achieved in these systems by proper selection of the polymer and metal (steel) to be used.

In the friction in no-polymer-on-polymer sliding contact two main components i.e. adhesive and mechanical properties are very important. The possibility of summing up of mechanical and adhesive component of friction force was proved in experiment [1–3]. The mechanical and adhesive interactions are located in very thin surface layer of polymer being in frictional contact. The ratio between mechanical and adhesive component depends in particular on roughness of the counterbody. The coefficient of friction is usually very high at small roughness because of high adhesion, and it decreases down to minimum value at increase of roughness and then increases at further increase of roughness when mechanical component of friction force becomes very high. The similar tendency was confirmed also experimentally in the case of wear rate. But the minimum value of friction coefficient, wear rate and also the shape of the characteristic curves are fairly similar.

The load and sliding speed influence strongly on friction coefficient and wear rate. When the load increases the friction coefficient decreases but only at elastic contact. When plastic deformation begins the coefficient of friction is small but increases due to further load increase. The sliding speed and temperature of the contact have a significant effect on this relation. Much more complex is the dependence of friction coefficient on sliding speed. Usually a maximum of the friction coefficient vs. sliding speed can be observed. For polymers with higher glass transition temperature the maximum value of friction coefficient appears at higher sliding speed [1–3].

Very important in polymeric tribosystems is the wear process. Adhesive and abrasive wear mechanisms often occur in many sliding systems. The wear rate is high at high $p\nu$ parameter (p – contact pressure, ν – sliding speed). The wear process in higher extent than the friction process is controlled by material transfer which is very characteristic phenomenon in polymeric contacts. This very complex phenomenon takes the most important role in friction and wear processes in polymeric tribosystems.

The transfer of polymer material onto non-polymer partner is initiated by local, strong adhesive bonds of rubbing surfaces. The cohesive strength of polymeric material is an important parameter which should be taken into consideration in the transfer mechanism.

Transfer film is very important to some polymer components, especially to those designed to be used under dry friction condition. The transfer film formed on a non-polymer counterface is controlled by the counterface material and roughness, and sliding conditions. Generally, transfer film formed during the friction process could effectively improve tribological condition of polymer, which means lower friction coefficient and remarkably reduced wear of material. For example, as a kind of very important tribological material, application of PTFE-based composite is just as this

situation. The cohesion between transfer film layers and the adhesion between transfer film and counterface are not completely understood.

The transfer of material, in particular, is very important in the tribosystem, where polymer composite rubs against non-polymer counter-body. Polymeric composites are very popular as materials for sliding components. The addition of fillers (fibers, powders) solid lubricants changes drastically physical properties of polymers and both friction and wear behaviors. Some fillers affect the development of transfer film and enhance its adhesion to the counterface. The crucial properties are mechanical behavior of composite, its thermal conductivity and “lubricity” (improved by solid lubricant(s)). The complex structure of polymer-based composites reflects in complex tribological behavior of polymeric tribosystems. Usually poor correlation between friction coefficient and wear rate characteristics can be observed [1–4]. Metallic, ceramic and, in particular, metal oxide nanoparticles are added to polymers in the expectation of obtaining unique physical and mechanical properties which can not be achieved by adding micron-sized particles [5].

Friction and wear are different, when evaluate on a small-scale and a large-scale tribometer to determine transitions in tribological behavior and application limits [6–8]. Frictional heating and transfer are important and interfere with the sliding or lubricant mechanisms. The wear behavior of test samples with small and large contact areas is significantly different for solid lubricated composites, with lower specific wear for large-scale samples [6, 8]. Transitions in lubrication mechanism due to softening and melting do not allow for extrapolation and justifies the use of large-scale tests. Only pure polyamides have identical specific wear rates on small-scale and large-scale under mild conditions [6, 8].

Nowadays the nano-scale studies of tribological behavior of polymers are becoming more and more important because of possible future applications of polymers as engineering materials in nanosystems or in nano-manufacturing processes. Tribological behavior of polymers is important for example in nanoimprint lithography (NIL) where ultrathin polymeric film deposited on silicon wafer is used to form nanostructures by imprinting them, at increased over glass transition temperature, with silicon stamp (usually coated by thin hard layer e.g. TiN or silicon nitride). The frictional and adhesive behaviors of ultrathin (200–300 nm thick) polymeric resist films for NIL is very important in the process and decides about quality of imprints [9].

3. Polymer-on-polymer contacts

As it was stated before polymers and polymer-based composites are widely used because of the combination of good mechanical and tribological properties, especially in dry friction conditions, where lubricants cannot be used. They are usually mated with metal materials, however, there are some circumstances, in which it might be advantageous for polymers sliding against polymers rather than against metal materials, because polymers are light weight, no corrosion can be expected and polymeric com-

ponents can be easily manufactured. However, very little information is known concerning the friction and wear of polymer–polymer combinations [1–3, 10].

The friction between polymers can be attributed to two main mechanisms: adhesion and deformation [1–3]. The friction coefficient of polymer–polymer combination increased with the increase of adhesive work between them [11–13]. Friction force of polymer–polymer combination was correlated with the adhesion hysteresis between two shearing polymer surfaces [14]. The population of chain “ends” at surfaces was the most important factor that determined the adhesion, adhesion hysteresis, friction and wear between two polymer surfaces [15].

Frictional heat, which would alter the physical state of polymer sliding surfaces, has a significant effect on the tribological behaviors of polymer–polymer sliding combinations under dry sliding condition, while oil lubrication could reduce or dissipate the frictional heat. Adhesion wear was the dominant wear mechanism for dry sliding condition, while adhesion wear combined with erosion wear was the main wear mechanism for oil-lubricated condition [10].

Dry sliding of polymer–polymer combinations always produces intermittent motion and seizure or stick–slip due to adhesion [16, 17]. The rough-on-rough surface sliding combinations show lower friction coefficients than smooth-on-smooth surface combinations [16].

Polymer-on-polymer contacts are widely used in miniature mechanisms because of very low manufacturing costs of completely polymeric devices (e.g. quartz clocks). The polymer-on-polymer miniature bearings are promising components but the knowledge about their tribological behavior is very limited. We tested many polymer-on-polymer material combinations in such bearings and the results shown that the frictional behavior is very dependent on the selection of the polymers [17–23]. The most popular polymers in practical application in the design of miniature mechanism are thermoplastics. The interfacial adhesion is very important in the tribological behavior in such polymer-on-polymer bearings [21]. During our and other studies [24] it was observed that the general trends in tribological behavior of the discussed bearings can be illustrated as shown in Figure 1.

Transfer of material in polymer-on-polymer contacts is very important in tribological processes. The studies [25] of transfer of material in polymer-on-polymer pairs (such polymers as polytetrafluorethylene, polyvinyl chloride, polypropylene, poly(methyl methacrylate) and polyethylene terephthalate were used) showed that the thickness of the layer of transferred material increased with increasing the sliding speed because of adhesion increased from temperature rise and decreased with increasing the load because of greater compaction and the likelihood of loose material being detached from the surface. The material transfer always occurred from polymer of low cohesive energy density to one of higher cohesive energy density.

The process of transition from static to kinetic friction in miniature polymer-on-polymer bearings was investigated [26]. The friction at starting phase of operation of the bearing was studied experimentally and was also modeled. The effect of load,

sliding speed and time of contact of the journal with bearing bush before the operation of the bearing was considered. The real area of contact, rheological processes in the contact area, roughness of contacting surfaces and adhesion played important role in the frictional behavior of the studied contacts. It was demonstrated that the prediction of the frictional behavior in polymer-on-polymer sliding contacts is possible.

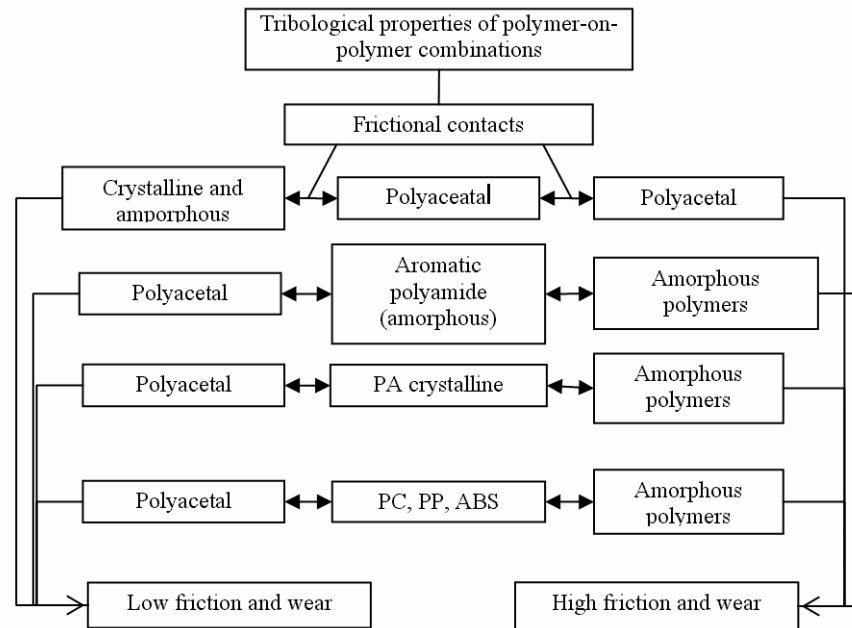


Fig. 1. Tribological properties of polymer-on-polymer contacts in miniature journal bearings; PA – polyamide, PC – polycarbonate, PP – polypropylene, ABS – Acrylonitrile/butadiene/styrene copolymer

4. Lubrication

Lubrication is very significant in tribological behavior of both non-polymer-on-polymer and polymer-on-polymer contacts. Friction and wear behaviors can be improved as well as friction and wear rate can also increase in the effect of lubrication [1-3]. It mainly depends on interactions between polymer and lubricant. The adsorption and even absorption of lubricant by polymer can effects in the plasticization of the surface layer and even of bulk polymer. The most important is to avoid the same solubility parameters of lubricant and polymer [27, 1–3]. The dielectric constant of oil should be higher than dielectric constant of the polymer in metal-on-polymer contacts [1]. In polymer-on-polymer contacts the dielectric contact of oil should be kept between the dielectric constants of applied polymers [1].

The used oils should be chemically inert and wet polymeric surface easily. For example polysiloxanes are interesting liquids therefore to be applied as lubricants of

polymeric contacts. Water is not a good lubricant, however can be used as cooling liquid [1, 28]. Also hydrodynamic effect can be easily and additionally obtained because of the high elasticity of the polymer element. In the case of miniature bearings special lubricants, mainly synthetic ones, are manufactured for mixed or boundary lubrication of non-polymer-on-polymer and polymer-on-polymer sliding contacts.

Self-lubrication in polymeric tribosystems is very interesting. Lubricant (oil) can be used as impregnation of polymer [29, 30] as well dispersion in the form of very small droplets inside the material (and even in polymeric thin coating) and perform lifetime lubrication.

5. Triboelectrification

As the effect of rubbing in non-polymer-on-polymer and polymer-on-polymer contacts electrical potential between contacting components occurs. The polarization does not depend on the fact which element is moving [1]. Triboelectrical potential depends on polymer and its position in the triboelectrical set of polymers [31].

The triboelectrification strongly depends on load and sliding speed and ambient conditions. The triboelectrification effects on friction and wear. The electrostatic forces increase adhesive interactions and the charge on rubbing components induces tribochemical reactions [1, 32]. The triboelectrification in lubricated contacts enables easy and strong adsorption of molecules of lubricant on rubbing surfaces.

It is possible to control the triboelectrification of rubbing elements by e.g. use of mixture of polymers which produces negative and positive charges. Such possibility exists at the use of compound polymeric material constructed by use of polyamide and polyethylene [1, 32]. Also permanent charge by the application of polymeric electrets is an effective way to control triboelectrification in polymeric tribosystems.

6. Summary

Polymers are very promising materials to be used for rubbing components in machines and devices. However, the selection of materials is critical. Understanding of frictional and wear mechanisms controlled in particular by intensive and decisive transfer of material during operation of polymeric tribosystems is a very important task for tribologists. Low cost, corrosion resistance, damping of vibrations, ability to adapt to work in presence of contamination and many other advantages of use of polymers in sliding (as well rolling) systems opens very interesting research area for tribology.

Polymeric tribosystems can operate without lubrication. Very wide possibilities to modify polymeric materials by fillers, lubricants and many other additives give very good perspectives to find polymeric composites that show excellent tribological properties both as matched with non-polymer or with another polymeric component. The lubrication enhanced these possibilities when the lubricant is optimized. The con-

struction of self-lubricating tribosystems is much easier to realize than in ceramic or metallic sliding or rolling contacts. Nowadays in technology polymers are seen as the most important future materials. The study shows that polymers as tribological materials are very good for low cost rubbing components in machines and devices.

References

- [1] Rymuza Z.: *Tribology of Anti-Friction Polymers*, WNT, Warszawa, 1986, in Polish.
- [2] Yamaguchi Y.: *Tribology of Plastic Materials*, Tribology Series, Vol. 16, Elsevier, New York, 1990.
- [3] Uetz H., Wiedemeyer J.: *Tribologie der Polymere*, Carl Hanser Verlag, München-Vienna, 1985.
- [4] Bahadur S.: *The development of transfer layers and their role in polymer tribology*, Wear, Vol. 245, 2000, pp. 92.
- [5] Sawyer W.G., Freudenberg K.D., Bhimaraj P., Schadler L.S.: *A study on the friction and wear behavior of PTFE filled with alumina nanoparticles*, Wear, Vol. 254, 2003, pp. 573.
- [6] Samyn P.: *Tribophysical interpretation of scaling effects in friction and wear for polymers*, Ph.D. Dissertation, Ghent University, 2006.
- [7] Zsidai L., De Baets P., Samyn P., Kalacska G., Van Peteghem A.P., Van Parys F.: *The tribological behaviour of engineering plastics during sliding friction investigated with small-scale specimens*, Wear, Vol. 253, 2002, pp. 673.
- [8] Samyn P., De Baets P., Schoukens G., Van Driessche I.: *Friction, wear and transfer of pure and internally lubricated cast polyamides at various testing scales*, Wear, Vol. 262, Issues 11–12, 2007, pp. 1433.
- [9] Bhushan B. (ed): *Springer Handbook of Nanotechnology*, Springer Verlag, Berlin, 2004.
- [10] Jia B.B., Li T.S., Liu X.J., Cong P.H.: *Tribological behaviors of several polymer–polymer sliding combinations under dry friction and oil-lubricated conditions*, Wear Vol. 262, Issue 11–12, 2007, pp. 1353.
- [11] Erhard G.: *Sliding friction behavior of polymer–polymer material combinations*, Wear, Vol. 84, 1983, pp. 167.
- [12] Czichos H.: *Influence of adhesive and abrasive mechanisms on the tribological behavior of thermoplastic polymers*, Wear, Vol. 88, 1983, pp. 27.
- [13] Lavielle L.: *Polymer–polymer friction: relation to adhesion*, Wear, Vol. 151, 1991, pp. 63.
- [14] Maeda N., Chen N.H., Tirrell M., Israelachvili J.N.: *Adhesion and friction mechanisms of polymer-on-polymer surfaces*, Science, Vol. 297, 2002, pp. 379.
- [15] Chen N.H., Maeda N., Tirrell M., Israelachvili J.N.: *Adhesion and friction of polymer surfaces: the effect of chain ends*, Macromolecules, Vol. 38, 2005, pp. 3491.
- [16] Eiss N.S., Mcann: *Frictional instabilities in polymer–polymer sliding*, Tribology Transactions, Vol. 36, 1993, pp. 686.
- [17] Norman S., Hanchi J.: *Stick-slip friction in dissimilar polymer pairs used in automobile interiors*, Tribology International, Vol. 32, No.11, 1998, pp. 653.
- [18] Rymuza Z.: *Friction, wear and lubrication in particular polymer-polymer pairs*, Zagadnienia Eksploatacji Maszyn, Vol. 2 (78), 1989, 125, in Polish.
- [19] Rymuza Z.: *Friction, wear and lubrication in particular polymer-polymer pairs*, Zagadnienia Eksploatacji Maszyn, Vol. 3 (79), 1989, 281, in Polish.

- [20] Rymuza Z., Kuszniereicz Z., Manturzyk G.: *Testing miniature, in particular, polymer-on-polymer journal bearings*, Wear, Vol. 174, 1994, pp. 39.
- [21] Rymuza Z., Kuszniereicz Z., Solariski T., Kwacz M., Chizhik S.A., Goldade A.V.: *Static friction and adhesion in polymer-polymer microbearings*, Wear, Vol. 238, 2000, pp. 56.
- [22] Karapetyan A.N., Rymuza Z., Kuszniereicz Z.: *Tribological properties of polymer-on-polymer pairs*, Trenie i Iznos, Vol. 25, No.3, 2004, 292, in Russian.
- [23] Karapetyan A.N., Rymuza Z., Kuszniereicz Z.: *Investigations of effect of clearance on static friction in polymer-on-polymer miniature journal bearings*, Trenie i Iznos, Vol. 25, No.2, 2004, pp. 207, in Russian.
- [24] Durr F.: *Das Reibungs- und Verschleissverhalten von technisch trocken und geschmierten Kunststoff-Kunststoff-Gleitpaarungen*, Uhrentechnik, 1975, nr 2, pp. 1.
- [25] Jain V.K., Bahadur S.: *Material transfer in polymer-polymer sliding*, Wear, Vol. 46, 1978, pp. 177.
- [26] Kwacz M.: *Minimization of energy losses in starting phase of operation of miniature polymeric sliding contacts*, PhD Thesis, Warsaw University of Technology, 2005, in Polish.
- [27] Hansen Ch.M.: *Hansen Solubility Parameters*, 2nd edition, CRC Press, Boca Raton, 2007.
- [28] Yamamoto Y.J., Takashina T.: *Friction and wear of water lubricated PEEK and PPS sliding contacts*, Wear, Vol. 253, 2002, pp. 820.
- [29] Yabe T., Takajo T., Kato S., Ueki F.: *Lubricant-supplying properties and durability of oil-impregnated polymers*, Tribology Transactions, Vol. 43, 2000, pp. 453.
- [30] Kang S.C., Chung D.W.: *The synthesis and frictional properties of lubricant-impregnated cast nylons*, Wear, Vol. 239, 2000, pp. 244.
- [31] Van Krevelen D.W.: *Properties of Polymers*, Elsevier, Amsterdam, 1990.
- [32] Rymuza Z.: *Triboelektryzacja polimerów*, Zagadnienia Eksploatacji Maszyn, 2 (74), 1988, pp. 61.

Tribologia polimerów

Polimery są atrakcyjnymi materiałami do zastosowania w węzłach tarcia maszyn i urządzeń. Mogą one być kojarzone z materiałami niepolimerowymi (metale, materiały ceramiczne) a także z polimerami. Większość prac badawczych poświęcona jest parom tarcia, w których tylko jeden element jest wykonany z polimeru. Zwykle są to skojarzenia stal-polimer. Równie interesujące właściwości tribologiczne mogą też wykazywać skojarzenia polimer-polimer przy starannym doborze materiałów na elementy trące. Szerokie możliwości stwarza zastosowanie kompozytów na osnowie polimerów. Skojarzenia polimerowe mogą pracować bez smaru i przy smarowaniu. Decydujący wpływ na tribologiczne zachowanie się polimerów ma zjawisko przenoszenia materiału przy tarcu. Także zjawisko triboelektryzacji ma istotnie wpływa na procesy tribologiczne w polimerowym węźle tarcia. Materiały polimerowe są materiałami przyszłości także w budowie odpowiedzialnych węzłów tarcia maszyn i urządzeń.



The Mechanism of Tribological Wear of Thermoplastic Materials

W. WIELEBA

Wrocław University of Technology, Wybrzeże Wyspiańskiego 25, 50-370 Wrocław

Sliding machine elements made of plastics co-operate mostly with metals. The friction of these materials engages several processes like mechanical and adhesion interactions, tribo-chemical and tribo-electrical reactions etc. In this paper, processes involved with the tribological wear of polymer materials under conditions of dry friction were discussed. The focus was on mechanical and adhesion reactions between co-operating surfaces. The role of the surface roughness of the metallic element on the creation of the polymer film and on the wear of the polymer material was stressed. Fundamental modes of wear characteristic for polymer materials were described. These include adhesion wear, abrasive wear, fatigue wear, thermal and chemical wear, asperities melting, creep wear, and fretting. A wear mechanism for different polymer materials (including composites) was presented. The mechanism includes chemical activity of the mating metals, the role of fillers in the transfer of load and creation of the polymer film. A mechanism accounting for additional heating of the material as a result of fluctuating friction force loading of the sliding metal/polymer pair and additional heating due to internal friction of the polymer materials was also presented.

Keywords: *polymer material, thermoplasts, wear tribological performance*

1. Introduction

Sliding machine elements made of plastics co-operate mostly with metallic materials and are subject to different processes involved with friction and wear. During the friction of polymer materials on steel, several processes [1, 3] like mechanical and adhesion interactions, tribo-chemical and tribo-electrical reactions etc. are present. A share of these interactions in the process of friction is dependent upon the loading of the friction pair with the normal force, sliding velocity, surface roughness and waviness of the co-operating metal element, mechanical properties of the rubbing materials, adhesion characteristic of the sliding pair and other operating conditions. The process of creation of the polymer film on the surface of the co-operating element as well as the film stability and its ability to regenerate is also of great importance.

The knowledge of the wear mechanism in polymer materials used in machine design makes it possible to select properly co-operating materials in the designed friction node as well as to ensure its proper exploitation in the future.

2. Characteristic tribological processes involved with the friction of polymer materials on steel

2.1. Mechanical interactions

Surfaces of mechanical elements, even those machined to the highest grade of finish, are never ideally smooth. Their geometric features are defined by the surface roughness, waviness, deviation in shape, and orientation of irregularities. The contact of two real surfaces subject to friction is done on the irregularity asperities. Many historical theories (Amontons, Coulomb) assumed that friction results from mechanical interactions of the contacting surfaces irregularities. In the so-called Coulomb model, the action of the wedge-shaped asperities causes the two surfaces to move apart as they slide from one position to another and then come close again. Work is done in raising the asperities from one position to another and most of the potential energy stored in this phase of the motion is recovered as surfaces move back.

Nowadays [1–5], it is generally acknowledged that apart of local adhesion contacts of the asperities of micro-irregularities, the energy of friction is required for micro-scale deformation of contacting surfaces during relative motion. If asperities of one surface (harder of the two, if dissimilar) plough through the other via plastic deformation, energy is required for this macro-scale deformation (grooving by ploughing). Macro-scale deformation can also occur by particles trapped between the sliding surfaces. A situation of this type is common during the friction of polymer materials on metals as the two co-operating materials feature a marked difference in hardness. Hard micro-irregularities of the metal element dig into a relatively soft surface of the polymer material causing ploughing, grooving or micro-machining during sliding friction (Figure 1).

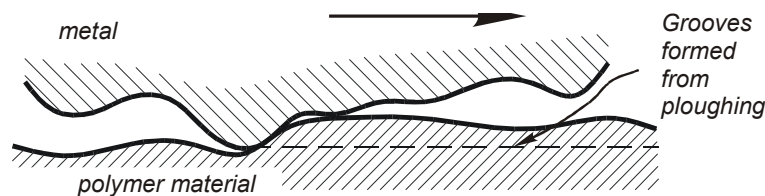


Fig. 1. Mechanical interactions between irregularities of the metal/polymer surfaces

2.2 Adhesion

In the process of contact formation, besides an elastic deformation process the asperities undergo some plastic deformation [1, 3]. Due to this deformation process, intimate contact between the partners occurs so that molecular surface forces may act through the interface, which results in “interfacial bonding” and the generation of adhesive “junctions”. Thus, the different types of molecular forces that can act within the

interface of two contacting bodies to produce “adhesion” and the energy of interfacial adhesion bonding must be considered. Theoretically, the attractive interaction forces between two contacting solids include, at least in principle, all those types of interaction that contribute to the cohesion of solids, such as metallic, covalent and ionic, i.e., primary chemical bonds (short-range forces), as well as secondary van der Waals bonds (long-range forces). Long-range van der Waals forces act in the adhesion between soft rubber-like materials and between polymeric solids.

Adhesion problems have been addressed in many research papers. There are a few theories concerning adhesion interactions: mechanical, adsorption, electrical, diffusion, and chemical ones. These were described, among others, in [4–7]. Artificial materials feature, as a rule, big adhesion to metals and relatively small shearing strength. As a result of rubbing, metal elements are being covered with a thin layer of the transferred polymer material. By virtue of this process, polymer materials display lower values of the friction coefficient under dry conditions than metals. The presence of strong adhesion, however, is detrimental to the wear rate.

Adhesion interactions may often be calculated in terms of free surface energies. The energy required to create a new surface, expressed over an area consisting of many atoms in the surface lattice, is referred to as the free surface energy. The higher the surface energy of a solid surface, the stronger the bonds it will form with a mating material. One obvious suggestion is to select materials that have a low surface energy. The use of lubricants at the interface reduces the surface energy. Materials with low work of adhesion result in low adhesion, where work of adhesion represents the energy that must be applied to separate a unit area of the interface or to create new surfaces.

2.3. Creation of the polymer film

The polymer film, i.e. a thin layer of polymer (Figure 2) forms on the surface of the co-operating metal element. It reduces the roughness of the steel surface influencing thus, among others, the friction and wear processes. Additionally, thanks to this layer, friction develops between two polymer layers and not between the polymer and metal layers. The rate of the film creation, its structure, durability and lubrication properties depend on forces of adhesion between the metal and the polymer, and, above all, on the properties of the very polymer material.

The explanation and role of this process have been subject to studies of many researchers [8–13]. A variety of offered explanations of the film creation process during sliding co-operation of polymer materials with steel is a prove that the process has not been fully recognized as yet. The majority of researchers is inclined to agree that the process of the film creation is a multi-stage one [8, 11, 12]. The prevalent opinion is that at the beginning stage of the sliding co-operation of polymer and steel, there is an adhesion transfer of the polymer onto the counter-element caused mainly by molecular and electrostatic forces and/or physical and chemical interactions.

At the same time, heat generated due to friction rises the temperature at the mating surface of the polymer, which in turn leads to the loosening of bonds between intermolecular polymer chains. Surface located polymer chains are subject to mechanical inputs like compression, shearing and tension, the inputs that cause chain cracking and creation of molecules of different radicals. This triggers tribo-chemical reactions between the broken chains of the polymer and complexes located at the surface of the mating metal. Generally speaking, the following factors influence tribo-chemical reactions: chemical composition and molecular structure of the polymer, friction conditions (unit pressure, sliding velocity, type of contact etc.), environment, temperature etc. The first layer of the polymer adheres strictly to the surface of the metal and is practically not removable during the whole friction process.

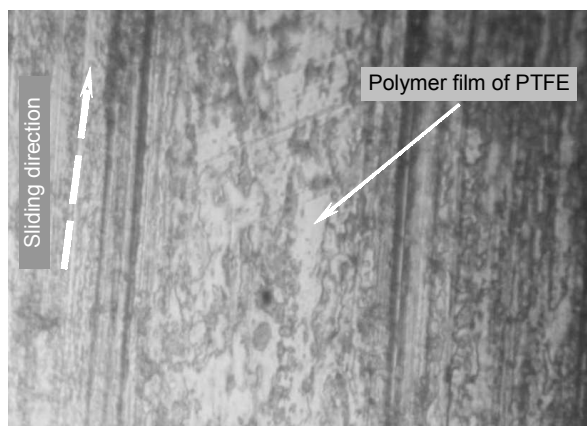


Fig. 2. Polymer film (PTFE) on the surface of steel after the friction process

The next layers of the polymer material may be easily removed and these very layers convert into wear products of the adhesion wear process. These products may also be created as a result of mutual abrasive interactions between the asperities of micro-irregularities of the metal surface and the surface of the polymer material. They fill gradually cavities between the asperities. Not all of the wear products are bound, however, to the surface of friction. In a further stage of the friction process these particles are compressed by the mating surfaces creating a layer of different thickness. The retaining of the transferred polymer material on the surface of the counter-specimen is possible due to the adhesion and locking of the material particles between micro-asperities of the metal surface. It was confirmed [12] that the greater the surface energy of polymer, the stronger sticks the polymer layer to the counter-specimen. Particles of fillers may increase the adhesion of the polymer layer to the surface of the counter-specimen by creating additional bonds. The thicker is the polymer film, the better protection of the polymer material against asperities of the counter-element surface. At the same time the strongly bonded polymer film protects the surface against the detri-

mental action of hard particles trapped in the friction zone. Materials featuring a high value of the surface energy form a film featuring higher coherency of particles or layers. Such layers are more wear resistant. At the same time, however, strong adhesion interactions cause that polymer particles are more easily removed from the surface of the polymer material.

Figure 3 shows differences in the formation process and retaining of a polymer layer depending upon the surface roughness of the steel element.

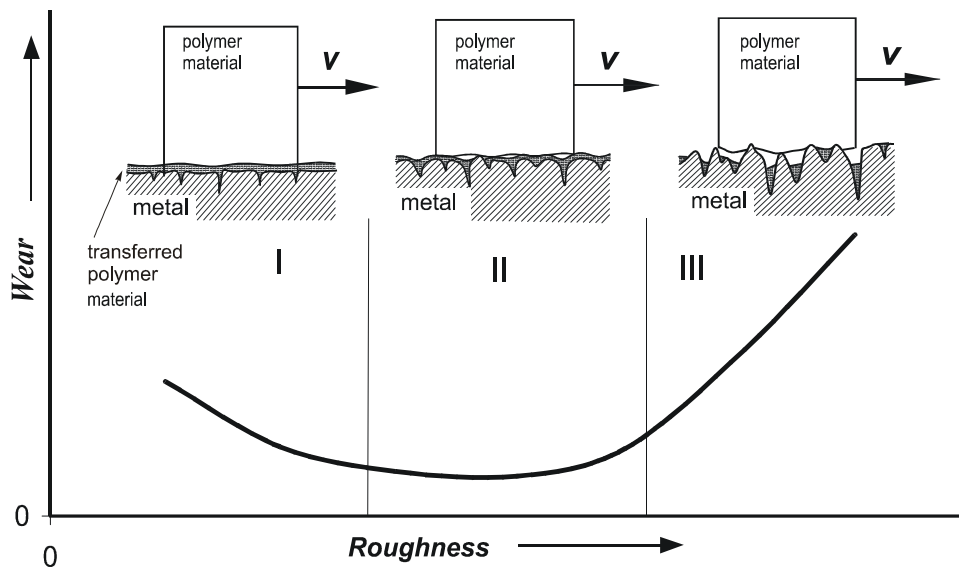


Fig. 3. Wear rate I_z versus surface roughness
I, II, III – formation of the polymer layer on surfaces with different roughness

With smooth surfaces, adhesion interactions at the surface of contacting materials are strong, which contributes to a relatively high value of the friction coefficient and to elevated wear of polymer materials. This is true even if mechanical interactions between the steel surface covered with a layer of the transferred material and the sliding surface of the composite are small. (Figure 3, zone I).

With the increasing roughness of steel, adhesive interactions decrease and the presence of the polymer layer (covering still the surface of the steel element) results with only a slight increase in mechanical interactions (Figure 3, zone II).

As a result, the wear rate of the composite is relatively low. With the high roughness of the steel surface (Figure 3, zone III), the formation and retaining of the polymer layer is difficult and adhesion interactions are weak. Lack of continuity in the layer of the transferred material and strong mechanical interactions of the steel surface against the sliding surface of the composite (micro-machining, ploughing etc) results with increased wear.

3. Types of wear in plastics

The process of tribological wear of polymer materials [4, 5, 7] is caused by the abrasion, cracking and spalling of material particles, surface adhesion of the co-operating elements and by tribo-chemical reactions present at the surface of contact. Of the many modes of wear characteristic for metallic materials, polymer materials are subject to abrasion, adhesion, and fatigue wear. On the other hand, creep wear, thermal wear and asperities melting are the wear processes inherently involved with polymers only.

The listed types of wear are practically never isolated. Depending upon friction conditions, different modes of wear may be dominant. Deciding is the state of the upper surface of the sliding counter-element (type of material, hardness, and roughness) and performance parameters (temperature, pressure, and sliding velocity). As tribological processes are dynamical ones (e.g. the creation of the polymer film) the share of individual types of wear may vary in individual phases of the friction process.

3.1 Adhesion wear

This type of wear is directly linked with the adhesion of the rubbing surfaces and is present mainly during the friction of polymer materials against smooth (e.g. polished) metal surfaces without lubrication. The mechanism of adhesion wear consists of the creation of strong local adhesion joints [3, 5, 7, 14–15] that produce deformations in the upper layer, rupture of cohesion links in the bulk of the polymer material and its transfer onto the counter-specimen surface. After a short period of friction, the creation of the polymer film on the steel surface follows, the surface of the polymer element becomes matt and characteristic in its appearance (numerous fine cavities after detached material particles). In a further phase of motion, the transferred material detaches from the counter-element and is removed from the friction zone as wear product. This process is a cyclical one and contributes, first of all, to the wear of the polymer material. The rate of occurrence of individual adhesion phenomena depends upon physical and chemical properties, mechanical properties and structure of the upper layer of the material as well as from properties of the co-operating material and its surface roughness. The surface energy of the polymer material and the surface roughness of the counter-element have also influence on adhesion.

3.2. Abrasion wear

Abrasion wear is present, first of all, during the rubbing of polymer materials against a metal surface featuring considerable roughness. The asperities of the harder material function as micro-blades. The loss of material is due to micromachining, scratching, or ploughing in the micro-zones of contact [1, 3, 5]. Abrasion wear may also follow as a result of the trapping of hard particles from the rubbing steel elements (or abrasive particles originating from the environment) between the two rubbing sur-

faces [16–19]. Characteristic for the co-operation of a sliding plastics/metal pair is the fact that abrasion grains or wear products embed into the more soft material and contribute to the wear of the metal surface. This mode of wear is also present when the polymer material is a composite containing hard filler particles, e.g. fibre glass, quartz powder etc. Abrasion wear features high intensity and often is a reason of a strong warm up of the polymer material. That is why, apart of mechanical wear, thermal and chemical wear processes are also present.

3.3. Fatigue and erosion wear

The reason of fatigue and erosion wear is a cyclical, variable deformation of the upper layer [1–3, 7]. As a result, small micro-cracks appear, the propagation and aggregation of which contribute to the spalling of the polymer material. The wear associated with this process grows very fast, especially when the deformations of the polymer material are of plastic nature. In the case of polymers, fatigue wear causes additionally the cracking of macromolecule chains. The result is a reduced molecular mass of the polymer within its surface layer and a reduction in the crystallinity rate of the polymer. In composites containing e.g. fibre or carbon glass, yet another form of wear is present. This one is a result of the propagation of dislocations due to a discontinuity of the material around fibres. Consequently, micro-cracks appear under the surface and particles of the polymer material are removed from the surface as a result of mechanical interactions and adhesion.

Erosion wear is a result of impacts of small particles against the metal surface. This results with small losses of material termed as erosion, a process little known and considered as a form of fatigue wear in the case of polymer materials.

3.4. Chemical (tribo-chemical) wear

Chemical wear develops due to chemical reactions evolving during friction between the rubbing materials. Forces of friction may cause the cracking of polymer chains in the surface layer and creation of molecules of different radicals. Highly-active radicals may react with chains that did not crack contributing to the creation of a new series of chain breakages. The radicals may also react with other radicals creating thus new polymer molecules. During the rubbing of polymers against steel, also other substances (e.g. O₂, H₂O, and the very metals and their oxides) may participate in reactions evolving on the friction surface. Generally, factors influencing tribo-chemical reactions are the chemical and molecular structure of the polymer, friction conditions (unit pressure, sliding velocity, type of contact), environment, temperature, etc.

Chemical wear may also be linked with reactions between the polymer material and the environment (e.g. oxidization) of the friction process. Degradation processes have big influence on the material transfer rate. Chemical wear goes together with other forms of wear.

3.5. Thermal wear

Thermal wear follows as a result of the dissipation of large amounts of friction energy in the form of heat, a process that results with an increase in the temperature of the polymer material and its softening in the upper layer. A temperature at which the thermal wear process starts depends upon the type of material. This temperature is usually higher than the temperature of the thermal resistance determined usually by the Martens, ASTM, or Vicata methods. It is usually given in the manufacturer's specifications of plastics. With this type of wear, the spreading of or even gluing of the rubbing surfaces often happens. In the ultimate case, the elevated temperature results with irreversible changes in the chemical structure of the polymer. That is why this type of wear is usually termed as the catastrophic one.

3.6. Asperity melting

The wear of polymer materials that results in the melting of asperities is prevalent mostly at the stage of run-in, i.e. during the initial stage of their rubbing against steel. At an appropriate loading (in terms of $p\nu$) of a rubbing pair and an appropriate roughness of the metal element, the melting of asperities of the polymer material starts. This leads to a quick smoothing of its surface and with a more uniform distribution of pressure at the contact surface (reduction in the stress concentration at the peaks of micro-irregularities). A precondition, however, is that abrasive wear at this stage of the friction process is not too intensive. Smoothing goes together with the working (hardening) of the upper layer of the polymer material. At a further stage, the asperity melting process terminates, the sliding surface of thermoplastic materials becomes lustrous and smooth. It may be assumed that the asperity melting wear is actually a beneficial part of the run-in process.

3.7. Wear as a result of creep

Wear as a result of creep is a characteristic process for polymer materials that leads to changes in the form and dimensions of elements made of these materials without any loss of mass. Wear as a result of creep is linked with the visco-elastic nature of polymers. It is due to deformations of form and volume aligned with the direction of loading. As a result of friction forces, periodically recurrent irregularities in the form of waves, which are transverse to the direction of motion, appear. The creation of these waves is not a result of a single plastic deformation but is a result of recurrent deformations of the surface layer of the material. The rate of this process is proportional to the viscosity of the material, value of the unit pressure, and the surface roughness of the co-operating surface. In the creep wear process, permanent deformations leading to changes in linear dimensions (due to the normal load) are, however, of greater importance. In polymer machine elements of considerable thickness and loaded with a big normal load this type of wear is overly dominant.

3.8. Fretting

Fretting is a specific type of wear that differs from other types of polymer wear in that it is present at a relatively low velocity of sliding and at cyclic micro-displacements. An additional condition is that the surfaces are in continuous contact [20]. Fretting is of fatigue-abrasion nature. Products of wear brought about by fretting are termed as the so called third body, which is of great importance in the wear process of polymer materials. These products remain practically all the time in the friction zone and are not removed outside of it. If they contain hard filler particles, the fretting process rate increases. The process and characteristics of fretting wear on the surface of polymers are determined by the thermal resistance of the polymer and the frictional heat produced, and these in turn depend on the molecular chain structure and aggregate state structure of the polymer.

4. Mechanism of polymer materials wear

4.1. Non-modified polymers

Non-modified polymer materials used in sliding machine nodes during normal operation are subject, first of all, to adhesion wear as this type of wear features the least rate of material loss. Other types of wear are more destructive and shall be eliminated by a skilful selection of parameters and conditions of the friction process.

The literature offers many descriptions of the polymer material wear [4, 7, 14–19]. The prevailing opinion among the researches is that an essential role in the case of polymer materials plays the process of formation and retaining of the polymer film on the steel element. Depending upon the chemical activity of the rubbing polymer/steel pair, products of wear may originate from the polymer film removed from the steel substrate (for small chemical activity) or from the sliding surface of the polymer material (for high chemical activity). Exemplary models of adhesion wear for different levels of chemical activity of the metal to a polymer material are presented in Figure 4.

4.2 Composite polymers

The process of wear of composite polymer materials is a very complex one [7, 10, 15, 21–24] as its course is markedly governed, apart of operational parameters and the state of the upper layer, also by fillers. A diversity of fillers, both with respect to their properties and their volumetric content, makes the analysis of this process even more difficult. In a set of fundamental factors that influence the friction and wear of composite materials these are the most important [5, 7, 21]: filler type, its volumetric content in the composite, the size, form and surface share of the filler particles as well as the structure of inter-phase border between the filler and the matrix.

It is assumed that the dominant wear during the regular exploitation of polymer composites is the adhesion one [14]. Depending however on the type of filler and fric-

tion conditions, other wear mechanisms may also be present with their marked impacts on the friction process. One of them is the modification of the surface layer of the polymer material. The share of the filler on the sliding surface becomes higher (when compared to its starting value). In some of the cases (e.g. a composite with metal powders) a situation may happen when the sliding surface consists predominantly of fillers (Figure 5, stage III). That means that the friction process is present mainly between fillers protecting the polymer matrix against wear and the surface of the counter-element. At the same time, both the sliding surface of the fillers and the surface of the counter-element may be coated with the polymer film decreasing the friction coefficient and temperature of the rubbing elements. In such composites, the polymer, apart of the role of matrix, performs also the function of grease. An example may be PTFE based composites [21–23].

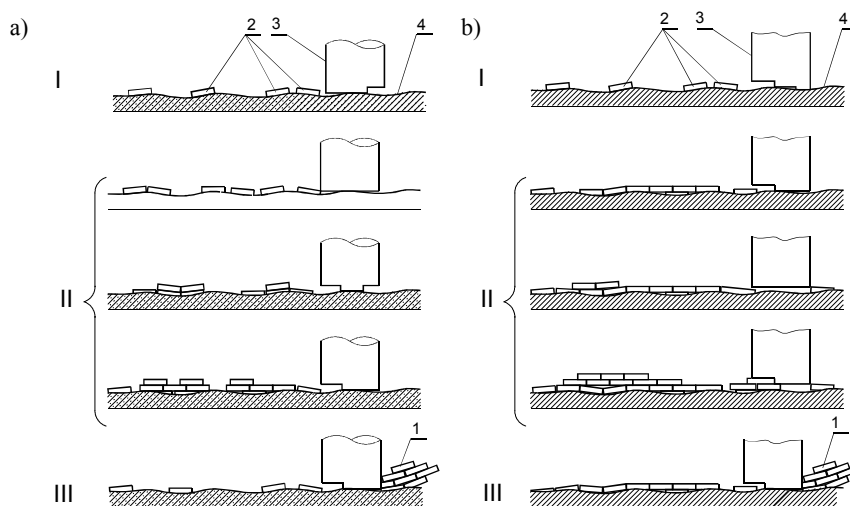


Fig. 4. Models of the adhesion wear of a polymer (PTFE) [14] when rubbing against materials with small (a) and high (b) chemical activity; 1 – wear products, 2 – PTFE lamellae, 3 – polymer specimen, 4 – counter-element; I, II, III stages in the transfer of material (explanations in the body of the text)

The research that has been done by many researchers [15, 22–23] confirms that dispersive fillers in most cases are also transferred to the polymer layer created on the surface of the co-operating steel element. By applying fillers with a big surface energy, the adhesion of the film to the metal may be increased and consequently, its durability. The application of bronze or molybdenum disulphide powder in PTFE based composites works to this effect.

The process of the tribological wear of a polymer material features periodically repeated micro-cycles [15, 21]. A discrete surface contact of the composite with the steel counter-element brings about big amounts of heat generated during the friction of

hard particles of the filler against steel. This contributes to local high temperatures, markedly higher than the average temperature of the rubbing elements. The elevation of the local temperature to its critical value brings about the softening of the matrix and a reduction of friction forces and, as a result, a reduction in the heat generated and an increase in the wear of the upper layer of the composite. Additionally, a certain amount of friction energy is dissipated as a result of internal friction [25], which leads to the appearance of new heat sources inside the polymer material. As a result, the temperature of layers located in the bulk of the material, just under the sliding surface, is higher. This difference in the temperature of PTFE composites may be as high as a dozen or so degrees. The higher temperature inside the polymer and comparatively high temperature gradients cause that the matrix becomes softer at a certain distance from the surface (approx. 1 mm) than just under the sliding surface.

In polymer composites there is usually a big difference between the stiffness of fillers and the polymer matrix (the modulus of longitudinal elasticity). This causes that particles of the filler transfer a large amount of loading into deeper layers of the composite (Figure 5a).

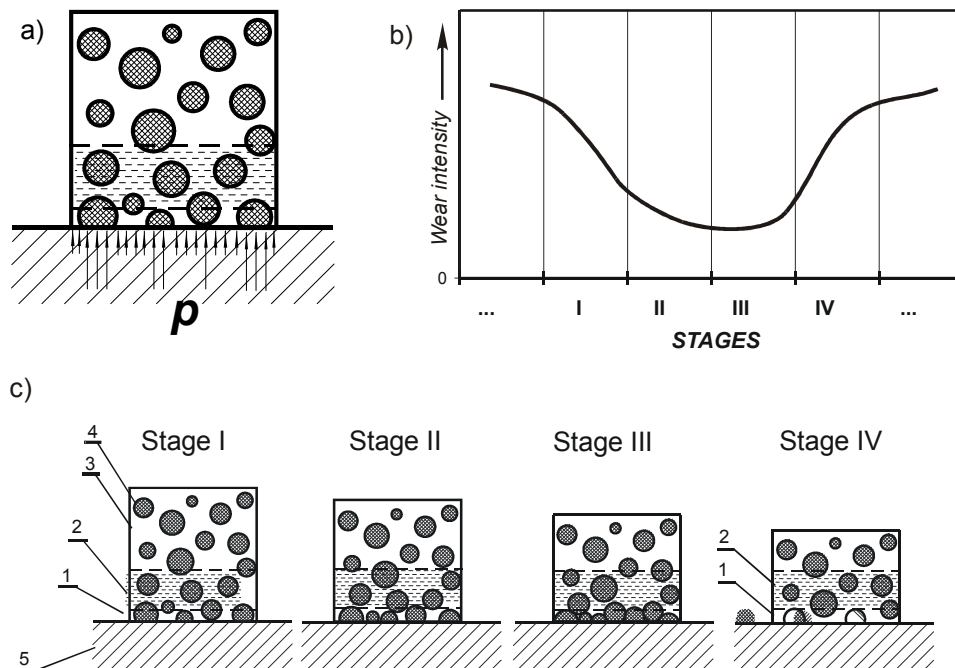


Fig. 5. Stages of the wear process for PTFE composites filled with dispersive fillers [21] (1 – surface layer, 2 – elevated temperature zone, 3 – polymer matrix (PTFE), 4 – filler grain, 5 – steel counterface) a) distribution of pressure on the surface of a composite with dispersive filler, b) wear intensity in subsequent stages of the wear process, c) stages in the wear process history

A markedly high loading of the filler grains located at the sliding surface causes their embedding in the polymer matrix (Figure 5c, stage I), especially—as earlier mentioned—it is softer in the bulk of the polymer material than in the closest proximity of the sliding surface. The stiffness of the polymer matrix just under the sliding surface causes that translations of the filler grains proceeding in line with the forces of friction is more difficult. On the other hand, the plastic deformation of these grains is possible, as is the case with bronze powder. With the wear proceeding, the grains of the filler being in the course of embedding encounter other grains located in the bulk of the material. The concentration of the filler in the upper layer of the composite material grows (Figure 5, stage II), what leads to a decrease in the wear rate of the composite, or to the increase of the wear resistance of this layer. During friction, the thin layer of the polymer may be transferred on the filler grains, which facilitates their sliding on the steel counter-element.

In the further stage, the filler concentration on the sliding surface is already so high (Figure 5c, stage III) that the renovated polymer layer is not capable to cover all grain located on the sliding surface. The value of the friction coefficient rises and accordingly – the temperature of the polymer material as well. As a result, the matrix becomes more and more soft and finally, is not able to detain the filler grains of the sliding surface. The grains are removed in part as products of wear and then, the enhanced wear period begins (Figure 5, stage IV). The diminishing concentration of the filler grains contributes to lower values of the friction coefficient and consequently, to the reduced amount of heat. This causes a reduction in the temperature of the composite material and another cycle in which the number of the filler grains in the surface layer increases.

The interactions of fibre fillers in polymer composites [24, 26] are a separate problem. In these materials, four processes of product removal dominate:

- wear of the polymer matrix,
- abrasive wear of fibres,
- cracking and spalling of fibres,
- separation of fibres from the matrix.

The last two of the listed processes are periodic ones. The removal of fibres from the matrix causes an increase in the matrix wear due to the weakening of the material at this place. Additionally, particles of the removed fibre get to the friction zone and start abrasion wear. The model of this mechanism is shown in Figure 6.

When the direction of fibres orientation is parallel to the line of loading in the friction node, the fibres participate in the transfer of load from the friction zone. Usually, the polymer matrix has a lesser value of the modulus of longitudinal stiffness. That is why, when assuming equal strains, a difference in the longitudinal stresses in the matrix and in the fibres occur. It shall be noted that the higher the ratio l/r (longer fibres), the more effective the composite strengthening. The above considerations witness to a significant role of fibres in this process [26].

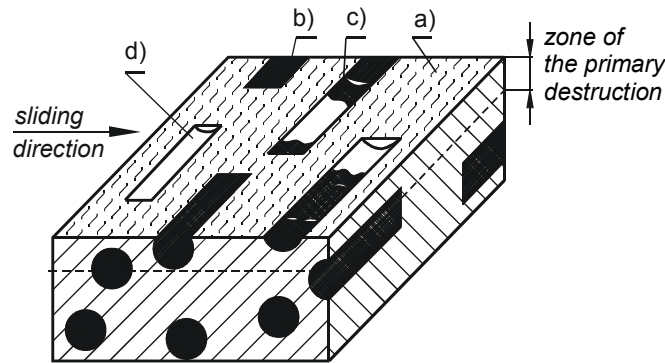


Fig. 6. Model of the wear mechanism of thermoplastic composites containing short cut fibres [25]
 a) polymer matrix, b) fibre, c) fibre rupture, d) cavities after the removed fibre

5. Summary

Mechanical and adhesion interactions and the creation of the polymer film transferred onto the steel surface play the most important role in the process of friction of polymer materials. The process of the film creation is triggered by tribo-chemical reactions between the broken chains of the polymer and complexes present on the surface of the co-operating material. The retention of the polymer layer is possible due to adhesion interactions. An essential influence on the durability of the film has the chemical activity of the metal to the polymer and the geometrical structure of the counter-element surface, which can make this detention process easier or more difficult. Additionally, the transferred layer of the polymer causes a modification of the geometrical structure of the metal surface. In the surface layer of the polymer and in the film transferred onto the steel surface, complex physical and chemical processes evolve.

The dominant type of wear in sliding elements of machines made of polymer materials during their regular operation is adhesion wear. This type of wear features the least rate of material loss. During the run-in process, asperities melting may occur as a beneficial type of wear. Other types of wear like abrasion wear, fatigue, creep, and especially thermal wear are to be avoided and shall be limited in their scope by a proper selection of parameters and conditions of the friction process.

Different and diversified physical and chemical interactions take place during the process of friction of polymer composites on metals due to the multi-phase structure of these materials. These interactions are related to the wear of the polymer matrix and the wear of individual fillers. Additionally, attention shall be given to a mutual influence of the fillers and the polymer matrix on the mode of wear as well as to the phenomena present on the surface of the metal counter-element. The properties of composites depend, to a high degree, on the volume and surface related characteristics of the components, which change the character of the friction process. Hard particles of

the filler increase local stresses during friction triggering increased head dissipation and changing mechanical processes when compared to those present in non-modified polymers.

References

- [1] Bhushan B.: *Modern tribology handbook*, CRC Press, Boca Raton, 2001.
- [2] Kragelsky I.V.: *Friction, wear, lubrication – Tribology handbook*, Moscow, 1981.
- [3] Czichos H.: *Tribology*, Elsevier, Amsterdam, 1978.
- [4] Belyj V.A., Sviridenok A.I., Petrokovec M.I., Savkin V.G.: *Trenie polimerov*, Moskva, Izd. Nauka, 1972.
- [5] Myshkin N.K., Petrokovets M.I., Kovalev A.V.: *Tribology of polymers: Adhesion, friction, wear, and mass-transfer*, Tribology International, 38, 2005, pp. 910.
- [6] Houwink R., Salomon G.: *Adhesion and adhesives*, Elsevier, Amsterdam, 1965.
- [7] Rymuza Z.: *Trybologia polimerów ślizgowych*, Warszawa, WNT, 1986.
- [8] Bahadur S.: *The development of transfer layers and their role in polymer tribology*, Wear, 2000, Vol. 245, pp. 92.
- [9] Evdokimov J.A., Kolesnikov V.I.: *Rol elektrizacii v mechanizme perenosa produktov iznašivaniya v sistemach polimer-metall*, Trenie i iznos, 1993, t. 14, No. 2, pp. 389.
- [10] Gong D., Zhang B., Xue Q.J., Wang H.L.: *Effect of tribochemical reaction of polytetrafluoroethylene transferred film with substrates on its wear behaviour*, Wear, 1990, Vol. 137, pp. 267.
- [11] Polak A.: *The mechanism of transfer film formation on metal surface*, Proc. of the International Conference "Problems of Non-Conventional Bearing Systems" NCBS '99, Zielona Góra, 1999, pp. 241.
- [12] Polak A.: *Wpływ energii powierzchniowej polimeru na zużycie podczas przenoszenia materiału w parze tribologicznej polimer-stal w obecności twardych cząstek ściernych*, Zagadnienia Eksploatacji Maszyn, 2000, Vol.123, z. 3, pp. 69.
- [13] Liu Y., Schaefer J.A.: *The sliding friction of thermoplastic polymer composites tested at low speeds*, Wear, 261, 2006, pp. 568.
- [14] Gong D., Xue Q.J., Wang H.L.: *Physical models of adhesive wear of polytetrafluoroethylene*, Proc. of the Japan International Tribology Conference, Nagoya, 1990, pp. 959.
- [15] Gong D., Zhang B., Xue Q.J., Wang H.L.: *Investigation of adhesion of filled polytetrafluoroethylene by ESCA, AES and XRD*, Wear, 1990, Vol. 137, pp. 25.
- [16] Yen B.K., Dharan C.K.H.: *A model for abrasive wear of fiber-reinforced polymer composites*, Wear, 1996, Vol.195, pp. 123.
- [17] Unal H., Sen U., Mimaroglu A.: *Abrasive wear behaviour of polymeric materials*, Materials and Design, 2005, Vol. 26, 705.
- [18] Sinha S.K., Chong W.L.M., Lim Seh-Chun: *Scratching of polymers—Modeling abrasive wear*, Wear, 2007, Vol. 262, pp. 1038.
- [19] Shipway P.H., Ngao N.K.: *Microscale abrasive wear of polymeric materials*, Wear, 2003, Vol. 255, pp. 742.
- [20] Guoa Q., Luoa W.: *Mechanisms of fretting wear resistance in terms of material structures for unfilled engineering polymers*, Wear, 2002, Vol. 249, pp. 924.

- [21] Wieleba W.: *Analiza procesów tribologicznych zachodzących podczas współpracy kompozytów PTFE ze stalą*, Oficyna Wydawnicza PWr., Wrocław, 2002.
- [22] Maškov J.K., Gadieva L.M. i in.: *Povyšenie iznosostojkosti napolnenogo politetraforetylena putem optimizacii sodieržanija nopolnitelej*. *Trenie i iznos*, 1988, t. 9, pp. 606.
- [23] Senatrev A.N., Birban V.V., Nevzorov V.V., Savkin V.G.: *Osobennosti processa iznašivaniija PTFE i kompozita na ego osnove*. *Trenie i iznos*, 1989, t. 10, No. 4, pp. 604.
- [24] Friedrich K., Walter R.: *Microstructure and tribological properties of short fiber-thermoplastic composites*, Proc. of a Conference "Tribology of Composite Materials", Oak Ridge (USA), 1990, pp. 217.
- [25] Wieleba W.: *The role of internal friction in the process of energy dissipation during PTFE composite sliding against steel*, *Wear*, 258, 2005, pp. 870.
- [26] Tanaka K., Kawakami S.: *Effect of various fillers on the friction and wear of polytetrafluoroethylene-based composites*, *Wear*, 1982, Vol. 79, pp. 221.

Mechanizm zużywania tribologicznego tworzyw termoplastycznych

Ślizgowe elementy maszyn wykonane z tworzyw sztucznych współpracują najczęściej w skojarzeniach z metalami. Podczas tarcia tych materiałów zachodzi szereg procesów takich jak oddziaływania mechaniczne i adhezyjne, reakcje tribochemiczne, triboelektryzacja, itp. W artykule przedstawiono procesy związane z tribologicznym zużywaniem materiałów polimerowych w warunkach tarcia suchego. Omówiono oddziaływania mechaniczne oraz adhezyjne pomiędzy współpracującymi powierzchniami par ślizgowych. Zwrócono uwagę na rolę chropowatości powierzchni elementu metalowego podczas tworzenia na nim filmu polimerowego a także w procesie zużywania materiału polimerowego. Opisano podstawowe rodzaje zużywania, charakterystyczne dla materiałów polimerowych m. in. zużywanie adhezyjne, ściernie, zmęczeniowe, cieplne, chemiczne, nadtapianie, zużywanie wskutek płynięcia oraz fretting. Zaprezentowano mechanizm zużywania różnych materiałów polimerowych, w tym kompozytów, uwzględniający między innymi aktywność chemiczną współpracujących metali, rolę wypełniaczy w przenoszeniu obciążenia oraz tworzeniu polimerowego filmu. Przedstawiono również mechanizm uwzględniający dodatkowo rozgrzewanie materiału polimerowego w wyniku tarcia wewnętrznego oraz zmiennego obciążenia siłą normalną oraz siłą tarcia zewnętrznego pary ślizgowej metal-polimer.

Information for Authors

Send to: *Archives of Civil and Mechanical Engineering*
Polish Academy of Sciences, Wrocław Branch
Podwale 75, 50-449 Wrocław, Poland

Archives of Civil and Mechanical Engineering (ACME) publishes both theoretical and experimental papers which explore or exploit new ideas and techniques in the following areas: structural engineering (structures, machines and mechanical systems), mechanics of materials (elasticity, plasticity, rheology, fatigue, fracture mechanics), materials science (metals, composites, ceramics, plastics, wood, concrete, etc., their structures and properties, methods of evaluation), manufacturing engineering (process design, simulation, diagnostics, maintenance, durability, reliability). In addition to research papers, the Editorial Board welcome: state-of-the-art reviews of specialized topics, letters to the Editor for quick publication, brief work-in-progress reports, brief accounts of completed doctoral thesis (one page is maximum), and bibliographical note on habilitation theses (maximum 250 words). All papers are subject to a referee procedure, except for letters, work-in-progress reports and doctoral and habilitation theses, which are briefly reviewed by the Editorial Board.

The papers submitted have to be unpublished works and should not be considered for publication elsewhere.

The Editorial Board would be grateful for all comments on the idea of the journal.

Submit three copies, each complete with abstract, tables, and figures.

Detailed information about the Journal on web:

<http://www.pan.wroc.pl>

www.ib.pwr.wroc.pl/wydzial/czasopismoACME.html

<http://www.wmech.pwr.wroc.pl>

Price 15 zł
(0% VAT)

Subscription orders should be addressed to:

Oficyna Wydawnicza Politechniki Wrocławskiej
Wybrzeże Wyspiańskiego 27
50-370 Wrocław